universität wien

DISSERTATION / DOCTORAL THESIS

Titel der Dissertation / Title of the Doctoral Thesis

"In-depth mass spectrometry-based proteome profiling of inflammation-related processes"

verfasst von / submitted by

Andrea Bileck, MSc

angestrebter akademischer Grad / in partial fulfilment of the requirements for the degree of

Doktorin der Naturwissenschaften (Dr.rer.nat.)
Doctor of Sciences (Dr.rer.nat.)

Wien, 2016 / Vienna 2016

Studienkennzahl lt. Studienblatt / degree programme code as it appears on the student record sheet:	A 796 605 419
Dissertationsgebiet lt. Studienblatt / field of study as it appears on the student record sheet:	Chemie / Chemistry
Betreut von / Supervisor:	Univ. Prof. Dr. Christopher Gerner

This doctoral thesis is based on the following publications and manuscripts:

Comprehensive assessment of proteins regulated by dexamethasone reveals novel effects in primary human peripheral blood mononuclear cells
Andrea Bileck, Dominique Kreutz, Besnik Muqaku, Astrid Slany, Christopher Gerner
Journal of Proteome Research, **2014,** 13, (12), 5989-6000

Impact of a synthetic cannabinoid (CP-47,497-C8) on protein expression in human cells: evidence for induction of inflammation and DNA damage
Andrea Bileck, Franziska Ferk, Halh Al-Serori, Verena J. Koller, Besnik Muqaku, Alexander Haslberger, Volker Auwärter, Christopher Gerner, Siegfried Knasmüller
Archives of Toxicology, **2015,** doi:10.1007/s00204-015-1569-7

Shotgun proteomics of primary human cells enables the analysis of signaling pathways and nuclear translocations related to inflammation
Andrea Bileck, Rupert L. Mayer, Dominique Kreutz, Tamara Weiss, Astrid Slany, Christopher Gerner
Journal of Proteome Research, **2015,** manuscript under revision

Contribution of human fibroblasts and endothelial cells to the hallmarks of inflammation as determined by proteome profiling
Astrid Slany, Andrea Bileck, Dominique Kreutz, Rupert L. Mayer, Besnik Muqaku, Christopher Gerner
Molecular & Cellular Proteomics, **2016,** manuscript in press

Acknowledgements

First and foremost, I want to express my sincere gratitude to my supervisor Univ.-Prof. Dr. **Christopher Gerner**. I especially want to thank him for giving me the great opportunity to perform my doctorate in his group as well as for his guidance, valuable support and for a lot of fruitful and inspiring discussions during this time. His tremendous enthusiasm and immense knowledge really motivated me to give my best and to learn something new every single day.

I would like to give my sincere thanks to Dr. **Astrid Slany** helping and supporting me in every stage of my doctorate. I especially want to thank her for always willing to listen to me, her valuable advice and loyalty.

Furthermore, I would like to thank my colleagues, which have become really good friends, **Rupert Mayer**, MSc, Mag. **Dominique Kreutz** and Mag. **Günter Walder** for their great support, advice and all the fun we had in the last years.

I want to express my sincere gratitude also to Dr. **Samuel Meier**. I especially want to thank him for his tremendous support in the final phase of my doctorate.

In addition, I want to thank all the other members of our working group, **Ammar Tahir**, MSc, **Besnik Muqaku**, MSc, Mag. **Denise Wolrab**, **Peter Frühauf** and Dr. **Johanna Mader** for their support, great discussions and the good working atmosphere.

I would also like to express my gratitude to my former colleagues Dr. **Michael Grössl** and **Editha Bayer** for introducing me in the field of mass spectrometry and sample preparation, as well as to our diploma students, especially **Raphael Ambros** for their help and assistance.

Last but not least, I want to thank my whole family and friends, especially my mother **Herta Bileck**, for their invaluable support, motivation, understanding and patience on every day of my life.

Table of Contents

1. Abbreviations

2D-DIGE, 2-dimensional difference gel electrophoresis; **2D-PAGE**, 2-dimensional polyacrylamide gel electrophoresis; **ACN**, acetonitrile; **AP-1**, transcription factor AP-1; **APCs**, antigen-presenting cells; **BM**, basement membrane; **CID**, collisional-induced fragmentation; **COX**, cyclooxygenase; **CTLs**, cytotoxic T cells; **DAMP**, damage-associated molecular pattern; **DCs**, dendritic cells; **DTT**, dithiothreitol; **ECs**, endothelial cells; **EI**, electron ionization; **ESI**, electrospray ionization; **ETD**, electron transfer dissociation; **FA**, formic acid; **FASP**, filter-aided sample preparation; **FCS**, fetal calf serum; **FDR**, false discovery rate; **GC**, glucocorticoid; **GRE**, glucocorticoid response element; **HCD**, higher energy collisional dissociation; **HIF1α**, hypoxia-inducible factor 1α; **IAA**, iodoacetamide; **ICAM-1**, intracellular adhesion molecule-1; **IL**, interleukin; **IPGs**, immobilized pH gradients; **LC**, liquid chromatography; **LOX**, lipoxygenase; **LPS**, lipopolysaccharide; **MALDI-TOF**, matrix-assisted laser/desorption ionization-time of flight; **MMPs**, matrix metalloproteinases; **MRM**, multiple reaction monitoring; **MS**, mass spectrometry; **MWCO**, molecular weight cut-off; **NF-κB**, nuclear factor- κB; **NK cells**, natural killer cells; **NSAIDs**, non-steroidal antiphlogistic drugs; **PAMP**, pathogen-associated molecular pattern; **PBMCs**, peripheral blood mononuclear cells; **PG**, prostaglandin; **PHA**, phytoheamagglutinin; **PMF**, peptide mass fingerprinting; **PPR**, pathogen recognition receptor; **PSMs**, peptide spectrum matches; **PTMs**, post-translational modifications; **ROS**, reactive oxygen species; **RP**, reversed phase; **SDS**, sodium dodecyl sulfate; **SRM**, single reaction monitoring; **STAT**, signal transducer and activator of transcription; **TCRs**, T cell receptors; **TEM**, transendothelial migration; **TFA**, trifluoroacetic acid; **TNF**, tumor necrosis factor; **Tregs**, regulatory T cells

2. Introduction

2.1. Immune System and Inflammation

Inflammation is the body's response to damaged cells or tissues triggered by a variety of pathogens, noxious stimuli and physical injury. Generally, the immune system is divided into two branches, namely the innate and the adaptive immune response, which provide an immediate as well as long-term immunity against specific pathogens, respectively[1]. While the innate immune system consists mainly of different kinds of phagocytes and the complement system, T- and B-lymphocytes belong to the adaptive immune system. In case of an infection, pathogens as well as cell or tissue damage are initially recognized by tissue-resident innate immune cells, *i.e.* macrophages and mast cells. These are responsible for the initiation of an inflammatory response. The innate immune response is then coordinated by different types of cells, such as neutrophils, monocytes, macrophages, dendritic cells (DCs) or natural killer (NK) cells, by protective plasma proteins and by epithelial barriers that block the entry of microbes[2]. This process is subdivided into the following four phases: (i) pathogen recognition, (ii) recruitment of immune cells to the site of inflammation, (iii) elimination of pathogens and (iv) the resolution of inflammation.

At the site of inflammation, the recognition of pathogens or tissue damage is the task of innate immune cells such as neutrophils or macrophages, which recognize pathogen- or damage-associated molecular patterns (PAMP/DAMP) by their pattern recognition receptors (PPR)[2]. The stimulation of these receptors results in the production of a wide range of inflammatory mediators such as cytokines and chemokines as well as vasoactive amines and eicosanoids leading to chemoattraction of further immune cells to the site of inflammation[3]. The process of leukocyte recruitment into damaged tissues is a very dynamic but tightly regulated process, which requires the extravasation of cells under flow conditions[4]. This cascade of extravasation involves 5 major steps: (1) capture and rolling, (2) firm adhesion and crawling, (3) transendothelial migration (TEM), (4) abluminal crawling and (5) exit from the vessel wall[5]. For the first step of neutrophil extravasation, an alteration and subsequent removal of the endothelial cell's (ECs) glycocalyx is required for neutrophil-EC contact via a specific class of glycoproteins called selectins and their glycoconjugate ligands. Second, firm adhesion of neutrophils on ECs is achieved through binding of adhesion interaction molecules to surface receptors on activated ECs, *e.g.* leukocyte β2 integrin LFA-1 or macrophage antigen-1, to the intercellular adhesion molecule-1 (ICAM-1). Depending on the inflammatory scenario TEM lasts for 5-10min and can occur via two main routes; either leukocytes migrate through EC-EC intercellular junctions (paracellular migration), or they migrate directly through ECs (transcellular migration, Figure 1). After TEM, leukocytes are embedded in a tight matrix of pericytes and the basement membrane (BM), which can be exited through enlarged gaps between pericytes. The mechanism of extravasation of cells other than neutrophils is similar but dependent on other receptor-ligand interactions[5]. A general scheme is shown in Figure 1 including known adhesion interaction molecules.

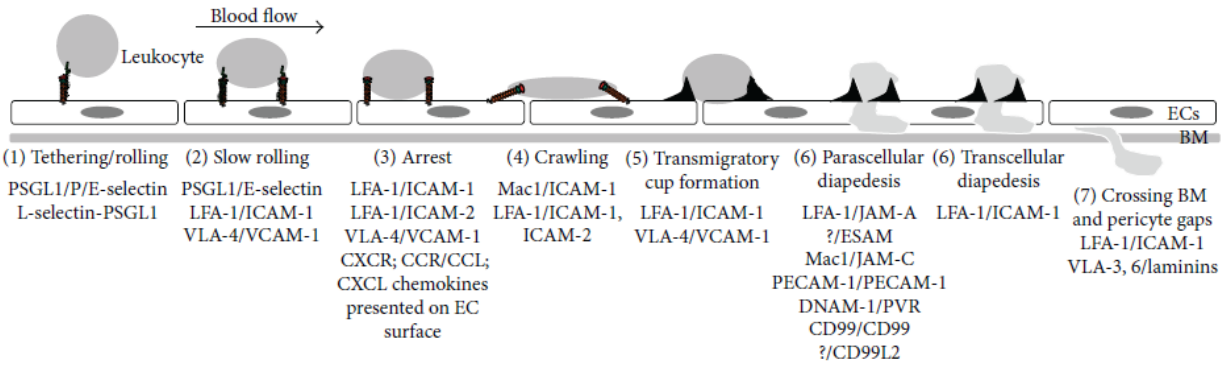

Figure 1: Extravasation cascade of leucocytes (Copyright © 2015 Michael Schnoor et al.)[5]

At the site of inflammation, the cooperative phagocytic activity of neutrophils, monocytes and macrophages leads to the elimination of pathogens[6]. Additionally, neutrophils are able to release lytic enzymes from their granules as well as to produce reactive oxygen species (ROS) with antimicrobial potential[7]. Beside their phagocytic and antimicrobial activity, monocyte-derived macrophages are also involved in wound repair[8]. The plasticity of these cells led to the classification of macrophages into different phenotypes. M1 macrophages display pro-inflammatory activities, whereas M2 macrophages display anti-inflammatory and wound healing phenotypes. A current study suggests that a further type of macrophages exists, *i.e.* M3 macrophages, which are able to reprogram their phenotype from a fully developed M1 macrophage to an M2-macrophage upon specific pro-inflammatory stimuli[9].

The last important step in the process of acute inflammation is the effective resolution of inflammation in order to prevent chronic inflammation. This phase of inflammation includes the reduction of neutrophil infiltration, the down-regulation of pro-inflammatory mediators such as chemokines and cytokines, the induction of apoptosis in remaining neutrophils and the phagocytosis thereof by macrophages as well as the up-regulation of pro-resolving mediators. The latter comprises not only proteins and peptides but also certain lipids such as lipoxins, resolvins and protectins, gaseous mediators as well as neurotransmitter and neuropeptides which are released uder the control of the vegetative nervous system[10].

Furthermore, acute inflammatory responses are not only based on the innate, but also on the adaptive immune response. However, the activation of the adaptive immune response is dependent on innate immune cells. As described above, the recognition of PAMPs by PRRs, which are mainly expressed on antigen-presenting cells (APCs) of the innate immune system such as DCs, leads to the activation of the adaptive immune response, resulting in a long-term and antigen-specific protection[11]. Specific signaling PPRs on APCs, such as Toll-like receptors, RIG-I-like receptors and NOD-like receptors exert a direct effect on lymphocytes[1]. DCs display the capability to present foreign peptides not only via MHC class I, which only accounts for all nucleated cells, but also via MHC class II resulting in the activation of naïve CD4 and CD8 T cells. The development of these cells starts in the thymus where a

stringent positive and negative selection takes place. After this process, naïve CD4 and CD8 T cells expressing a comprehensive collection of T cell receptors (TCRs) are released from the thymus into the peripheral blood system.

Three independent signals are required for an accurate activation of the adaptive immune response in order to reach the full potential of effector and memory CD4 and CD8 T cells: (i) direct signals through the TCRs, (ii) signals from co-stimulatory molecules such as CD80/CD86 and (iii) cytokine signals[12]. After T-cells are primed to a specific antigen, a clonal expansion takes place before cells gain their effector functions. While CD8 T cells consist of one main subset which displays cytotoxic activity, i.e. cytotoxic T cells (CTLs), CD4 T cells are not only responsible for helping B cells to produce antibodies, but they also orchestrate macrophage and CD8 T cell functions. Therefore they can be distinguished in two main subsets: T helper cells (mainly Th1, Th2 and Th17 cells) and regulatory T cells (Tregs). Furthermore, two main functional subsets of T helper cells are subdivided according to their immunological functions including defined expression patterns of transcription factors, cytokines and homing receptors. While the differentiation of naïve CD4 cells to Th1 cells is dependent on interleukin (IL) 12, the polarization to Th2 cells is based on the presence of IL4. In comparison to Th1 cells, which are responsible for the activation of phagocytes and for the opsonizing antibodies, Th2 cells provide protection against helminths and other allergens[13]. Tregs are characterized based on their surface molecules CD4 and CD25 as well as the specific expression of the forkhead family transcription factor FoxP3. They are responsible for the maintenance of immune homeostasis and immunological self-tolerance[14].

The second branch of the adaptive immune response consists of B-cells, which become mature upon antigen binding by APCs. They are then activated in an autocrine fashion or with the support of CD4 T cells. After selection and clonal expansion, B cells differentiate into antibody-secreting plasma cells and in a second step into memory cells[15]. In general, plasma cell based antibody secretion is of great importance to protect the immune system against acutely cytopathic viruses as well as to ensure long-term defense. The success of this humoral memory is based on at least two layers of defense. In a first step, pre-existing antibodies which are secreted by long-lived plasma cells provide defense against reinfection. If this consecutive humoral memory is not enough, a reactive humoral memory can be induced, which is based on a rapid reactivation of pathogen-experienced memory B cells in order to produce antibodies. This reactivation process leads typically to a faster and more intense immune response compared to the primary antibody response[16].

2.2. Chronic Inflammation and Cancer

As mentioned above, the resolution of inflammation is an important step in the acute immune response. An incompletely resolved inflammatory response may lead to a dysregulated or persistent inflammation which has a major impact on the pathogenesis of many diseases, especially chronic diseases such as rheumatoid arthritis, psoriasis and inflammatory bowel disease[10]. Nowadays, up to 25% of malignancies are associated with chronic inflammation[17]. Many research fields focus on investigating the pathophysiological mechanisms underlying chronic inflammation such as the transition from acute to chronic inflammation or the interplay of key molecules which could serve as therapeutic targets. The interaction between immune and stromal cells is tightly regulated during the resolution of inflammation and is dependent on a sequential expression of chemokines, cytokines and adhesion molecules. If this expression of proteins and receptors is disarranged, leukocytes are persistently restrained and are able to survive in the stromal cell microenvironment[18]. In general, chronic inflammation displays many features of acute inflammation and is based on the following possible mechanisms: (i) activation of a positive feedback loop and hence a long-lasting immune response caused by repetitive stimuli, (ii) maintenance of inflammation facilitated by changing active cell populations in the affected tissue or (iii) tissue remodeling[19].

Furthermore, chronic inflammation seems to be a driving force for cell transformation during cancer initiation. In addition, inflammatory conditions at the site of tumor cells may promote tumor progression as well as metastasis[20]. Many triggers which are related to chronic inflammation-based tumor development are already known, e.g. microbial infections, autoimmune diseases or other inflammatory conditions of unknown origin. The association of chronic inflammation and cancer development was clearly demonstrated for gastrointestinal carcinogenesis based on a chronic *Helicobacter pylori* infection. Furthermore, inflammatory bowel disease, an autoimmune disorder, was correlated with colon cancer and prostatitis with the development of prostate cancer[21]. Mantovani et.al further defined hallmarks of cancer-related inflammation including the presence of inflammatory cells and mediators within tumor tissues as well as tissue remodeling and angiogenesis which is similar to that present in chronic inflammatory conditions or tissue repair[21].

The molecular link between inflammation and cancer development is based on the following two pathways: (i) an extrinsic pathway based on inflammatory conditions which increase the risk of cancer development and (ii) an intrinsic pathway based on genetic alterations resulting in inflammation and neoplasia (Figure 2).

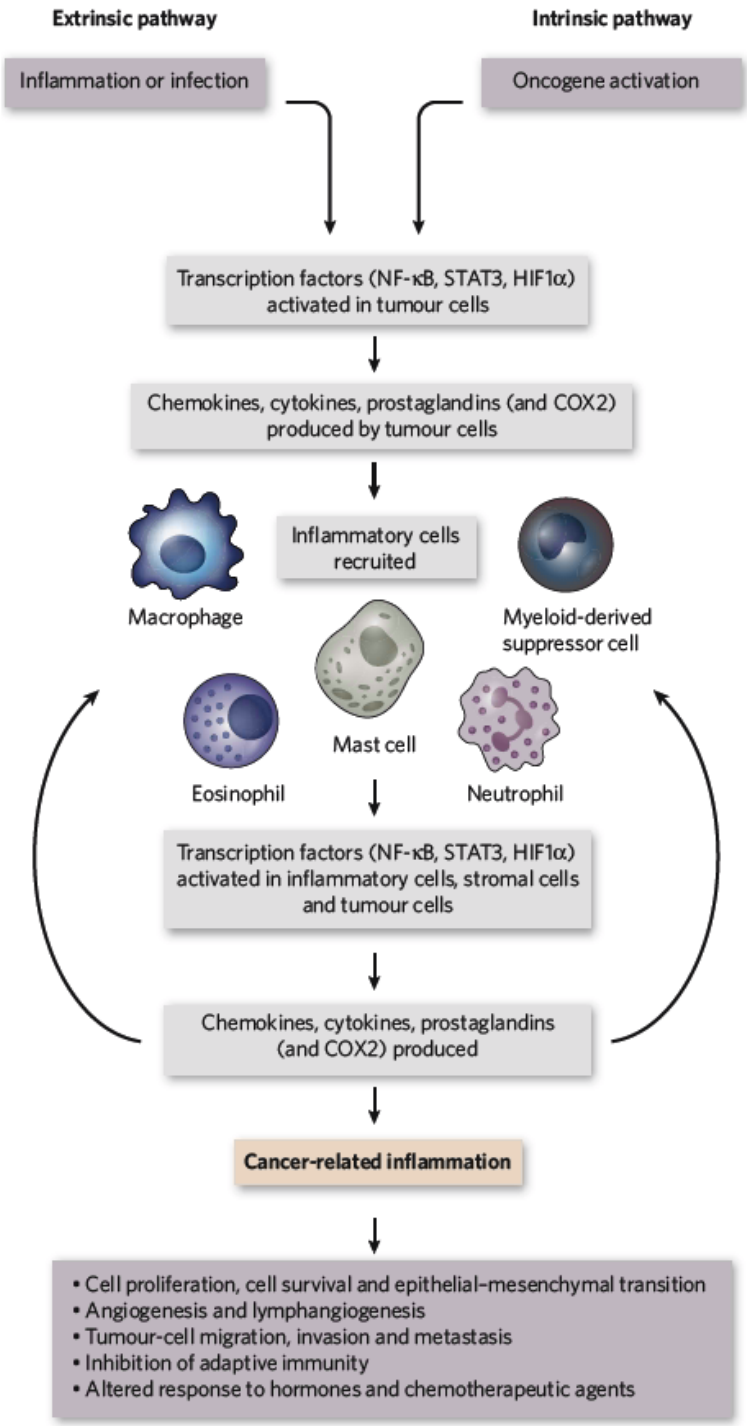

Figure 2: Molecular pathways connecting inflammation and cancer. (Reprinted by permission from Macmillan Publishers Ltd: NATURE, copyright © 2008, Mantovani et al.) [21]

Both pathways, the extrinsic and the intrinsic, result in the activation of transcription factors such as nuclear factor-κB (NF- κB), signal transducer and activator of transcription 3 (STAT3) or hypoxia-inducible factor 1α (HIF1α). The activation of these transcription factors leads to the production of inflammatory mediators such as cytokines and chemokines as well as of cyclooxygenase 2 (COX2) and prostaglandins, together resulting in the recruitment and activation of leukocytes. Since the

activation of these key transcription factors is not limited to leukocytes, stromal cells as well as tumor cells may be activated, generating a cancer-related inflammatory microenvironment.

Additionally to the pathways described above, the development of cancer is based on a progressive transformation of cells caused by the accumulation of genetic and epigenetic alterations. Such mutations are often observed in non-cancerous tissues under chronic inflammatory conditions prior to cancer development. For example, the inactivation of tumor suppressor p53, one of the most frequent genetic targets in human cancers, is present in inflammatory bowel disease, Barret's esophagus or HCV-associated chronic hepatitis[22]. However, inflammation is not only associated with point mutations in various tumor suppressor genes but also with epigenetic alterations such as DNA methylation or histone modifications[23]. DNA methylation of CpG islands within promotor regions of tumor suppressor genes may result in their permanent inactivation, contributing to cancer development. This aberrant DNA methylation of tumor suppressor genes cannot only be determined in tumor tissue but also for example in non-cancerous colonic mucosae of patients with inflammatory bowel disease. Furthermore, animal model systems demonstrated that *Helicobacter pylori*-induced inflammation is able to induce aberrant DNA methylation[22]. The potential of cancer-related inflammation to induce genetic instability resulting in the accumulation of random genetic alteration in tumor cells leads to the inclusion of inflammation as a hallmark of cancer[24]; now consisting of (i) sustaining proliferative signaling, (ii) evading growth suppressors, (iii) resisting cell death, (iv) enabling replicative immortality, (v) inducing angiogenesis, (vi) activating invasion and metastasis, (vii) deregulating cellular energetics, (viii) avoiding immune destruction, (ix) genome instability and mutation, and (x) tumor-promoting inflammation[25,26].

Beside the pro-tumorigenic activity of inflammation, evidence exists that in certain types of tumors, the presence of inflammatory cells is associated with better prognosis. This accounts, for example, for tumor-associated macrophages in certain breast and pancreatic tumors or for eosinophils in colon cancer. Especially macrophages display pro- and anti-tumorigenic properties which apparently depend on NF-κB expression. The importance of the balance between pro- and anti-tumorigenic macrophages seems to be evident in psoriasis, an inflammatory skin disease. Here, an overexpression of NF-κB inhibits invasive epidermal neoplasia, whereas in other types of tumors such as liver and colon cancer, the blockage of NF-κB activity inhibits tumor development[21]. In addition, interactions between immune and tumor cells display high functional plasticity, which determines whether inflammation supports pro- or anti-tumorigenic responses[27].

2.3. Therapeutic Modulation of Inflammation

Although inflammation is an important physiological process necessary for the elimination of a magnitude of pathogens, a prolonged inflammatory response might result in pathogenesis and progression of certain inflammation-associated diseases. Therapeutic strategies exist which usually aim at decreasing or neutralizing pro-inflammatory mediators or at inhibiting leukocyte recruitment and activation. The following therapeutic classes exist: (i) non-steroidal antiphlogistic drugs (NSAID), (ii) glucocorticoid (GC) receptor agonists and (iii) inhibitors or antibodies which target specific pro-inflammatory cytokines such as TNFα or IL-1[28].

The most commonly known representatives of NSAIDs are aspirin, naproxen and ibuprofen, which are inhibiting COX-1 and COX-2 activity and are therefore leading to the inhibition of prostaglandin (PG) synthesis. COX as well as lipoxygenase (LOX) are essential enzymes catalyzing the oxidation of arachidonic acid, which is released from membrane phospholipids by phospholipase A_2 or phospholipase C. PGs are the main mediators of inflammatory symptoms such as fever and pain. By blocking COX activity, NSAIDs decrease the inflammatory response by reducing pain and vasodilation, which is mainly caused by PGE2 and prostacyclin (PGI2). Generally, two main classes of NSAIDs can be distinguished: non-selective NSAIDs such as ibuprofen, paracetamol or aspirin and COX-2 selective NSAIDs such as etodoloac, diclofenac or valdecoxib[29,30]. Although NSAIDs belong to the most frequently applied anti-inflammatory drugs worldwide, chronic use of this class of therapeutics cause asymptomatic enteropathy in many individuals. This side effect is characterized by an increased intestinal permeability and mucosal inflammation. Furthermore, non-acetylated NSAIDs can cause focal lesions in the small intestine as well as ulcerations which are associated with acute or chronic bleeding[31].

In contrast to NSAIDs, which are acting through the blockage of COX, the mode of action of glucocorticoids depends on their effect on signaling pathways including NF-κB and transcription factor AP1 (AP-1) as well as their capacity to induce the production of anti-inflammatory molecules[28]. Furthermore, glucocorticoids lead to the reduction of circulating monocytes resulting in a decreased synthesis of pro-inflammatory cytokines and prostaglandins[32]. The most commonly known glucocorticoids are 17-hydroxy-11-dehydro-corticosterone (cortisone) and the synthetic agents' prednisolone and dexamethasone. The anti-inflammatory effects of glucocorticoids are mediated by the glucocorticoid receptor, which is released from a protein complex upon activation. The released receptor then translocates into the nucleus and regulates gene expression by binding glucocorticoid response elements (GRE) of target genes[33]. This leads to the activation of either the transcription of anti-inflammatory molecules, such as IL-10 or Annexin 1, or of regulatory proteins which are involved in metabolic processes such as enzymes of the gluconeogenesis. This process of transcription activation is called transactivation. Furthermore, a second mechanism exists concerning the mode of action of glucocorticoids, namely the transrepression, which blocks the expression of pro-

inflammatory molecules[32]. Although glucocorticoids are potent anti-inflammatory drugs, long-term use of these drugs may result in glucocorticoid resistance as unwanted side effect. This may limit the therapeutic response and outcome of patients with chronic inflammatory diseases. A potential reason for the development of glucocorticoid resistances are alterations in the cellular microenvironment caused by chronic inflammation such as oxidative stress and hypoxia[34,35].

Therapeutic antibodies are used for the treatment of inflammatory and autoimmune diseases, as well as in cancer therapies. They target single, well-defined effector molecules such as tumor necrosis factor α (TNFα) or IL-6, which are important in the therapy of rheumatoid arthritis and Crohn's disease, respectively[36]. In general, these monoclonal antibody-based drugs target a variety of cytokines, chemokines, adhesion molecules as well as certain cell types[37]. Especially cytokines are important molecules which regulate tissue homeostasis and immune cell function like activation, proliferation and differentiation. Since these molecules are involved in the pathogenesis and spreading of many diseases like allergy, autoimmune disorders or infections, blockage of the cytokine response via antibodies against their receptors or themselves lead to the termination of cytokine reaction[38]. For example, IL-6 is recognized as key molecule for linking chronic inflammation and cancer, thus IL-6 and downstream signaling molecules became targets for drug development. Tocilizumab was the first anti-IL-6 antibody which prevents the IL-6 mediated signaling by blocking the binding of IL-6 to the transmembrane as well as to soluble IL-6 receptors[39].

Other important classes of therapeutic targets regarding inflammation are lipases, especially those upstream of the production of eicosanoids including prostaglandins, leukotrienes and thromboxane. The cardinal symptoms of an inflammatory response, namely pain, heat development, swelling, redness and loss of function are mediated by these lipids, which are derived from arachidonic acid. Prostaglandins are end products of the arachidonic acid metabolism which is catalyzed by COX and prostaglandin synthase. Therefore, the inhibition of COX, as mentioned above, leads to an interruption of their synthesis. Alternatively, the upstream located phospholipase A_2 is also a potential therapeutic target for the inhibition of prostaglandin synthesis. A few phospholipase A_2 inhibitors are already developed which exert *in vivo* efficacy in inflammatory animal models[40].

2.4. Mass Spectrometry-based Proteomics

Bioanalysis, part of the analytical chemistry, involves the quantitative assessment of biomolecules, such as DNA, proteins, metabolites and lipids, in complex biological matrices such as blood, cells or tissues. Studies on the whole entity of a subset of these molecules has the suffix "-omics", for example the analysis of all proteins within a biological system, the proteome, is called proteomics. For each of these "-omics" approaches, bioanalytical techniques are of great relevance. Concerning the analysis of proteins, mass spectrometry (MS)-based technologies, especially LC-MS/MS analysis, has become most important in the last decade. With current state-of-the-art analytical instruments it is possible to analyze thousands of proteins within one measurement.

2.4.1. General Overview of Mass Spectrometry-based Proteomics

Proteomics was introduced almost 20 years ago, pursuing the target of comprehensive analysis of protein expression under varying biological conditions such as disease or drug treatment[41]. Although the technologies in the field of proteomics have been tremendously improved, the main goal is still the same: the qualitative and/or quantitative analysis of proteins as well as their isoforms, post-translational modifications (PTMs) and potential interaction partners in different functional cell states. In principle, the following main analysis strategies are used for protein analysis; (i) antibody-based methods such as Western blot, ELISA or even CHIP-arrays, (ii) 2-dimensional polyacrylamide gel electrophoresis (2D-PAGE) or LC-based MS methods and (iii) combination of both such as phosphopeptide enrichment using antibody-based techniques prior to LC-MS/MS analysis or affinity purification for the characterization of protein-protein interaction partners. However, regarding common analytical characteristics such as sensitivity and specificity, antibody-based strategies are dependent on the quality of the used antibody; LC-MS/MS based strategies however, are less dependent on external factors. Furthermore, the main difference between these two strategies is the possibility of an untargeted screening analysis which is only feasible using LC-MS/MS analysis. When applying antibody-based techniques for the analysis of proteins, it is necessary to exactly know the target molecules. In contrast, LC-MS/MS analysis allows both, a screening and a targeted analysis of proteins only depending on the instrumentation. In general, two different approaches in MS-based proteomics can be distinguished: Gel-based proteomics which mainly includes protein separation via 2D-PAGE prior to MS analysis. In contrast, gel-free proteomics is based on protein separation using liquid chromatography prior to MS analysis.

2.4.2. Gel-based Proteomics

Since proteomics was first introduced, especially mass spectrometric-based protein analysis underwent multiple technological improvements. In earlier days, the method of choice was a combination of 2D-PAGE and MS/MS analysis[42]. This approach allows protein separation usually under denaturing conditions prior to MS analysis. Proteins are separated based on two independent characteristics, namely charge and molecular weight. The first dimension encompasses an isoelectric focusing allowing a separation of proteins according to their isoelectric point. This can be achieved either using carrier ampholytes-based pH gradients or immobilized pH gradients (IPGs). With the establishment of IPGs, difficulties, which were present using carrier ampholytes such as poor reproducibility due to unstable ampholytes causing cathodic drifts, could be overcome[43]. In contrast to the first dimension, the second dimension allows an orthogonal separation according to the molecular weight of proteins. This strategy reveals distinct protein spots within the gel, which can be stained with MS-compatible methodologies, for example using silver or Coomassie Blue[44]. Protein spots can be easily cut out from the gel and enzymatically digested for subsequent MS analysis. The whole procedure of 2D-PAGE-based protein separation, enzymatic digestion and MS analysis, mainly using matrix-assisted laser/desorption ionization – Time of Flight (MALDI-TOF) mass spectrometry, is called peptide mass fingerprinting (PMF). PMF is an effective tool for protein identification, as long as proteins are pure and not in complex mixtures. The possible combination of PMF with tandem mass spectrometry (MS/MS) usually results in high sequence coverage[45,46].

An alternative strategy to 2D-PAGE-based protein analysis is the development of 2D difference gel electrophoresis (2D DIGE), which allows a multiplexed analysis of proteins in a quantitative fashion. Protein samples have to be labeled with charge and size-matched fluorescent dyes, namely CyDye DIGE flours, prior to 2D-PAGE. The labeled samples are then pooled and separated on the same 2D-gel enabling a comparative and quantitative protein expression analysis. The identification of differentially expressed proteins can be carried out applying PMF or MS/MS analysis[47,48]. Another protein identification methodology in gel-based proteomics are antibody-based strategies, which do not require subsequent MS-analysis. Especially after 1D-SDS-PAGE, whereby protein samples were separated only due to their molecular weight, antibody-based protein identification has become a conventional strategy in protein analysis. In this targeted approach, namely Western blot analysis, separated proteins have to be transferred from the 1D-gel to a membrane such as nitrocellulose or PVDF membranes via electroblotting. Afterwards, proteins can be incubated with a primary antibody detecting the protein of interest. A secondary antibody, usually labeled with an enzyme such as horseradish peroxidase, is used to visualize the respective protein. By comparing the intensities of a distinct protein in different samples, a relative quantification can be performed by means of Western blot analysis[49].

2.4.3. Gel-free Proteomics

In contrast to gel-based proteomic approaches, gel-free strategies are based on an in-solution digestion of proteins instead of in-gel digestion as well as protein separation via liquid chromatography (LC) prior to MS/MS analysis instead of 2D-PAGE. Therefore, methods such as filter-aided sample preparation (FASP) were introduced, which enable digestion of proteins directly on top of molecular weight cut-off (MWCO) filters. While in-solution digestion procedures are more susceptible to impurities due to the missing purification which is obtained by an SDS-PAGE, these methodologies allow a higher peptide recovery and the possibility for automation[50].

Initially, LC-MS/MS was introduced as a substitute for MALDI-TOF analyses of protein spots. In particular, the analysis of complex peptide mixtures benefits from the separation via LC with respect to accurate protein identifications, when compared to PMF[51]. The detection of low abundant peptides in complex samples such as cell lysates is a key challenge in LC-MS/MS-based proteomics[52]. Therefore, very low flow as well as narrow-bore LC is coupled directly via electrospray ionization (ESI) to the mass spectrometer[53]. This can be achieved using nano-LC with flow rates of around 300nL/min. Large-scale proteomics experiments then most commonly employ reversed phase (RP) LC, especially under gradient conditions. Increasing the amount of organic modifier such as acetonitrile (ACN) or methanol enables a separation based on hydrophobicity[54]. Furthermore, trifluoroacetic acid (TFA) or formic acid (FA) are used as essential additives because of their ion-pairing properties. Again, the LC instrument can be directly coupled to the mass spectrometer using an ESI source. The two most frequently used ionization sources in proteomics are discussed below.

2.4.4. Ionization Sources in Mass Spectrometry-based Proteomics

In general, two different ionization strategies can be distinguished, i.e. soft and hard ionization. Both, MALDI as well as ESI are soft ionization techniques imparting little residual energy and therefore resulting in basically no fragmentation of molecules compared to hard ionization techniques such as electron ionization (EI). Therefore, in the field of proteomics soft ionization techniques are preferred. For example, MALDI is based on the rapid photo-volatilization of a peptide sample, which is embedded in a UV-absorbing matrix. Different chemical and physical pathways are discussed concerning the generation of ions during the MALDI process, for example gas-phase photoionization, ion-molecule reactions, excited-state proton transfer or desorption of preformed ions[55]. Proteomics analysis by MS relies on the identification of intact peptides or proteins. The need for LC-MS hyphenation then requires an ESI source. The mechanism of ESI involves three major processes: First, charged droplets have to be produced from the high-voltage capillary tip. Second, continuous solvent evaporation and droplet shrinking has to take place, resulting in very small charged droplets, wherefrom charged solvent-free analytes are obtained. Two different potential mechanisms are proposed that explain the formation of pas-phase ions[56], but the exact mechanism is still disputed: (i)

the ion evaporation model[57] and (ii) the charge residue model[58]. According to the ion evaporation model, generated droplets shrink by evaporation until the electric field strength at the surface of a droplet is so high that solvated ions can be expelled due to Coulombic repulsion. This results in individual solvated ions leaving a charged droplet. In contrast, the charge residue model describes the shrinking of droplets solely by evaporation. In this continuous process droplets are generated, which contain only one molecule. Based on solvent evaporation and declustering, the molecule within a droplet can be released as an ion[59].

Although ESI sources allow facile ionization of solvents, it can be susceptible to potential interference from complex biological sample matrices, which may result in ion suppression leading to difficulties concerning reproducibility and accuracy. Sources for ion suppression are either endogenous or exogenous components. Endogenous ion suppressors are ionic species such as salts or inorganic electrolytes and various other organic molecules displaying a similar chemical structure as the target analyte. In case of proteomics, highly concentrated peptides, which are co-eluting with the peptide of interest, are potential candidates for ion suppression. In contrast to these endogenous components, exogenous ion suppressors are accidentally introduced during sample preparation, including for example plastic components (phthalates), polymers (PEGs) or detergent residues (SDS) as well as ion-pairing reagents[60]. For example, the ion-pairing reagent TFA, preferentially used as additive in LC-UV analyses due to its capability of improving peak shape, causes ion suppression throughout the entire measurement if it is present in the mobile phase. Therefore, weaker acids like formic acid are mainly used for ion-pairing in LC-MS-based analysis[61].

2.4.5. Mass Analyzers Commonly Used in the Field of Proteomics

In principle, the identification of peptides using MS is based on the determination of distinct ions and their fragmentation in order to gain information of the amino acid sequence by measuring mass-to-charge ratios. Historically, MALDI-time of flight (TOF)-MS was one of the first analysis strategies for peptide identification in the field of proteomics. In case of TOF analyzers, after desorption and ionization, molecules are accelerated in an electric field before they were ejected in a metal flight tube. The detection of the ions takes place through their collision with a detector at the end of the flight tube. TOF analysis can be repeated at a frequency of up to 50 Hertz[62].

The development of a high-resolution orbitrap mass analyzer by Alexander Makarov[63,64] was a great improvement in the field of shotgun proteomics, a bottom up screening approach. The orbitrap provides high mass accuracy due to the axial motion of ions along the central spindle. This motion of ions is only dependent on the m/z of an ion but not on initial sample conditions[65]. The combination of the high resolution orbitrap and a quadrupole which serves as mass filter was first realized in the QExactive orbitrap, a high performance instrument in shotgun proteomics. In a QExactive, ions are generated in an ion source at the front of the instrument, which are then guided through a transfer tube

into the S-lens and a bent flatapole. In the bent flatapole, collisional cooling of the ions takes place before they are transmitted into a hyperbolic quadrupole. The quadrupole is capable of isolating ions with an isolation width of 0.4 Th at m/z 400. After the quadrupole, ions are guided through an exit lens and a short octapole before they enter the C-trap. In case of MS1 Scans, which are used as survey scans of precursor ions present at a distinct time point, ions are directly ejected from the C-trap into the orbitrap analyzer. However, when performing an MS2 scan, which detects specific fragments of a distinct precursor m/z selected from the previous MS1 scan, ions are transferred into a fragmentation cell (see 2.1.5), which is separated from the C-trap by a diaphragm. All ion fragments are then transferred back into the C-trap before they are ejected into the orbitrap analyzer[66]. A schematic overview of a QExactive is shown in Figure 3.

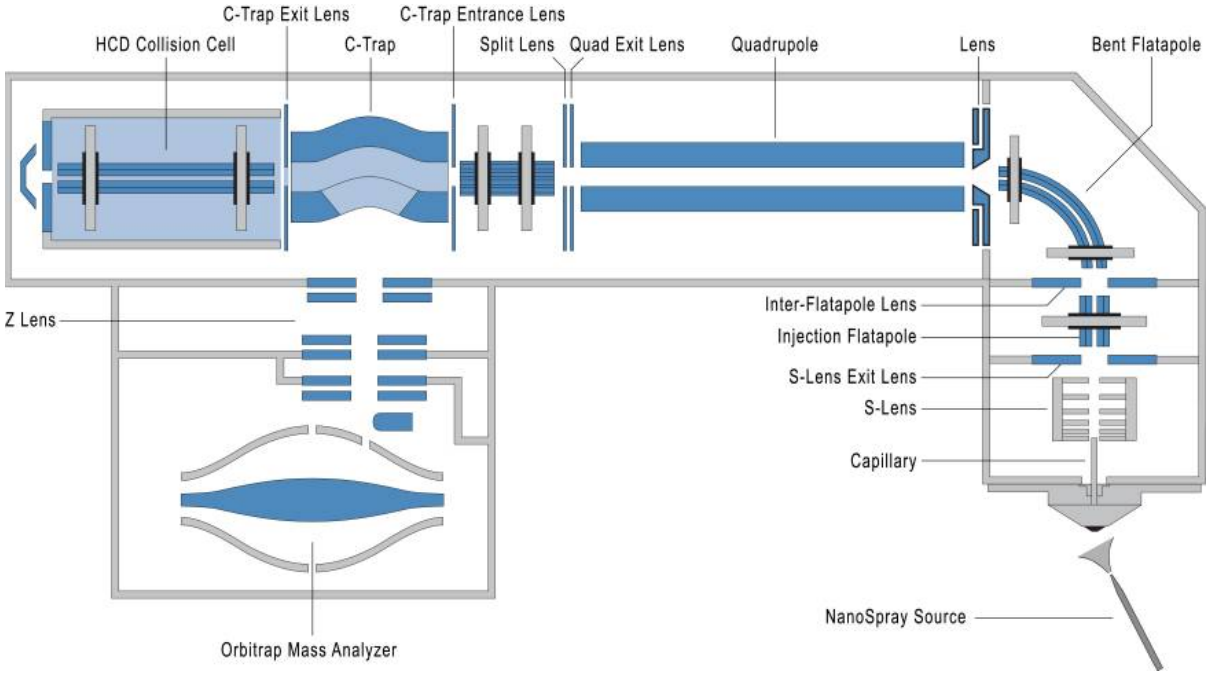

Figure 3: Schematic overview of a QExactive (Copyright © 2011 Michalski et al.)[66]

In contrast to the orbitrap mass analyzer, which is usually applied in screening methodologies aiming at identifying a high number of proteins, triple quadrupoles are used as tools for the targeted and quantitative analysis of selected proteins in a data-dependent fashion as demonstrated in Figure 4. In principle, a precursor ion of interest is isolated in the first quadrupole (Q1) and fragmented in the second quadrupole (Q2) using collisional-induced dissociation. The third quadrupole (Q3) acts as a mass filter for the fragmented ions. Only a few desired fragments displaying the best transitions are then transmitted to the detector and analyzed[67]. This process refers to multiple reaction monitoring (MRM) or single reaction monitoring (SRM).

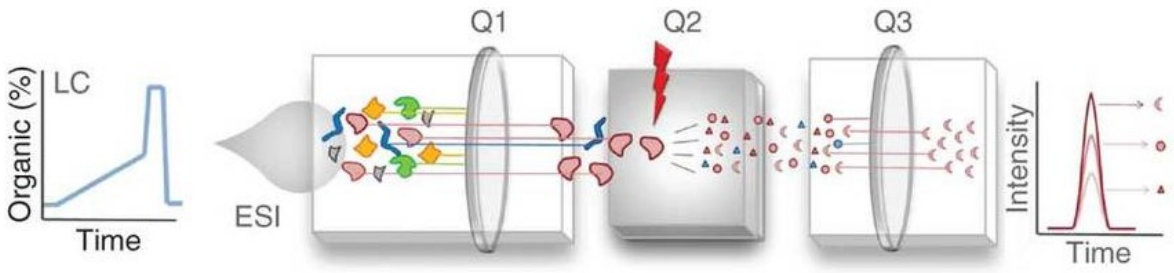

Figure 4: Principle of multiple reaction monitoring. (Reprinted by permission from Macmillan Publishers Ltd: NATURE METHODS, copyright © 2012, Picotti et al.)[68]

2.4.6. Ion Activation Methods in Mass Spectrometry-based Proteomics

As described above, the identification of proteins or peptides in MS-based proteomics is not only based on exact mass-to-charge (m/z) ratios (MS1 scans) but also on amino acid sequence information, which can be obtained using controlled fragmentation of peptides (MS2 scans). The most common ion activation techniques are collision-induced dissociation (CID), higher energy collisional dissociation (HCD) and electron transfer dissociation (ETD). Fragmentations based on collisional dissociation are the most commonly used ion activation methods in MS-based bottom-up proteomics. They rely on energetic collisions between peptides and a neutral gas such as nitrogen, helium or argon in the ion trap[69]. This predominantly generates b- and y-type ions resulting from the dissociation of the amide bond (-C(O)–N-)[70,71]. However, CID tends to bias experiments towards medium-length peptides, which are doubly or triply charged and suffers from a low-molecular weight cut-off[72]. The introduction of HCD in the orbitrap technology allows a more efficient terminal fragmentation and evades the low molecular weight cut-off. This ion activation method, originally named higher-energy C-trap dissociation, takes place in an external collision cell (HCD cell). Therefore, ions have to pass through the C-trap before they are fragmented in the HCD cell. The resulting fragment ions are analyzed in the orbitrap upon passing the C-trap a second time[73]. In contrast to the activation mechanisms of CID and HCD, in which ions are fragmented using neutral gases, the underlying mechanism of ETD is based on radical chemistry. Therefore, fluoranthene is most commonly used as a radical anion, which transfers an electron to multiply protonated peptides. During subsequent electron-induced fragmentation, c- and z-type product ions are generated resulting from the rupture of N-Cα bonds within a peptide.

The applied ion activation technique tremendously contributes to the success rate of identifications, especially when it comes to the identification of post-translational modifications (PTMs). For example, CID-labile PTMs can be identified using ETD, which provides not only information about the sequence but also about the localization of the modified site. Regarding protein phosphorylation, CID is often associated with a neutral loss of phosphoric acid, whereas ETD causes effective

fragmentation without corrupting the modification. In addition, HCD displays great potential for phosphoproteomics due to rich fragment ion spectra and fast scan rates compared to ETD. Generally, stable modifications, for example acetylation and methylation, can be easily analyzed using CID or HCD, whereas for the identification of other modifications such as phosphorylation, glycosylation and ubiquitination, other fragmentation techniques or combination of different ion activation strategies need to be combined[74]. Although ETD is especially interesting for analyzing PTMs, it may suffer from slightly longer activation times.

2.5. General Overview of Applied Methods in this Doctoral Thesis

For the comprehensive investigation of proteome alterations caused by certain stimuli, peripheral blood mononuclear cells (PBMCs) were isolated from whole blood, inflammatory stimulated *in vitro* and drug treated. Due to the highly complex mixture of proteins within cells, fractionation and/or separation were fundamental principles of the applied methodologies of this thesis. To reduce the protein complexity, several fractionation steps were included in the workflow, *e.g. subcellular fractionation in* secreted, cytoplasmic and nuclear protein fractions. Additionally, this fractionation step was essential to get a deeper insight into the cellular proteome and for the determination of nuclear translocations of proteins. Then, these fractions were further separated according to their molecular weight using sodium dodecyl sulfate-polyacrylamide gel electrophoresis (SDS-PAGE) giving four sub-fractions, each, which were separated according to their hydrophobicity using a nanoLC system.

2.5.1. Isolation and Treatment of PBMCs

PBMCs were isolated from whole blood of healthy donors with written consent and ethical approval. The blood was collected in CPDA tubes using Ficoll Paque, a sucrose solution and applying density centrifugation. Cells were isolated from an interphase layer above the erythrocytes, washed and cultivated in autologous plasma to keep the cells under physiological conditions. Furthermore, PBMCs were treated with different stimuli according to the respective study, such as lipopolysaccharide (LPS) and phytoheamagglutinin (PHA) in case of inflammatory stimulation. After 1h inflammatory activation, a time point when inflammatory signaling is already fully developed, cells were further treated with dexamethasone to investigate the cellular response to an antiphlogistic drug as well as to determine unwanted side effects of this drug. This time point of drug treatment was chosen to better represent *in vivo* situation, where typically first an inflammation is detected before a therapeutic intervention is performed. In the other study, PBMCs were treated with CP47,497-C8, a synthetic cannabinoid. This drug was investigated to determine alterations of the proteome in response to drug treatment especially focusing on inflammation-related processes.

2.5.2. Subcellular Fractionation

After *in vitro* cell experiments, cells were fractionated into secreted, cytoplasmic and nuclear proteins. This was an essential step in this thesis due to the following reasons: (i) a reduced protein complexity compared to the analysis of whole cell lysates enabling a deeper proteome profiling and (ii) the possibility to monitor intracellular protein translocations upon specific stimuli. To obtain secreted proteins, the cultivation of the cells in plasma-free cell culture medium was a necessity. In the context of inflammation, the main focus in terms of secreted proteins was laid especially on cytokines, chemokines and growth factors. To ensure an accurate and sensitive analysis of these low-abundant proteins, the removal of contaminating high-abundant proteins was an important step. Therefore, PBMCs were washed after 4 hours of cultivation and treatment in autologous plasma, and were then cultivated in serum-free cell culture medium for 3 hours prior to the subcellular fractionation. Concerning the harvesting of secreted proteins, the medium was collected and proteins were precipitated over night with ethanol.

After collecting the secreted proteins, cells were lysed using both, fractionation buffer containing Triton-X100 as detergent, which allows the permeabilization of the outer cell membrane[75] as well as mechanical shear stress. Using centrifugation, cytoplasmic proteins were then separated from the nuclei. The intact cell nuclei were disrupted using a high-salt solution. A further centrifugation is required to separate the soluble nuclear proteins from nuclear matrix proteins and DNA fragments[76]. Cytoplasmic as well as nuclear protein fractions were then precipitated over night with ethanol.

2.5.3. Sample Preparation for Mass Spectrometric Analysis

The precipitated proteins were solubilized by denaturing in sample buffer, which contains dithiothreitol (DTT), urea, thiourea, CHAPS and SDS, and protein concentrations were determined by the a Bradford photometric assay. Cytoplasmic and nuclear proteins were additionally separated according to their molecular weight by SDS-PAGE. Samples were only run for one cm and after silver staining cut into four slices, which were further processed separately. Concerning the digestion of proteins, secreted proteins were directly digested in-solution on top of 3kDa molecular weight filters, whereas cytoplasmic and nuclear proteins were digested in-gel. However, the principle behind these two digestion strategies is the same. After a washing step with ammonium bicarbonate buffer, DTT is applied to disrupt quantitatively covalent disulfide bonds between cysteine groups. To prevent their reformation by oxidation, cysteins were carbamidomethylated using iodoacetamide (IAA). Then, proteins were enzymatically digested at 37°C using a mixture of trypsin and lys-C. Trypsin is a serine protease displaying a pH optimum at 7.0-8.0 and cleaves peptide chains specifically at the C-terminal side of the amino acids lysine and arginine. However, it is evident that trypsin displays proteolytic deficiency at lysine sites. In contrast, lys-C shows exceptional efficiency and specificity concerning the cleavage of lysines[77]. Thus, the mixture of both enzymes allows an efficient proteolytic digestion

of the protein samples. After overnight digestion, peptides were eluted, dried and stored at -20°C until LC-MS/MS analysis.

2.5.4. LC-MS/MS Analysis

In this thesis, the general strategy of LC-MS/MS analysis was based on a combination of two different instrument types. For in-depth proteome screening analysis, a QExactive orbitrap was used providing a deep insight into cellular responses to a given stimulus. Furthermore, relative quantification of all proteins between different cell states was achieved by this approach using MS1-based label-free quantification. Proteins of interest or significantly regulated proteins, which were determined by this shotgun approach, were selected and further analyzed using a triple quadrupole mass spectrometer. The application of a targeted MRM approach then allowed an MS2-based quantification of a subset of proteins.

For shotgun proteomics, a nanoLC system was used and multi-step gradients were applied with a run time of 235min for the analysis of cytoplasmic and nuclear protein fractions and 95min for the analysis of secreted proteins. In general, each gradient includes a washing phase using high amounts of organic solvents, i.e. acetonitrile and a sufficiently long equilibration phase. In contrast to these relatively long gradients, MRM analyses can be performed using shorter gradients. For example, in case of the analysis of secreted proteins, chromatographic separation for MRM analysis can be performed in 20min. The quality of each LC-MS/MS run was verified using four synthetic internal standard peptides, which were spiked in each sample after protein digestion. These standard peptides give information about the quality of the chromatography and of the mass spectrometer performance. Thus, potential retention time shifts or other separation problems as well as ion intensity problems can be recognized immediately.

Mass spectrometric analyses for in-depth proteome profiling were performed in the range from m/z 400 to 1'400 at a resolution of 70'000 (at m/z = 200) when concerning MS1 scans. MS2 scans of the 12 most abundant ions in an MS1 scan (*i.e.* top 12 method) in case of cytoplasmic and nuclear protein fractions and the 8 most abundant ions in case of secreted proteins fractions were achieved using HCD fragmentation at 30% normalized collision energy and analyzed in the orbitrap at a resolution of 14'000 (at m/z = 200). For MRM analyses, transitions of each peptide as well as the corresponding collision energies for each peptide fragmentation were manually determined and optimized.

2.6. Challenge of Secretome Analysis

The establishment of adequate cell culture model systems as well as the optimization of cell culture conditions in order to provide a platform for the analysis of low-abundant, secreted effector molecules was a major goal of this thesis. Thus, an optimal workflow had to be determined which on the one hand keeps cells in the most possible physiological conditions but otherwise allows the analysis of main players during inflammation-related processes, such as cytokines, chemokines and growth factors without contaminations of high-abundant plasma proteins. Therefore, isolated PBMCs were first cultured and treated in 1:2 diluted autologous plasma of each donor, respectively, ensuring conditions which are more similar to the *in vivo* situation than using 5-10% fetal calf serum (FCS) in commercially available cell culture media. However, human-derived plasma consists of a majority of high-abundant proteins such as albumin, α1-antitrypsin, α2-macroglobulin, transferrin, fibrinogen, haptoglobin and different immunoglobulins[78], as demonstrated in Figure 5.

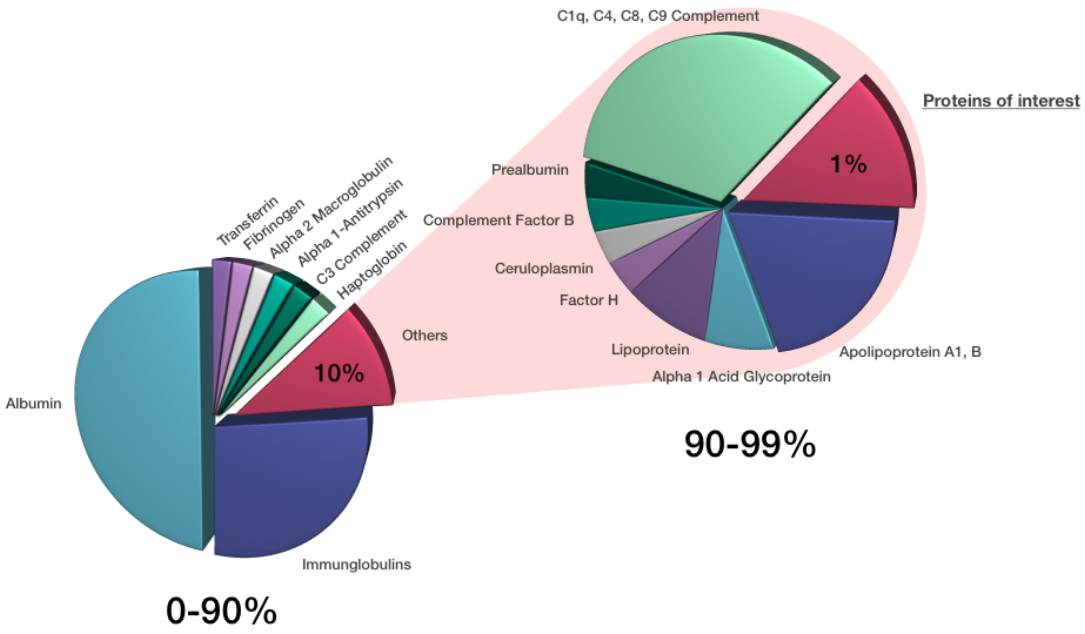

Figure 5: Plasma protein composition

Taking into account that PBMCs are cultivated in 4ml 1:2 diluted plasma, a final protein amount of 160mg can be expected when assuming an average plasma protein concentration of 80mg/ml. For the in-solution digest, 20µg total protein amount is used, whereof 99% are high abundant plasma proteins and only 1% represents low-abundant proteins of interest. This corresponds to a total of 19.8µg and 0.2µg protein amount, respectively. Considering also the protein concentration of high-abundant proteins (mg/ml) and low-abundant proteins (pg/ml) such as chemokines and cytokines[79], it would be necessary that an analytical methodology covers more than 10 orders of magnitude, which is not yet feasible. Due to this, it is necessary to culture cells under serum-free conditions prior to secretome analysis, thus providing a matrix free of high-abundant plasma proteins.

In addition, sample preparation steps as well as LC-MS/MS analysis had to be reconsidered when analyzing cell supernatants. In comparison to cytoplasmic and nuclear protein fractions, where SDS-PAGE was performed to reduce sample complexity, secreted proteins were digested directly in-solution in order to prevent loss of proteins as a consequence of more manipulation steps as well as to shorten analysis time. Figure 6 demonstrates chromatograms of secretome analysis of inflammatory activated PBMCs (A) before and (B) after optimization.

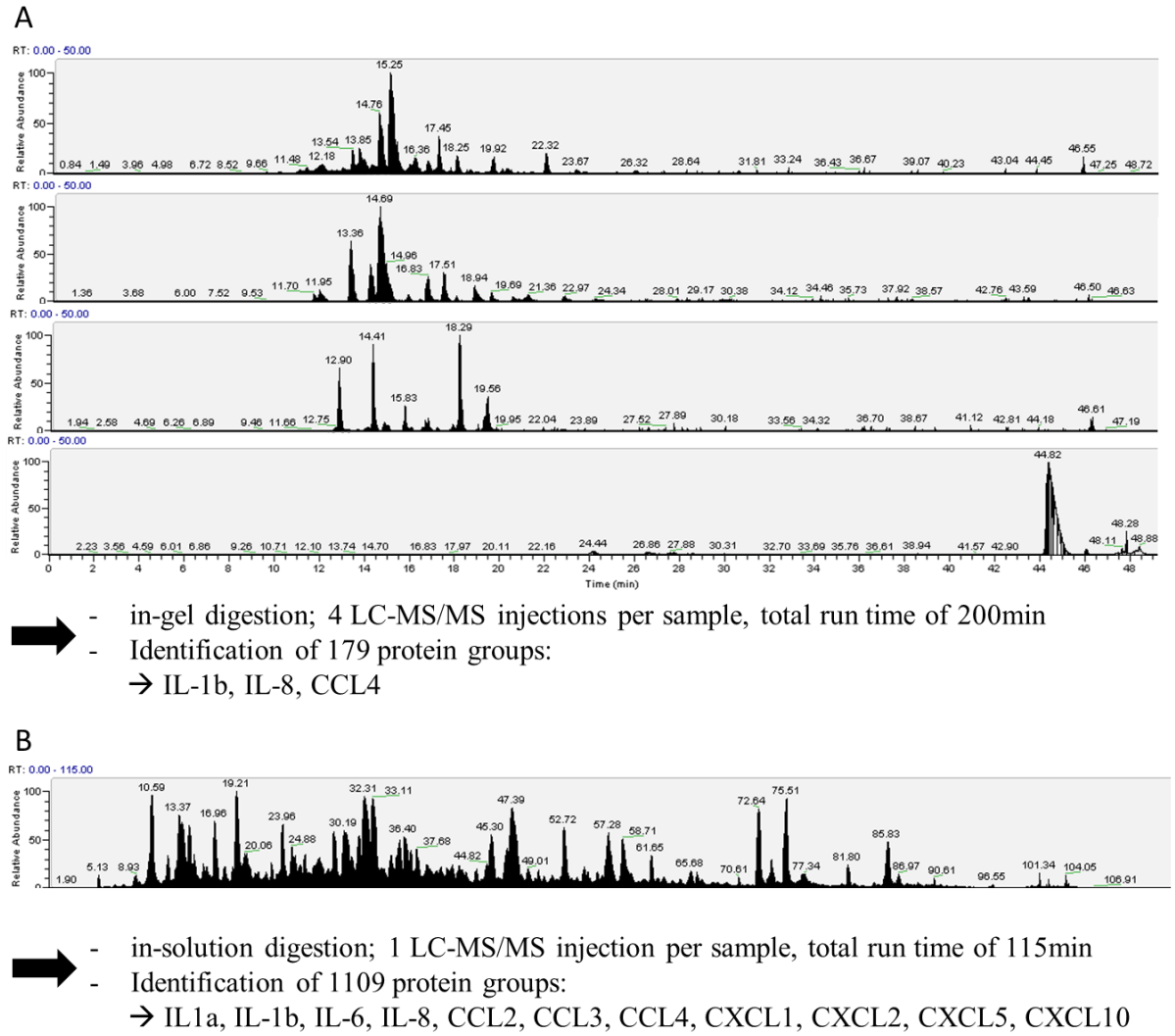

Figure 6: Optimization of secretome analysis

Figure 6 displays total ion chromatograms of secretome analysis (A) before and (B) after optimization. Before optimization SDS-PAGE was performed prior to LC-MS/MS analysis resulting in an analysis of 4 fractions per sample. Furthermore, contaminations of peptides derived from remaining high-abundant plasma proteins were observed allowing the identification of only 179 protein groups. After optimization regarding cell culture conditions, washing procedures, digestion protocol as well as LC-MS/MS method, 1 injection per sample was performed and a total number of 1109 protein groups was identified. Concerning the analysis of cytokines and chemokines, which is important when investigating inflammatory activated PBMCs, we were able to detect only IL-1β, IL-8 and CCL4 before optimization. However, after optimization IL-1α, IL-1β, IL-6, IL-8, CCL2, CCL3, CCL4, CXCL1, CXCL2, CXCL5 and CXCL10 were identified.

2.7. High Data Density Obtained by Mass Spectrometry-based Proteomics

Shotgun proteomics, the main analytical approach applied in this thesis, is used to identify the most proteins possible with high confidence. Here, this strategy is applied in order to characterize various cell types in different functional states to gain a better insight into cellular responses to external stimuli, which is based on very high data density as demonstrated in Figure 7.

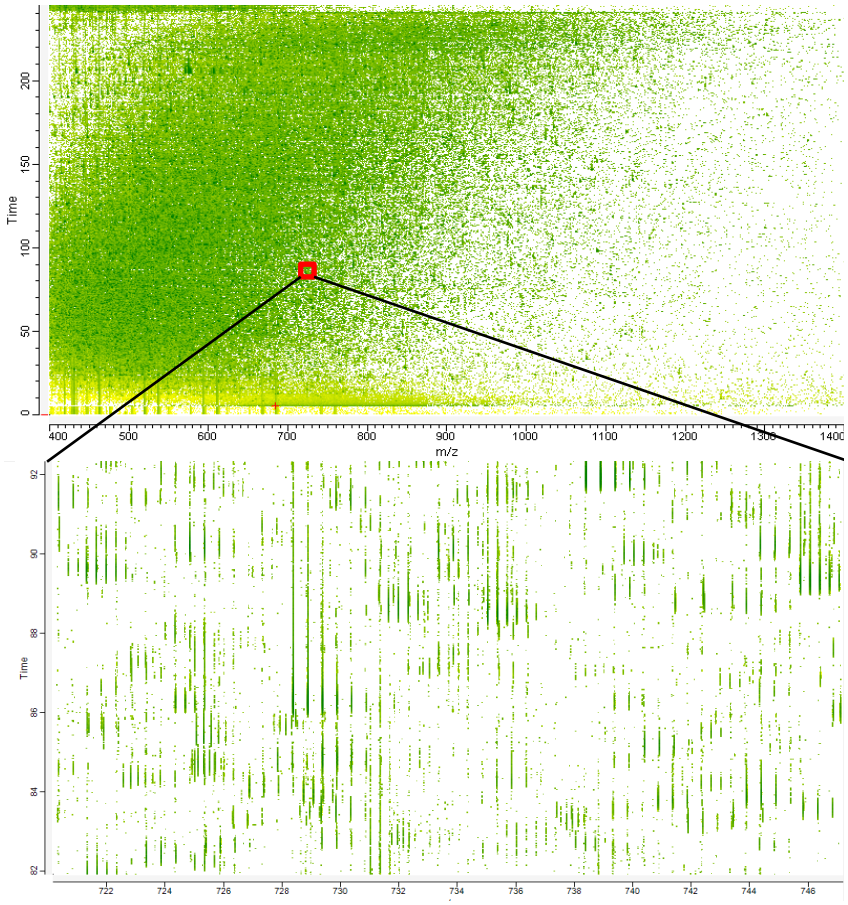

Figure 7: MaxQuant plot of a cytoplasmic protein fraction demonstrating data density

This plot, created with MaxQuant Viewer[80,81], demonstrates a typical LC-MS/MS analysis of an enzymatically digested cytoplasmic protein fraction after SDS-PAGE. While the x-axis displays the applied m/z range, the y-axis reflects the retention time and the color of each spot indicates the intensity of a distinct m/z to a given time point (the more green the more intense). When zooming in a certain time and m/z window (for example between 82-92 min retention time and m/z=720-748 as demonstrated in Figure 9), the distributions of isotopes belonging to specific peptide can also be distinguished. The ion intensity as a third dimension is used subsequently to determine ion abundances and from those relative protein abundance levels assigned as a basis for label free quantification.

As mentioned above, proteins within complex samples display high differences in abundances. Due to this fact, a high dynamic range of the analytical measurement is required in order to cover low as well as high abundant proteins. To demonstrate the power of our shotgun proteomics approach in terms of dynamic range, ion intensity profiles are shown in Figure 8.

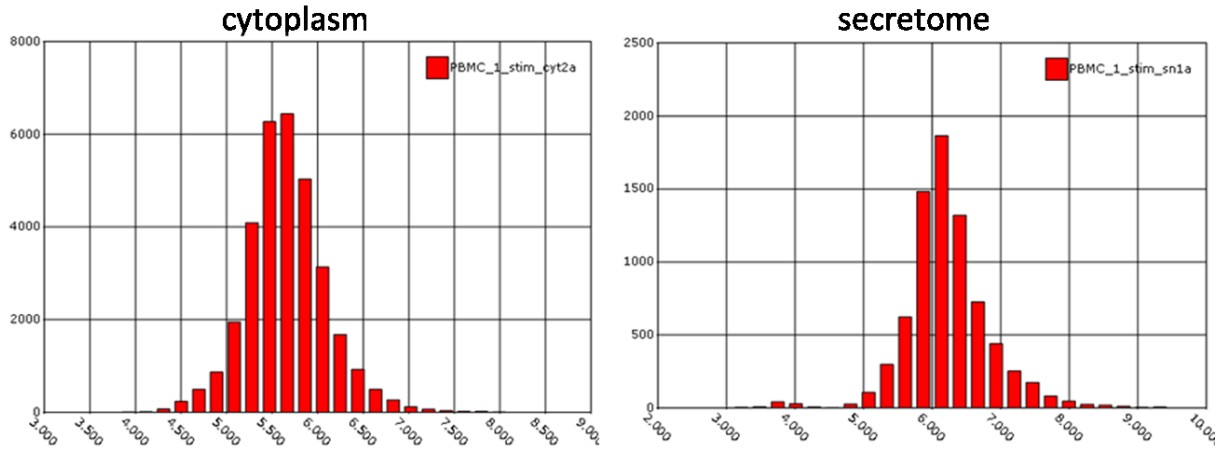

Figure 8: Distribution of precursor ion intensities during LC-MS/MS analysis

The shown histograms display the log10 precursor intensities of the cytoplasmic protein fractions as well as of secreted proteins, respectively. While the x-axis indicates the log10 intensity (6 refers to 10^6), the y-axis shows the counts per bin. It can be observed, that 4 orders of magnitude concerning the precursor ion intensities of a cytoplasmic protein fraction derived from inflammatory activated PBMCs can easily be covered. In case of secretome analysis, precursor ions were detected even in a range of 6 orders of magnitude during an LC-MS/MS analysis demonstrating the high dynamic range of this analytical methodology.

Based on this high data density and on the high identification rate of differently abundant proteins, it is thus possible to comprehensively represent cellular pathways involved in distinct biological processes such as inflammation. Therefore, all proteins identified in control as well as inflammatory activated PBMCs are mapped to KEGG pathways using DAVID bioinformatics resources[82,83]. The coverage of cellular pathways is exemplified on the T-cell receptor signaling pathway as shown in Figure 9.

Regarding this pathways, all proteins which are marked with red asterisks were positively identified in our dataset resulting in a pathway coverage of 79,4%.

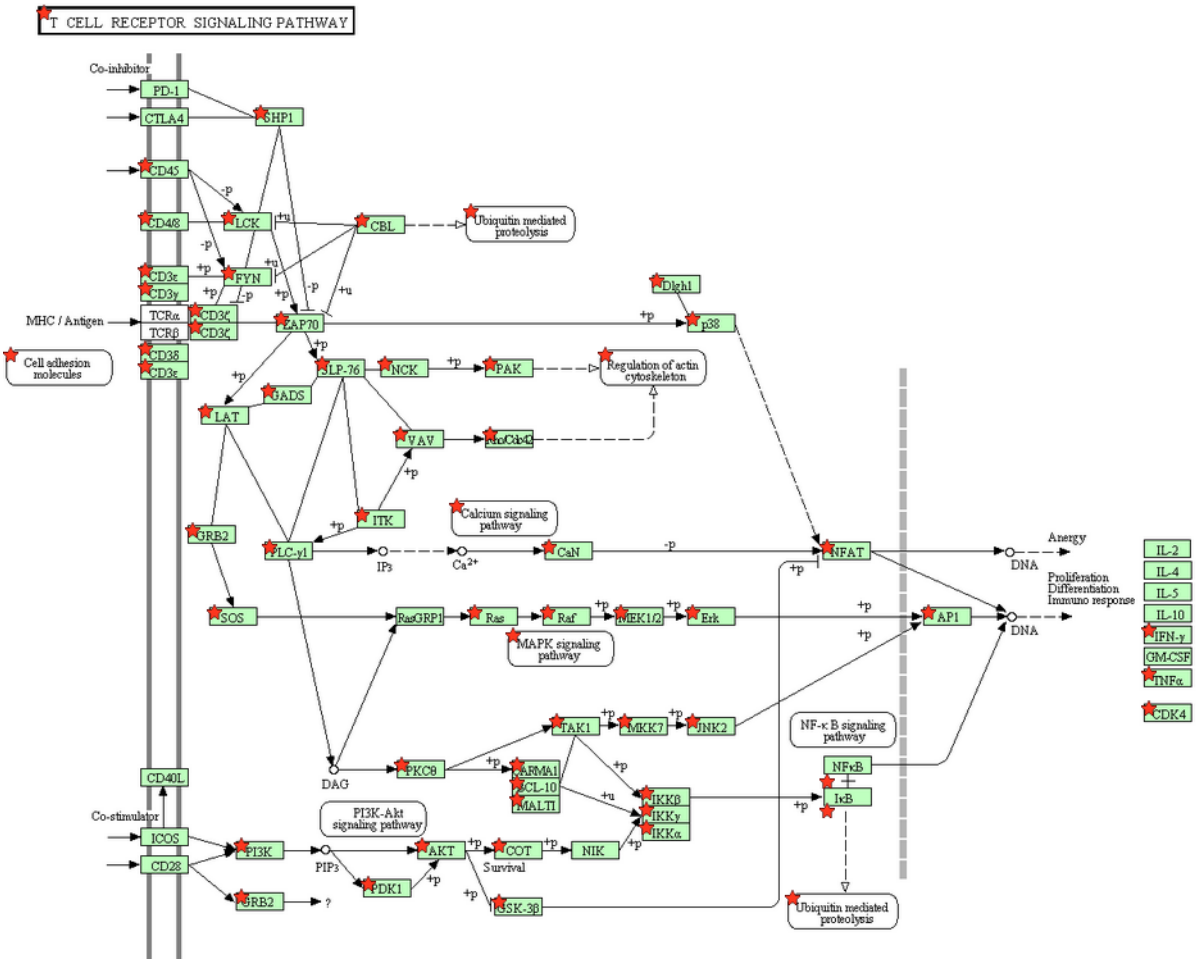

Figure 9: Coverage of proteins involved in the T-cell receptor signaling pathway

2.8. Challenges in the Analysis of PTMs using Mass Spectrometry

The high data density achievable using MS-based proteomics enables the identification of thousands of proteins, thus allowing a comprehensive coverage of proteins involved in signaling pathways. However, for the full assessment of the activation states of signaling pathways, not only the identification of involved proteins is necessary but also the analysis of specific PTMs. For example, the activation states of kinases, which are involved in many pathways such as in the MAPK pathway, are dependent on their phosphorylation state. Thus, the analysis of PTMs, especially of phosphorylation events, seems to be necessary concerning the comprehensive investigation of signaling pathways.

But, owing to the nature of phosphorylation sites, their assessment is not trivial. The phosphate groups of phosphopeptides are acidic and thus negatively charged, which may interfere with their MS-detection due to charge neutralization in the positive ion mode. In addition, the low-stoichiometry of phosphopeptides in comparison to non-phosphorylated proteins may be a reason for their inefficient ionization[84]. Furthermore, the MS-based analysis of phosphopeptides can lead to the generation of MS2 spectra with lower quality compared to those of non-phosphorylated peptides. This is due to the fact that phosphate moieties are relatively labile and are often released during fragmentation which leads to a less informative fragmentation of the peptides backbone[85]. Apart from these challenges in the analytical analysis of phosphopeptides, difficulties in the experimental design can occur. Phosphorylations of receptors like PDGF or IGF-1 receptor occur on a time scale of 13 to 35 seconds whereas phosphorylations of downstream kinases like Akt or GSK3β last between 25 and 200 seconds[86]. Due to these characteristics, phosphorylation events can easily be missed using a phospho-proteomic profiling approach which usually represents a snapshot of phosphorylated proteins at a given time point.

Generally, different phosphoprotein or –peptide enrichment strategies are used prior to LC-MS/MS analysis. This can be performed either by using titanium dioxide and antibody-based enrichment strategies or by using immobilized metal affinity chromatography. However, it is also possible to comprehensively assess phosphopeptides in a shotgun proteomics dataset without using any enrichment strategy, as demonstrated in Paper III of this thesis. Therefore, an existing data set was re-evaluated concerning the assessment of phosphopeptides. Although such an analysis strategy is susceptible to have less phosphopeptide identifications because no specific enrichment was performed, it is possible to obtain an overview of high confident phosphorylation events during cellular processes.

2.9. Peptide Identification and False Discovery Rate Estimation

The large scale identification of proteins using shotgun proteomics is based on the generation of thousands of MS2 spectra during an LC-MS/MS analysis. These spectra are then interpreted to determine amino acid sequences and assigned to the corresponding peptides and proteins using database search engines such as Mascot, SEQUEST, OMSSA or Andromeda[87]. Therefore, the input for search engines are MS2 spectra generated during LC-MS/MS analyses and a database containing amino acid sequences of proteins of interest. In the course of this thesis, all existing reviewed human proteins which are contained in the Uniprot database were used for peptide and protein identification. The output of the search engines are peptide-spectrum matches (PSMs) displaying the best scoring peptide to each spectrum out of a database. These PSM assignments are usually defined by scores; the higher the score the more confident the peptide identification. However, a substantial overlap of correct and incorrect PSM assignments exists. Due to this, peptide identification is limited either by allowing a large number of false positive PSM assignments to maximize true positive assignments or by the elimination of a large number of true positive PSM assignments to reduce the number of false

positive identifications[88]. Therefore, a threshold has to be defined which enables the differentiation of positive discoveries (positive PSMs) among all assignments, which is usually referred to as false discovery rate (FDR)[87,89]. Thus, the FDR displays a metric for global confidence assessment in shotgun proteomics[90]. The estimation of the FDR in proteomics is mainly based on a target-decoy database search strategy. This strategy includes not only the search of all spectra against the target protein database but also against a decoy database which displays a shuffled, reversed or otherwise randomized version of the corresponding database. Since the likelihood of false positive identifications should be the same when searching against the target and the decoy database, an estimation of the FDR can be performed in a given dataset[91]. For example, an FDR of 1% in a shotgun proteomics experiment means that 99% of all identifications are true positives whereas 1% of them are false positive identifications[92]. In addition, it is not only possible to calculate the FDR at the level of PSM assignments but also on the level of peptide and protein identification[91].

Furthermore, statistical analysis of proteomic datasets may suffer from the "large p small n" problem[93]. This problem refers to a typical proteomics experiment, where thousands of proteins are identified out of a relatively small sample size. Typically, Students t-tests are used to identify quantitative changes of proteins between different samples, for example control and treated cells as demonstrated in this thesis. This results in the repeated application of statistical tests to the same set of proteins, which is called the "multiple testing problem"[94]. As a consequence, 5% of all tests display p values ≤ 0.05 purely by chance. Thus, it is important to include multiple testing corrections for the statistical analysis of proteomic datasets. The Bonferroni correction is known to have a strong control over false positive identifications but seems to be too conservative for proteomic experiments in terms of reducing the number of differentially abundant proteins in a dataset[94,95]. Due to this, FDR-based corrections are mainly used for statistical testing, which allow the identification of a higher number of differentially abundant proteins compared to Bonferroni correction, but greatly limit the number of false positives compared to statistical testing without using multiple testing correction[94].

2.10. Research Justification

Cellular responses to inflammatory stimuli are based on a complex crosstalk between various cell types, *i.e.* immune and stromal cells via a plethora of effector molecules as demonstrated in Figure 10[96]. The crosstalk among these cells is mainly based on secreted effector molecules such as interleukins, chemokines and matrix metalloproteinases (MMPs). The interplay of these cells and molecules is further dependent on different signaling cascades which are able to interlock at certain steps thus constructing a tight network capable to defend the organism against pathogens as well as tissue damage.

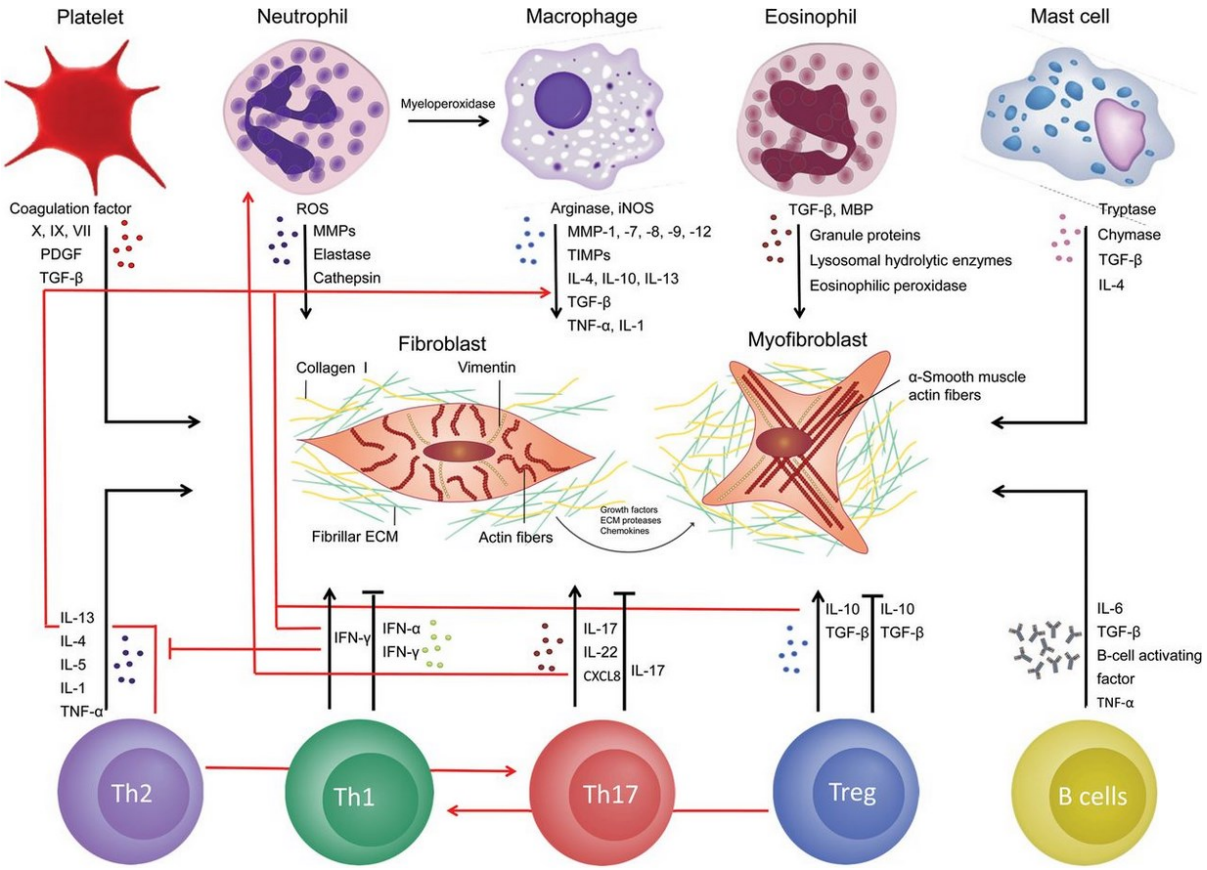

Figure 10: Complex cellular crosstalk between immune and stromal cells. (Reprinted by permission from Macmillan Publishers Ltd: CARDIOVASCULAR RESEARCH, copyright © 2014, Van Linthout et al.)[96]

In acute inflammatory responses the therapeutic inhibition of COX is usually sufficient to prevent an unwanted escalation of inflammation. However, in chronic inflammation, such a monocausal blockage of for example COX-2 is no longer sufficient. Obviously, cells learn to circumvent such an inhibition by manipulating other signaling pathways. A similar phenomenon can be observed during therapeutic interventions which can cause the development of cellular resistance mechanisms. The intake of certain drugs over a long period of time can lead to a loss of the drug's action. This is not due to the fact that the active component is old or loses its activity by chance but rather because cells are able to change their responses to drugs. It seems that they adapt their phenotypes to varying surrounding conditions via different intracellular mechanisms which are not fully understood yet[97]. An example for the alteration of cellular responses during drug treatment is the long-term cellular response to the treatment with the glucocorticoid dexamethasone. A long term administration of this compound can lead to a reduction and/or loss of drug activity, which may result in chronic inflammation[98]. This example demonstrates a potential "learning effect" of cells.

However, before better understanding these mechanisms, it is necessary to take a step backwards in order to get a deep insight into functional cellular processes under well controlled physiological

conditions such as acute inflammation. Therefore, this thesis focuses on the investigation of basic inflammation-related processes in immune cells by proteomics trying to cover processes from ligand-induced receptor activation, the exertion of downstream signaling cascades involving kinase activities, the translocation of transcription factors and the subsequent transcriptional activation of target genes resulting in protein synthesis. Nevertheless, a comprehensive investigation of such highly complex cellular mechanisms, involved in any kind of physiological as well as pathophysiological processes, represent serious problems in biomedical research. Any analytical methodology which is capable of providing deep insight into cellular processes has to fulfill the following main criteria: (i) high sensitivity allowing the identification of low-abundant effector molecules such as cytokines, chemokines or transcription factors and (ii) the possibility of multiplexing enabling the analysis of a number of important effector molecules in parallel.

The aim of this thesis is to establish a powerful analysis strategy, *i.e.* mass spectrometry-based proteomics, to comprehensively assess molecular regulatory processes involved in acute inflammation. This analytical methodology was applied to assess inflammation-related cellular processes caused by external stimuli as well as the cellular responses to therapeutic interventions. Primary human peripheral blood mononuclear cells (PBMCs) were chosen as an *in vitro* model system. They were treated with LPS and PHA to simulate an inflammatory cell state. Cells were fractionated into the supernatant of cells, which contains all secreted effector molecules including chemokines and cytokines, the cytoplasmic and the nuclear protein fractions. All protein samples were subsequently enzymatically digested and analyzed applying a bottom-up proteomics platform using a combination of nanoLC system coupled to a QExactive orbitrap (Thermo Fisher Scientific) and nano CHIP-LC coupled to a triple quadrupole QQQ6490 (Agilent) mass spectrometer.

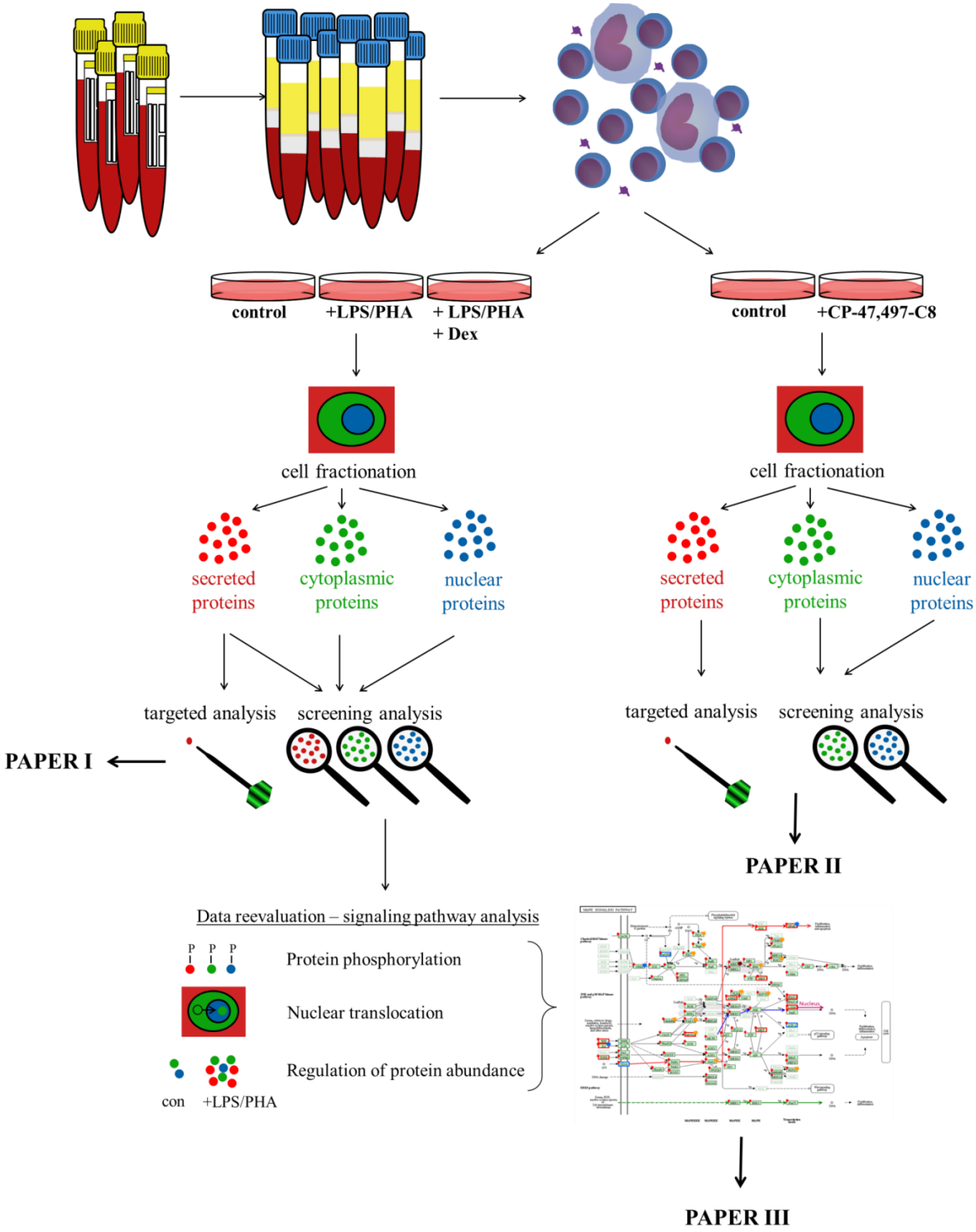

Figure 11: Overview of research articles

Figure 11 displays a methodological and thematic overview of the three main research articles which are presented in this thesis. For each study, PBMCs were first isolated from whole blood using density centrifugation prior to cultivation and treatment. While the treatment of cells was the same for Paper I and III using LPS and PHA as well as dexamethasone, cells in Paper II were treated with the synthetic cannabinoid CP47,497-C8. A short introduction of the three main research articles is given below.

In Paper I, cellular proteome changes were evaluated upon inflammatory stimulation as well as dexamethasone treatment. Therefore, PBMCs were inflammatory activated and afterwards treated with dexamethasone. This proof of principle study with the title "Comprehensive assessment of proteins regulated by dexamethasone reveals novel effects in primary human peripheral blood mononuclear cells" was published in the *Journal of Proteome Research*. After method evaluation with an established drug (Paper I), a novel drug with unknown modes of action was investigated in order to determine their capacity to modulate inflammation-related processes. Therefore, in Paper II, cellular responses of PBMCs were evaluated in similar setup to the cyclohexylphenol CP47,497-C8, a synthetic cannabinoid used as legal surrogate for marihuana. PBMCs were treated *in vitro* with this drug in order to investigate potential health effects in consumers and to elucidate the underlying mechanisms of action. This study with the title "Impact of a synthetic cannabinoid (CP-47,497-C8) on protein expression in human cells: evidence for induction of inflammation and DNA damage" was published in *Archives of Toxicology*. Paper III is based on the data set of study I but includes not only the analysis of overall changes in the proteome and protein abundance upon external stimulation but also the analysis of signaling cascades, nuclear translocation and post-translational modifications of proteins. This study with the title "Shotgun proteomics of primary human cells enables the analysis of signaling pathways and nuclear translocations related to inflammation" was submitted to the *Journal of Proteome Research* and is currently under revision.

Beside these main three articles, which focus on the role of PBMCs during acute inflammation-related processes and their underlying mechanism, in Paper IV the role of other cell types contributing to inflammation was investigated in the same fashion. Therefore, fibroblasts as well as endothelial cells, both representatives of stromal cells, were inflammatory activated using IL-1β. A comparative proteome analysis of fibroblasts, endothelial cell and PBMCs was performed in order to investigate cell-type specific contributions to acute inflammation. This study with the title "Contribution of human fibroblasts and endothelial cells to the hallmarks of inflammation as determined by proteome profiling" was published in the Journal *Molecular and Cellular Proteomics*.

2.11. References

1. Eisenbarth, S.C. & Flavell, R.A. Innate instruction of adaptive immunity revisited: the inflammasome. *EMBO Mol Med* **1**, 92-98 (2009).
2. Nowarski, R.*, et al.* Innate Immune Cells in Inflammation and Cancer. *Cancer Immunol Res* **1**, 77-84 (2013).
3. Medzhitov, R. Origin and physiological roles of inflammation. *Nature* **454**, 428-435 (2008).
4. Kelly, M.*, et al.* Modulating leukocyte recruitment in inflammation. *J Allergy Clin Immun* **120**, 3-10 (2007).
5. Schnoor, M.*, et al.* Crossing the Vascular Wall: Common and Unique Mechanisms Exploited by Different Leukocyte Subsets during Extravasation. *Mediat Inflamm* (2015) 10.1155/2015/946509.
6. Soehnlein, O. & Lindbom, L. Phagocyte partnership during the onset and resolution of inflammation. *Nat Rev Immunol* **10**, 427-439 (2010).
7. Mantovani, A.*, et al.* Neutrophils in the activation and regulation of innate and adaptive immunity. *Nat Rev Immunol* **11**, 519-531 (2011).
8. Galli, S.J.*, et al.* Phenotypic and functional plasticity of cells of innate immunity: macrophages, mast cells and neutrophils. *Nat Immunol* **12**, 1035-1044 (2011).
9. Malyshev, I. & Malyshev, Y. Current Concept and Update of the Macrophage Plasticity Concept: Intracellular Mechanisms of Reprogramming and M3 Macrophage "Switch" Phenotype. *Biomed Res Int* **2015**, 341308 (2015).
10. Headland, S.E. & Norling, L.V. The resolution of inflammation: Principles and challenges. *Semin Immunol* **27**, 149-160 (2015).
11. Iwasaki, A. & Medzhitov, R. Control of adaptive immunity by the innate immune system. *Nat Immunol* **16**, 343-353 (2015).
12. den Haan, J.M.*, et al.* The activation of the adaptive immune system: cross-talk between antigen-presenting cells, T cells and B cells. *Immunol Lett* **162**, 103-112 (2014).
13. Cosmi, L.*, et al.* T helper cells plasticity in inflammation. *Cytometry A* **85**, 36-42 (2014).
14. Ohkura, N. & Sakaguchi, S. Regulatory T cells: roles of T cell receptor for their development and function. *Semin Immunopathol* **32**, 95-106 (2010).
15. Ollila, J. & Vihinen, M. B cells. *Int J Biochem Cell B* **37**, 518-523 (2005).
16. Kurosaki, T.*, et al.* Memory B cells. *Nat Rev Immunol* **15**, 149-159 (2015).
17. Hussain, S.P. & Harris, C.C. Inflammation and cancer: an ancient link with novel potentials. *Int J Cancer* **121**, 2373-2380 (2007).
18. Barone, F.*, et al.* The role of non-hematopoietic stromal cells in the persistence of inflammation. *Front Immunol **3**,* (2012) 10.3389/fimmu.2012.00416.
19. Aoki, T. & Narumiya, S. Prostaglandins and chronic inflammation. *Trends Pharmacol Sci* **33**, 304-311 (2012).
20. Ben-Baruch, A. Inflammation-associated immune suppression in cancer: the roles played by cytokines, chemokines and additional mediators. *Semin Cancer Biol* **16**, 38-52 (2006).
21. Mantovani, A.*, et al.* Cancer-related inflammation. *Nature* **454**, 436-444 (2008).
22. Chiba, T.*, et al.* Inflammation-associated cancer development in digestive organs: mechanisms and roles for genetic and epigenetic modulation. *Gastroenterology* **143**, 550-563 (2012).
23. Nishizawa, T. & Suzuki, H. Gastric Carcinogenesis and Underlying Molecular Mechanisms: Helicobacter pylori and Novel Targeted Therapy. *Biomed Res Int **2015**,* (2015) 10.1155/2015/794378.
24. Colotta, F.*, et al.* Cancer-related inflammation, the seventh hallmark of cancer: links to genetic instability. *Carcinogenesis* **30**, 1073-1081 (2009).
25. Hanahan, D. & Weinberg, R.A. The hallmarks of cancer. *Cell* **100**, 57-70 (2000).
26. Hanahan, D. & Weinberg, R.A. Hallmarks of cancer: the next generation. *Cell* **144**, 646-674 (2011).
27. Jinushi, M. Yin and yang of tumor inflammation: how innate immune suppressors shape the tumor microenvironments. *Int J Cancer* **135**, 1277-1285 (2014).
28. Alessandri, A.L.*, et al.* Resolution of inflammation: mechanisms and opportunity for drug development. *Pharmacol Ther* **139**, 189-212 (2013).

29. Dwivedi, A.K., *et al.* Molecular basis for nonspecificity of nonsteroidal anti-inflammatory drugs (NSAIDs). *Drug Discov Today* **20**, 863-873 (2015).
30. Bertolini, A., *et al.* Selective COX-2 inhibitors and dual acting anti-inflammatory drugs: critical remarks. *Curr Med Chem* **9**, 1033-1043 (2002).
31. Beaugerie, L. & Thiefin, G. [Gastrointestinal complications related to NSAIDs]. *Gastroenterol Clin Biol* **28**, 62-72 (2004).
32. Strehl, C. & Buttgereit, F. Optimized glucocorticoid therapy: teaching old drugs new tricks. *Mol Cell Endocrinol* **380**, 32-40 (2013).
33. Clark, A.R. Anti-inflammatory functions of glucocorticoid-induced genes. *Mol Cell Endocrinol* **275**, 79-97 (2007).
34. Barnes, P.J. & Adcock, I.M. Glucocorticoid resistance in inflammatory diseases. *Lancet* **373**, 1905-1917 (2009).
35. Yang, N., *et al.* Current concepts in glucocorticoid resistance. *Steroids* **77**, 1041-1049 (2012).
36. Enever, C., *et al.* Next generation immunotherapeutics--honing the magic bullet. *Curr Opin Biotechnol* **20**, 405-411 (2009).
37. Kotsovilis, S. & Andreakos, E. Therapeutic human monoclonal antibodies in inflammatory diseases. *Methods Mol Biol* **1060**, 37-59 (2014).
38. Zagury, D. & Gallo, R.C. Anti-cytokine Ab immune therapy: present status and perspectives. *Drug Discov Today* **9**, 72-81 (2004).
39. Rath, T., *et al.* From physiology to disease and targeted therapy: interleukin-6 in inflammation and inflammation-associated carcinogenesis. *Arch Toxicol* **89**, 541-554 (2015).
40. Huwiler, A. & Pfeilschifter, J. Lipids as targets for novel anti-inflammatory therapies. *Pharmacol Ther* **124**, 96-112 (2009).
41. Anderson, N.L. & Anderson, N.G. Proteome and proteomics: new technologies, new concepts, and new words. *Electrophoresis* **19**, 1853-1861 (1998).
42. Packer, N.H. & Harrison, M.J. Glycobiology and proteomics: is mass spectrometry the Holy Grail? *Electrophoresis* **19**, 1872-1882 (1998).
43. Rabilloud, T., *et al.* Two-dimensional gel electrophoresis in proteomics: Past, present and future. *J Proteomics* **73**, 2064-2077 (2010).
44. Steinberg, T.H. Protein gel staining methods: an introduction and overview. *Methods Enzymol* **463**, 541-563 (2009).
45. Thiede, B., *et al.* Peptide mass fingerprinting. *Methods* **35**, 237-247 (2005).
46. Zimny-Arndt, U., *et al.* Classical proteomics: two-dimensional electrophoresis/MALDI mass spectrometry. *Methods Mol Biol* **492**, 65-91 (2009).
47. Rozanas, C.R. & Loyland, S.M. Capabilities using 2-D DIGE in proteomics research : the new gold standard for 2-D gel electrophoresis. *Methods Mol Biol* **441**, 1-18 (2008).
48. Marouga, R., *et al.* The development of the DIGE system: 2D fluorescence difference gel analysis technology. *Anal Bioanal Chem* **382**, 669-678 (2005).
49. Mahmood, T. & Yang, P.C. Western blot: technique, theory, and trouble shooting. *N Am J Med Sci* **4**, 429-434 (2012).
50. Wisniewski, J.R., *et al.* Universal sample preparation method for proteome analysis. *Nat Methods* **6**, 359-362 (2009).
51. Camerini, S. & Mauri, P. The role of protein and peptide separation before mass spectrometry analysis in clinical proteomics. *J Chromatogr A* **1381**, 1-12 (2015).
52. Wilson, S.R., *et al.* Nano-LC in proteomics: recent advances and approaches. *Bioanalysis* **7**, 1799-1815 (2015).
53. Walther, T.C. & Mann, M. Mass spectrometry-based proteomics in cell biology. *J Cell Biol* **190**, 491-500 (2010).
54. Sandra, K., *et al.* Highly efficient peptide separations in proteomics Part 1. Unidimensional high performance liquid chromatography. *J Chromatogr B Analyt Technol Biomed Life Sci* **866**, 48-63 (2008).
55. Marvin, L.F., *et al.* Matrix-assisted laser desorption/ionization time-of-flight mass spectrometry in clinical chemistry. *Clin Chim Acta* **337**, 11-21 (2003).
56. Banerjee, S. & Mazumdar, S. Electrospray ionization mass spectrometry: a technique to access the information beyond the molecular weight of the analyte. *Int J Anal Chem* ***2012,*** (2012) 10.1155/2012/282574.

57. Thomson, B.A. & Iribarne, J.V. Field-Induced Ion Evaporation from Liquid Surfaces at Atmospheric-Pressure. *J Chem Phys* **71**, 4451-4463 (1979).
58. Wilm, M.S. & Mann, M. Electrospray and Taylor-Cone Theory, Doles Beam of Macromolecules at Last. *Int J Mass Spectrom* **136**, 167-180 (1994).
59. Wilm, M. Principles of electrospray ionization. *Mol Cell Proteomics* **10**, (2011) 10.1074/mcp.M111.009407.
60. Furey, A.*, et al.* Ion suppression; a critical review on causes, evaluation, prevention and applications. *Talanta* **115**, 104-122 (2013).
61. Annesley, T.M. Ion suppression in mass spectrometry. *Clin Chem* **49**, 1041-1044 (2003).
62. Cobo, F. Application of maldi-tof mass spectrometry in clinical virology: a review. *Open Virol J* **7**, 84-90 (2013).
63. Makarov, A. Electrostatic axially harmonic orbital trapping: a high-performance technique of mass analysis. *Anal Chem* **72**, 1156-1162 (2000).
64. Makarov, A.*, et al.* Performance evaluation of a hybrid linear ion trap/orbitrap mass spectrometer. *Anal Chem* **78**, 2113-2120 (2006).
65. Cox, J. & Mann, M. Computational principles of determining and improving mass precision and accuracy for proteome measurements in an Orbitrap. *J Am Soc Mass Spectrom* **20**, 1477-1485 (2009).
66. Michalski, A.*, et al.* Mass spectrometry-based proteomics using Q Exactive, a high-performance benchtop quadrupole Orbitrap mass spectrometer. *Mol Cell Proteomics* **10**, (2011) 10.1074/mcp.M111.011015.
67. Elschenbroich, S. & Kislinger, T. Targeted proteomics by selected reaction monitoring mass spectrometry: applications to systems biology and biomarker discovery. *Mol Biosyst* **7**, 292-303 (2011).
68. Picotti, P. & Aebersold, R. Selected reaction monitoring-based proteomics: workflows, potential, pitfalls and future directions. *Nat Methods* **9**, 555-566 (2012).
69. Wells, J.M. & McLuckey, S.A. Collision-induced dissociation (CID) of peptides and proteins. *Biol Mass Spectrom* **402**, 148-185 (2005).
70. Syka, J.E.P.*, et al.* Peptide and protein sequence analysis by electron transfer dissociation mass spectrometry. *P Natl Acad Sci USA* **101**, 9528-9533 (2004).
71. Oh, H.B. & Moon, B. Radical-driven peptide backbone dissociation tandem mass spectrometry. *Mass Spectrom Rev* **34**, 116-132 (2015).
72. Guthals, A. & Bandeira, N. Peptide Identification by Tandem Mass Spectrometry with Alternate Fragmentation Modes. *Mol Cell Proteomics* **11**, 550-557 (2012).
73. Olsen, J.V.*, et al.* Higher-energy C-trap dissociation for peptide modification analysis. *Nat Methods* **4**, 709-712 (2007).
74. Quan, L. & Liu, M. CID, ETD and HCD Fragmentation to Study Protein Post-Translational Modifications. *Mod Chem appl* (2013) 10.4172/2329-6798.1000e102.
75. Koley, D. & Bard, A.J. Triton X-100 concentration effects on membrane permeability of a single HeLa cell by scanning electrochemical microscopy (SECM). *Proc Natl Acad Sci U S A* **107**, 16783-16787 (2010).
76. Gerner, C.*, et al.* Similarity between nuclear matrix proteins of various cells revealed by an improved isolation method. *J Cell Biochem* **71**, 363-374 (1998).
77. Saveliev, S.*, et al.* Trypsin/Lys-C protease mix for enhanced protein mass spectrometry analysis. *Nat Methods* **10,** (2013).
78. Cunningham, R.*, et al.* Mass Spectrometry-based Proteomics and Peptidomics for Systems Biology and Biomarker Discovery. *Front Biol (Beijing)* **7**, 313-335 (2012).
79. Schiess, R.*, et al.* Targeted proteomic strategy for clinical biomarker discovery. *Mol Oncol* **3**, 33-44 (2009).
80. Tyanova, S.*, et al.* Visualization of LC-MS/MS proteomics data in MaxQuant. *Proteomics* **15**, 1453-1456 (2015).
81. Cox, J. & Mann, M. MaxQuant enables high peptide identification rates, individualized p.p.b.-range mass accuracies and proteome-wide protein quantification. *Nat Biotechnol* **26**, 1367-1372 (2008).
82. Huang da, W.*, et al.* Systematic and integrative analysis of large gene lists using DAVID bioinformatics resources. *Nat Protoc* **4**, 44-57 (2009).

83. Huang da, W., *et al.* Bioinformatics enrichment tools: paths toward the comprehensive functional analysis of large gene lists. *Nucleic Acids Res* **37**, 1-13 (2009).
84. Pan, N., *et al.* Highly efficient ionization of phosphopeptides at low pH by desorption electrospray ionization mass spectrometry. *Analyst* **138**, 1321-1324 (2013).
85. Dephoure, N., *et al.* Mapping and analysis of phosphorylation sites: a quick guide for cell biologists. *Mol Biol Cell* **24**, 535-542 (2013).
86. Blazek, M., *et al.* Analysis of fast protein phosphorylation kinetics in single cells on a microfluidic chip. *Lab Chip* **15**, 726-734 (2015).
87. Jeong, K., *et al.* False discovery rates in spectral identification. *BMC Bioinformatics* **13**, (2012) 10.1186/1471-2105-13-S16-S2.
88. Kall, L., *et al.* Assigning significance to peptides identified by tandem mass spectrometry using decoy databases. *J Proteome Res* **7**, 29-34 (2008).
89. Keich, U., *et al.* Improved False Discovery Rate Estimation Procedure for Shotgun Proteomics. *J Proteome Res* **14**, 3148-3161 (2015).
90. Aggarwal, S. & Yadav, A.K. False Discovery Rate Estimation in Proteomics. *Methods Mol Biol* **1362**, 119-128 (2016).
91. Savitski, M.M., *et al.* A Scalable Approach for Protein False Discovery Rate Estimation in Large Proteomic Data Sets. *Mol Cell Proteomics* **14**, 2394-2404 (2015).
92. Kall, L., *et al.* Posterior error probabilities and false discovery rates: two sides of the same coin. *J Proteome Res* **7**, 40-44 (2008).
93. Johnstone, I.M. & Titterington, D.M. Statistical challenges of high-dimensional data. *Philos Trans A Math Phys Eng Sci* **367**, 4237-4253 (2009).
94. Ting, L., *et al.* Normalization and statistical analysis of quantitative proteomics data generated by metabolic labeling. *Mol Cell Proteomics* **8**, 2227-2242 (2009).
95. Diz, A.P., *et al.* Multiple hypothesis testing in proteomics: A strategy for experimental work. *Mol Cell Proteomics* (2011) 10.1074/mcp.O110.004374.
96. Van Linthout, S., *et al.* Crosstalk between fibroblasts and inflammatory cells. *Cardiovasc Res* **102**, 258-269 (2014).
97. de la Puente, P. & Azab, A.K. Contemporary drug therapies for multiple myeloma. *Drugs Today (Barc)* **49**, 563-573 (2013).
98. Newton, R. Anti-inflammatory glucocorticoids: changing concepts. *Eur J Pharmacol* **724**, 231-236 (2014).

3. Results and Discussion

3.1. Comprehensive assessment of proteins regulated by dexamethasone reveals novel effects in primary human peripheral blood mononuclear cells

Andrea Bileck[a], Dominique Kreutz[a], Besnik Muqaku[a], Astrid Slany[a], Christopher Gerner[a]

Journal of Proteome Research, **2014,** 13, (12), 5989-6000

[a] Department of Analytical Chemistry, Faculty of Chemistry, University of Vienna, Währinger Str. 38, A-1090 Vienna, Austria

Contributions to this publication:

- Conduction of experiments
- Organization of required materials
- Creation of figures
- Involved in the planning of the experiments, data interpretation and writing of the manuscript

Journal of proteome research

Article

pubs.acs.org/jpr

Comprehensive Assessment of Proteins Regulated by Dexamethasone Reveals Novel Effects in Primary Human Peripheral Blood Mononuclear Cells

Andrea Bileck, Dominique Kreutz, Besnik Muqaku, Astrid Slany, and Christopher Gerner*

Institute of Analytical Chemistry, Faculty of Chemistry, University of Vienna, Vienna 1090, Austria

Supporting Information

ABSTRACT: Inflammation is a physiological process involved in many diseases. Monitoring proteins involved in regulatory effects may help to improve our understanding of inflammation. We have analyzed proteome alterations induced in peripheral blood mononuclear cells (PBMCs) upon inflammatory activation in great detail using high-resolution mass spectrometry. Moreover, the activated cells were treated with dexamethasone to investigate their response to this antiphlogistic drug. From a total of 6886 identified proteins, 469 proteins were significantly regulated upon inflammatory activation. Data are available via ProteomeXchange with identifiers PXD001415−23. Most of these proteins were counter-regulated by dexamethasone, with some exceptions concerning members of the interferon-induced protein family. To confirm some of these results, we performed targeted MRM analyses of selected peptides. The inflammation-induced upregulation of proteins such as IL-1β, IL-6, CXCL2, and GROα was confirmed, however, with strong quantitative interindividual differences. Furthermore, the inability of dexamethasone to downregulate inflammation-induced proteins such as PTX3 and TSG6 was clearly demonstrated. In conclusion, the relation of cell function as well as drug-induced modulation thereof was successfully mapped to proteomes, suggesting targeted analysis as a novel and powerful drug evaluation method. Although most consequences of dexamethasone were found to be compatible with the expected mode of action, some unexpected but significant observations may be related to adverse effects.

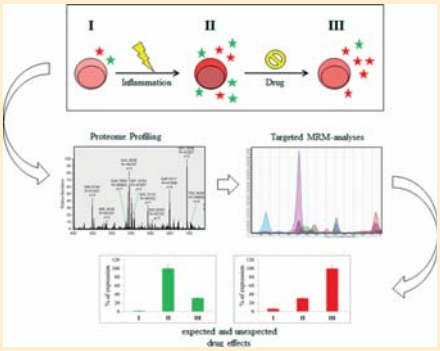

KEYWORDS: *Adverse drug effects, cell biology, drug effects, inflammatory response, mass spectrometry, PBMCs, proteomics, secretome*

INTRODUCTION

Peripheral blood mononuclear cells (PBMCs) are important constituents of the immune system and play an essential role in a large number of diseases. PBMCs consist of different cell types such as T- and B-lymphocytes and monocytes, which cooperate in inflammatory processes. Inflammatory stimulation of these cells is a rather dynamic process associated with an alteration of protein synthesis within a short period of time.[1] Since the underlying mechanisms of inflammatory processes are very complex, a powerful screening technique is required to investigate regulatory proteins. We have previously performed functional studies with these cells using 2D-PAGE and ion trap-based shotgun analysis, resulting in the identification of 1774 proteins.[1] A recent study provided more in-depth proteome analysis data for untreated PBMCs, with 4129 proteins built from 25 503 distinct peptides identifications.[2] Although this provides a reference for normal cells, the characterization of inflammation-related proteins is of greater functional relevance. Most importantly, the effect of antiphlogisitc drugs on the proteome of inflammatory activated cells has not been investigated until now. With improved technologies, now using a QExactive Orbitrap, we therefore investigated these cells at three different cell states: (i) untreated, (ii) inflammatory activated, and (iii) inflammatory activated and treated with dexamethasone. This approach actually allowed us to identify 6886 protein groups built from 85 501 high-quality peptide identifications.

Dexamethasone is a synthetic glucocorticoid that is applied worldwide, mainly for the treatment of acute and chronic inflammatory diseases such as allergy, rheumatoid arthritis, and others. However, its long-term application may be accompanied by adverse effects including osteoporosis and acne as well as the development of drug resistance, based on effects that are not yet fully understood.[3,4] So far, it is known that dexamethasone acts mainly on immune cells and that the effects of this potent anti-inflammatory drug are mediated through different intracellular mechanisms including the binding to the widely expressed glucocorticoid (GC) receptor. One of the most important anti-inflammatory effects of dexamethasone is the inhibition of prostaglandin production and activity, which is achieved through three different mechanisms: (i) repression of cyclooxygenase 2 (COX2) transcription via the NFκB signaling pathway, (ii) induction of MAPK phosphatase 1, and (iii)

Received: August 18, 2014
Published: October 27, 2014

ACS Publications © 2014 American Chemical Society

induction of Annexin 1.[5−8] In addition, dexamethasone is meant to efficiently reduce the activity of inflammatory modulators such as cytokines and chemokines at the site of inflammation. However, systematic studies of proteome alterations subsequent to dexamethasone or other glucocorticoid treatments have not been performed so far. In this study, we focused on this question by investigating the extent to which white blood cells may return to their original functional state after their inflammatory activation and subsequent treatment with this antiphlogistic drug. Hence, we focused on the most significantly altered functionalities during stimulation and followed their regulation in response to application of the drug.

Understanding the mode of action of routinely administered drugs is relevant to improving those that already exist as well as to developing new therapeutic strategies. Currently, many studies are focusing on the discovery of new drugs and on better understanding a drug's effects by characterizing its specific target molecules. For example, mRNA expression and protein synthesis of CXCR4 were found to be upregulated in dexamethasone-treated PBMCs.[9] Also, a loss of tumor suppressor protein p53 activity has been shown to affect the repression of dexamethasone-induced NFκB target gene transcription; therefore, aberrant p53 activity in tumors should be considered in common treatment strategies.[10] In contrast to this, a more broadly based screening approach is also possible that focuses on more complex cellular mechanisms. Here, the focus lies on the characterization of overall cellular responses to a drug challenge rather than on selected molecules, as practiced by the use of enzymatic assays. Therefore, proteomics seems to be one of the most promising screening techniques to investigate such drug effects.[11] In-depth proteome profiling could also help to understand possible adverse effects as well as resistance mechanisms and to identify the involved proteins. Following this strategy, it was, for example, possible to characterize resistance signatures in human melanoma cells as well as in breast cancer cells.[12,13]

Obviously, much is already known about characteristic effects of dexamethasone, especially at the transcriptomic level. However, no in-depth proteome analysis focusing on the effects of this anti-inflammatory drug has been performed so far. The aim of this study was to gain insight into the anti-inflammatory mechanisms induced by dexamethasone and to better understand its complex intracellular mechanisms by means of comprehensive proteome profiling. To investigate the potency of the drug to suppress pro-inflammatory activities, we treated inflammatory activated primary human PBMCs with dexamethasone. PBMCs were stimulated in vitro with lipopolysaccharide (LPS) and phytohemagglutinin (PHA) in order to induce an inflammatory activation, simulating an in vivo situation.[1] After 1 h of activation, a time point when transcriptional activation has already been fully accomplished, cells were treated with dexamethasone and further cultivated for 6 h. Thereafter, PBMCs were fractionated into secretome, cytoplasmic, and nuclear proteins. Proteome analysis was performed by means of QExactive Orbitrap mass spectrometry, and data analysis was supported by label-free quantification via MaxQuant software.[14] On the basis of this proteomic approach and on the comprehensive data analysis, we were able to characterize molecular mechanisms strongly regulated through inflammatory activation as well as the cell's response to the applied antiphlogistic drug.

EXPERIMENTAL SECTION

Isolation and Treatment of PBMCs

PBMCs were isolated from three different healthy volunteers with the written consent of each donor and approval of the Ethics Committee of the Medical University of Vienna (Application 2011/296 by C.G. entitled *Charakterisierung von entzündlich aktivierten Zellen des peripheren Blutes...*). The donors reported no ailments and had not taken any medication for at least 2 weeks. Fifty milliliters of noncoagulated whole blood was collected in 6 mL CPDA tubes (Greiner Bio-One GmbH, Austria) and immediately processed by diluting it 1:2 with RPMI1640 medium (Gibco, Life Technologies, Austria) supplemented with 100 U/mL penicillin and 100 μg/mL streptomycin (ATCC, LGC Standards GmbH, Germany). Afterward, the diluted blood suspension was carefully overlaid on Ficoll Paque (GE Healthcare, Bio-Sciences AB, Uppsala, Sweden) and centrifuged at 500*g* for 20 min at 24 °C. The interphase was then collected and washed with PBS. The washed cell pellet was resuspendend in diluted autologous plasma and divided into three Petri dishes: one for the control, one for inflammatory activation, and one for inflammatory activation and subsequent dexamethasone treatment. For activation, 1 μg/mL LPS (Sigma-Aldrich) and 5 μg/mL PHA (Sigma-Aldrich) were added to the respective approach, and the cells were incubated at 37 °C under 5% CO_2. In the case of dexamethasone treatment, 100 ng/mL dexamethasone (Sigma-Aldrich) was added after 1 h of activation. Following 4 h of cultivation, cells were further grown for 3 h in serum-free medium for secretome analysis and were harvested afterward.

Subcellular Fractionation

Supernatants were sterile-filtered through a 0.2 μm filter and precipitated overnight with ice-cold ethanol at −20 °C for isolation of secreted proteins as described previously.[1] All fractionation steps were performed on ice. To obtain the cytoplasmic fraction, cells were lysed in isotonic lysis buffer (10 mM HEPES/NaOH, pH 7.4, 0.25 M sucrose, 10 mM NaCl, 3 mM MgCl2, 0.5% Triton X-100) supplemented with protease inhibitors (pepstatin, leupeptin, aprotinin, each at 1 μg/mL, and 1 mM PMSF) under mechanical shear stress. By centrifugation at 2300*g* and 4 °C for 5 min, the cytoplasmic proteins were separated from the nuclei and precipitated overnight with ice-cold ethanol at −20 °C. For obtaining nuclear proteins, pellets were swelled for 10 min in extraction buffer (500 mM NaCl) and 1:10 diluted with NP-40 buffer for another 15 min. To obtain the nuclear fraction, centrifugation at 2300*g* and 4 °C for 5 min was performed. The extracted proteins were then precipitated overnight with ice-cold ethanol at −20 °C. After precipitation, all samples were dissolved in sample buffer (7.5 M urea, 1.5 M thiourea, 4% CHAPS, 0.05% SDS, 100 mM DDT), and the protein concentrations were determined by Bradford assay (Bio-Rad Laboratories, Germany).

MS Sample Preparation

For the separation of the cytoplasmic and nuclear fractions, 20 μg of each sample was loaded on an SDS-PAGE gel, which allowed us to prefractionate the sample in order to reduce the complexity thereof. This was not necessary for supernatants, which contain a lower number of proteins. Proteins in the gels were stained by MS-compatible silver staining. After fixation with 50% methanol/10% acetic acid, the gels were washed and sensitized with 0.02% $Na_2S_2O_3$. Gels were then stained with

0.1% $AgNO_3$ for 10 min, rinsed, and developed with 3% Na_2CO_3/0.05% formaldehyde. Afterward, each protein band was cut into 4 slices and destained. Upon reduction with DTT and alkylation with IAA, the proteins were digested enzymatically overnight at 37 °C using trypsin (Roche Diagnostics, Germany), as described previously.[15,16] The peptides were eluted, dried ,and stored at −20 °C until LC−MS analysis.

In contrast to the cytoplasmic and nuclear fractions, a variation of the FASP protocol was used for the digestion of secreted proteins.[17] Therefore, 3 kD MWCO filters (Pall Austria Filter GmbH) were rinsed with LC−MS grade water (Millipore GesmbH) by centrifugation at 14 000*g* for 10 min. Twenty micrograms of each protein sample was concentrated onto the prewashed filter by centrifugation at 15 000*g* for 15 min to obtain a final sample volume of 10−20 μL. For reduction, 200 μL of DTT solution (5 mg/mL dissolved in 8 M guanidinium hydrochloride in 50 mM ammonium bicarbonate buffer (ABC buffer), pH 8) was added, and incubation was performed at 56 °C for 30 min. After centrifugation at 14 000*g* for 10 min, a washing step with ABC buffer was performed. For alkylation, 200 μL of IAA solution (10 mg/mL in 8 M guanidinium hydrochloride in 50 mM ABC buffer) was added, and incubation was performed in the dark for 45 min. After centrifugation at 14 000*g* for 10 min, proteins on top of the filter were washed with ABC buffer. Afterward, filters (with a maximum of 50 μL sample volume) were placed in a new Eppendorf tube, and 100 μL of ABC buffer as well as 10 μL of trypsin solution (0.1 μg/μL) were added, and incubation was performed at 37 °C for 18 h. After trypsin digestion, peptide samples were cleaned up with C-18 spin columns (Pierce, Thermo Scientific). Therefore, columns were prewashed two times with 500 μL of ACN and equilibrated with 200 μL of 5% ACN and 0.5% trifluoroacetic acid (TFA) by centrifugation at 1500*g* for 1 min. The peptide samples were acidified to a final concentration of 1% TFA and transferred from the MWCO filters to spin columns. After centrifugation at 1500*g* for 1 min, the flow-through was reloaded on the column to maximize peptide binding and again centrifuged. After a washing step with 5% ACN and 0.5% TFA, the peptides were eluted two times with 40 μL of 50% ACN and 0.1% TFA and once with 40 μL of 80% ACN and 0.1% TFA into a new Eppendorf tube. Finally, the digested peptide samples in the flow-through were dried and stored at −20 °C until further MS analyses.

LC−MS Analysis

Dried samples were reconstituted in 5 μL of 30% formic acid (FA) containing 10 fmol each of 4 synthetic standard peptides and diluted with 40 μL of mobile phase A (98% H_2O, 2% ACN, 0.1% FA). Synthetic peptides [Glu1-Fribrinopeptide B, EGVNDNEEGFFSAR; M28, TTPAVLDSDGSYFLYSK; HK0, VLETKSLYVR; HK1, VLETK(ε-AC)SLYVR] were spiked into each sample as an internal quality control for monitoring LC−MS system stability. Ten microliters of this solution was then injected into the Dionex Ultimate 3000 nano LC system coupled to a QExactive Orbitrap mass spectrometer equipped with a nanospray ion source (Thermo Fisher Scientific, Austria). All samples were analyzed in duplicate. As a preconcentration step, peptides were loaded on a 2 cm × 75 μm C18 Pepmap100 precolumn (Thermo Fisher Scientific, Austria) at a flow rate of 10 μL/min using mobile phase A. Elution from the precolumn to a 50 cm × 75 μm Pepmap100 analytical column (Thermo Fisher Scientific, Austria) and subsequent separation was achieved at a flow rate of 300 nL/min using a gradient of 8−40% mobile phase B (80% ACN, 2% H_2O, 0.1% FA) over 235 min for the analysis of the cytoplasmic and nuclear fractions and over 95 min in the case of secretome analysis. For mass spectrometric detection, MS scans were performed in the range from m/z 400 to 1400 at a resolution of 70 000 (at m/z = 200). MS/MS scans of the 12 most abundant ions (cytoplasm and nuclear fractions) or 8 most abundant ions (secretome) were achieved through HCD fragmentation at 30% normalized collision energy and analyzed in the Orbitrap at a resolution of 17 500 (at m/z = 200). The mass spectrometry proteomics data have been deposited to the ProteomeXchange Consortium[18] via the proteomics identification database (PRIDE) repository with the data set identifiers PXD001415−23 (DOI: 10.6019/PXD001415−23; Supporting Information Table S1).

LC−MS Data Analysis

ProteomeDiscoverer 1.3 (Thermo Fisher Scientific, Austria) running Mascot 2.4 (Matrix Science, UK) was used for protein identification and qualitative data analysis. Protein identification was achieved searching against the SwissProt Database (version 012013 with 20 264 entries), allowing a mass tolerance of 5 ppm for MS spectra and 20 ppm for MS/MS spectra as well as a maximum of 2 missed cleavages. Furthermore, search criteria included carbamidomethylation on cysteins as fixed modification as well as methionine oxidation and N-terminal protein acetylation as variable modifications. A list of lab-characteristic contaminants including various keratins was excluded manually. After setting the FDR < 0.01 and filtering all peptides meeting a highly stringent Mascot significance threshold of less than 0.01, we obtained a total of 85 501 peptides compiled to 6886 protein groups. The Mascot significance threshold filters out all peptides with a score lower than the specified significance score. In Table S2, the SwissProt accession numbers, the sequence coverage, the number of unique peptides, the number of distinct peptides, and the number of peptide spectrum matches per protein identification are indicated for all of these proteins. Six-thousand seventy nine proteins were identified with two or more distinct and confident peptides. The data displayed in Figure 1 were generated using these settings.

For label-free quantitative (LFQ) data analysis, we used the open source software MaxQuant 1.3.0.5 including the Andromeda search engine and the Perseus statistical analysis package.[14,19] Here, the same SwissProt database and mass tolerance values as well as fixed and variable modifications were used, again with a minimum of 2 peptide identifications per protein, with at least one of them being unique, and the FDR calculation based on q-values, here performed both for peptide and protein identifications, was set to less than 0.01. Protein identifications obtained from MaxQuant were further analyzed using Perseus (version 1.3.0.4), with proteins being filtered for reversed sequences, contaminants, and a minimum of three independent identifications per protein. As a result, a total of 6963 proteins compiled from 127 756 distinct peptides were identified (not shown). The number of peptide and protein identifications using Andromeda thus clearly outnumbered the results obtained with Mascot, but it reproduced almost all protein identifications from Mascot (data not shown). Therefore, we concluded that the FDR of the proteins identified using Mascot and listed in Table S2 is better than 0.01. Using Perseus, the determination of significantly up- and downregulated proteins was achieved by applying a two-sided t-test with $p < 0.05$. All significant protein regulations are listed in

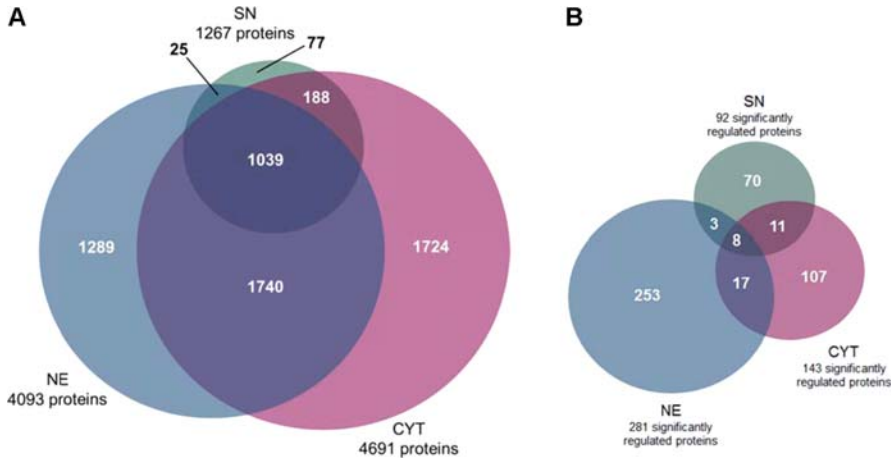

Figure 1. Quantitative Venn diagrams of control and inflammatory activated PBMCs. (A) For each subcellular fraction, the number of proteins identified in three biological and two technical replicates is represented. In total, we identified 4691 proteins in cytoplasmic fractions (CYT), 4093 proteins in nuclear extracts (NE), and 1267 proteins in supernatants (SN). (B) For each subcellular fraction, the number of significantly ($p \leq 0.05$) regulated proteins with a minimum of 2-fold change between control and inflammatory activated PBMCs is represented.

Table S3. In addition, using Perseus, a 2D Annotation enrichment analysis was performed based on GO terms for molecular functions (GOMF) according to Geiger et al.[20]

Multiple Reaction Monitoring (MRM)

Dried peptide samples from the secretome of control, inflammatory activated, and dexamethasone-treated activated PBMCs of three donors were reconstituted in 2 μL of 30% FA containing 10 fmol each of 4 synthetic standard peptides and diluted with 20 μL of 30% FA. One microliter of this solution was then injected to a nanoflow LC system (1260 Infinity Series, Agilent, Palo Alto, CA) using the HPLC-Chip cube (Agilent) coupled to the 6490 triple quadrupole mass spectrometer (Agilent). Peptides were separated by a protein ID HPLC-Chip equipped with a 40 nL Zorbax 300SB-C18 trapping column and a 150 mm × 75 μm Zorbax 300SB-C18 analytical column (Agilent) at a flow rate of 400nL/min using a gradient from 8% mobile phase A (99.8% H_2O, 0.2% FA) to 30% mobile phase B (99.8% ACN, 0.2% FA) over 20 min. All samples were analyzed in triplicate. For MRM analysis, peptides were selected from the Orbitrap data based on the following rationale: only well-ionizing peptides were chosen with good fragmentation properties. Potential matrix effects derived from the original blood samples were investigated by obtaining extracted ion chromatograms using mass ranges actually realized by our first quadrupole in the QQQ-MS. As a result, 9 peptides were selected: (i) ANDQYLTAAALHNLDEAVK (m/z precursor ion: 686.35; m/z product ions: 1038.56, 936.48, and 878.97; eV collision energy: 19.9) belonging to IL-1β, (ii) EALAENNLNLPK (m/z precursor ion: 663.37; m/z product ions: 1012.54, 941.51, and 812.46; eV collision energy: 19.1) and YILDGISALR (m/z precursor ion: 560.82; m/z product ions: 844.49, 731.40, and 446.27; eV collision energy: 15.4) belonging to IL-6, (iii) ACLNPASPMVK (m/z precursor ion: 594.30; m/z product ions: 956.52, 843.44, and 729.40; eV collision energy: 16.6) belonging to CXCL2, (iv) CQCLQT-LQGIHPK (m/z precursor ion: 528.24; m/z product ions: 679.39, 551.33, and 647.85; eV collision energy: 14.2) and ACLNPASPIVK (m/z precursor ion: 585.32; m/z product ions: 938.57, 825.48, and 711.44; eV collision energy: 16.3) belonging to GROα, (v) LTSALDELLQATR (m/z precursor ion: 477.60; m/z product ions: 588.35 and 475.26; eV collision energy: 14.7) and ADLHAVQGWAAR (m/z precursor ion: 432.23; m/z product ions: 560.30 and 503.27; eV collision energy: 10.8) belonging to PTX3, and (vi) TGIIDYGIR (m/z precursor ion: 504.28; m/z product ions: 906.50, 623.31, and 508.29; eV collision energy: 13.4) belonging to TSG6. As an internal standard, one of the standard peptides, Glu1-Fribrinopeptide B (EGVNDNEEGFFSAR; m/z precursor ion: 785.84; m/z product ion: 480.26; eV collision energy: 23.5) was used. For this peptide, we included a calibration curve spanning 4 orders of magnitude in protein concentration (0.05−500 fmol on-column) spiked into cell culture supernatants of normal human dermal fibroblasts with R^2 values greater than 0.999 (Supporting Information Figure S1).

LC−MRM Data Analysis

Each measurement was performed with two different digests per sample and in technical triplicates. The results obtained from one representative series of digests are shown in Figure 4. Data analysis was supported by Skyline version 1.5.[21] The total peak area of each peptide was related to the cell number per assay (total peak area per million cells) and further normalized to the internal standard peptide. Note that normalization here differed from the normalization performed using Perseus, which is based on total protein amount. Afterward, the mean and standard deviation of the normalized peak areas were calculated for each protein separately for the different donors and conditions. For graphical representation, for each protein, the highest determined peak area was set to 100%, and the other peak areas were calculated relative to this.

RESULTS

Inflammatory Activation Induces Significant Changes in Protein Regulation in PBMCs

Proteome profiles of PBMCs were generated using cells from three different healthy donors. PBMCs were analyzed either in their nonactivated state (controls) or in an inflammatory activated state obtained by stimulating the cells in vitro with LPS and PHA. Secreted, cytoplasmic, and nuclear proteins were isolated from the cells, and each of these subcellular fractions was analyzed separately. Each biological replicate was measured as technical duplicate with LC−MS/MS. Comprehensive

Table 1. Inflammatory Response

accession	protein name		fold change SN	*p*-value SN	fold change CYT	*p*-value CYT	fold change NE	*p*-value NE
P00973	2−5-oligoadenylate synthase 1	con vs act	2.3	0.07	2.4	0.39	**4.6**	**0.045**
		act vs dex	−1.5	0.09	−1.0	0.99	−1.9	0.41
Q9Y6K5	2−5-oligoadenylate synthase 3	con vs act	n.d.	n.d.	2.2	0.35	**3.0**	**0.019**
		act vs dex	n.d.	n.d.	−1.5	0.32	−1.9	0.03
Q10588	ADP-ribosyl cyclase 2	con vs act	**−4.7**	**7.7×10^{-4}**	−1.7	0.27	1.0	0.97
		act vs dex	−1.1	0.84	−1.0	0.92	−1.8	0.48
P13500	C-C motif chemokine 2	con vs act	**156.4**	**2.3×10^{-5}**	n.d.	n.d.	n.d.	n.d.
		act vs dex	**−4.7**	**8.6×10^{-4}**	n.d.	n.d.	n.d.	n.d.
P78556	C-C motif chemokine 20	con vs act	n.d.	n.d.	**7.4**	**5.6×10^{-5}**	1.6	0.50
		act vs dex	n.d.	n.d.	−1.9	0.07	−1.6	0.54
P10147	C-C motif chemokine 3	con vs act	**54.6**	**4.1×10^{-4}**	**6.2**	**0.043**	**2.5**	**0.042**
		act vs dex	**−7.4**	**8.5×10^{-5}**	**−26.6**	**2.4×10^{-6}**	−2.0	0.09
P13236	C-C motif chemokine 4	con vs act	3.0	0.13	**30.6**	**4.3×10^{-4}**	**5.9**	**7.4×10^{-3}**
		act vs dex	−1.4	0.68	**-18.1**	**0.027**	−2.4	0.34
P19875	C-X-C motif chemokine 2	con vs act	**9.6**	**6.7×10^{-7}**	**7.9**	**3.8×10^{-3}**	1.8	0.65
		act vs dex	**−6.1**	**1.5×10^{-6}**	−3.2	0.09	−1.6	0.70
P42830	C-X-C motif chemokine 5	con vs act	**13.8**	**1.0×10^{-6}**	n.d.	n.d.	n.d.	n.d.
		act vs dex	−1.4	0.47	n.d.	n.d.	n.d.	n.d.
Q14314	Fibroleukin	con vs act	**−22.3**	**3.7×10^{-3}**	−2.0	0.47	**−9.5**	**0.013**
		act vs dex	**2.1**	**0.043**	−3.0	0.26	2.8	0.21
P09341	Growth-regulated alpha protein	con vs act	**15.3**	**1.9×10^{-3}**	n.d.	n.d.	2.1	0.06
		act vs dex	−3.6	0.15	n.d.	n.d.	−1.3	0.62
P14902	Indoleamine 2,3-dioxygenase 1	con vs act	1.9	0.024	**5.3**	**5.4×10^{-3}**	n.d.	n.d.
		act vs dex	**−2.0**	**0.035**	−1.8	0.20	n.d.	n.d.
P09914	Interferon-induced protein with tetratricopeptide repeats 1	con vs act	1.2	0.76	**10.3**	**0.011**	1.3	0.54
		act vs dex	1.2	0.79	−1.7	0.31	−1.2	0.69
P09913	Interferon-induced protein with tetratricopeptide repeats 2	con vs act	**18.4**	**1.2×10^{-4}**	**17.5**	**8.5×10^{-5}**	n.d.	n.d.
		act vs dex	−2.4	0.35	−2.0	0.10	n.d.	n.d.
O14879	Interferon-induced protein with tetratricopeptide repeats 3	con vs act	**6.5**	**3.4×10^{-3}**	**23.7**	**4.1×10^{-4}**	1.2	0.62
		act vs dex	−1.4	0.62	−2.0	0.14	−1.0	0.93
P01583	Interleukin-1 alpha	con vs act	**11.0**	**1.1×10^{-4}**	**63.6**	**3.1×10^{-4}**	n.d.	n.d.
		act vs dex	**−4.9**	**0.015**	**−7.1**	**0.016**	n.d.	n.d.
P01584	Interleukin-1 beta	con vs act	**53.1**	**5.9×10^{-7}**	**21.9**	**5.0×10^{-5}**	**6.5**	**1.4×10^{-3}**
		act vs dex	**−12.6**	**0.027**	**−4.8**	**7.0×10^{-4}**	−2.3	0.06
Q14213	Interleukin-27 subunit beta	con vs act	n.d.	n.d.	**5.5**	**1.3×10^{-3}**	1.6	0.30
		act vs dex	n.d.	n.d.	2.9	0.14	−1.3	0.55
Q9NZH8	Interleukin-36 gamma	con vs act	n.d.	n.d.	**7.0**	**0.014**	−1.5	0.54
		act vs dex	n.d.	n.d.	−3.5	0.11	1.7	0.36
P05231	Interleukin-6	con vs act	**132.6**	**3.6×10^{-6}**	**35.8**	**1.3×10^{-4}**	**2.2**	**0.048**
		act vs dex	**−6.0**	**6.3×10^{-3}**	**-9.3**	**1.3×10^{-3}**	−1.8	0.21
P10145	Interleukin-8	con vs act	**4.4**	**4.0×10^{-4}**	**14.8**	**1.1×10^{-3}**	**7.0**	**0.026**
		act vs dex	**−5.9**	**3.2×10^{-5}**	**−4.0**	**0.014**	**-5.6**	**0.024**
P07333	Macrophage colony-stimulating factor 1 receptor	con vs act	**−10.3**	**0.016**	n.d.	n.d.	n.d.	n.d.
		act vs dex	−1.2	0.28	n.d.	n.d.	n.d.	n.d.
P08571	Monocyte differentiation antigen CD14	con vs act	**−4.4**	**0.014**	−2.8	0.16	−2.8	0.21
		act vs dex	1.0	0.97	−1.3	0.66	2.5	0.16
P26022	Pentraxin-related protein PTX3	con vs act	**7.3**	**4.5×10^{-7}**	2.2	0.56	n.d.	n.d.
		act vs dex	1.2	0.52	1.3	0.80	n.d.	n.d.
P35354	Prostaglandin G/H synthase 2	con vs act	n.d.	n.d.	**37.8**	**6.4×10^{-4}**	3.2	0.08
		act vs dex	n.d.	n.d.	**−15.5**	**4.2×10^{-3}**	**-3.6**	**0.047**
Q86VB7	Scavenger receptor cysteine-rich type 1 protein M130	con vs act	**−7.7**	**3.4×10^{-9}**	−5.1	0.06	n.d.	n.d.
		act vs dex	2.0	0.031	**12.0**	**9.1×10^{-4}**	n.d.	n.d.
P01137	Transforming growth factor beta-1	con vs act	**6.4**	**0.030**	−1.1	0.80	1.3	0.72
		act vs dex	−1.3	0.51	−1.9	0.38	−1.9	0.46
P01375	Tumor necrosis factor	con vs act	**11.7**	**2.6×10^{-4}**	**7.1**	**4.6×10^{-3}**	n.d.	n.d.
		act vs dex	**−8.0**	**5.5×10^{-3}**	−2.8	0.19	n.d.	n.d.

proteome profiles of PBMCs were generated by combining all data related to one cell state. As a result, 6079 protein groups were identified with at least two distinct peptides in control and inflammatory activated cells taken together. In the secretome, cytoplasm, and nuclear fractions, 1267, 4691, and 4093 proteins were found, respectively, or an exclusive list of 77, 1724, and

Table 2. Transcriptional Regulation

accession	protein name		fold change SN	*p*-value SN	fold change CYT	*p*-value CYT	fold change NE	*p*-value NE
P49716	CCAAT/enhancer-binding protein delta	con vs act	n.d.	n.d.	n.d.	n.d.	**5.2**	**0.012**
		act vs dex	n.d.	n.d.	n.d.	n.d.	−1.1	0.84
Q14527	Helicase-like transcription factor	con vs act	n.d.	n.d.	−1.1	0.90	**5.8**	**0.016**
		act vs dex	n.d.	n.d.	1.1	0.93	**−4.4**	**0.016**
Q92570	Nuclear receptor subfamily 4 group A member 3	con vs act	n.d.	n.d.	n.d.	n.d.	**8.0**	**7.7×10^{-3}**
		act vs dex	n.d.	n.d.	n.d.	n.d.	−3.3	0.06
Q13395	Probable methyltransferase TARBP1	con vs act	n.d.	n.d.	3.0	0.21	**6.4**	**0.016**
		act vs dex	n.d.	n.d.	−1.3	0.80	−1.8	0.50
P42224	Signal transducer and activator of transcription 1-alpha/beta	con vs act	1.6	0.55	−1.2	0.75	**4.4**	**1.3×10^{-3}**
		act vs dex	−1.6	0.16	−1.7	0.25	**−2.6**	**3.0×10^{-3}**
P52630	Signal transducer and activator of transcription 2	con vs act	n.d.	n.d.	1.2	0.78	**8.9**	**2.7×10^{-4}**
		act vs dex	n.d.	n.d.	−1.3	0.63	**−4.6**	**8.0×10^{-4}**
P42226	Signal transducer and activator of transcription 6	con vs act	n.d.	n.d.	1.1	0.94	**4.2**	**0.037**
		act vs dex	n.d.	n.d.	−1.9	0.14	−3.2	0.09
P05412	Transcription factor AP-1	con vs act	n.d.	n.d.	−4.0	0.23	**3.0**	**0.014**
		act vs dex	n.d.	n.d.	−1.2	0.84	−3.0	0.10
Q04206	Transcription factor p65	con vs act	n.d.	n.d.	1.3	0.57	**2.3**	**0.012**
		act vs dex	n.d.	n.d.	−2.1	0.07	−1.6	0.17
Q01201	Transcription factor RelB	con vs act	n.d.	n.d.	1.8	0.47	**4.4**	**1.5×10^{-3}**
		act vs dex	n.d.	n.d.	−2.3	0.15	−1.6	0.22
Q16670	Zinc finger protein 187	con vs act	n.d.	n.d.	**3.0**	**2.4×10^{-3}**	**10.0**	**9.2×10^{-3}**
		act vs dex	n.d.	n.d.	−1.4	0.32	−1.0	0.95

Table 3. Redox Regulation

accession	protein name		fold change SN	*p*-value SN	fold change CYT	*p*-value CYT	fold change NE	*p*-value NE
Q9Y305	Acyl-coenzyme A thioesterase 9, mitochondrial	con vs act	n.d.	n.d.	1.5	0.16	**2.3**	**0.033**
		act vs dex	n.d.	n.d.	−2.0	0.16	−1.7	0.27
P00390	Glutathione reductase, mitochondrial	con vs act	−1.1	0.73	1.1	0.83	**−2.8**	**5.5×10^{-3}**
		act vs dex	1.1	0.45	−1.5	0.37	−1.2	0.64
P09488	Glutathione S-transferase Mu 1	con vs act	−1.5	0.71	2.4	0.57	**−2.9**	**3.9×10^{-3}**
		act vs dex	2.0	0.43	1.2	0.89	−1.3	0.70
Q86U28	Iron−sulfur cluster assembly 2 homologue, mitochondrial	con vs act	n.d.	n.d.	**5.4**	**0.050**	n.d.	n.d.
		act vs dex	n.d.	n.d.	−2.0	0.39	n.d.	n.d.
O75438	NADH dehydrogenase [ubiquinone] 1 beta subcomplex subunit 1	con vs act	n.d.	n.d.	**6.6**	**0.029**	−2.2	0.49
		act vs dex	n.d.	n.d.	−2.0	0.25	3.7	0.15
Q7RTP6	Protein-methionine sulfoxide oxidase MICAL3	con vs act	n.d.	n.d.	**−5.0**	**0.033**	2.2	0.08
		act vs dex	n.d.	n.d.	**4.8**	**2.4×10^{-3}**	−1.9	0.27
Q8WU10	Pyridine nucleotide-disulfide oxidoreductase domain-containing protein 1	con vs act	n.d.	n.d.	**−3.8**	**0.017**	−1.0	0.94
		act vs dex	n.d.	n.d.	2.8	0.10	1.2	0.75
Q9BV79	Trans-2-enoyl-CoA reductase, mitochondrial	con vs act	n.d.	n.d.	1.7	0.65	**4.1**	**0.027**
		act vs dex	n.d.	n.d.	−1.0	0.98	−1.4	0.57

1289 when considering proteins that were identified only in one subcellular fraction (Figure 1A). Comparative proteome profiling of the two cell states was performed to determine proteins that were significantly up- or downregulated in inflammatory activated in comparison to their level in nonactivated PBMCs. Four-hundred sixty nine proteins were significantly ($p < 0.05$) up- or downregulated with a minimum of 2-fold change of LFQ value between control and inflammatory activated cells, as determined by label-free quantification using the Max Quant software. Out of these, 92, 143, and 281 proteins were found in the secretome, cytoplasm, and nuclear fractions, respectively, or 70, 107, and 253 when considering only those proteins that were found exclusively in one subcellular fraction (Figure 1B). Otherwise expressed, 6.9, 3.0, and 6.8% of the secreted, cytoplasmic, and nuclear proteins, respectively, were found to be differentially regulated in activated PBMCs versus control cells.

In order to obtain a better general overview of the data, we organized the 469 significantly regulated proteins into groups according to their cellular functionalities, which were inflammatory response, transcriptional regulation, redox regulation, organization of cytoskeleton, cell adhesion/migration, cell cycle/apoptosis, DNA repair, metabolism, protein degradation, protein transport, signaling, and others (Supporting Information Table S3 lists difference and significance values for each protein in each of the three subcellular fractions). Tables 1−3 list selected extracts from Table S3 with representatives for the most relevant functionalities. First, Table 1 lists proteins known to play a general role in inflammation, such as chemokines and interleukins. Upregulation of these proteins actually proved that induction of

inflammatory activation in PBMCs was successful. Thereby, the most significantly upregulated chemokines, C-C motif chemokine 2 (CCL2), C-X-C motif chemokine 5 (CXCL5), and growth-regulated alpha protein (GROα), were exclusively detected in the secretome of the activated cells. Other chemokines and interleukins were found to be upregulated in the cytoplasm as well, indicating that these proteins were secreted not only in increased amounts but also were indeed newly synthesized by the activated cells. This applied for CCL3, CXCL2, interleukin-1 alpha (IL-1α), IL-1β, IL-6, and IL-8. Interestingly, some inflammatory mediators such as CCL20, CCL4, IL-27 subunit beta, and IL-36 gamma were found to be upregulated in the cytoplasm but not in the secretome. This may indicate that these proteins were synthesized in the cytoplasm of activated cells but their secretion was not yet induced, suggesting that they may become relevant in a later step of inflammation. Other inflammatory mediators found to be upregulated in activated PBMCs were several members of the interferon (IFN) family, such as 2−3-oligoadenylate synthase 1 and 3, which are responsible for antiviral responses. In particular, IFN-induced proteins with tetratricopeptide repeats (IFITs) were also found to be upregulated: IFIT2 and IFIT3 in the secretome and the cytoplasm and IFIT1 only in the cytoplasm of activated PBMCs. Furthermore, members of the tumor necrosis factor alpha (TNFα) and the transforming growth factor beta-1 (TGFβ1) families were upregulated likewise in addition to other proteins known to be involved in inflammation such as indoleamine 2,3-dioxygenase 1 (IDO1), pentraxin-related protein 3 (PTX3), and prostaglandin G/H synthase 2 (COX2). On the other hand, some of the proteins in this group were found to be downregulated upon inflammatory activation. This applied, for example, for scavenger receptor cysteine-rich type 1 protein M130 (CD163), fibroleukin, macrophage colony-stimulating factor 1 receptor, monocyte differentiation antigen CD14 (CD14), and ADP ribosyl cyclase 2.

Several proteins apparently involved in transcriptional regulation are listed in Table 2. Some of those are already known to play a role in inflammatory processes. This applies to many transcription factors, such as AP-1, CCAAT/enhancer-binding protein delta, p65, and RelB, and several signal transducers and activators of transcription, such as STAT 1-alpha/beta, STAT 2, and STAT 6, which were found to be upregulated in inflammatory activated cells, as expected. Other proteins involved in transcription, such as helicase-like transcription factor, nuclear receptor subfamily 4 group A member 3, probable methyltransferase TARBP1, and zinc finger proteins were found to be significantly upregulated as well, even though their role in inflammatory processes has not yet been established. Concerning proteins related to redox processes (Table 3), we found both significant up- and downregulation in the cytoplasm as well as in the nuclear extract of activated cells. Downregulated proteins were, for example, glutathione S-transferase mu 1 and glutathione reductase in the nuclear extract as well as protein-methionine sulfoxide oxidase MICAL3 and pyridine nucleotide-disulfide oxidoreductase domain-containing protein 1 in the cytoplasm. Upregulated proteins were acyl-coenzyme A thioesterase 9 and trans-2-enoyl-CoA reductase in the nuclear fraction as well as iron−sulfur cluster assembly 2 homologue and NADH dehydrogenase [ubiquinone] 1 beta subcomplex subunit 1 in the cytoplasm.

Dexamethasone-Induced Reversion of Inflammatory Activation Is Not Fully Reconstituting the Original Cell State in Normal Primary Human PBMCs

Inflammatory activated PBMCs were treated with dexamethasone in order to analyze the capability of this antiphlogistic drug to counter-regulate protein synthesis previously induced by an inflammatory process in these cells. For this purpose, 1 h after stimulation, the inflammatory activated PBMCs were treated with dexamethasone for a further 3 h. Proteome profiling was then performed, and the obtained results were compared to those of activated cells that had not been treated. In combination with untreated and inflammatory stimulated cells, a total of 85 501 highly confident distinct peptides corresponding to 6886 proteins were identified (Supporting Information Table S2). All data sets have been made publicly available via ProteomeXchange (Supporting Information Table S1; DOI 10.6019/PXD001415−23). Here, all raw-files comprised 6 748 700 MS^2 spectra with 2 046 004 peptide spectrum matches containing 108 195 distinct peptides with the default Mascot significance score better than 0.05, assembling a total list of 8088 distinct protein groups. All results obtained from searching the data with Mascot can be freely downloaded. Comparative data analysis was supported by the 2D annotation enrichment tool included in Perseus, a statistical package of MaxQuant. In this way, it became apparent that almost all upregulated chemokines and interleukins previously described were successfully downregulated upon treatment with dexamethasone (Table 1). In particular, interleukins such as IL-1α, IL-1β, IL-6, and IL-8, which were upregulated in the secretome as well as in the cytoplasm of activated PBMCs, were now significantly downregulated in both fractions. In the case of transcriptional regulation, all proteins upregulated upon inflammatory activation were downregulated upon treatment with the antiphlogistic drug. For helicase-like transcription factor, STAT 1-alpha/beta and STAT 2, this effect was significant (Table 2). In contrast to this consistent effect on transcription factors, redox-regulating enzymes were affected by the dexamethasone treatment in differing ways. From three proteins that were upregulated upon inflammatory activation, one was significantly downregulated upon dexamethasone treatment, namely, protein-methionine sulfoxide oxidase MICAL3, whereas the others, glutathione S-transferase mu 1 and glutathione reductase, showed a further, yet lower, increase, detected in the nuclear extract (Table 3).

In order to classify the predominant molecular functionalities in the cells that are upregulated by LPS/PHA and then downregulated by dexamethasone, we organized the proteins according to gene ontology terms for molecular functions (MFs). For each subcellular fraction, we selected the five MFs in which the highest effects of dexamethasone with regard to counter-regulating the inflammation process were observed. In Figure 2, the relative amounts of proteins measured for each of these MFs are compared. In the secretome, proteins related to cytokine and chemokine activity and chemokine-, cytokine-, and G-protein coupled receptor binding were upregulated in activated PBMCs, an effect that was largely reversed upon treatment with dexamethasone. In the nuclear extracts, proteins related to helicase activity, DNA binding, DNA-dependent ATPase activity, and structural constituents of cytoskeleton upregulated in inflammatory activated PBMCs were found to be downregulated when applying dexamethasone. In contrast to this, proteins were also observed that were downregulated in activated cells and upregulated in drug-treated cells, which, in

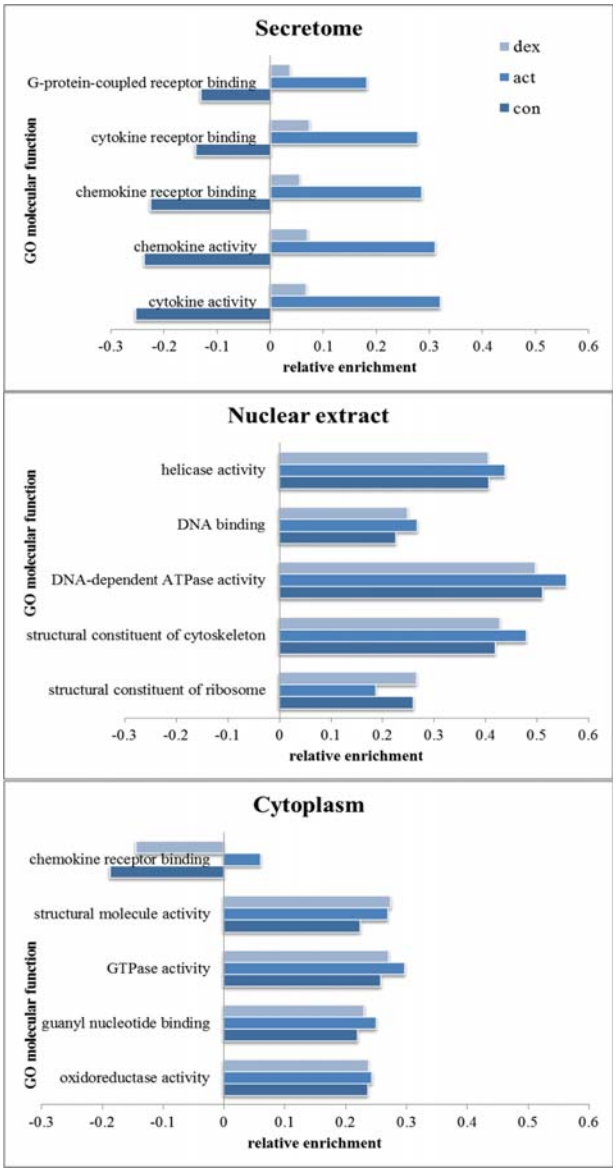

Figure 2. Two-dimensional annotation enrichment of control PBMCs, inflammatory activated PBMCs, and activated PBMCs after treatment with dexamethasone. Two-dimensional annotation enrichment of molecular functions according to gene ontology (GO) terms was performed using Perseus. Categories for each subcellular fraction, in which proteins were most highly regulated between control (con) and activated (act) PBMCs, were selected for enrichment analysis. Additionally, enrichment analysis was performed between nontreated (act) and treated (dex) inflammatory activated cells. Average ranks, indicating relative protein abundances in the respective categories, were determined according to Geiger et al.[20] The corresponding *p*-values, corrected for multiple parameters according to Benjamini–Hochberg, are less than 1×10^{-4} in the case of SN, less than 0.02 in the case of NE, and less than 0.005 in the case of CYT.

this regard, is reconstituting the functional state of control cells. These proteins were related to structural constituents of ribosomes. In the cytoplasmic fraction, counter-regulation of inflammatory effects upon dexamethasone treatment were observed for proteins related to chemokine receptor binding, GTPase activity, guanyl nucleotide binding, and oxidoreductase activity. Counter-regulation was not observed in all cases, as demonstrated for proteins related to structural molecule activity, which were not reconstituted to the original cellular state upon drug treatment.

Actually, we were able to differentiate four groups of proteins distinguished by different regulation patterns (Figure 3). The first group encompassed proteins that were significantly upregulated in inflammatory activated PBMCs and significantly downregulated upon treatment with dexamethasone. This group contained proteins such as inhibin beta A chain, IL-6, and CCL2. The second group contained proteins that showed a significant downregulation upon inflammatory activation and a further significant upregulation upon dexamethasone treatment. This applied to scavenger receptor cysteine-rich type 1 protein M130, fibroleukin, and metalloproteinase inhibitor 2. The third group concerned proteins such as IFN-stimulated gene 20 kDa protein, IFIT2, and PTX3, which were significantly upregulated in activated PBMCs but showed no successful counter-regulation when applying dexamethasone. Other IFN-family members, such as IFIT1 and IFIT3, also belonged to this group. Finally, the last group applied to proteins that were significantly downregulated in inflammatory activated PBMCs such as ADP-ribosyl cyclase 2, macrophage colony-stimulating factor 1 receptor, and CD14. Concerning the regulation of these proteins, no responsiveness to the treatment with dexamethasone was observed.

In order to verify the results obtained with the label-free quantification technique, an independent targeted MS approach using MRM was applied. Six well-known inflammatory mediators were analyzed, namely, IL-1β, IL-6, CXCL2, GROα, PTX3, and tumor necrosis factor-inducible gene 6 protein (TSG6). As demonstrated in Figure 4, PBMCs of all donors showed upregulation of IL-1β, IL-6, CXCL2, and GROα upon inflammatory activation, followed by a down-regulation when applying dexamethasone. In contrast to these counter-regulated proteins, PTX3 and TSG6 showed a further upregulation upon treatment with dexamethasone in all donors. Although, especially in the case of PTX3, high individual variances in protein abundance were observed, the tendency toward up- and downregulation was consistent in the different donors.

DISCUSSION

In this study, we demonstrated that in-depth proteome profiling can be used to characterize a cell's response to a functional stimulation as well as to an applied drug on the level of protein regulation. Indeed, treatment of inflammatory activated primary human PBMCs with an antiphlogistic drug resulted in readily detectable proteome alterations, in accordance with expectations. However, although the regulation of known inflammatory mediators such as interleukins and chemokines showed very good responsiveness to dexamethasone, members of the IFN family remained rather unaffected upon drug treatment. These data indicate that the original cell state, i.e., before inflammatory activation, cannot be fully reconstituted by the application of dexamethasone to stimulated PBMCs. Since glucocorticoids are frequently used drugs for the treatment of inflammatory diseases and the development of resistance is a common drawback, the analysis of drug effects is an important research topic. In contrast to other strategies, such as different functional genomics approaches[22,23] or flow cytometric analysis of immune cells,[24] here we provide a proteome profiling approach to investigate

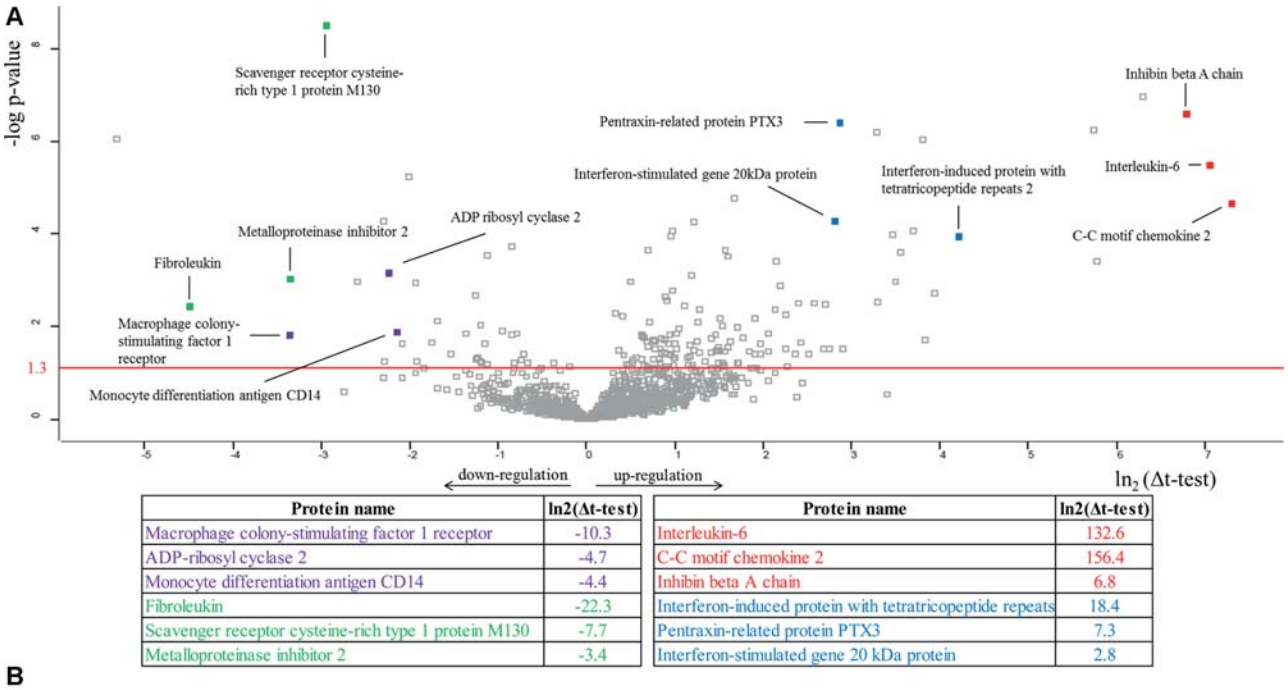

Protein name	ln2(Δt-test)
Macrophage colony-stimulating factor 1 receptor	-10.3
ADP-ribosyl cyclase 2	-4.7
Monocyte differentiation antigen CD14	-4.4
Fibroleukin	-22.3
Scavenger receptor cysteine-rich type 1 protein M130	-7.7
Metalloproteinase inhibitor 2	-3.4

Protein name	ln2(Δt-test)
Interleukin-6	132.6
C-C motif chemokine 2	156.4
Inhibin beta A chain	6.8
Interferon-induced protein with tetratricopeptide repeats	18.4
Pentraxin-related protein PTX3	7.3
Interferon-stimulated gene 20 kDa protein	2.8

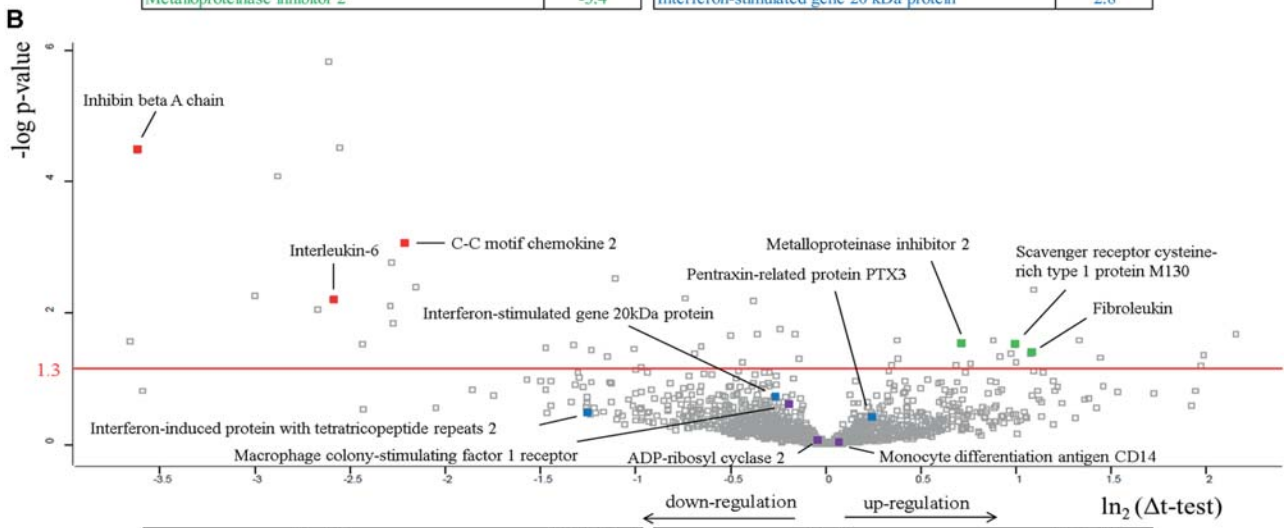

Protein name	ln2(Δt-test)
Interleukin-6	-6.0
C-C motif chemokine 2	-4.7
Inhibin beta A chain	-3.6
Interferon-induced protein with tetratricopeptide repeats 2	-2.4
Pentraxin-related protein PTX3	1.2
Interferon-stimulated gene 20 kDa protein	-0.3

Protein name	ln2(Δt-test)
Macrophage colony-stimulating factor 1 receptor	-1.2
ADP-ribosyl cyclase 2	-1.1
Monocyte differentiation antigen CD14	1.0
Fibroleukin	2.1
Scavenger receptor cysteine-rich type 1 protein M130	2.0
Metalloproteinase inhibitor 2	0.7

Figure 3. Protein regulation patterns related to inflammatory activation and subsequent treatment with dexamethasone. Volcano plots show the *p*-value and fold-change of secreted proteins in (A) control versus activated PBMC and (B) activated versus dexamethasone-treated PBMCs. Red-labeled proteins show a significant upregulation in inflammatory activated PBMCs and a significant downregulation upon treatment with dexamethasone. In contrast, green-labeled proteins are significantly downregulated upon inflammatory activation and significantly counter-regulated. Blue- and purple-labeled proteins show a significant up- or downregulation in activated cells, but, concerning the regulation of these proteins, hardly any responsiveness to dexamethasone was observed. The LFQ-based difference values of the means (logarithmic values based on 2) corresponding to the highlighted proteins are indicated.

cellular responses associated with drug application in inflammatory activated PBMCs in great detail.

In the secretome of PBMCs, the proportion of proteins that were significantly up- and downregulated upon inflammatory activation or treatment with dexamethasone was higher when compared to that in the cytoplasm and nuclear extracts. The present data confirmed that many cytokines such as IL-1α, IL-1β, IL-6, IL-8, CCL2, CCL3, and CXCL2 showed an increase upon inflammatory activation and a successful decrease upon treatment with dexamethasone. Therefore, the analyzed differences in the secretomes seem to reflect drug effects adequately and therefore we suggest that such an assay could be

dx.doi.org/10.1021/pr5008625 | *J. Proteome Res.* 2014, 13, 5989−6000

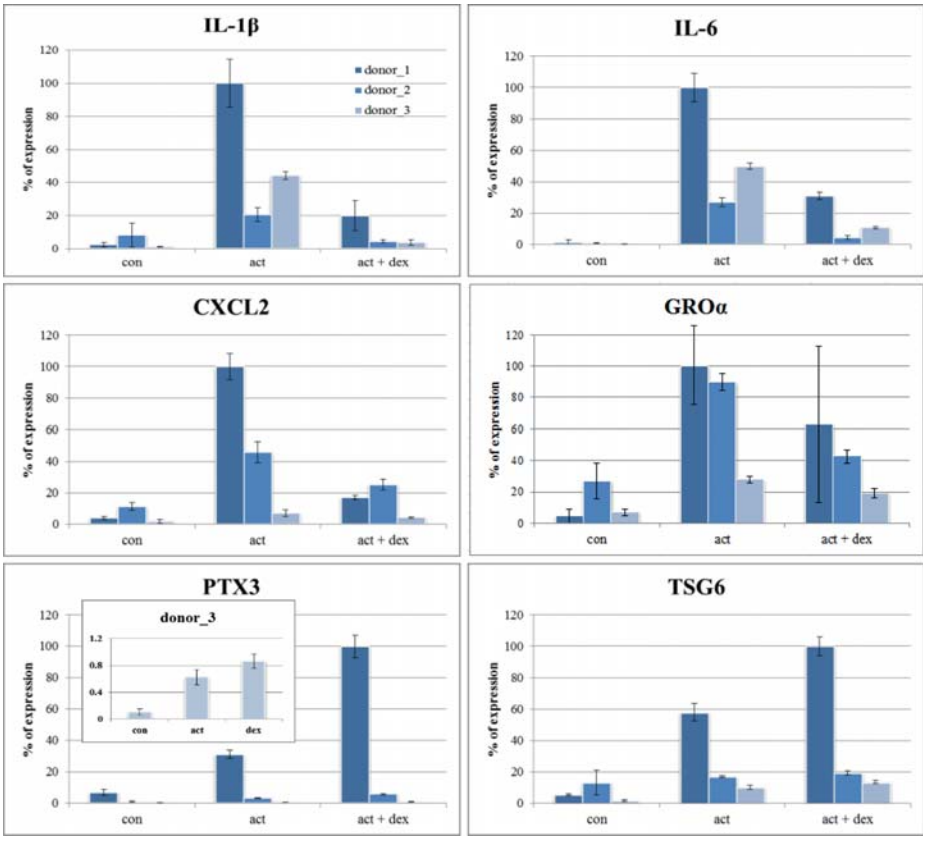

Figure 4. Targeted MS analysis of secreted proteins. Data obtained from MRM analysis of selected proteins isolated from PBMCs of three healthy donors at three different conditions, i.e., controls (con), inflammatory activated (act), and inflammatory activated and dexamethasone-treated PBMCs (act + dex), are represented. IL-1β, IL-6, CXCL2, GROα, PTX3, and TSG6 were analyzed. The mean and standard deviation were calculated from three technical replicates. The highest peak area determined for a protein was set to 100%, and the other peak areas were calculated relative to this.

used for comprehensive drug evaluations. Other inflammatory molecules such as CCL20, IL-27 subunit beta, and IL-36 gamma were found to be upregulated only in the cytoplasm, but not in the secretome, of activated PBMCs. The secretion of these proteins might not yet be fully induced, since we investigated an early step of inflammation. In addition, with regard to the regulation of these proteins, hardly any responsiveness to dexamethasone was observed. Such cytokines, which accumulated in the cells and were found to be hardly downregulated by dexamethasone, may be of great physiological relevance since they may be released upon specific stimulation at later time points or the release may occur nonspecifically in the case of secondary necrosis. The latter scenario, which may be relevant in the case of joint diseases or other types of inflammation occurring in tissues with poor blood supply, would explain the escalation of local inflammatory signaling and thus represent an undesirable mechanism supporting the establishment of chronic inflammation.

Members of the IFN-family, i.e., IFIT1, IFIT2, and IFIT3, as well as 2−5-oligoadenylate synthase 1 and 2−5-oligoadenylate synthase 3, showed upregulation upon stimulation, but regulation of these proteins showed hardly any responsiveness to dexamethasone. IFITs and 2−5-oligoadenylate synthases are main players in the antiviral host defense and activation-induced cell death.[25] Therefore, the inability of dexamethasone to downregulate these proteins is compatible with the known induction of apoptosis in T-cells by dexamethasone.[26] The normal physiologic consequence of inflammatory activation in T-cells is 2-fold: induction of pro-inflammatory mediators and subsequent induction of activation-induced cell death in order to avoid uncontrolled escalation of inflammation.[27,28] As demonstrated above, dexamethasone successfully inhibited the induction of pro-inflammatory mediators. However, mediators of activation-induced cell death were not switched off by dexamethasone; consequently, apoptosis can still occur. This consideration, pointing both to functional inhibition of inflammatory signaling together with induction of apoptosis in main inflammatory players, may help to better understand the great therapeutic efficiency of this drug demonstrated in clinical practice.

As the interindividual variations in the proteome of human PBMCs may be very high,[31] for a more accurate evaluation, we performed an independent targeted MRM approach for selected molecules. Indeed, not only did basal protein concentrations vary by up to 30-fold as demonstrated in the case of PTX3 (donor 1 vs 3) but also the individual induction rates varied by more than 10-fold as exemplified for IL-1β (donor 1 vs 2). Remarkably, the relative effects of dexamethasone treatment were still highly similar in these donors. In addition, these data suggest that dexamethasone can either act as agonist or antagonist of protein synthesis. In the case of pro-inflammatory molecules such as IL-1β, IL-6, CXCL2, and GROα, the application of dexamethasone resulted in down-regulation. In the case of inflammation-modulating molecules

like PTX3 and TSG6,[29,30] dexamethasone further increased protein synthesis in all three donors. Furthermore, these data clearly demonstrate the technical feasibility of assessing cellular responsiveness and drug effects in an individualized fashion. We are currently establishing a MRM-based cytokine, chemokine, and growth factor quantitation assay comprising almost a hundred different proteins, which will allow us to meaningfully assess cell functionalities as well as drug responsiveness in an individualized fashion.

The experimental design of the present project can actually support many more investigations based on the data set, which was made publicly available via ProteomeXchange. To give an example, the systematic comparison of proteins downregulated in the cytoplasm but concomitantly upregulated in the nuclear fractions identifies protein translocation events accompanying inflammatory activation or drug responsiveness, respectively. Functional studies are currently being conducted that will corroborate the biological significance of such events.

Thus, in this study, the known clinical effects of dexamethasone were very well-reflected by the drug-induced cellular effects on protein regulation. This observation clearly indicated that drug effects may well be evaluated by proteome profiling. Using a targeted approach that screens for drug effects by quantitative determination of specific protein regulation events is becoming a realistic option.

CONCLUSIONS

This work demonstrates that the combination of in-depth proteome profiling and targeted analysis of the most relevant molecules is a powerful strategy for investigating drug effects in an individualized fashion. Expected drug effects such as the dexamethasone-induced downregulation of inflammatory cytokines were clearly observed, whereas several other inflammation-induced proteins were unexpectedly further aggravated by this anti-inflammatory drug. Overall, proteome-based drug evaluation may provide a comprehensive overview of the regulation of cellular activities comprising the observation of expected effects as well as unexpected adverse drug effects.

ASSOCIATED CONTENT

Supporting Information

Figure S1: Calibration curve for internal standard peptide Glu1-Fribrinopeptide B. Table S1. Assignment of PRIDE Identifiers and DOIs to the corresponding data set. Mass spectrometry proteomics data have been deposited to the ProteomeXchange Consortium via the PRIDE partner repository with specific data set identifiers and corresponding accession numbers (DOIs). In this table, each identifier and DOI has been assigned to the corresponding data set. Table S2: Proteins identified in control, inflammatory activated, and dexamethasone-treated PBMCs. Table S3: Significantly regulated proteins in inflammatory activated PBMCs and their regulation upon treatment with dexamethasone. This material is available free of charge via the Internet at http://pubs.acs.org.

AUTHOR INFORMATION

Corresponding Author

*E-mail: christopher.gerner@univie.ac.at. Tel.: +43-1-4277-52302.

Notes

The authors declare no competing financial interest.

ACKNOWLEDGMENTS

We thank the Faculty of Chemistry for continuous support. We are thankful to Attila Csordas and all other members of the PRIDE team for helping us with the deposition of our data to the ProteomeXchange Consortium.

ABBREVIATIONS

CCL, C-C motif chemokine; COX, cyclooxygenase; CPDA, citrate−phosphate−dextrose solution with adenine; CXCL, C-X-C motif chemokine; FA, formic acid; FDR, false discovery rate; GO, gene ontology; GROα, growth-regulated alpha protein; IAA, iodoacetamide; IFIT, IFN-induced proteins with tetratricopeptide repeats; IFN, interferon; LFQ, label-free quantification; LPS, lipopolysaccharide; MFs, molecular functions; MRM, multiple reaction monitoring; MWCO, molecular weight cutoff; NFκB, nuclear factor kappa-light-chain-enhancer of activated B cells; PBMCs, peripheral blood mononuclear cells; PHA, phythemeagglutinin; PRIDE, Proteomics Identification Database; PTX3, pentraxin-related protein 3; STAT, signal transducers and activators of transcription; TSG6, tumor necrosis factor-inducible gene 6 protein

REFERENCES

(1) Haudek-Prinz, V. J.; Klepeisz, P.; Slany, A.; Griss, J.; Meshcheryakova, A.; Paulitschke, V.; Mitulovic, G.; Stockl, J.; Gerner, C. Proteome signatures of inflammatory activated primary human peripheral blood mononuclear cells. *J. Proteomics* **2012**, *76*, 150−62.

(2) Koncarevic, S.; Lossner, C.; Kuhn, K.; Prinz, T.; Pike, I.; Zucht, H. D. In-depth profiling of the peripheral blood mononuclear cells proteome for clinical blood proteomics. *Int. J. Proteomics* **2014**, *2014*, 129259.

(3) Curtis, J. R.; Westfall, A. O.; Allison, J.; Bijlsma, J. W.; Freeman, A.; George, V.; Kovac, S. H.; Spettell, C. M.; Saag, K. G. Population-based assessment of adverse events associated with long-term glucocorticoid use. *Arthritis Rheum.* **2006**, *55*, 420−6.

(4) Samuels, A. L.; Heng, J. Y.; Beesley, A. H.; Kees, U. R. Bioenergetic modulation overcomes glucocorticoid resistance in T-lineage acute lymphoblastic leukaemia. *Br. J. Hamaetol.* **2014**, *165*, 57−66.

(5) Coutinho, A. E.; Chapman, K. E. The anti-inflammatory and immunosuppressive effects of glucocorticoids, recent developments and mechanistic insights. *Mol. Cell. Endocrinol.* **2011**, *335*, 2−13.

(6) Newton, R. Molecular mechanisms of glucocorticoid action: what is important? *Thorax* **2000**, *55*, 603−13.

(7) Lowenberg, M.; Stahn, C.; Hommes, D. W.; Buttgereit, F. Novel insights into mechanisms of glucocorticoid action and the development of new glucocorticoid receptor ligands. *Steroids* **2008**, *73*, 1025−9.

(8) Rhen, T.; Cidlowski, J. A. Antiinflammatory action of glucocorticoids—new mechanisms for old drugs. *N. Engl. J. Med.* **2005**, *353*, 1711−23.

(9) Caulfield, J.; Fernandez, M.; Snetkov, V.; Lee, T.; Hawrylowicz, C. CXCR4 expression on monocytes is up-regulated by dexamethasone and is modulated by autologous $CD3^+$ T cells. *Immunology* **2002**, *105*, 155−62.

(10) Murphy, S. H.; Suzuki, K.; Downes, M.; Welch, G. L.; De Jesus, P.; Miraglia, L. J.; Orth, A. P.; Chanda, S. K.; Evans, R. M.; Verma, I. M. Tumor suppressor protein (p)53, is a regulator of NF-kappaB repression by the glucocorticoid receptor. *Proc. Natl. Acad. Sci. U.S.A.* **2011**, *108*, 17117−22.

(11) Zhang, C. C.; Kast, J. Applications of current proteomics techniques in modern drug design. *Curr. Comput.-Aided Drug Des.* **2010**, *6*, 147−64.

(12) Paulitschke, V.; Haudek-Prinz, V.; Griss, J.; Berger, W.; Mohr, T.; Pehamberger, H.; Kunstfeld, R.; Gerner, C. Functional

classification of cellular proteome profiles support the identification of drug resistance signatures in melanoma cells. *J. Proteome Res.* **2013**, *12*, 3264−76.
(13) Chen, S.; Dong, Q.; Hu, S.; Cai, J.; Zhang, W.; Sun, J.; Wang, T.; Xie, J.; He, H.; Xing, J.; Lu, J.; Dong, Y. Proteomic analysis of the proteins that are associated with the resistance to paclitaxel in human breast cancer cells. *Mol. BioSyst.* **2014**, *10*, 294−303.
(14) Cox, J.; Mann, M. MaxQuant enables high peptide identification rates, individualized p.p.b.-range mass accuracies and proteome-wide protein quantification. *Nat. Biotechnol.* **2008**, *26*, 1367−72.
(15) Slany, A.; Haudek, V. J.; Gundacker, N. C.; Griss, J.; Mohr, T.; Wimmer, H.; Eisenbauer, M.; Elbling, L.; Gerner, C. Introducing a new parameter for quality control of proteome profiles: consideration of commonly expressed proteins. *Electrophoresis* **2009**, *30*, 1306−28.
(16) Mortz, E.; Krogh, T. N.; Vorum, H.; Gorg, A. Improved silver staining protocols for high sensitivity protein identification using matrix-assisted laser desorption/ionization-time of flight analysis. *Proteomics* **2001**, *1*, 1359−63.
(17) Wisniewski, J. R.; Zougman, A.; Nagaraj, N.; Mann, M. Universal sample preparation method for proteome analysis. *Nat. Methods* **2009**, *6*, 359−62.
(18) Vizcaino, J. A.; Deutsch, E. W.; Wang, R.; Csordas, A.; Reisinger, F.; Rios, D.; Dianes, J. A.; Sun, Z.; Farrah, T.; Bandeira, N.; Binz, P. A.; Xenarios, I.; Eisenacher, M.; Mayer, G.; Gatto, L.; Campos, A.; Chalkley, R. J.; Kraus, H. J.; Albar, J. P.; Martinez-Bartolome, S.; Apweiler, R.; Omenn, G. S.; Martens, L.; Jones, A. R.; Hermjakob, H. ProteomeXchange provides globally coordinated proteomics data submission and dissemination. *Nat. Biotechnol.* **2014**, *32*, 223−6.
(19) Cox, J.; Mann, M. 1D and 2D annotation enrichment: a statistical method integrating quantitative proteomics with complementary high-throughput data. *BMC Bioinf.* **2012**, *13*, S12.
(20) Geiger, T.; Cox, J.; Mann, M. Proteomic changes resulting from gene copy number variations in cancer cells. *PLoS Genet.* **2010**, *6*, e1001090.
(21) MacLean, B.; Tomazela, D. M.; Shulman, N.; Chambers, M.; Finney, G. L.; Frewen, B.; Kern, R.; Tabb, D. L.; Liebler, D. C.; MacCoss, M. J. Skyline: an open source document editor for creating and analyzing targeted proteomics experiments. *Bioinformatics* **2010**, *26*, 966−8.
(22) Luca, F.; Maranville, J. C.; Richards, A. L.; Witonsky, D. B.; Stephens, M.; Di Rienzo, A. Genetic, functional and molecular features of glucocorticoid receptor binding. *PLoS One* **2013**, *8*, e61654.
(23) Xiang, L.; Marshall, G. D., Jr. Immunomodulatory effects of dexamethasone on gene expression of cytokine and stress hormone receptors in peripheral blood mononuclear cells. *Int. Immunopharmacol.* **2013**, *17*, 556−60.
(24) Zhang, H.; Cardell, L. O.; Bjorkander, J.; Benson, M.; Wang, H. Comprehensive profiling of peripheral immune cells and subsets in patients with intermittent allergic rhinitis compared to healthy controls and after treatment with glucocorticoids. *Inflammation* **2013**, *36*, 821−9.
(25) Zhou, X.; Michal, J. J.; Zhang, L.; Ding, B.; Lunney, J. K.; Liu, B.; Jiang, Z. Interferon induced IFIT family genes in host antiviral defense. *Int. J. Biol. Sci.* **2013**, *9*, 200−8.
(26) Miller, A. L.; Webb, M. S.; Copik, A. J.; Wang, Y.; Johnson, B. H.; Kumar, R.; Thompson, E. B. p38 mitogen-activated protein kinase (MAPK) is a key mediator in glucocorticoid-induced apoptosis of lymphoid cells: correlation between p38 MAPK activation and site-specific phosphorylation of the human glucocorticoid receptor at serine 211. *Mol. Endocrinol.* **2005**, *19*, 1569−83.
(27) Barber, G. N. Host defense, viruses and apoptosis. *Cell Death Differ.* **2001**, *8*, 113−26.
(28) Takaoka, A.; Hayakawa, S.; Yanai, H.; Stoiber, D.; Negishi, H.; Kikuchi, H.; Sasaki, S.; Imai, K.; Shibue, T.; Honda, K.; Taniguchi, T. Integration of interferon-alpha/beta signalling to p53 responses in tumour suppression and antiviral defence. *Nature* **2003**, *424*, 516−23.
(29) Wisniewski, H. G.; Vilcek, J. Cytokine-induced gene expression at the crossroads of innate immunity, inflammation and fertility: TSG-6 and PTX3/TSG-14. *Cytokine Growth Factor Rev.* **2004**, *15*, 129−46.
(30) Nauta, A. J.; Bottazzi, B.; Mantovani, A.; Salvatori, G.; Kishore, U.; Schwaeble, W. J.; Gingras, A. R.; Tzima, S.; Vivanco, F.; Egido, J.; Tijsma, O.; Hack, E. C.; Daha, M. R.; Roos, A. Biochemical and functional characterization of the interaction between pentraxin 3 and C1q. *Eur. J. Immunol.* **2003**, *33*, 465−73.
(31) Vizcaino, J. A.; Cote, R. G.; Csordas, A.; Dianes, J. A.; Fabregat, A.; Foster, J. M.; Griss, J.; Alpi, E.; Birim, M.; Contell, J.; O'Kelly, G.; Schoenegger, A.; Ovelleiro, D.; Perez-Riverol, Y.; Reisinger, F.; Rios, D.; Wang, R.; Hermjakob, H. The PRoteomics IDEntifications (PRIDE) database and associated tools: status in 2013. *Nucleic Acids Res.* **2013**, *41*, D1063−9.

3.2. Impact of a synthetic cannabinoid (CP-47,497-C8) on protein expression in human cells: evidence for induction of inflammation and DNA damage

Andrea Bileck[a], Franziska Ferk[b], Halh Al-Serori[b], Verena J. Koller[b], Besnik Muqaku[a], Alexander Haslberger[c], Volker Auwärter[d], Christopher Gerner[a], Siegfried Knasmüller[b]

Archives of Toxicology, **2015,** doi:10.1007/s00204-015-1569-7

[a] Department of Analytical Chemistry, Faculty of Chemistry, University of Vienna, Währinger Str. 38, A-1090 Vienna, Austria

[b] Department of Internal Medicine 1, Comprehensive Cancer Center, Institute of Cancer Research, Medical University of Vienna, Borschkegasse 8A, A-1090 Vienna, Austria

[c] Department of Nutritional Sciences, University of Vienna, UZA 2/2D541, Althanstrasse 14, A-1090, Austria

[d] Institute of Forensic Medicine, University Medical Center Freiburg, Albertstraße 9, 79104 Freiburg, Germany

Contributions to this publication:

- Conduction of shotgun proteomics experiments
- Creation of figures for shotgun proteomics data
- Involved in the planning of the experiments, data interpretation and writing of the manuscript

Arch Toxicol
DOI 10.1007/s00204-015-1569-7

MOLECULAR TOXICOLOGY

Impact of a synthetic cannabinoid (CP-47,497-C8) on protein expression in human cells: evidence for induction of inflammation and DNA damage

Andrea Bileck[1] · Franziska Ferk[2] · Halh Al-Serori[2] · Verena J. Koller[2] · Besnik Muqaku[1] · Alexander Haslberger[3] · Volker Auwärter[4] · Christopher Gerner[1] · Siegfried Knasmüller[2]

Received: 30 January 2015 / Accepted: 6 July 2015
© Springer-Verlag Berlin Heidelberg 2015

Abstract Synthetic cannabinoids (SCs) are marketed worldwide as legal surrogates for marihuana. In order to predict potential health effects in consumers and to elucidate the underlying mechanisms of action, we investigated the impact of a representative of the cyclohexylphenols, CP47,497-C8, which binds to both cannabinoid receptors, on protein expression patterns, genomic stability and on induction of inflammatory cytokines in human lymphocytes. After treatment of the cells with the drug, we found pronounced up-regulation of a variety of enzymes in nuclear extracts which are involved in lipid metabolism and inflammatory signaling; some of the identified proteins are also involved in the endogenous synthesis of endocannabinoids. The assumption that the drug causes inflammation is further supported by results obtained in additional experiments with cytosols of LPS-stimulated lymphocytes which showed that the SC induces pro-inflammatory cytokines (IL12p40 and IL-6) as well as TNF-α. Furthermore, the proteome analyses revealed that the drug causes down-regulation of proteins which are involved in DNA repair. This observation provides an explanation for the formation of comets which was seen in single-cell gel electrophoresis assays and for the induction of micronuclei (which reflect structural and numerical chromosomal aberrations) by the drug. These effects were seen in experiments with human lymphocytes which were conducted under identical conditions as the proteome analysis. Taken together, the present findings indicate that the drug (and possibly other structurally related SCs) may cause DNA damage and inflammation in directly exposed cells of consumers.

Keywords Synthetic cannabinoid · Comet assay · Lymphocytes · Proteomics

Abbreviations

B(a)P	Benzo(*a*)pyrene
BSA	Bovine serum albumin
CBs	Cannabinoid receptors
DDT	Dithiothreitol
IAA	Iodacetamide
FDR	False discovery rate
GC–MS	Gas chromatography–mass spectrometry
^{1}H NMR	Proton nuclear magnetic resonance
LC–MS	Liquid chromatography–mass spectrometry
LFQ	Label-free quantification
MNi	Micronuclei
Nbuds	Nuclear buds
NDI	Nuclear division indices
NPBs	Nucleoplasmatic bridges
PAGE	Polyacrylamide gel electrophoresis
PBMCs	Peripheral blood mononuclear cells
PHA	Phytohemagglutinin
SCs	Synthetic cannabinoids
SCGE	Single-cell gel electrophoresis

Electronic supplementary material The online version of this article (doi:10.1007/s00204-015-1569-7) contains supplementary material, which is available to authorized users.

✉ Siegfried Knasmüller
siegfried.knasmueller@meduniwien.ac.at

[1] Faculty of Chemistry, Institute of Analytical Chemistry, University of Vienna, Währingerstr. 38, 1090 Vienna, Austria

[2] Department of Internal Medicine 1, Comprehensive Cancer Center, Institute of Cancer Research, Medical University of Vienna, Borschkegasse 8A, 1090 Vienna, Austria

[3] Department of Nutritional Sciences, University of Vienna, UZA 2/2D541, Althanstrasse 14, 1090 Vienna, Austria

[4] Institute of Forensic Medicine, University Medical Center Freiburg, Albertstraße 9, 79104 Freiburg, Germany

Published online: 21 July 2015

SDS Sodium dodecyl sulfate
THC Tetrahydrocannabinol

Introduction

Synthetic cannabinoids (SCs) are marketed worldwide as substitutes for cannabis. These drugs bind to cannabinoid receptors (CBs) and cause psychotropic effects which are similar to those of natural phytocannabinoids (Uchiyama et al. 2009). The chemical structures of SCs are heterogeneous (Presley et al. 2013). "Classical" representatives are structurally related to tetrahydrocannabinol (THC), while "non-classical" compounds which entered the market later belong to various chemical groups. Cannabicyclohexanol (CP-47,497-C8) was used in the present study as a model for SCs which bind to both CB receptors. It is a representative of the cyclohexylphenols and was detected for the first time in a herbal mix termed "Spice" in Germany and Japan in 2008 (Auwärter et al. 2009; Uchiyama et al. 2009). In the following years, several structurally related compounds (e.g., CP-47,497 and CP-55,940) were detected in smoking mixtures (Presley et al. 2013). Figure S1 depicts the chemical structure of different SCs.

Only few investigations have been conducted which concern the toxicological properties of SCs apart from their neurological effects. Recent findings indicate that some of these drugs, including CP-47,497-C8, cause damage of the genetic material (Koller et al. 2014). Furthermore, also acute toxic effects were observed in human-derived cells which were caused by interference with protein synthesis and damage of the cell membranes (Koller et al. 2013, 2014).

In order to elucidate the molecular mechanisms which cause these effects and other biological processes, which may have a negative impact on the health of drug users, we applied in the present investigation a proteomic-based screening approach which focused on a broad spectrum of cellular proteins. This method was successfully used in previous studies to improve the understanding of the toxicological properties of pharmaceuticals (Bileck et al. 2014; Klepeisz et al. 2013; Lorenz et al. 2009). Apart from damage of the genetic material, also inflammatory processes are associated with long-term effects of drugs including cancer (Okada 2014). Therefore, we focused in the present study particularly on expression patterns of proteins which are involved in DNA damage and repair and on changes of proteins which reflect inflammatory reactions.

For the proteome analysis, peripheral blood mononuclear cells (PBMCs) from different donors were exposed to CP-47,497-C8. Subsequently, nuclear proteins were isolated, and protein patterns were determined by means of a QExactive orbitrap mass spectrometer. The data analyses were supported by label-free quantification with MaxQuant software (Cox and Mann 2008). Furthermore, the altered expression of individual cytokines under identical experimental conditions was quantitatively determined with an additional approach, i.e., multiple reaction monitoring.

To find out whether alterations of the signatures of proteins which are involved in the maintenance of DNA stability are associated with damage of the genetic material, single-cell gel electrophoresis assays (SCGE) were performed which are based on the measurement of DNA migration in an electric field and enable the detection of single-, double-strand breaks and apurinic sites (Tice et al. 2000). Furthermore, also cytome experiments were conducted with the same indicator cells under identical conditions in which we monitored the impact of the drug on the formation of micronuclei (MNi) which reflects chromosome breakage and/or aneuploidy (Norppa and Falck 2003). In addition, also other nuclear anomalies which reflect genomic instability were scored in the cytome experiments, namely nuclear buds (Nbuds) which are caused by gene amplification and nucleoplasmatic bridges (NPBs), which are formed as a consequence of dicentric chromosomes (Fenech et al. 2003).

The observed alterations of the protein pattern indicated also the involvement of immune functions that are associated with inflammation. Therefore, additional experiments were conducted which concerned the impact of the drug on the immune status. The nuclear division indices (NDI), which were determined in the cytome experiments, provide information about the mitotic activity of lymphocytes. Furthermore, changes of the levels of important pro- and anti-inflammatory cytokines (IL-10, IL-6, IL12p40 and TNF-α) were measured under identical conditions as those used in the proteome experiments and in the genotoxicity assays.

Materials and methods

Test compound

Pure CP-47,497-C8 (CAS 70434-92-3) was obtained by extraction from commercial "Spice" products and subsequent purification by flash chromatography (Moosmann et al. 2012). The purity of the drug was assessed by GC-MS and ^{1}H NMR analysis and was >99 %. Stock solutions were prepared in DMSO and stored at −20 °C.

Proteomics

Isolation and treatment of peripheral blood mononuclear cells

Peripheral blood mononuclear cells (PBMCs) were collected from four male healthy non-smoking volunteers (age

25–32 years) with their written consent. None had a history of a recent disease and exposure to toxic chemicals and drugs. A total of 30.0 mL of whole blood were collected in 6.0-mL CPDA tubes (Greiner Bio-One GmbH, Austria) and subsequently diluted 1:2 with RPMI 1640 medium (Gibco, Life Technologies, Austria) supplemented with 100 U/mL penicillin and 100.0 µg/mL streptomycin (ATCC, LGC Standards GmbH, Germany). Subsequently, the suspensions were carefully overlaid on Ficoll Paque (GE Healthcare, Bio-Sciences AB, Uppsala, Sweden) and centrifuged at 500×*g* for 20 min at 24 °C. PBMCs were collected from the interphase and washed with PBS. Afterward, the cell pellets were re-suspended in RPMI 1640 medium and transferred to Petri dishes (Greiner Bio-One GmbH, Austria). The cell suspensions of the individual donors were treated separately either with a solvent control or with a solution of the test compound (final concentration 10.0 µM). We used in all experiments a 3-h exposure time since we aimed to find changes in protein pattern which may provide an explanation for the results of the SCGE experiments which were also conducted with a 3-h treatment protocol. The subsequent proteome analyses were conducted separately with samples from the different donors.

Subcellular fractionation

After removal of the supernatants, the cells were lysed by addition of isotonic lysis buffer (10 mM HEPES/NaOH, pH 7.4, 0.25 M sucrose, 10.0 mM NaCl, 3 mM $MgCl_2$, 0.5 % Triton X-100) containing protease inhibitors (pepstatin, leupeptin and aprotinin, each at 1.0 µg/mL; 1.0 mM PMSF) and by mechanical shear stress as described previously (Slany et al. 2014). After centrifugation at 2300×*g* (4 °C for 5 min), the cytoplasmic proteins were separated from the nuclei and subsequently precipitated overnight with ice-cold ethanol at −20 °C. The nuclear pellets were treated with extraction buffer (500.0 mM NaCl) for 10 min and diluted 1:10 with NP-40 buffer (Nonidet P40 Substitute, BioXtra, mixture of 15 homologs, Sigma-Aldrich). After 15-min incubation, the samples were again centrifuged, and the supernatants were precipitated by addition of ethanol.

MS sample preparation

Subsequently, the samples were solubilized in buffer (7.5 M urea, 1.5 M thiourea, 4 % CHAPS, 0.05 % SDS, 100 mM DDT) and the protein concentrations were determined with the Bradford assay (Bio-Rad-Laboratories, Germany). As described previously, 20.0-µg protein of each sample was loaded on SDS-PAGE and stained with MS-compatible silver stain (Mortz et al. 2001; Slany et al. 2009). Before enzymatic digestion of the proteins at 37 °C by using trypsin (Roche Diagnostics, Germany) overnight, each protein band was cut into four slices, reduced with DTT and alkylated with IAA. The peptides were then eluted, dried and kept at −20 °C until further analysis.

LC–MS analysis

For LC–MS analysis, samples were dissolved in 5.0 µL 30 % formic acid (FA) containing four synthetic standard peptides (each 10 fmol) and diluted with 40.0 µL mobile phase A (98 % H_2O, 2 % ACN, 0.1 % FA). A total of 10.0 µL of the solutions were injected into a Dionex Ultimate 3000 nano-LC-system combined with a QExactive orbitrap mass spectrometer (Thermo Fisher Scientific, Waltham, MA USA). A 2 cm × 75 µm C18 Pepmap100 pre-column (Thermo Fisher Scientific, Waltham, MA USA) was used for pre-concentration, on which peptides were loaded at a flow rate of 10.0 µL/min using mobile phase A. A 50 cm × 75 µm Pepmap 100 (Thermo Fisher Scientific, Waltham, MA USA) was used as an analytical column. Peptides were eluted from the pre-column and separated on the analytical column using a gradient of 8–40 % mobile phase B (80 % ACN, 20 % H2O, 0.1 % FA) over 235 min at a flow rate of 300 nL/min. Mass spectrometric analyses were performed with a nanospray ion source. MS scans were achieved in the range from *m/z* 400–1400 at a resolution of 70,000 (at $m/z = 200$). HCD fragmentation at 30 % normalized collision energy and an isolation window of 2.0 *m/z* were used to generate MS/MS scans of the 12 most abundant ions, which were further analyzed in the orbitrap at a resolution of 17,500 (at $m/z = 200$).

Multiple reaction monitoring (MRM)

For targeted analyses, supernatants of CP 47,497-C8-treated PBMCs from further three male healthy volunteers were obtained after 3-h incubation and digested in-solution using trypsin as described previously (Bileck et al. 2014). Briefly, protein samples were concentrated and washed on 3kD MWCO filters (Pall Austria Filter GmbH) by centrifugation at 15,000*g* for 15 min. Again, DTT (5 mg/mL dissolved in 8 M guanidinium hydrochloride in 50 mM ammonium bicarbonate buffer (ABC buffer), pH 8) and IAA (10 mg/mL in 8 M guanidinium hydrochloride in 50 mM ABC buffer) were used for reduction and alkylation, respectively. Afterward, trypsin (0.1 µg/µL) was added and incubated at 37 °C for 18 h. Peptides were eluted using 25 mM ABC buffer and dried and stored at −20 °C until further MS analyses. For targeted LC–MS/MS analyses, dried peptide samples were reconstituted in 30 µL of 30 % FA containing 10 fmol each of the four synthetic standard

peptides. MRM analysis was performed as described in detail recently (Muqaku et al. 2015): 1 µL of this solution was then injected to a nano-flow LC-system (1260 Infinity Series, Agilent, Palo Alto, CA) using the HPLC-Chip cube (Agilent) coupled to the 6490 triple quadrupole mass spectrometer (Agilent). Peptides were separated by large-capacity protein chip (G4240-62010) with a 160-nl enrichment column and a 150mm × 75 µm separation column (5-µm ZORBAX 300SB-C18, 30-Å pore size) at a flow rate of 400 nl/min using a gradient from 8 % mobile phase A (99.8 % H2O, 0.2 % FA) to 30 % mobile phase B (99.8 % ACN, 0.2 % FA) over 20 min. All samples were analyzed in triplicates.

Genotoxicity experiments (SCGE and MN assay)

Isolation of human lymphocytes

Peripheral blood samples were collected from four non-smoking healthy male volunteers (aged between 25 and 32 years) without any history of recent disease or exposure to chemical toxins. The samples were collected by venipuncture in heparinized tubes (Vacutainer Systems, Becton, Dickinson, Erembodegem, Belgium). Venous heparinized blood was collected for comet and MN assays on separate days.

For comet assays, the blood samples were centrifuged (650×*g*, 10 min at 4 °C) immediately after collection. Plasma was removed, and lymphocytes were isolated by gradient centrifugation (800×*g*, 16 °C min, 16 °C) with Histopaque (Sigma-Aldrich, Steinheim, Germany) in Accupin tubes (Sigma-Aldrich, Steinheim, Germany). Lymphocytes were collected and washed twice in RPMI 1640 (332×*g*, 10 min 16 °C). Subsequently, aliquots were dispersed in serum-free freezing medium (1:10 dilution in Biofreeze, Biochrom AG, Berlin, Germany), frozen and stored at −80 °C. The SCGE experiments were performed within 2 weeks after sampling.

The lymphocytes for CBMN assays were isolated separately under sterile conditions from the same donors.

Single-cell gel electrophoresis (SCGE) assays

SCGE assays which reflect the formation of single- and double-strand breaks and apurinic sites were conducted under standard alkaline conditions as described by Tice et al. (2000).

Briefly, frozen lymphocytes were thawed in a water bath (37 °C) and centrifuged (200×*g*, 5 min at 16 °C). Subsequently, the pellets were dissolved in RPMI and washed twice under identical conditions. Thereafter, the vitality and number of cells were determined with the trypan blue dye exclusion test with a Neubauer chamber (LO-Laboroptik GmbH, Germany).

Aliquots of the lymphocytes were treated with different concentrations (5.0, 7.5, 10.0, 15.0 and 20.0 µM, 3 h) of the synthetic cannabinoid with and without metabolic activation with S9 mix (10 %). Aroclor™ 1254-induced rat liver S9 was purchased from Trinova Biochem GmbH (Giessen, Germany), and the S9-activation mix was freshly prepared before the experiments according to Maron and Ames (1983) prior to the experiments.

The indicator cells were incubated with serum-free medium containing 1 % DMSO (negative control) or with H_2O_2 (50 µM, 10 min) in experiments without S9 mix or with benzo(a)pyrene (B[a]P, 4 µM, 4 h, CAS no. 50-32-8, Sigma-Aldrich, Steinheim, Germany) in assays with S9-activation mix as a positive control. We used rat-derived liver homogenate as it is the most widely used activation mix for routine testing in genetic toxicology. In contrast to expensive, standardized liver preparations from humans, it is easily available, and a validated procedure for the composition of the homogenate has been published (for details see Maron and Ames 1983). Stock solutions of the drug were freshly made and further dissolved in serum-free medium. After incubation in the dark (37 °C; shaking 250 rpm) in presence and absence of S9-activation mix for 3 h, the cells were washed twice with RPMI (containing 10 % FCS), centrifugated (200×*g*, 8 min, 16 °C). The incubation time was chosen for reasons of comparison with earlier SCs studies in which positive results were obtained with various representatives (Koller et al. 2015). Subsequently, the pellets were resuspended in low-melting agarose (LMA, 0.5 %), spread on pre-coated agarose slides (1.5 % normal melting agarose) and lysed in the dark at 4 °C overnight. After 30-min unwinding under alkaline conditions (pH > 13), electrophoresis was carried out for 30 min (300 mA, 25 V). Subsequently, neutralization was performed twice for 8 min. Air-dried slides were stained with propidium iodide (10.0 µg/mL, Sigma-Aldrich, Steinheim, Germany).

The percentage of DNA in tail was measured by use of a computer-aided image analysis system (Comet IV, Perceptive Instruments Ltd., Haverhill, UK). For each experimental point, three slides were prepared from each person, and 50 randomly distributed cells were evaluated per slide.

Cytokinesis-blocked micronucleus (CBMN) assay with mitogen-stimulated human lymphocytes

The experiments were conducted according to OECD guideline # 487 (OECD 2012). Human lymphocytes are more sensitive toward genotoxic effects during S, G2 and M phase; therefore, we used cells which were stimulated

with phytohemagglutinin (PHA, Remel Inc., USA) before treatment with the test compound.

Briefly, 1 × 10^6 lymphocytes were added to 750.0 µL culture medium (RPMI 1640 containing 10 % FCS, 2.0 mM L-glutamine and 1.0 mM sodium pyruvate) and 10 µL PHA solution (30.0 µg/mL, Sigma-Aldrich, Steinheim, Germany). Four cultures were set up per concentration for each experimental point. The cells were incubated at 37 °C in a humidified atmosphere with 5 % CO_2 for 44 h. After PHA stimulation, the medium was replaced by fresh medium without FCS (Sigma-Aldrich, Steinheim, Germany) containing different concentrations of CP-47,497-C8 (1.0, 2.5, 5.0, 7.5 and 10.0 µM). Treatment was performed for 3 h (37 °C, 250-rpm shaking in the dark). Mitomycin C (1.0 µg/mL, Sigma-Aldrich Chemical Co., USA) was used as a positive control. The solvent (DMSO, 1.0 %) was added to untreated cultures as a negative control. After treatment, the cells were washed twice in RPMI (332×*g*, 10 min, 16 °C), and the pellets were re-suspended in culture medium. Cytochalasin B (Sigma-Aldrich Chemical Co., USA) was added to the cultures at a final concentration of 4.5 µg/mL to block cytokinesis. The cells were harvested 72–73 h after stimulation with PHA. Slides were made by use of cytocentrifugation (Fenech 2007) and were air-dried, fixed and stained with Diff-Quick (Dade Behring, Deerfield, IL, USA).

From each culture, 2000 cells were evaluated. Different endpoints were scored, namely the number of binucleated (BN) cells with micronuclei (BN-MN), the total number of micronuclei in binucleated cells (MNi), nuclear buds (Nbuds) and nucleoplasmic bridges (NPBs). Furthermore, the cytokinesis-blocked proliferation indices (CBPI) were calculated according to the formula CBPI = (M1 + 2M2 + 3(M3 + M4))/N (N is the total number of scored cells, and M1–M4 refers to the number of cells with one to four nuclei). The toxicity of the compound was indirectly assessed by the assumption that a CBPI of 1.0 corresponds to 100 % cytotoxicity (OECD Guideline 2012). Five concentrations of each drug were used to determine the CBPI values. In agreement with OECD guideline 487 (OECD), only doses were analyzed in regard to formation of MN which caused less than 60 % cytotoxicity.

Cell isolation and measurement of cytokine induction

The experiments were performed as described by Saemann et al. (2000) with slight modifications. Briefly, heparinized blood was collected from four healthy donors, and peripheral blood mononuclear cells (PBMCs) were isolated by density gradient centrifugation over Lymphoprep (AXIS-SHIELD PoC AS, Oslo, Norway). To evaluate the impact of the drugs on the production of cytokines, the cells were cultivated in RPMI 1640 (Gibco BRL, Grand Island, NY) supplemented with 2.0 mM L-glutamine, 100.0 µg/mL streptomycin, 100 U/mL penicillin (Sigma-Aldrich Chemical Co., St. Louis, MO, USA) and 10 % FCS (Hyclone, Logan, UT, USA) and stimulated with LPS (100 ng/mL, *Escherichia coli* 0111:B4; Sigma-Aldrich Chemical Co., St. Louis, MO) in the presence and absence of increasing concentrations of the drug (0.1, 0.3, 1.0, 3.0 and 10.0 µM). The solvent (DMSO, 1.0 %) was added to untreated cultures as a negative control.

All experiments were conducted in 96-well plates in humidified atmosphere with 5 % CO_2. After exposure for 24 h, the supernatants were collected and stored at −80 °C after centrifugation. The treatment period was chosen on the basis of the experimental design of earlier investigations with SCs (Berdyshev et al. 1997). Cytokines (TNF-α, IL12/23p40, IL-6 and IL10) were determined in the samples by Luminex using matched-pair antibodies specific for the respective cytokines and recombinant cytokines as standards. Coating and detection antibodies for human IL-6, IL-10 and IL-12/23p40 were obtained from R&D (Minneapolis, MIN), and antibodies to human TNF-α were from PharMingen (San Diego, CA, USA).

Statistical analysis

Cytokines, comet formation and nuclear anomalies

Determination of cytokine levels was performed by use of the software package SoftMax Pro (Molecular Devices, Sunnyvale CA). The statistical evaluation of results of the SCGE experiments, and evaluation of the CBMN assays was performed with the GraphPad Prism 5 Project software system (La Jolla, CA, USA). Results are reported as means ± standard deviations (SD). Results of the comet assay and cytokines were analyzed with one-way ANOVA and Dunnett's multiple comparisons Test. The results of cytome assays were analyzed with the Kruskal–Wallis test followed by the Dunn's test; p values ≤ 0.05 were considered as statistically significant.

LC–MS data analysis

MaxQuant 1.3.0.5 comprising the Andromeda search engine, and the Perseus statistical analysis package (Cox and Mann 2008, 2012) was employed for label-free quantitative data analysis. For protein identification, the SwissProt database (version 012013 with 20 264 entries) was used, allowing a 5-ppm mass tolerance for peptide *m*/*z* values as well as a maximum of two missed cleavages. Additionally, carbamidomethylation on cysteines was set as fixed modification and methionine oxidation as well as N-terminal protein acetylation as variable modifications. Search criteria further included a minimum of two peptide identifications per protein, at least one of them unique and a FDR

calculation based on q values less than 0.01 for both peptide and protein identification. Further data analysis was performed using Perseus (version 1.3.0.4). The proteins were filtered for reversed sequences and contaminants as well as a minimum of three independent identifications. Applying a two-sided t test with $p < 0.05$, significantly up- and down-regulated proteins were determined. Additionally, a 2D annotation enrichment analysis based on GO terms for molecular functions (GOMF) and biological processes (GOBP) was performed according to (Geiger et al. 2010).

Analysis of LC-MRM data

Data analysis was accomplished using Skyline version 1.5 (MacLean et al. 2010). The total peak area of each peptide was normalized to the internal standard peptides. Afterward, means and SDs of normalized peak areas were calculated for each protein separately for the different donors and conditions. For graphical representation, the highest determined peak area was set to 100 %, and the other peak areas were calculated relative to it.

Results

Alterations in protein regulation in PBMC by CP-47,497-C8

In total 6883 proteins were identified with at least two distinct peptides per protein. Comprehensive profiling of the status of untreated and CP-47,497-C8 treated cells showed that in total 249 proteins were significantly up- or down-regulated with a minimum of a twofold change of the LFQ values. Figure 1 depicts the results of a volcano plot analysis and shows the pattern of up- and down-regulation of individual proteins; Table S1 contains a list of all proteins which were found significantly up- or down-regulated in our study.

The results of a cluster analysis using gene ontology terms performed with Perseus (Geiger et al.) show that most up-regulated genes fall in three categories, namely, regulation of metabolic processes, signal transduction involved in mitosis and antigen processing and presentation. Most down-regulated proteins are involved in the metabolism of macromolecules, RNA splicing and in the activation of transcription cofactor activities (Fig. S2A–B—supplementary material).

Since the formation of endocannabinoids is linked to interactions with lipid metabolism (see "Discussion" section), we anticipated that CP-47,497-C8 may interact with these pathways. Indeed, significant up-regulation of a number of proteins which are involved in lipid metabolism was observed after treatment of the cells with the drug. It can be seen in Fig. 2, that the level of arachidonate 5-lipoxygenase was induced more than 26-fold, and fatty acid synthase was induced 2.7-fold upon treatment of the cells. Interestingly, also monoacylglycerol lipase ABHD12, a regulator of the endocannabinoid signaling pathway, was clearly increased after treatment of the cells with the drug.

Some of these proteins are important regulators of inflammatory processes. Therefore, we looked on further interactions of the drug with inflammatory signaling. The results are summarized in Fig. 3. It can be seen that a

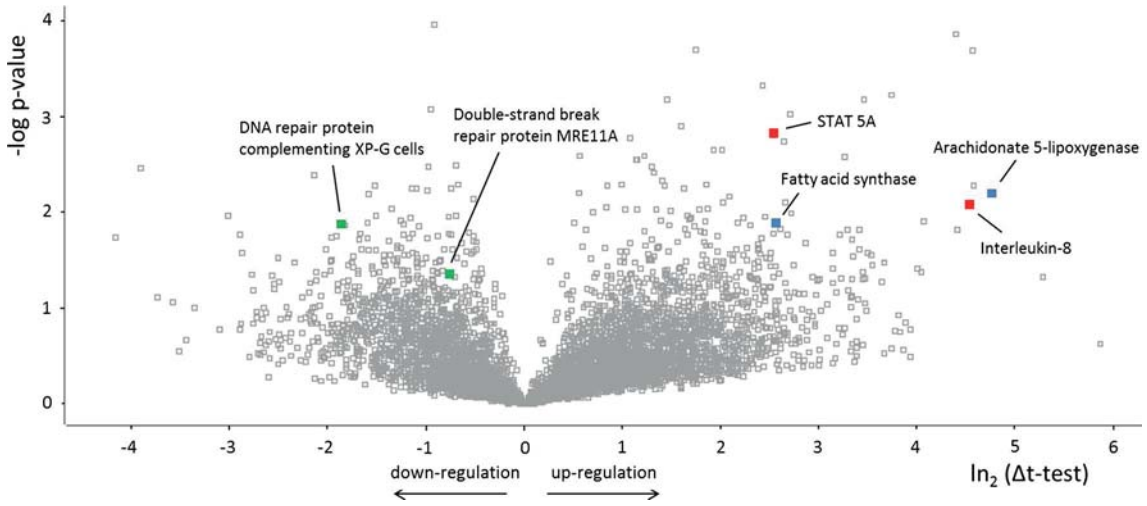

Fig. 1 Protein regulation in lymphocytes upon treatment with CP-47,497-C8 (exposure concentration 10 µM; treatment time 3 h). The distribution of up- and down-regulated nuclear proteins upon treatment with CP-47,497-C8 is displayed by a volcano plot. For each identified protein the fold-change in a logarithmic scale to the basis of 2 ($\ln_2 \Delta t$ test) and the corresponding p value ($-\log p$) are indicated

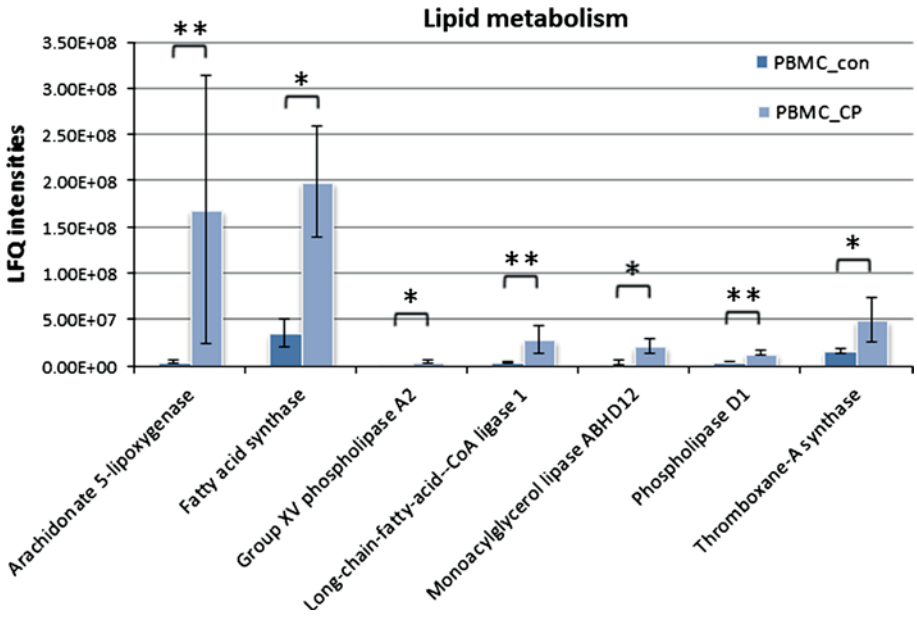

Fig. 2 Regulation of proteins related to lipid metabolism (exposure concentration 10 µM; treatment time 3 h). Label-free quantification (LFQ) intensities of proteins are shown. *Bars* represent mean ± SD of results obtained with samples from four donors. The samples were analyzed separately. These proteins were significantly (*t* test, $*p \leq 0.05$; $**p \leq 0.01$) up-regulated in PBMC upon treatment with CP-47,497-C8 (PBMC_CP; *light colored*) in comparison with control PBMC (PBMC_con; *dark colored*) (color figure online)

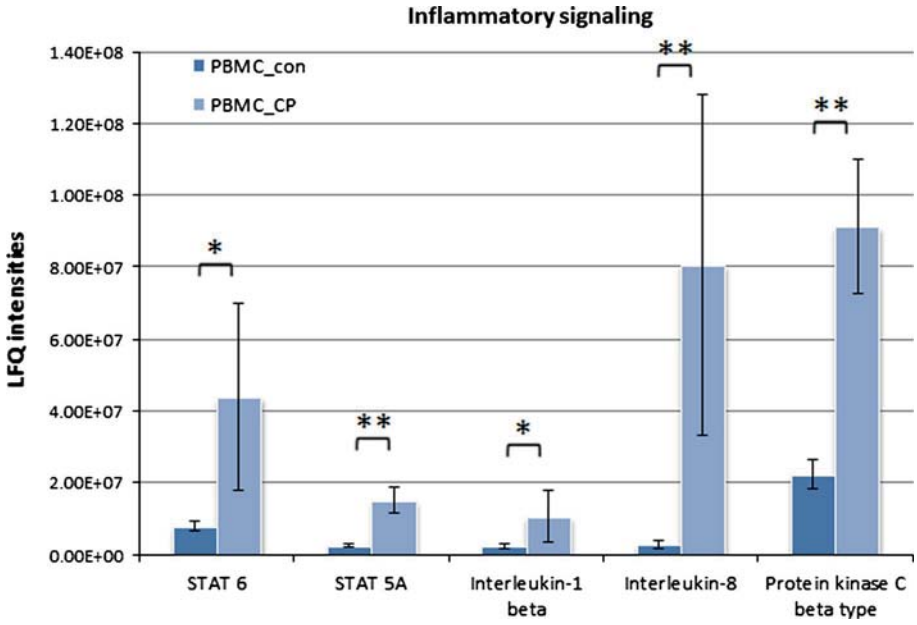

Fig. 3 Regulation of proteins related to inflammatory signaling (exposure concentration 10 µM; treatment time 3 h). Label-free quantification (LFQ) intensities of proteins are shown. *Bars* represent mean ± SD of results obtained with samples from four donors. The samples were analyzed separately. These proteins were significantly (*t* test, $*p \leq 0.05$; $**p \leq 0.01$) up-regulated in PBMC after treatment with CP-47,497-C8 (PBMC_CP; *light colored*) in comparison with control cells (PBMC_con; *dark colored*) (color figure online)

number of cytokines and also STAT proteins were up-regulated by CP-47,497-C8.

As mentioned in the "Introduction" section, we found in earlier investigations that several SCs including CP-47,497-C8 cause DNA damage in human-derived cells. The molecular mechanisms by which SCs cause instability of the genetic material are not known at present. The results of the present proteome analysis can be seen in Fig. 4. It was found that proteins which play a role in DNA excision repair and in double-strand break repair were down-regulated after treatment of the cells.

Cytokine analysis with multiple reaction monitoring (MRM)

An independent targeted MS analysis was used in order to verify data obtained from the shotgun proteomics approach. Therefore, two important pro-inflammatory mediators were selected, namely IL-8 and IL-1α. As demonstrated in Fig. 5, these cytokines were significantly up-regulated in the PBMCs of two (out of three) donors.

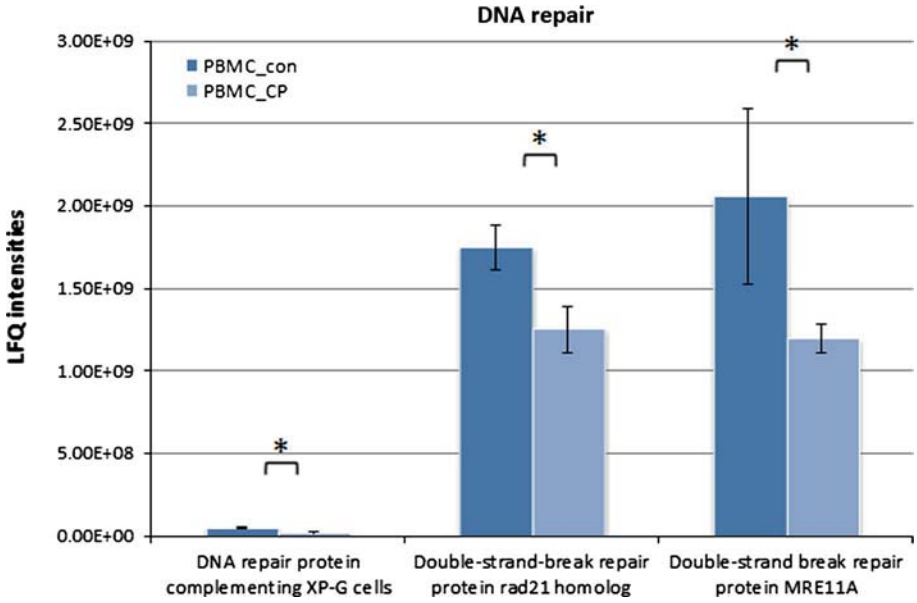

Fig. 4 Regulation of proteins related to DNA repair (exposure concentration 10 µM; treatment time 3 h). Label-free quantification (LFQ) intensities of proteins are shown. *Bars* represent mean ± SD of results obtained with samples from four donors. The samples were analyzed separately. These proteins were significantly (*t* test, $*p \leq 0.05$) up-regulated in PBMC upon treatment with 10 µM CP-47,497-C8 (PBMC_CP; *light colored*) in comparison with control cells (PBMC_con; *dark colored*) (color figure online)

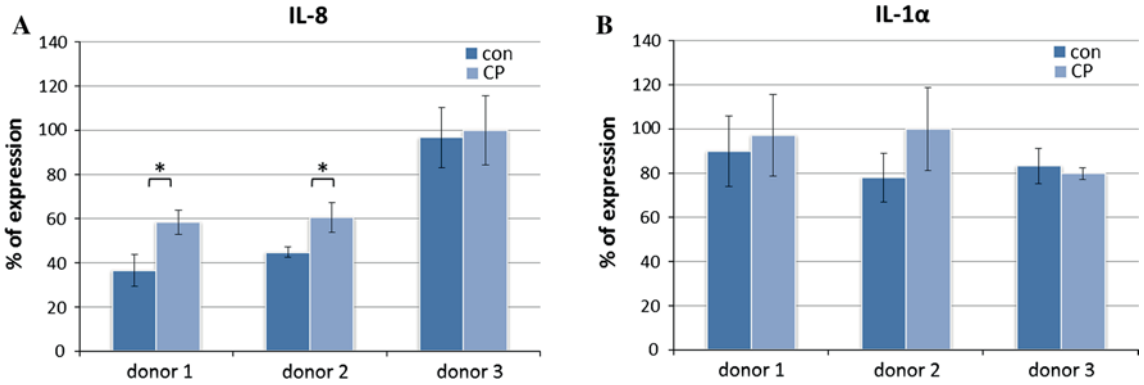

Fig. 5 Impact of exposure on PBMCs from three different donors on the levels of IL-1α and IL-8. The proteins were quantified with MRM as described in the "Materials and methods" section. *Bars* represent results obtained with cells from individual participants. The highest peak area determined for a protein was set to 100 %, and the other peak areas were calculated relative to it. *Stars* indicate statistical significance (*t* test, $p \leq 0.05$)

Induction of DNA damage in lymphocytes by CP-47,497-C8

To find out whether the drug causes DNA damage in human lymphocyte under identical experimental conditions as those used in the protein analyses, SCGE experiments were carried out in which the cells were treated with CP-47,497-C8 in the presence and absence of liver-derived metabolic activation mix (S-9). The results are summarized in Fig. 6a–f. Exposure of the indicator cells to the drugs had no impact on their vitality (see Fig. 6a, c and e), but significant induction of comets was seen which reflect single- and double-strand breaks and apurinic sites (Fig. 6b, d and f).This effect was less pronounced in presence of liver S9 mix. This observation indicates that the compound may be detoxified via protein binding. In order to verify this assumption, additional experiments were conducted in which the drug was incubated with BSA and heat-inactivated S9. Both suspensions contained identical protein concentrations (final protein concentration 0.3 mg/mL). It can be seen in Fig. 6f, that addition of the proteins and of the enzyme mix to the incubation mix reduced the genotoxic activity of the drug.

To find out whether the interaction of the drug with DNA leads to persisting chromosomal aberrations, cytome experiments were conducted in which MN were scored which reflect structural and numerical chromosomal aberrations. Furthermore, also other nuclear anomalies were evaluated, namely Nbuds and NPBs.

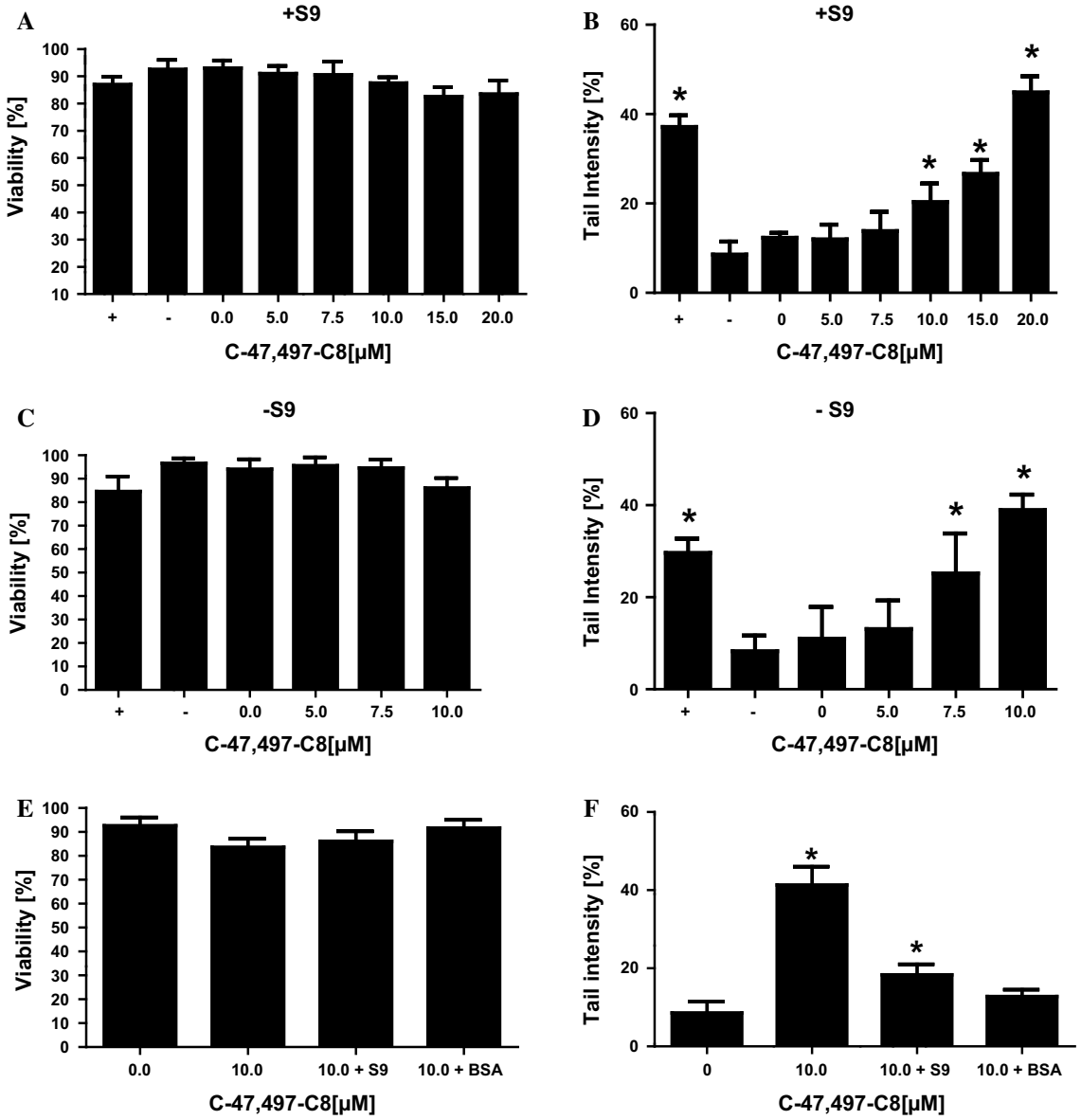

Fig. 6 Results of SCGE experiments with CP-47,497-C8. Human lymphocytes were treated in the presence and absence of rat-derived liver S9 mix with CP-47,497-C8 (treatment time 3 h; 5.0–20 µM). Furthermore, experiments were conducted in which the cells were incubated under identical conditions with S9 activation mix and heat-inactivated BSA (final protein concentration 0.4 mg/mL). **a**, **c** and **e** depict the impact of the drugs on the vitality of the indicator cells (which was monitored with *trypan blue*). **b**, **d** and **f** shows results which were conducted in SCGE assay which were conducted under identical experimental conditions. Cells were exposed in experiments without metabolic activation to the drug for 3 h or to 50 µM H_2O_2 as positive control for 10 min. In the positive control experiments with S9 mix, cells were treated with 4 µM B(a)P for 4 h. Subsequently, the nuclei were isolated and the percentage of DNA in comet determined as described in "Materials and methods." *Bars* represent mean ± SD of results obtained with three cultures per experimental point. From each culture, three slides were made, and 50 cells from each slide were analyzed for comet formation. The viability of the cells was determined after treatment with trypan blue and was in all experiments ≥95 % (data not shown). *Stars* indicate statistical significance (ANOVA, $p \leq 0.05$)

The results of a representative experiment are summarized in Table 1. It can be seen, that exposure of the cells to CP-47,497-C8 at concentrations ≥7.5 µM caused a significant increase in the frequencies of two endpoints (MN and BN-MN), and also the number of NPBs was elevated, but this latter effect did not reach significance. The impact of the drug on the nuclear division indices (NDI) of the cells is listed in the first column. It can be seen that no significant effects were detected under any experimental conditions.

Table 1 Impact of CP-47,497-C8 on human lymphocytes on the nuclear division index and various chromosomal anomalies

Compounds	Concentration	NDI	BN-MN	MNi	Nbuds	NPBs
	µM	Mean ± SD	Mean (‰) ± SD	Mean (‰) ± SD	Mean (‰) ± SD	Mean (‰) ± SD
Neg. Cont.	0.0	2.04 ± 0.12	4.14 ± 0.52	4.26 ± 0.50	2.96 ± 1.56	1.67 ± 0.76
CP-47,497-C8	1.0	1.99 ± 0.14	4.40 ± 0.79	4.40 ± 0.79	3.91 ± 2.08	2.10 ± 1.67
	2.5	2.02 ± 0.12	4.89 ± 1.01	4.89 ± 1.01	4.33 ± 1.61	2.05 ± 0.79
	5.0	2.01 ± 0.14	5.26 ± 0.98	5.37 ± 1.20	2.57 ± 1.90	2.24 ± 2.79
	7.5	2.01 ± 0.15	**6.03 ± 1.28**	**6.03 ± 1.28**	3.97 ± 1.45	2.45 ± 2.41
	10.0	1.93 ± 0.19	**6.37 ± 1.83**	**6.58 ± 2.03**	4.48 ± 2.24	1.89 ± 0.96
Pos. Cont.	1.0 µg/mL	1.74 ± 0.16	**48.60 ± 9.35**	**50.62 ± 10.10**	**12.44 ± 5.92**	2.68 ± 1.16

Human mitogen-stimulated lymphocytes from four individuals were treated with different concentrations of the test compound for 3 h. Subsequently, the nuclear division indices (NDI) and nuclear aberrations were analyzed after incubation of the cells with cytochalasin B as described in "Materials and methods." Each experimental point represents results (mean ± SD) obtained from duplicate cultures from four donors

NDI Nuclear Division Indices, *BN-MN* binucleated cells with micronuclei, *MN* micronuclei, *Nbuds* nuclear buds, *NPB* nucleoplasmic bridges, *Neg. Control* solvent control (DMSO 1 %), *Pos. Control* mitomycin C (1.0 µg/mL)

Bold values indicate significant differences from negative control values (Kuskal–Wallis test followed by Dunnett's test, $p \leq 0.05$)

Table 2 Impact of CP-47,497-C8 on the cytokine production in human PBMCs

LPS + CP (µM)	IL-10 (ng/mL)	Δ[a] (%)	IL-6 (ng/mL)	Δ[a] (%)	IL12p40 (ng/mL)	Δ[a] (%)	TNFα (ng/mL)	Δ[a] (%)
	Mean ± SD		Mean ± SD		Mean ± SD		Mean ± SD	
0.0	0.97 ± 0.22	–	12.30 ± 1.18	–	0.64 ± 0.30	–	1.01 ± 0.35	–
0.1	0.84 ± 0.20	−13	12.23 ± 4.67	−1	0.71 ± 0.26	+14	1.07 ± 0.41	+6
0.3	1.01 ± 0.28	+4	10.15 ± 1.31	−17	0.64 ± 0.22	0	0.91 ± 0.28	−10
1.0	0.95 ± 0.11	−2	10.64 ± 1.76	−13	0.56 ± 0.30	−12	0.93 ± 0.27	−8
3.0	0.92 ± 0.13	−5	14.45 ± 1.15	+17	0.69 ± 0.26	+8	1.04 ± 0.30	+3
10.0	**0.78 ± 0.22**	−20	**15.83 ± 2.10**	+29	**0.91 ± 0.26**	+42	**1.46 ± 0.39**	+45

Human PBMCs were exposed to the synthetic cannabinoid CP-47,497-C8 for 24 h and processed as described in the "Materials and methods" section. Values indicate mean ± SD from triplicate measurements conducted with samples from four different donors. Statistical analyses were performed by one-way ANOVA and Dunnett's multiple comparison test

Bold values are significantly different from those found in the respective controls ($p < 0.05$)

[a] Δ Alteration in %

Impact of CP-47,497-C8 on the production of inflammatory cytokines

Since the results of proteome profiling indicated that the drug induces the synthesis of proteins which are involved in inflammation, experiments were conducted in which we measured the levels of cytokines after treatment of LPS-stimulated lymphocytes with the drug. The results are summarized in Table 2. It can be seen that inductions of several cytokines (IL-10, IL-6 and IL12p40) and of TNF-α were detected. The strongest effect was seen with the tumor necrosis factor, and its concentration was increased by approximately 40 % after exposure of the cells to the drug. On the contrary, we found down-regulation of IL-10; its level was decreased by approximately 20 % after treatment of the cells. It is notable that all these effects were not dose-related; up to concentrations of 3.0 µM, no differences were seen in comparison with the background levels, whereas only at the highest dose (10.0 µM), significant alterations were detected.

Discussion

This is the first investigation using proteome profiling to assess the impact of a synthetic cannabinoid on primary human cells. In contrast, several studies have been published which describe cellular alterations by THC, the most relevant phytocannabinoid (for review see Wang et al. 2011). However, these earlier investigations concerned the impact of the drug on global and psychotropic effects and were conducted with cytosolic extracts of neuronal cells (Bindukumar et al. 2008; Colombo et al. 2009; Quinn et al. 2008; Rubino et al. 2009); therefore, their findings can hardly be compared with the present results.

As described in the "Results" section, we observed up-regulation of several proteins by the SC which are involved in the metabolism of amino acids as well as in signal transduction involved in mitotic cell cycle; most down-regulated proteins play a role in the biosynthesis of macromolecules (Fig. S2A–B—supplementary material).

Furthermore, we detected a number of specific alterations which concern lipid metabolism, inflammatory reactions and other functions of the immune system as well as inhibition of DNA repair processes. These effects are of particular interest in regard to possible adverse health effects in drug users.

The impact of the drug on lipid metabolism was not unexpected. The lipophilic character of phytocannabinoids led to the assumption that they exert part of their physiological effects via disturbance of the structures of the lipid part of the cell membranes (Leuschner et al. 1984; Paton 1975). THC and related compounds are incorporated in the lipid bilayers of cell membranes (Herbette et al. 1986) and cause their effects via interactions with microdomains of plasma membranes which are modulators of immune receptors and cannabinoid receptors (Fisar 2009). As described in the "Results" section (Fig. 2), we found in the present study significant alterations of a number of proteins which are involved in lipid metabolism. The most pronounced up-regulation concerned arachidonate 5-lipoxygenase. Furthermore, several other enzymes which were induced by CP-47,497-C8, for example fatty acid synthase and long-chain fatty acid CoA ligase 1, are also involved in inflammation (Kanter et al. 2012; Matsuo et al. 2014). The observation of increased levels of phospholipase D1 indicates that SCs may have an impact on the synthesis of endogenous cannabinoids. This enzyme is involved in the biosynthesis of anandamide (Fisar 2009) and is also required for TNF-α induced production of cytokines such as IL-1, IL-5, IL-6 and IL-13 (Sethu et al. 2008). Also monoacylglycerol lipase ABHD12, which was clearly activated by CP-47,497-C8, is involved in the synthesis of endocannabinoids (Chen et al. 2013).

It is notable that all lipid metabolism-associated proteins, which were up-regulated after exposure of the cells to CP-47,497-C8, are involved in inflammatory processes. Numerous studies have been published which concern the effects of pro- and anti-inflammatory properties of phyto- and endocannabinoids (Cabral and Griffin-Thomas 2009; Kaplan 2013; Suarez-Pinilla et al. 2014; Tanasescu and Constantinescu 2010). Also synthetic antagonists which bind selectively to both types of cannabinoid receptors (CB1 and CB2) were used in some of these investigations. In addition to the findings which are described in the previous chapter, we detected up-regulation of further inflammation-related proteins, for example induction of STAT5A and 6, which are involved in both, pro- and anti-inflammatory processes (Goenka and Kaplan 2011; Lu et al. 2007). Furthermore, we found also evidence for up-regulation of interleukin-1β, one of the most important pro-inflammatory cytokines in the human body, which is involved in the pathogenesis of several neurological disorders (Fogal and Hewett 2008). Notably, it is known that this protein regulates also the sensitivity of cannabinoid receptor CB1-controlled GABA transmission in the striatum (De Chiara et al. 2013). Other cytokines which are induced by the drug are interleukin-8 (its production is controlled by TNF-α and by IL-1 which are up-regulated by the drug) and tryptophan tRNA ligase, which has not only an enzymatic function, but is also induced upon inflammatory activation and acts also as a pro-inflammatory cytokine (Haudek-Prinz et al. 2012; Ivakhno and Kornelyuk 2004). Finally, we observed also significant induction of PKC-β, which is involved in the activation of NFκB1 and causes up-regulation of numerous inflammatory mediators (Kang et al. 2001; Kong et al. 2013).

Also in the cytoplasmic fractions, up-regulation of pro-inflammatory proteins was detected in LPS-stimulated cells. As shown in Table 2, we found that TNFα was significantly increased, and this protein activates NFkB1, the most important transcription factor regulating inflammatory responses. Furthermore, also the cytokines IL-6 and IL-12, which are involved in numerous inflammatory diseases (Mihara et al. 2012; Vignali and Kuchroo 2012), were induced by the SC. On the contrary, a reduction in IL-10 was observed under identical experimental conditions. IL-10 is an inhibitor of the synthesis of pro-inflammatory cytokines and controls the inducible form of COX (Sikka et al. 2013).

The former observations seem to contradict previous reports in which the effects of phytocannabinoids and SCs (JWH-015 and JWH133) on cytokine production were monitored in T cells (for review see Suarez-Pinilla et al. 2014). In these previous investigations, induction of IL-10 and suppression of IL-1β and IL-6 were observed in contrast to our findings. Also in experiments with LPS-stimulated human PBMCs, low concentrations of Δ9-THC (3 nM) were found to inhibit pro-inflammatory cytokine production (e.g., TNF-α, IL-8, IL-6), while a high dose (3 μM) which is similar to those we used caused stimulation of these proteins. These findings of Berdyshev et al. (1997) indicate that the responses of mammalian cells toward SCs depend strongly on the exposure concentrations and provide an explanation for the discrepancy between earlier findings and our results.

It is not known at present which molecular mechanisms trigger the up-regulation of inflammatory cytokines. One of the modes of action potentially involved is oxidative stress which may cause activation of a variety of transcription factors leading to expression of hundreds of genes

including those which encode for inflammatory cytokines (for details see (Reuter et al. 2010).

As mentioned in the introduction, recent investigations indicate that SCs of different chemical groups including CP-47,497-C8 cause chromosomal damage in human-derived cells (Koller et al. 2013). The molecular mechanisms which cause these effects are not known. The results of the present study provide a possible explanation; they indicate that CP-47,497-C8 inhibits several enzymes which are involved in DNA repair processes (see Fig. 4). ERCC5 is a synthetic endonuclease involved in excision repair (Kiyohara and Yoshimasu 2007), while MRE11A plays a causal role in double-strand break repair (Errico and Costanzo 2012). Both proteins were significantly down-regulated after exposure of the cells to CP-47,497-C8. These findings indicate that indirect effects may account for the induction of MNi (Table 1) and also for the formation of comets (Fig. 6b, d and f) in lymphocytes. This assumption is supported by results obtained with liver-S9-mix, which indicate that the drug is not converted by phase I enzymes to DNA-reactive metabolites. The reduction in the genotoxic activity of the compound after addition of BSA and also with heat-inactivated enzyme mix indicates that the drug is inactivated by proteins probably due to direct binding. Similar detoxification effects were seen in earlier studies with other direct acting genotoxic carcinogens for example with alkylating drugs and isothiocyanates (Kassie et al. 2003).

It can be seen in Figs. 2, 3 and 4 that the standard derivations in the proteome analyses are quite high indicating that strong inter-individual variations of the responses exist. Also the findings of the MRM experiments (Fig. 5) underline this assumption: As described above, only in two out of three participants induction of cytokines was detected. Nevertheless, it is obvious that the alterations of protein expression patterns which we described in the previous chapters were pronounced and highly significant.

In conclusion, the results of the present investigations indicate that the drug causes two main effects which may lead to adverse health effects in users, namely induction of inflammation via up-regulation of pro-inflammatory cytokines as well as induction of damage of the genetic material via inhibition of repair enzymes. It is notable that the concentrations which caused these effects in the present study in human cells are substantially (10^2–10^3 orders of magnitude) higher than the blood levels which were detected after consumption of selected SCs in humans (Kneisel and Auwärter 2012; Teske et al. 2010). However, it is likely that relatively high concentrations, which may cause inflammation as well as chromosomal damage in drug users, are reached in epithelia of the respiratory tract of drug users. Therefore, further investigations concerning possible adverse effects in consumers are warranted.

Acknowledgments This study was funded by the EU Commission in the frame of the coordinated Project "SPICE and synthetic cannabinoids" (JUST/2009/DPIP/AG/0948).

Compliance with ethical standards

Conflict of interest The authors state that they have no conflict of interest.

References

Auwärter V, Dresen S, Weinmann W et al (2009) 'Spice' and other herbal blends: harmless incense or cannabinoid designer drugs? J Mass Spectrom 44(5):832–837. doi:10.1002/jms.1558

Berdyshev EV, Boichot E, Germain N, Allain N, Anger JP, Lagente V (1997) Influence of fatty acid ethanolamides and Delta(9)-tetrahydrocannabinol on cytokine and arachidonate release by mononuclear cells. Eur J Pharmacol 330(2–3):231–240. doi:10.1016/S0014-2999(97)01007-8

Bileck A, Kreutz D, Muqaku B, Slany A, Gerner C (2014) Comprehensive assessment of proteins regulated by dexamethasone reveals novel effects in primary human peripheral blood mononuclear cells. J Proteome Res 13(12):5989–6000. doi:10.1021/pr5008625

Bindukumar B, Mahajan SD, Reynolds JL et al (2008) Genomic and proteomic analysis of the effects of cannabinoids on normal human astrocytes. Brain Res 1191:1–11. doi:10.1016/j.brainres.2007.10.062

Cabral GA, Griffin-Thomas L (2009) Emerging role of the cannabinoid receptor CB2 in immune regulation: therapeutic prospects for neuroinflammation. Expert Rev Mol Med 11:e3. doi:10.1017/S1462399409000957

Chen DH, Naydenov A, Blankman JL et al (2013) Two novel mutations in ABHD12: expansion of the mutation spectrum in PHARC and assessment of their functional effects. Hum Mutat 34(12):1672–1678. doi:10.1002/humu.22437

Colombo G, Rusconi F, Rubino T et al (2009) Transcriptomic and proteomic analyses of mouse cerebellum reveals alterations in RasGRF1 expression following in vivo chronic treatment with delta 9-tetrahydrocannabinol. J Mol Neurosci MN 37(2):111–122. doi:10.1007/s12031-008-9114-2

Cox J, Mann M (2008) MaxQuant enables high peptide identification rates, individualized p.p.b.-range mass accuracies and proteome-wide protein quantification. Nat Biotechnol 26(12):1367–1372. doi:10.1038/nbt.1511

Cox J, Mann M (2012) 1D and 2D annotation enrichment: a statistical method integrating quantitative proteomics with complementary high-throughput data. BMC Bioinf 13(Suppl 16):S12. doi:10.1186/1471-2105-13-S16-S12

De Chiara V, Motta C, Rossi S et al (2013) Interleukin-1beta alters the sensitivity of cannabinoid CB1 receptors controlling glutamate transmission in the striatum. Neuroscience 250:232–239. doi:10.1016/j.neuroscience.2013.06.069

Errico A, Costanzo V (2012) Mechanisms of replication fork protection: a safeguard for genome stability. Crit Rev Biochem Mol Biol 47(3):222–235. doi:10.3109/10409238.2012.655374

Fenech M (2007) Cytokinesis-block micronucleus cytome assay. Nat Protoc 2(5):1084–1104. doi:10.1038/nprot.2007.77

Fenech M, Chang WP, Kirsch-Volders M et al (2003) HUMN project: detailed description of the scoring criteria for the cytokinesis-block micronucleus assay using isolated human lymphocyte cultures. Mutat Res 534(1–2):65–75

Fisar Z (2009) Phytocannabinoids and endocannabinoids. Curr Drug Abuse Rev 2(1):51–75

Fogal B, Hewett SJ (2008) Interleukin-1 beta: a bridge between inflammation and excitotoxicity? J Neurochem 106(1):1–23. doi:10.1111/j.1471-4159.2008.05315.x

Geiger T, Cox J, Mann M (2010) Proteomic changes resulting from gene copy number variations in cancer cells. PLoS Genet 6(9):e1001090. doi:10.1371/journal.pgen.1001090

Goenka S, Kaplan MH (2011) Transcriptional regulation by STAT6. Immunol Res 50(1):87–96. doi:10.1007/s12026-011-8205-2

Haudek-Prinz VJ, Klepeisz P, Slany A, et al (2012) Proteome signatures of inflammatory activated primary human peripheral blood mononuclear cells. J Proteom 76 Spec No.: 150-62. doi:10.1016/j.jprot.2012.07.012

Herbette LG, Chester DW, Rhodes DG (1986) Structural analysis of drug molecules in biological membranes. Biophys J 49(1):91–94

Ivakhno SS, Kornelyuk AI (2004) Cytokine-like activities of some aminoacyl-tRNA synthetases and auxiliary p43 cofactor of aminoacylation reaction and their role in oncogenesis. Exp Oncol 26(4):250–255

Kang SW, Wahl MI, Chu J et al (2001) PKCbeta modulates antigen receptor signaling via regulation of Btk membrane localization. The EMBO journal 20(20):5692–5702. doi:10.1093/emboj/20.20.5692

Kanter JE, Kramer F, Barnhart S et al (2012) Diabetes promotes an inflammatory macrophage phenotype and atherosclerosis through acyl-CoA synthetase 1. Proc Natl Acad Sci USA 109(12):E715–E724. doi:10.1073/pnas.1111600109

Kaplan BL (2013) The role of CB1 in immune modulation by cannabinoids. Pharmacol Ther 137(3):365–374. doi:10.1016/j.pharmthera.2012.12.004

Kassie F, Laky B, Gminski R et al (2003) Effects of garden and water cress juices and their constituents, benzyl and phenethyl isothiocyanates, towards benzo(a)pyrene-induced DNA damage: a model study with the single cell gel electrophoresis/Hep G2 assay. Chem Biol Interact 142(3):285–296

Kiyohara C, Yoshimasu K (2007) Genetic polymorphisms in the nucleotide excision repair pathway and lung cancer risk: a meta-analysis. Int J Med Sci 4(2):59–71

Klepeisz P, Sagmeister S, Haudek-Prinz V, Pichlbauer M, Grasl-Kraupp B, Gerner C (2013) Phenobarbital induces alterations in the proteome of hepatocytes and mesenchymal cells of rat livers. PLoS ONE 8(10):e76137. doi:10.1371/journal.pone.0076137

Kneisel S, Auwärter V (2012) Analysis of 30 synthetic cannabinoids in serum by liquid chromatography-electrospray ionization tandem mass spectrometry after liquid–liquid extraction. J Mass Spectrom 47(7):825–835. doi:10.1002/jms.3020

Koller VJ, Zlabinger GJ, Auwärter V, Fuchs S, Knasmueller S (2013) Toxicological profiles of selected synthetic cannabinoids showing high binding affinities to the cannabinoid receptor subtype CB1. Arch Toxicol 87(7):1287–1297. doi:10.1007/s00204-013-1029-1

Koller VJ, Auwärter V, Grummt T, Moosmann B, Misik M, Knasmuller S (2014) Investigation of the in vitro toxicological properties of the synthetic cannabimimetic drug CP-47,497-C8. Toxicol Appl Pharmacol 277(2):164–171. doi:10.1016/j.taap.2014.03.014

Koller VJ, Ferk F, Al-Serori H et al (2015) Genotoxic properties of representatives of alkylindazoles and aminoalkyl-indoles which are consumed as synthetic cannabinoids. Food Chem Toxicol 80:130–136. doi:10.1016/j.fct.2015.03.004

Kong L, Shen X, Lin L et al (2013) PKCbeta promotes vascular inflammation and acceleration of atherosclerosis in diabetic ApoE null mice. Arterioscler Thromb Vasc Biol 33(8):1779–1787. doi:10.1161/ATVBAHA.112.301113

Leuschner JT, Wing DR, Harvey DJ et al (1984) The partitioning of delta 1-tetrahydrocannabinol into erythrocyte membranes in vivo and its effect on membrane fluidity. Experientia 40(8):866–868

Lorenz O, Parzefall W, Kainzbauer E et al (2009) Proteomics reveals acute pro-inflammatory and protective responses in rat Kupffer cells and hepatocytes after chemical initiation of liver cancer and after LPS and IL-6. Proteomics Clinical applications 3(8):947–967. doi:10.1002/prca.200800173

Lu X, Chen J, Sasmono RT et al (2007) T-cell protein tyrosine phosphatase, distinctively expressed in activated-B-cell-like diffuse large B-cell lymphomas, is the nuclear phosphatase of STAT6. Mol Cell Biol 27(6):2166–2179. doi:10.1128/MCB.01234-06

MacLean B, Tomazela DM, Shulman N et al (2010) Skyline: an open source document editor for creating and analyzing targeted proteomics experiments. Bioinformatics 26(7):966–968. doi:10.1093/bioinformatics/btq054

Maron DM, Ames BN (1983) Revised methods for the Salmonella mutagenicity test. Mutat Res 113(3–4):173–215

Matsuo S, Yang WL, Aziz M, Kameoka S, Wang P (2014) Fatty acid synthase inhibitor C75 ameliorates experimental colitis. Mol Med 20:1–9. doi:10.2119/molmed.2013.00113

Mihara M, Hashizume M, Yoshida H, Suzuki M, Shiina M (2012) IL-6/IL-6 receptor system and its role in physiological and pathological conditions. Clin Sci 122(3–4):143–159. doi:10.1042/Cs20110340

Moosmann B, Kneisel S, Wohlfarth A, Brecht V, Auwärter V (2012) A fast and inexpensive procedure for the isolation of synthetic cannabinoids from 'Spice' products using a flash chromatography system. Anal Bioanal Chem. doi:10.1007/s00216-012-6462-0

Mortz E, Krogh TN, Vorum H, Gorg A (2001) Improved silver staining protocols for high sensitivity protein identification using matrix-assisted laser desorption/ionization-time of flight analysis. Proteomics 1(11):1359–1363. doi:10.1002/1615-9861(200111)1:11<1359:AID-PROT1359>3.0.CO;2-Q

Muqaku B, Slany A, Bileck A, Kreutz D, Gerner C. (2015) Quantification of cytokines secreted by primary human cells using multiple reaction monitoring: evaluation of analytical parameters. Anal Bioanal Chem. doi:10.1007/s00216-015-8817-9

Norppa H, Falck GC (2003) What do human micronuclei contain? Mutagenesis 18(3):221–233

OECD (2012) Test No. 487: in vitro mammalian cell micronucleus test. OECD Publishing, Paris

Okada F (2014) Inflammation-related carcinogenesis: current findings in epidemiological trends, causes and mechanisms. Yonago Acta Med 57(2):65–72

Paton WD (1975) Pharmacology of marijuana. Annu Rev Pharmacol 15:191–220. doi:10.1146/annurev.pa.15.040175.001203

Presley B, Jansen-Varnum S, Logan B (2013) Analysis of synthetic cannabinoids in botanical materials: a review of analytical methods and findings. Forensic Sci Rev 25:27–46

Quinn HR, Matsumoto I, Callaghan PD et al (2008) Adolescent rats find repeated Delta(9)-THC less aversive than adult rats but display greater residual cognitive deficits and changes in hippocampal protein expression following exposure. Neuropsychopharmacology 33(5):1113–1126. doi:10.1038/sj.npp.1301475

Reuter S, Gupta SC, Chaturvedi MM, Aggarwal BB (2010) Oxidative stress, inflammation, and cancer: How are they linked? Free Radic Biol Med 49(11):1603–1616. doi:10.1016/j.freeradbiomed.2010.09.006

Rubino T, Realini N, Braida D et al (2009) The depressive phenotype induced in adult female rats by adolescent exposure to THC is associated with cognitive impairment and altered neuroplasticity in the prefrontal cortex. Neurotox Res 15(4):291–302. doi:10.1007/s12640-009-9031-3

Saemann MD, Bohmig GA, Osterreicher CH et al (2000) Anti-inflammatory effects of sodium butyrate on human monocytes: potent inhibition of IL-12 and up-regulation of IL-10 production. FASEB J 14(15):2380–2382. doi:10.1096/fj.00-0359fje

Sethu S, Mendez-Corao G, Melendez AJ (2008) Phospholipase D1 plays a key role in TNF-alpha signaling. J Immunol 180(9):6027–6034

Sikka G, Miller KL, Steppan J et al (2013) Interleukin 10 knockout frail mice develop cardiac and vascular dysfunction with increased age. Exp Gerontol 48(2):128–135. doi:10.1016/j.exger.2012.11.001

Slany A, Haudek VJ, Gundacker NC et al (2009) Introducing a new parameter for quality control of proteome profiles: consideration of commonly expressed proteins. Electrophoresis 30(8):1306–1328. doi:10.1002/elps.200800440

Slany A, Paulitschke V, Haudek-Prinz V, Meshcheryakova A, Gerner C (2014) Determination of cell type-specific proteome signatures of primary human leukocytes, endothelial cells, keratinocytes, hepatocytes, fibroblasts and melanocytes by comparative proteome profiling. Electrophoresis 35(10):1428–1438. doi:10.1002/elps.201300581

Suarez-Pinilla P, Lopez-Gil J, Crespo-Facorro B (2014) Immune system: a possible nexus between cannabinoids and psychosis. Brain Behav Immun 40:269–282. doi:10.1016/j.bbi.2014.01.018

Tanasescu R, Constantinescu CS (2010) Cannabinoids and the immune system: an overview. Immunobiology 215(8):588–597. doi:10.1016/j.imbio.2009.12.005

Teske J, Weller JP, Fieguth A, Rothamel T, Schulz Y, Troger HD (2010) Sensitive and rapid quantification of the cannabinoid receptor agonist naphthalen-1-yl-(1-pentylindol-3-yl)methanone (JWH-018) in human serum by liquid chromatography-tandem mass spectrometry. J Chromatogr B Anal Technol Biomed Life Sci 878(27):2659–2663. doi:10.1016/j.jchromb.2010.03.016

Tice RR, Agurell E, Anderson D et al (2000) Single cell gel/comet assay: guidelines for in vitro and in vivo genetic toxicology testing. Environ Mol Mutagen 35(3):206–221

Uchiyama N, Kikura-Hanajiri R, Kawahara N, Haishima Y, Goda Y (2009) Identification of a cannabinoid analog as a new type of designer drug in a herbal product. Chem Pharm Bull (Tokyo) 57(4):439–441

Vignali DA, Kuchroo VK (2012) IL-12 family cytokines: immunological playmakers. Nat Immunol 13(8):722–728. doi:10.1038/ni.2366

Wang J, Yuan W, Li MD (2011) Genes and pathways co-associated with the exposure to multiple drugs of abuse, including alcohol, amphetamine/methamphetamine, cocaine, marijuana, morphine, and/or nicotine: a review of proteomics analyses. Mol Neurobiol 44(3):269–286. doi:10.1007/s12035-011-8202-4

3.3. Shotgun proteomics of primary human cells enables the analysis of signaling pathways and nuclear translocations related to inflammation

Andrea Bileck[a], Rupert L. Mayer[a], Dominique Kreutz[a], Tamara Weiss[b], Astrid Slany[a], Christopher Gerner[a]

Journal of Proteome Research, **2015, manuscript submitted on 05-Oct-2015 (ID: pr-2015-00929f), currently under revision**

[a] Department of Analytical Chemistry, Faculty of Chemistry, University of Vienna, Währinger Str. 38, A-1090 Vienna, Austria

[b] Department of Tumor Biology, CCRI, Children's Cancer Research Institute, St. Anna Kinderkrebsforschung, A-1090 Vienna, Austria

Contributions to this publication:

- Conduction of experiments
- Organization of required materials
- Creation of figures
- Involved in the planning of the experiments, data interpretation and writing of the manuscript

This document is confidential and is proprietary to the American Chemical Society and its authors. Do not copy or disclose without written permission. If you have received this item in error, notify the sender and delete all copies.

Shotgun proteomics of primary human cells enables the analysis of signaling pathways and nuclear translocations related to inflammation

Journal:	*Journal of Proteome Research*
Manuscript ID	Draft
Manuscript Type:	Article
Date Submitted by the Author:	n/a
Complete List of Authors:	Bileck, Andrea; University of Vienna, Department of Analytical Chemistry, Faculty of Chemistry Mayer, Rupert; University of Vienna, Department of Analytical Chemistry, Faculty of Chemistry Kreutz, Dominique; University of Vienna, Department of Analytical Chemistry, Faculty of Chemistry Weiss, Tamara; Department of Tumor Biology, CCRI, Children's Cancer Research Institute, St. Anna Kinderkrebsforschung Slany, Astrid; University of Vienna, Department of Analytical Chemistry, Faculty of Chemistry Gerner, Christopher; University of Vienna, Department of Analytical Chemistry, Faculty of Chemistry

SCHOLARONE™
Manuscripts

Shotgun proteomics of primary human cells enables the analysis of signaling pathways and nuclear translocations related to inflammation

Andrea Bileck[1], Rupert L. Mayer[1], Dominique Kreutz[1], Tamara Weiss[2], Astrid Slany[1], Christopher Gerner[1*]

[1] Department of Analytical Chemistry, Faculty of Chemistry, University of Vienna, Vienna, Austria

[2] Department of Tumor Biology, CCRI, Children's Cancer Research Institute, St. Anna Kinderkrebsforschung, Vienna, Austria

Corresponding author

Christopher Gerner

Department of Analytical Chemistry

University of Vienna

Währingerstraße 38

1090 Vienna

Austria

christopher.gerner@univie.ac.at

+43-1-4277-52302

Keywords

Proteome profiling, signaling pathways, nuclear translocation, inflammation, protein phosphorylation, primary human cells

Abbreviations

FDR, false discovery rate; **IL,** interleukin; **JUN,** transcription factor AP-1; **LC**, liquid chromatography; **LFQ,** label-free quantification; **LPS,** lipopolysaccharide; **MAPK,** mitogen-activated protein kinase; **MS**, mass spectrometry; **NFκB,** nuclear factor 'kappa-light-chain-enhancer' of activated B-cells**; NFKB1**, NF-kappa-B p105 subunit; **PAK**, serine/threonine-protein kinase PAK; **PBMCs**, peripheral blood mononuclear cells; **PEP**, posterior error probability; **PHA**, phytoheamagglutinin; **PKA**, cAMP-dependent protein kinase catalytic subunit alpha; **PRIDE**, proteomics identification database; **PTM**, post-translational modification; **RT**, room temperature; **RUNX2**, runt-related transcription factor 2; **STAT3**, signal transducer and activator of transcription 3; **TiO2**, titanium dioxide; **ZFP161,** zinc finger protein 161 homolog

Abstract

Peripheral blood mononuclear cells are important players in immune regulation relying on a complex network of signaling pathways. In this study, we evaluated the power of label-free quantitative shotgun proteomics regarding the comprehensive characterisation of signaling pathways in such primary cells by studying regulation of protein abundance, post-translational modifications and nuclear translocation events. A dataset made accessible via ProteomeXchange consisting of 6901 identified proteins was evaluated. These data enabled us to map the entire c-JUN, ERK5 and NF-κB signaling cascade in a semi-quantitative fashion. Without the application of any enrichment, 2731 highly confident phosphopeptides derived from 991 proteins including 60 kinases were identified. Efficient subcellular fractionation enabled us assessing inflammation-associated nuclear translocation of proteins including histone-modifying proteins, zinc finger proteins as well as transcription factors. In conclusion, we demonstrate that multiple regulatory events related to the activity of signaling pathways can be determined out of untargeted shotgun proteomics data.

Introduction

Signaling pathways are based on complex networks of interacting proteins displaying different functionalities, involving ligands, receptors, intracellular effector molecules and transcription factors. The dysregulation or activation of one single protein or protein complex within such pathways may be sufficient to induce pathophysiological processes like inflammation. On this account, proteins within an affected signaling pathway may be important targets for therapeutic interventions. Although the use of immunoblots and gene expression analysis methods are still the most common ways to systematically evaluate signaling pathways, high-end proteomic techniques are getting more and more attractive for this field of research (1-3). Mass spectrometry (MS)-based proteomics is the method of choice with regard to complex protein mixtures covering a large dynamic range (4). Large-scale proteome profiling strategies enable the analysis of various sample types such as tissues and cells at different functional states, thereby contributing to the draft map of the human proteome (5).

However, for the evaluation of signaling pathways, classical protein identification data resulting from shotgun proteomics may hardly be sufficient. Because the phosphorylation state may determine the functionality of many signaling pathway players, analysis of phosphoproteins has become indispensable (6). Furthermore, additional information such as that about the subcellular location of proteins may be relevant. The main approaches for the analysis of phosphoproteins using proteomics are based on the selective enrichment of phosphopeptides by immobilized metal affinity chromatography (IMAC) and titanium dioxide (TiO_2) or antibody-based enrichment strategies (7). Recent studies have demonstrated that the use of label-free phosphoproteomics using TiO_2-based enrichment may provide high reproducibility. More than 6000 phosphopeptides were identified within 2h measuring time, starting from a total of 500µg protein amount (8). In this way, functional studies on the phosphoproteome of transforming growth factor-β (TGF-β) stimulated keratinocytes allowed the identification of more than 22000 phosphopeptides corresponding to more than 5300 proteins (9). In contrast to these phosphopeptide enrichment approaches, evaluation of different phosphoprotein enrichment strategies

using lanthanum chloride or customized affinity micro columns in combination with two dimensional gel electrophoresis was recently performed to characterize peripheral blood mononuclear cells (PBMCs) (10).

The effort and costs necessary for such proteomics experiments, including enrichment strategies, MS-based analysis as well as data interpretation is a common drawback in many research areas. Nevertheless, because of the availability of proteomic datasets via collaboration partners, core facilities and public repositories such as proteomics identifications database (PRIDE) (11), it is nowadays possible to get access to very comprehensive proteomics data. These datasets mostly comprise quantitative information about proteins, resulting from either label-free quantification, *in vivo* metabolic stable-isotope labeling, e.g. stable isotope labeling by amino acids in cell culture (SILAC), or *in vitro* stable-isotope labeling, like tandem mass tags (TMT) or isobaric tags for relative and absolute quantification (iTRAQ). Using biological and bio-computational knowledge, it is possible to interpret such data in order to integrate information about protein abundance, isoform expression, turnover rate, subcellular localization and post-translational modifications, thereby answering relevant cellular, physiological as well as pathophysiological questions (12).

Though much is already known about acute inflammatory diseases, chronic inflammation is still poorly understood. Detailed analysis of processes related to inflammatory regulation at the level of signaling pathways may therefore contribute to a better understanding of pathophysiological mechanisms during inflammation. In this study, we demonstrate the feasibility of a signaling pathway analysis based on a dataset obtained from a standard label-free shotgun proteomics experiment, without any phosphopeptide enrichment strategy. Therefore, a well-known model system was used, namely inflammatory activated PBMCs. The dataset, accessible via PRIDE, comprises proteome profiles of secreted, cytoplasmic and nuclear fractions from control as well as from inflammatory activated PBMCs (13). Comprehensive re-evaluation of this dataset provided new data regarding subcellular inflammation-associated phosphorylation and translocations of proteins in PBMCs.

Experimental Section

A dataset published previously by us (13), available via ProteomeXchange with identifiers PXD001415-23 was used for this study. Briefly, this dataset was obtained from three control as well as three inflammatory activated PBMCs and generated with a nanoLC-MS system using a QExactive orbitrap. Subcellular fractionation of PBMCs was performed prior to LC-MS analysis.

MaxQuant data analysis for the evaluation of subcellular fractionation and protein translocation

For protein identification as well as label-free quantitative data analysis, the open source software MaxQuant 1.3.0.5 including the Andromeda search engine and the Perseus statistical analysis package (14, 15) was used. Search criteria included the use of the SwissProt database (version 012013 with 20 264 entries) and a peptide tolerance of 25ppm as well as a maximum of 2 missed cleavages. Furthermore, carbamidomethylation on cysteins was set as fixed modification and methionine oxidation as well as N-terminal protein acetylation as variable modifications. For positive protein identification, a minimum of two peptide identifications per protein, at least one of them unique, were required. Match between runs was performed using a 5min match time window and a 15min alignment time window. All peptides and proteins were meeting an FDR<0.01. Statistical analysis was performed using Perseus (version 1.3.0.4), filtering proteins for reversed sequences, contaminants and a minimum of three independent experimental identifications per protein. To determine significant differences of protein abundance between cytoplasmic and nuclear fractions, a two-sided t-test with a significance threshold of $p<0.05$ was applied for control and inflammatory activated PBMCs, respectively.

For the evaluation of subcellular fractionation, these fold-change values of the control PBMCs obtained from the t-test statistics between cytoplasmic and nuclear fraction were sorted from the highest to the lowest and categorized into 7 groups using Excel. Proteins of each group were also classified as “nucleus” and/or “cytoplasm” according to Uniprot keyword attributes and visualized using pie charts.

Furthermore, LFQ-values of three biological replicates including two technical measurements were used for heat map analysis using R (16).

For the determination of protein translocation, these proteins were sorted from the highest to the lowest difference values between nucleus and cytoplasm from control cells and plotted as black line. The corresponding difference values derived from the inflammatory activated cells were plotted in grey (Figure 2a). Data evaluation was performed using Excel.

Immunofluorescence

PBMCs were purified with written consent and approval of the Ethics Committee of the Medical University of Vienna (Application 2011/296 by C.G. entitled:"Charakterisierung von entzündlich aktivierten Zellen des peripheren Blutes…") as described previously (13, 17). Briefly, 30ml of non-coagulated whole blood were collected in 6ml CPDA tubes (Greiner Bio-One GmbH, Austria) and immediately processed by diluting it 1:2 with RPMI1640 medium (Gibco, Life Technologies, Austria) supplemented with 100U/ml penicillin and 100µg/ml streptomycin (ATCC, LGC Standards GmbH, Germany). Afterwards, the diluted blood suspension was carefully overlaid on Ficoll Paque (GE Healthcare, Bio-Sciences AB, Uppsala, Sweden) and centrifuged at 500g for 20min at 24°C. The interphase was then collected and washed with PBS. The washed cell pellet was resuspendend in diluted autologous plasma, divided for the analysis of two functional states, namely control and inflammatory activated cells and incubated at 37°C and 5% CO_2. Activation was performed using 1µg/ml LPS (Sigma-Aldrich) and 5µg/ml PHA (Sigma-Aldrich). After 4h cultivation, cells were washed with PBS and spun against microscope slides (Marienfeld, #0810000) using Shandons' Cytospin 2. Slides were allowed to dry 30min at room temperature (RT) and fixed in Roti-Histofix 4% (ROTH #P087.3) at 4°C for 15min. After washing twice with PBS, cells were blocked in PBS containing 3% goat serum for 30min at RT. Subsequently, slides were incubated overnight at 4°C with the following primary antibodies: ZFP161 (1:50, Acris, #H00007541-B01P) and Vimentin (1:200, Millipore #AB5733) in PBS containing 1% BSA,

0.1% Triton-X and 1% goat serum. The next day, slides were washed twice with PBS and incubated with following secondary antibodies: goat anti-mouse TRITC (1:350, Dinova #115-025-072) and goat anti-chicken DL650 (1:300, Thermo Scientific #SA5-10073) diluted in PBS containing 2% BSA, 0.1% Triton-X and 1% goat serum for 1h at RT. After washing slides in PBS, 2 µg/ml DAPI solution was added for 2min at RT. Slides were then washed again and cells embedded in VECTASHIELD mounting medium (Vector Laboratories, Inc., CA, #H-1000) and cover glasses (0.17 ± 0.01 mm, Hecht-Assistent, #1014/2424) were sealed with glue. Afterwards, pictures were taken with the confocal microscope LEICA TCS SP8X.

Proteome Discoverer data analysis for the determination of phosphorylated proteins

For the determination of phosphorylated proteins, ProteomeDiscoverer 1.3 (Thermo Fisher Scientific, Austria) running Mascot 2.4 (Matrix Science, UK) was used. Protein identification was achieved searching against the SwissProt Database (version 012013 with 20 264 entries) allowing a mass tolerance of 5ppm for MS spectra and 20ppm for MS/MS spectra as well as a maximum of 2 missed cleavages. Furthermore, search criteria included carbamidomethylation on cysteins as fixed modification and methionine oxidation, N-terminal protein acetylation as well as phosphorylation on serine, threonine and tyrosine as variable modifications. After setting the FDR<0.01 and filtering all peptides meeting a Mascot significance threshold better than 0.01, highly confident phosphopeptides (PEP<0.05) were exported to Excel. A subsequent qualitative analysis of phosphorylated proteins was performed separately for control and inflammatory activated PBMCs.

Results

Subcellular fractionation of cytoplasmic and nuclear proteins

The analysis is based on LC-MS/MS proteome profiles obtained from control and inflammatory activated PBMCs fractionated into secreted, cytoplasmic and nuclear proteins. Differences in protein abundance levels determined via label-free quantification values between nuclear and cytoplasmic fractions were calculated using t-test statistics. Fold-change values were sorted in descending order and categorized into 7 groups (Figure 1a). The resulting protein distribution was compared with subcellular location of proteins in "nucleus" and/or "cytoplasm" according to Uniprot. Actually, a strong correlation of the experimental data with Uniprot classification was evident (Figure 1). However, some apparent discrepancies were also observed. Vimentin, A-kinase anchor protein 9 and eukaryotic translation initiation factor 2D were assigned to "cytoplasm" but displayed higher LFQ values in the nuclear fraction. These proteins are components of large protein complexes, such as the cytoskeleton, which mainly reside in the cytoplasm but typically become co-purified together with nuclei. Thus, the atypical abundance distribution of these proteins can be considered as artifacts. On the other hand, e.g. c-myc promoter-binding protein, apoptosis regulator Bcl-2 and nuclear receptor coactivator 7 were found enriched in the cytoplasm (group VI), but are classified as nuclear proteins according to Uniprot. Here the experimental evidence of predominant cytoplasmic localization is striking, but does not contradict a potential main biological activity which could take place within nuclei. This observation calls for a more accurate classification of proteins. This notion is further supported by our finding of a relatively large number of proteins showing strong enrichment in one of the two fractions but being not yet classified according to Uniprot (725 proteins in group VI, 310 in group III and 85 in group II). Figure 1b illustrates how the here presented data could be used for a more comprehensive annotation of proteins regarding their subcellular location. Heat maps representing abundances of selected proteins in control cells were generated. Abundances of 12 proteins which were correctly classified according to Uniprot regarding

their subcellular location were represented together with those of 12 candidates which are not yet annotated, but, which could be assigned according to our here presented data set, are illustrated.

Monitoring of specific intracellular protein translocation events during inflammation – transcriptions factors, zinc finger proteins and histone-modifying proteins

For the detection of intracellular protein translocation events upon inflammatory activation, we compared protein abundance ratios between the nuclear and cytoplasmic fractions of control and inflammatory stimulated PBMCs. The nuclear versus cytoplasmic protein abundance rations of control cells were sorted in descending order, resulting in a graph depicted in Figure 2A. The corresponding values obtained from the inflammatory activated cells were plotted on the same graph in grey (Figure 2A). In a first step, this analysis strategy was performed for the entire 6901 identified proteins (Supplementary Table S1). To find those proteins most plausibly translocating from the cytoplasm in the nucleus upon inflammatory activation, the following filtering criteria were set: (i) proteins had to show a positive fold-change between cytoplasm and nucleus of control cells; (ii) proteins had to be at least two-fold up-regulated in the nuclear fraction upon inflammatory stimulation and (iii) proteins had to show an at least two-fold higher fold-change between nucleus and cytoplasm in activated cells in comparison to control cells. 271 out of the initial 6901 proteins met these criteria and were consequently considered as proteins translocating into the nucleus upon inflammatory activation.

The most prominent translocating proteins out of these 271 encompass for example histone H3.1 and H3.2 (29 and 19-fold enriched in the nucleus, respectively), high mobility group protein HMG-I/HMG-Y (3.6-fold), lysine-specific demethylase 6A and zinc finger protein 397 (Tables 1-3). Actually, three groups of proteins were found most prominently represented amongst the translocating proteins: histone-modifying proteins, transcription factors and zinc finger proteins. Transcription factor AP-1, RFX3 and runt-related transcription factor 2 (RUNX2) displayed the most outstanding enrichment values (Table 1). Table 2 lists the group of zinc finger proteins showing similar properties, with the highest enrichment

(17-fold) in case of zinc finger protein 397. Even less dramatic translocation values were found to be clearly discernible via immunofluorescence staining, as exemplified for zinc finger protein 161 homolog (ZFP161), visually demonstrating nuclear translocation (Figure 2b). The third group includes histone-modifying proteins such as histone-lysine N-methyltransferase EZH1, histone lysine demethylase PHF8 and lysine-specific histone demethylase 1B, as shown in Table 3.

Three-dimensional assessment of the MAPK signaling pathway

A complete proteome analysis dataset may support the evaluation of protein regulation, translocation and phosphorylation, thus encompassing three independent dimensions regarding the regulation of a signaling cascade. Actually, any signaling pathway can be evaluated in this way; this is exemplified here for the MAPK signaling pathway. For this purpose, the MAPK signaling pathway was downloaded via KEGG (18) and all events accessible from our dataset mapped to this pathway. As demonstrated in Figure 3, we were able to identify almost 70% of all known proteins involved in this pathway, which allowed us to completely track the ERK5, NF-κB as well as the transcription factor AP-1 (c-JUN) cascade. In total, 17 proteins of the MAPK signaling pathway showed significant changes in protein abundance (Table 4). Out of these proteins, 14 proteins were significantly up- and 3 down-regulated. In case of transcription factor AP-1, the observed nuclear translocation was described above.

For the assessment of the phosphorylation state of proteins, the dataset was separately searched using Mascot with phosphorylation of serine, tyrosine and/or threonine set as dynamic modification. As a result, 24 members of the MAPK signaling pathway were found to be phosphoproteins. These proteins included mitogen-activated protein kinase 1 (MAPK1), serine/threonine-protein kinase 4 (STK4), mitogen-activated protein kinase kinase kinase 7 (TAK1), ribosomal protein S6 kinase alpha-3 (RSK2), serine/threonine-protein kinase PAK 1 and 2 (PAK1/2), cAMP-dependent protein kinase catalytic subunit alpha (PKA) as well as protein kinase C alpha and beta type. Four proteins, growth factor receptor-bound protein 2 (GRB2), IL-1α, IL-1β and nuclear factor NF-kappa-B p105 subunit (NFKB1) were identified as

phosphoproteins only in inflammatory stimulated cells. A single candidate, dual specificity mitogen-activated protein kinase kinase 1 (MEK1) was found phosphorylated only in control PBMCs.

Identification of novel phosphorylation sites in interleukins

Although no phosphopeptide enrichment step was included, a total of 2731 phosphopeptides with a PEP-value better than 0.05 was identified, making up 991 phosphoproteins (Supplementary Table S2). 79% of those were already classified as phosphoproteins according to Uniprot PTM keywords, for example annexin-1, 2, 4, 6, and 11. Furthermore, more than 60 phosphorylated kinases were identified, for example 13 serine/threonine-protein kinase 4, 10, MARK2, MST4, PAK1/2, NEK9 and WNK1, seven different tyrosine-protein kinases, including CSK, Lyn, Fyn, Syk and ZAP70, and the serine-protein kinase ATM.

Several known inflammation-associated phosphorylation events were further observed, including phosphorylation sites of signal transducer and activator of transcription 3 (STAT3), nuclear factor NF-kappa-B p105 subunit as well as nuclear factor of activated T-cells, cytoplasmic 2. Remarkably, phosphorylation of IL-1α and IL-1β in the cytoplasm was observed, whereas IL-6 was found to be phosphorylated in the secretome of activated primary human PBMCs. As demonstrated in Figure 4, highly confident MS1 and MS2 spectra of the IL-1α-derived peptide RLSLSQSITDDDLEAIANDSEEEIIKPR were obtained in three different modification states, i.e non-phosphorylated, mono- and bi-phosphorylated.

In addition, we investigated whether combination of post-translational modification and nuclear translocation of proteins could be identified. 46 candidate proteins translocating into the nucleus upon inflammatory activation also displayed phosphorylation sites (Supplementary Table S3). These proteins included for example transcription factor Sp110 nuclear body protein as well as a variety of transcriptional regulators such as deoxynucleotidyltransferase terminal-interacting protein 2, myeloid cell nuclear differentiation antigen, protein polybromo-1, high mobility group protein HMG-I/HMG-Y,

transcriptional regulator ATRX and transcriptional-regulating factor 1. Furthermore, six histones as well as histone-lysine N-methyltransferase MLL and lysine-specific demethylase PHF2 were identified as phosphoproteins undergoing nuclear translocation.

Discussion

For the comprehensive assessment of complex physiological as well as pathophysiological processes, such as inflammation, the analysis of a variety of intracellular events may be considered. In this context, translocations of proteins, post-translational modifications of proteins as well as protein regulation upon treatment of cells with a specific stimulus are of great relevance. Up until now, rather specified methodologies were applied to investigate each of these aspects. So, antibody-based techniques and enrichment strategies are typical for the assessment of phosphoproteins (19-21); immunofluorescence staining for the analysis of protein translocation (22-24); antibody-based techniques as well as MS-based methods for the determination of differences in abundance and regulation of proteins between different functional cell states (25, 26). In this study, we have demonstrated for the first time to what extent such information can be retrieved from a classical non-targeted shotgun proteomics approach. The presently described comprehensive screening approach not only allowed us to confirm already published findings, but also to discover novel intracellular events occurring upon inflammatory activation of PBMCs.

An in-depth analysis of functional processes occurring within cells relies on the efficient fractionation into subcellular compartments. Therefore, in a first step, we successfully evaluated the efficiency of our in-house established subcellular fractionation protocol (27). As demonstrated in Figure 1, the subcellular localization of proteins as determined by us showed a good correlation with the corresponding local assignments according to Uniprot, as far as they were specified. This also points to the possibility that a dataset as presented here may contribute to a better annotation of proteins. Furthermore, the reliable classification of proteins is essential for monitoring translocation events. In this way, we were able to confirm known events, such as, for example, nuclear translocation of transcription factor AP-1 upon inflammatory activation of cells (28). The involvement of high mobility group protein HMG-I/HMG-Y in inflammation, which was described previously (29), and translocation of the protein into the nucleus, until now only observed in other context (30), was demonstrated. In addition, yet unknown translocation events, such as that of regulator of G-protein signaling 19 were observed and may be of great relevance.

Not only single proteins were assessed, also larger groups such as histone-modifying proteins were found to translocate into the nucleus upon inflammatory activation. Histone methylation accomplished by histone methyltransferases is known to play a role in the inflammatory response of T-cells as well as in the regulation of pro-inflammatory genes in monocyte-derived macrophages (31, 32). However, up until now, this activity was not yet linked to translocation events. This observation may indicate inflammation-associated epigenetic alterations of histones, as already suggested by others (33).

The assessment of PTMs such as protein phosphorylation may be the first association with regard to the investigation of cellular processes. Obviously the activity of several kinases involved in signaling cascades as well as in cell cycle control is regulated via phosphorylation (34). Also transcription factors, such as STAT3, are known to be regulated by phosphorylation in association with inflammation (35). Although antibody-based techniques are still the method of choice for the detection of STAT3 phosphorylation (36), we were able to observe these events likewise, indicating the validity of this experimental approach. A main strength of the shotgun approach is the concomitant detection of kinases and corresponding kinase substrates. To give an example, PKA was found phosphorylated as well as its targets NFKB1 and vasodilator-stimulated phosphoprotein (37, 38). Thus we were able to confirm phosphorylation events in human cells which were described only in other species up until now. Most importantly, novel phosphorylation events were observed as well. The inflammasome component caspase-1, responsible for the cleavage, activation and thus secretion of IL-1β (39), was identified here as phosphoprotein in inflammatory activated primary human PBMCs (Supplementary Table S2). Several phosphorylation sites were also assigned to other key players of inflammation, such as IL-1α, IL-1β as well as IL-6. Interestingly, phosphorylated IL-1α and IL-1β were only detected in the cytoplasm, whereas phosphorylated IL-6 was only determined in the secretome of inflammatory activated cells. A potential regulation of the secretion of these most important players via phosphorylation remains to be further investigated. Alterations in the phosphorylation state of such mediators may also account for cell type-specific responses to inflammatory stimuli. Actually, the combined analysis of inflammation-associated

phosphorylation and nuclear translocation may provide completely novel understanding for inflammatory mechanisms. For example, the presently identified phosphoproteins transcription factor Sp110 nuclear body protein and transcriptional-regulating factor 1 were also found by us to be translocated into the nucleus. While phosphorylation of these two proteins has been described previously (40), inflammation-related nuclear translocation represents a novel finding.

At the present state, shotgun proteomics proves to provide comprehensive information about different regulatory events in complex biological systems. Most importantly, this information is gained in an unbiased manner. The different kinds of observations can now be obtained and calculated from one data set, also rendering multiple ways of normalization unnecessary. In this way, the shotgun approach may deliver relevant information about any conceivable signaling pathway without the necessity of preliminary assumptions. Despite the fact that classical shotgun proteomics approaches are prone to a certain degree of variability, constant improvements of this methodology concerning sequence coverage and reproducibility (41, 42) are making this methodology applicable to the comprehensive analysis of complex signaling pathway.

Conclusions

This work demonstrates the power of untargeted shotgun proteomics regarding the assessment of signaling pathway activities. The incredible improvement in data comprehensiveness and accuracy by modern mass spectrometry allows the coverage of three dimensions of protein regulation, including abundance, subcellular localization and phosphorylation status of proteins. This study highlights the present and future potential of shotgun proteomics for the assessment of multiple regulatory events related to complex biological processes.

Acknowledgements

We would like to thank Samuel M. Gerner for computational support and Samuel M. Meier for his help during the preparation of the manuscript.

References

1. Graves, P. R.; Haystead, T. A., A functional proteomics approach to signal transduction. *Recent Prog Horm Res* **2003,** 58, 1-24.

2. Harsha, H. C.; Pinto, S. M.; Pandey, A., Proteomic strategies to characterize signaling pathways. *Methods Mol Biol* **2013,** 1007, 359-77.

3. Marko-Varga, G., Pathway proteomics: global and focused approaches. *Am J Pharmacogenomics* **2005,** 5, (2), 113-22.

4. Aebersold, R.; Mann, M., Mass spectrometry-based proteomics. *Nature* **2003,** 422, (6928), 198-207.

5. Wilhelm, M.; Schlegl, J.; Hahne, H.; Moghaddas Gholami, A.; Lieberenz, M.; Savitski, M. M.; Ziegler, E.; Butzmann, L.; Gessulat, S.; Marx, H.; Mathieson, T.; Lemeer, S.; Schnatbaum, K.; Reimer, U.; Wenschuh, H.; Mollenhauer, M.; Slotta-Huspenina, J.; Boese, J. H.; Bantscheff, M.; Gerstmair, A.; Faerber, F.; Kuster, B., Mass-spectrometry-based draft of the human proteome. *Nature* **2014,** 509, (7502), 582-7.

6. Oppermann, F. S.; Gnad, F.; Olsen, J. V.; Hornberger, R.; Greff, Z.; Keri, G.; Mann, M.; Daub, H., Large-scale proteomics analysis of the human kinome. *Mol Cell Proteomics* **2009,** 8, (7), 1751-64.

7. Doll, S.; Burlingame, A. L., Mass spectrometry-based detection and assignment of protein posttranslational modifications. *ACS Chem Biol* **2015,** 10, (1), 63-71.

8. Piersma, S. R.; Knol, J. C.; de Reus, I.; Labots, M.; Sampadi, B. K.; Pham, T. V.; Ishihama, Y.; Verheul, H. M.; Jimenez, C. R., Feasibility of label-free phosphoproteomics and application to base-line signaling of colorectal cancer cell lines. *J Proteomics* **2015**.

9. D'Souza, R. C.; Knittle, A. M.; Nagaraj, N.; van Dinther, M.; Choudhary, C.; ten Dijke, P.; Mann, M.; Sharma, K., Time-resolved dissection of early phosphoproteome and ensuing proteome changes in response to TGF-beta. *Sci Signal* **2014,** 7, (335), rs5.

10. Rocchetti, M. T.; Alfarano, M.; Varraso, L.; Di Paolo, S.; Papale, M.; Ranieri, E.; Grandaliano, G.; Gesualdo, L., Two dimensional gel phosphoproteome of peripheral blood mononuclear cells: comparison between two enrichment methods. *Proteome Sci* **2014,** 12, (1), 46.

11. Vizcaino, J. A.; Cote, R. G.; Csordas, A.; Dianes, J. A.; Fabregat, A.; Foster, J. M.; Griss, J.; Alpi, E.; Birim, M.; Contell, J.; O'Kelly, G.; Schoenegger, A.; Ovelleiro, D.; Perez-Riverol, Y.; Reisinger, F.; Rios, D.; Wang, R.; Hermjakob, H., The PRoteomics IDEntifications (PRIDE) database and associated tools: status in 2013. *Nucleic Acids Res* **2013,** 41, (Database issue), D1063-9.

12. Larance, M.; Lamond, A. I., Multidimensional proteomics for cell biology. *Nat Rev Mol Cell Biol* **2015,** 16, (5), 269-80.

13. Bileck, A.; Kreutz, D.; Muqaku, B.; Slany, A.; Gerner, C., Comprehensive assessment of proteins regulated by dexamethasone reveals novel effects in primary human peripheral blood mononuclear cells. *J Proteome Res* **2014,** 13, (12), 5989-6000.

14. Cox, J.; Mann, M., MaxQuant enables high peptide identification rates, individualized p.p.b.-range mass accuracies and proteome-wide protein quantification. *Nat Biotechnol* **2008,** 26, (12), 1367-72.

15. Cox, J.; Mann, M., 1D and 2D annotation enrichment: a statistical method integrating quantitative proteomics with complementary high-throughput data. *BMC Bioinformatics* **2012,** 13 Suppl 16, S12.

16. R Development Core Team, R: A language and environment for statistical computing. *R Foundation for Statistical Computing, Vienna, Austria* **2010**.

17. Haudek, V. J.; Gundacker, N. C.; Slany, A.; Wimmer, H.; Bayer, E.; Pable, K.; Gerner, C., Consequences of acute and chronic oxidative stress upon the expression pattern of proteins in peripheral blood mononuclear cells. *J Proteome Res* **2008,** 7, (12), 5138-47.

18. Kanehisa, M.; Goto, S., KEGG: kyoto encyclopedia of genes and genomes. *Nucleic Acids Res* **2000,** 28, (1), 27-30.

19. Barbosa, S.; Carreira, S.; Bailey, D.; Abaitua, F.; O'Hare, P., Phosphorylation and SCF-mediated degradation regulate CREB-H transcription of metabolic targets. *Mol Biol Cell* **2015,** 26, (16), 2939-54.

20. Whiteaker, J. R.; Zhao, L.; Yan, P.; Ivey, R. G.; Voytovich, U. J.; Moore, H. D.; Lin, C.; Paulovich, A. G., Peptide Immunoaffinity Enrichment and Targeted Mass Spectrometry Enables Multiplex, Quantitative Pharmacodynamic Studies of Phospho-Signaling. *Mol Cell Proteomics* **2015,** 14, (8), 2261-73.

21. Fila, J.; Honys, D., Enrichment techniques employed in phosphoproteomics. *Amino Acids* **2012,** 43, (3), 1025-47.

22. Ishii, Y.; Yamaizumi, A.; Kawakami, A.; Islam, A.; Choudhury, M. E.; Takahashi, H.; Yano, H.; Tanaka, J., Anti-inflammatory effects of noradrenaline on LPS-treated microglial cells: Suppression of NFkappaB nuclear translocation and subsequent STAT1 phosphorylation. *Neurochem Int* **2015**.

23. Zhang, Y.; Chen, Y.; Wu, J.; Manaenko, A.; Yang, P.; Tang, J.; Fu, W.; Zhang, J. H., Activation of Dopamine D2 Receptor Suppresses Neuroinflammation Through alphaB-Crystalline by Inhibition of NF-kappaB Nuclear Translocation in Experimental ICH Mice Model. *Stroke* **2015,** 46, (9), 2637-46.

24. Kil, S. H.; Kalinec, F., Expression and dexamethasone-induced nuclear translocation of glucocorticoid and mineralocorticoid receptors in guinea pig cochlear cells. *Hear Res* **2013,** 299, 63-78.

25. Stevenson, S. E.; Houston, N. L.; Thelen, J. J., Evolution of seed allergen quantification--from antibodies to mass spectrometry. *Regul Toxicol Pharmacol* **2010,** 58, (3 Suppl), S36-41.

26. Ackermann, B. L.; Berna, M. J., Coupling immunoaffinity techniques with MS for quantitative analysis of low-abundance protein biomarkers. *Expert Rev Proteomics* **2007,** 4, (2), 175-86.

27. Gundacker, N.; Bayer, E.; Traxler, E.; Zwickl, H.; Kubicek, M.; Stockl, J.; Gerner, C., Knowledge-based proteome profiling: considering identified proteins to evaluate separation efficiency by 2-D PAGE. *Electrophoresis* **2006,** 27, (13), 2712-21.

28. Lam, A. P.; Dean, D. A., Cyclic stretch-induced nuclear localization of transcription factors results in increased nuclear targeting of plasmids in alveolar epithelial cells. *J Gene Med* **2008,** 10, (6), 668-78.

29. Schuldenfrei, A.; Belton, A.; Kowalski, J.; Talbot, C. C., Jr.; Di Cello, F.; Poh, W.; Tsai, H. L.; Shah, S. N.; Huso, T. H.; Huso, D. L.; Resar, L. M., HMGA1 drives stem cell, inflammatory pathway, and cell cycle progression genes during lymphoid tumorigenesis. *BMC Genomics* **2011,** 12, 549.

30. Dement, G. A.; Treff, N. R.; Magnuson, N. S.; Franceschi, V.; Reeves, R., Dynamic mitochondrial localization of nuclear transcription factor HMGA1. *Exp Cell Res* **2005,** 307, (2), 388-401.

31. He, S.; Tong, Q.; Bishop, D. K.; Zhang, Y., Histone methyltransferase and histone methylation in inflammatory T-cell responses. *Immunotherapy* **2013,** 5, (9), 989-1004.

32. Palma, L.; Amatori, S.; Cruz Chamorro, I.; Fanelli, M.; Magnani, M., Promoter-specific relevance of histone modifications induced by dexamethasone during the regulation of pro-inflammatory mediators. *Biochim Biophys Acta* **2014,** 1839, (7), 571-8.

33. Shanmugam, M. K.; Sethi, G., Role of epigenetics in inflammation-associated diseases. *Subcell Biochem* **2013,** 61, 627-57.

34. Sefton, B. M., Overview of protein phosphorylation. *Curr Protoc Cell Biol* **2001,** Chapter 14, Unit 14 1.

35. Aggarwal, B. B.; Kunnumakkara, A. B.; Harikumar, K. B.; Gupta, S. R.; Tharakan, S. T.; Koca, C.; Dey, S.; Sung, B., Signal transducer and activator of transcription-3, inflammation, and cancer: how intimate is the relationship? *Ann N Y Acad Sci* **2009,** 1171, 59-76.

36. Clemente, A.; Pons, J.; Lanio, N.; Cunill, V.; Frontera, G.; Crespi, C.; Matamoros, N.; Ferrer, J. M., Increased STAT3 phosphorylation on CD27 B-cells from common variable immunodeficiency disease patients. *Clin Immunol* **2015**.

37. Guan, H.; Hou, S.; Ricciardi, R. P., DNA binding of repressor nuclear factor-kappaB p50/p50 depends on phosphorylation of Ser337 by the protein kinase A catalytic subunit. *J Biol Chem* **2005,** 280, (11), 9957-62.

38. Howe, A. K.; Hogan, B. P.; Juliano, R. L., Regulation of vasodilator-stimulated phosphoprotein phosphorylation and interaction with Abl by protein kinase A and cell adhesion. *J Biol Chem* **2002,** 277, (41), 38121-6.

39. Franchi, L.; Eigenbrod, T.; Munoz-Planillo, R.; Nunez, G., The inflammasome: a caspase-1-activation platform that regulates immune responses and disease pathogenesis. *Nat Immunol* **2009,** 10, (3), 241-7.

40. Mayya, V.; Lundgren, D. H.; Hwang, S. I.; Rezaul, K.; Wu, L.; Eng, J. K.; Rodionov, V.; Han, D. K., Quantitative phosphoproteomic analysis of T cell receptor signaling reveals system-wide modulation of protein-protein interactions. *Sci Signal* **2009,** 2, (84), ra46.

41. Nilsson, T.; Mann, M.; Aebersold, R.; Yates, J. R., 3rd; Bairoch, A.; Bergeron, J. J., Mass spectrometry in high-throughput proteomics: ready for the big time. *Nat Methods* **2010,** 7, (9), 681-5.

42. Deeb, S. J.; Tyanova, S.; Hummel, M.; Schmidt-Supprian, M.; Cox, J.; Mann, M., Machine Learning Based Classification of Diffuse Large B-cell Lymphoma Patients by their Protein Expression Profiles. *Mol Cell Proteomics* **2015**.

Figure Legends

Figure 1: Efficiency of subcellular fractionation and annotation of proteins. (A) Fold-change values of control PBMCs obtained from the t-test statistics between cytoplasmic and nuclear fraction were sorted in a descending fashion and categorized into 7 groups using Excel. Proteins of each group were then classified as "nucleus" and/or "cytoplasm" according to Uniprot subcellular location and visualized using pie charts. (B) Heat map analysis of LFQ-values of the cytoplasmic (cyt) and nuclear fraction (ne) of three biological replicates, each including two technical measurements, were used to demonstrate how proteins may be annotated using shotgun proteomics data.

Figure 2: Translocation events of proteins. (A) Fold-change values of control PBMCs obtained from the t-test statistics between cytoplasmic and nuclear fraction were sorted in a descending fashion. The corresponding differences from the inflammatory activated cells were outlined in grey. (B) Immunofluorescence staining of zinc finger protein 161 homolog (ZFP161), vimentin and DAPI in control and inflammatory activated PBMCs.

Figure 3: Evaluation of the MAPK signaling pathway. The status of the MAPK signaling pathway of inflammatory activated PBMCs was investigated in detail, using a classical shotgun proteomics approach. All events accessible from our dataset were mapped to the pathway downloaded via KEGG. The NFκB, AP1 and ERK4 cascade were outlined using a red, blue and green arrow, respectively.

Figure 4: Identification of the IL-1α-derived peptide RLSLSQSITDDDLEAIANDSEE-EIIKPR. Chromatogram, peak intensity, MS1 spectrum, m/z values as well as charge state of the non-, mono- and bi-phosphorylated state of this peptide are shown. For each state, the MS2 spectrum and the corresponding PEP value are indicated.

Table Legends

Table 1: Nuclear translocation of transcription factors. Uniprot accessions, protein name as well as the extent of nuclear translocation upon inflammatory activation (con ne vs cyt/ act ne vs cyt) are listed.

Table 2: Nuclear translocation of zinc finger proteins. Uniprot accessions, protein name as well as the extent of nuclear translocation upon inflammatory activation (con ne vs cyt/ act ne vs cyt) are listed.

Table 3: Nuclear Translocation of histone-modifying proteins. Uniprot accessions, protein name as well as the extent of nuclear translocation upon inflammatory activation (con ne vs cyt/ act ne vs cyt) are listed.

Table 4: Significantly regulated proteins of MAPK signaling pathway upon inflammatory activation. For each subcellular fraction (secretome, cytoplasm and nuclear extract), fold changes of protein levels between control versus activated PBMCs as well as corresponding p-values are listed.

Supplementary Table S1: Identified proteins. Uniprot accession and protein name of all identified proteins contained in the present data set are listed.

Supplementary Table S2: Identified phosphopeptides and corresponding phosphoproteins. Phosphorylated amino acids, ion score and PEP values for all identifies phosphopeptides and corresponding phosphoproteins are listed separately for each subcellular location (cytoplasm, nucleus and supernatant), donor (donor 1, 2, 3) and functional state (con = control PBMCs; act = inflammatory activated PBMCs). Identified phosphoproteins which are also annotated as phosphoproteins according to Uniprot are marked.

Supplementary Table S3: Phosphoproteins found to translocate into the nucleus upon inflammatory activation. Uniprot accession and protein names are listed.

Table 1: Nuclear translocation of transcription factors

Accession	Protein name	con ne vs cyt/ act ne vs cyt
P23511	Nuclear transcription factor Y subunit alpha	3.2
Q13950	Runt-related transcription factor 2	5.7
P05412	Transcription factor AP-1	12.0
Q9ULX9	Transcription factor MafF	4.4
P48380	Transcription factor RFX3	5.8
P21675	Transcription initiation factor TFIID subunit 1	3.4
Q5VWG9	Transcription initiation factor TFIID subunit 3	3.2
P49848	Transcription initiation factor TFIID subunit 6	3.8
Q7Z7C8	Transcription initiation factor TFIID subunit 8	3.7
P46100	Transcriptional regulator ATRX	2.5
P49711	Transcriptional repressor CTCF	3.4
Q96PN7	Transcriptional-regulating factor 1	5.4

Table 2: Nuclear translocation of zinc finger proteins

Accession	Protein name	con ne vs cyt/ act ne vs cyt
O75626	PR domain zinc finger protein 1	4.6
Q9NQV6	PR domain zinc finger protein 10	2.8
Q9UBW7	Zinc finger MYM-type protein 2	2.5
Q9UQR1	Zinc finger protein 148	4.2
O43829	Zinc finger protein 161 homolog	2.8
Q16670	Zinc finger protein 187	3.3
Q8NF99	Zinc finger protein 397	17.2
Q96C55	Zinc finger protein 524	5.4
Q92610	Zinc finger protein 592	6.7
Q8N1G0	Zinc finger protein 687	6.0
Q15072	Zinc finger protein OZF	5.3
Q9UHF7	Zinc finger transcription factor Trps1	3.8
P17010	Zinc finger X-chromosomal protein	2.0

Table 3: Nuclear Translocation of histone-modifying proteins

Accession	Protein name	con ne vs cyt/ act ne vs cyt
Q92993	Histone acetyltransferase KAT5	3.0
Q9UPP1	Histone lysine demethylase PHF8	6.7
Q9H9B1	Histone-lysine N-methyltransferase EHMT1	4.0
Q96KQ7	Histone-lysine N-methyltransferase EHMT2	3.0
Q92800	Histone-lysine N-methyltransferase EZH1	9.2
Q03164	Histone-lysine N-methyltransferase MLL	3.4
Q9UPS6	Histone-lysine N-methyltransferase SETD1B	2.0
Q15047	Histone-lysine N-methyltransferase SETDB1	2.1
Q8NB78	Lysine-specific histone demethylase 1B	6.4

Table 4: Significantly regulated proteins of MAPK signaling pathway upon inflammatory activation

		secretome		cytoplasm		nuclear extract	
Accession	Protein name	ln_2 (Δt-test)	p-value	ln_2 (Δt-test)	p-value	ln_2 (Δt-test)	p-value
P01375	Tumor necrosis factor	3.54	2.57E-04	2.84	4.60E-03	-	-
P01583	Interleukin-1 alpha	3.45	1.08E-04	5.99	3.11E-04	-	-
P01584	Interleukin-1 beta	5.73	5.91E-07	4.45	4.97E-05	2.71	1.45E-03
P01137	Transforming growth factor beta-1	2.67	3.05E-02	-0.16	8.01E-01	0.41	7.23E-01
P20333	Tumor necrosis factor receptor superfamily member 1B	1.55	6.93E-02	2.33	2.88E-02	1.45	1.17E-02
P32121	Beta-arrestin-2	1.45	3.51E-02	-0.34	6.69E-01	0.38	3.49E-01
Q13188	Serine/threonine-protein kinase 3	-	-	1.07	1.89E-01	1.16	2.29E-02
Q16690	Dual specificity protein phosphatase 5	-	-	-	-	1.57	2.25E-02
P05412	Transcription factor AP-1	-	-	-1.99	2.32E-01	1.59	1.37E-02
Q9BYH8	NF-kappa-B inhibitor zeta	-	-	-1.03	1.94E-01	2.97	7.25E-04
O95644	Nuclear factor of activated T-cells, cytoplasmic 1	-	-	-0.36	7.47E-01	2.87	7.16E-03
Q13469	Nuclear factor of activated T-cells, cytoplasmic 2	-	-	-0.08	8.80E-01	1.93	6.70E-04
Q04206	Transcription factor p65	-	-	0.36	5.66E-01	1.21	1.17E-02
Q01201	Transcription factor RelB	-	-	0.82	4.72E-01	2.13	1.45E-03
P08571	Monocyte differentiation antigen CD14	-2.14	1.38E-02	-1.47	1.63E-01	-1.51	2.11E-01
Q8TDF6	RAS guanyl-releasing protein 4	-	-	-1.65	2.40E-01	1.46	1.42E-02
P15336	Cyclic AMP-dependent transcription factor ATF-2	-	-	-1.02	3.95E-02	0.04	9.68E-01

Graphical abstract

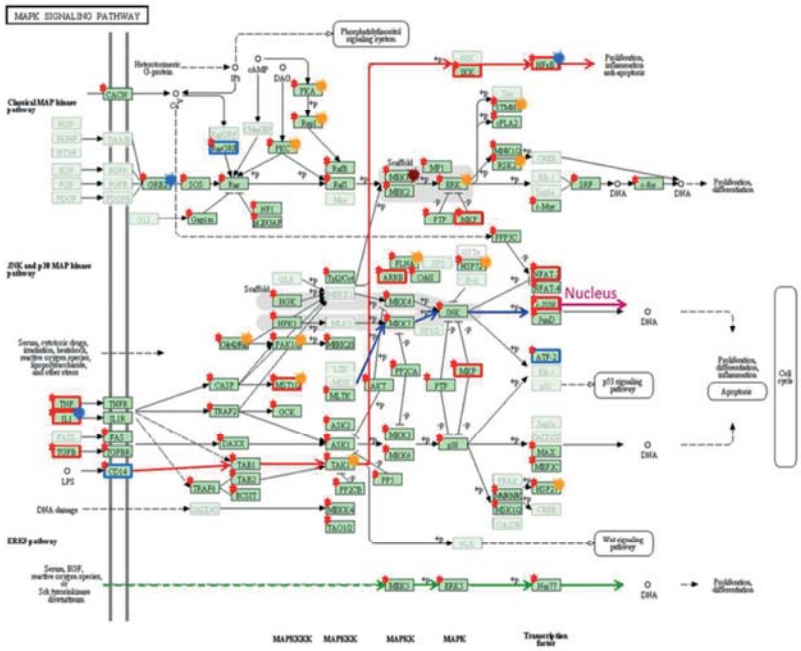

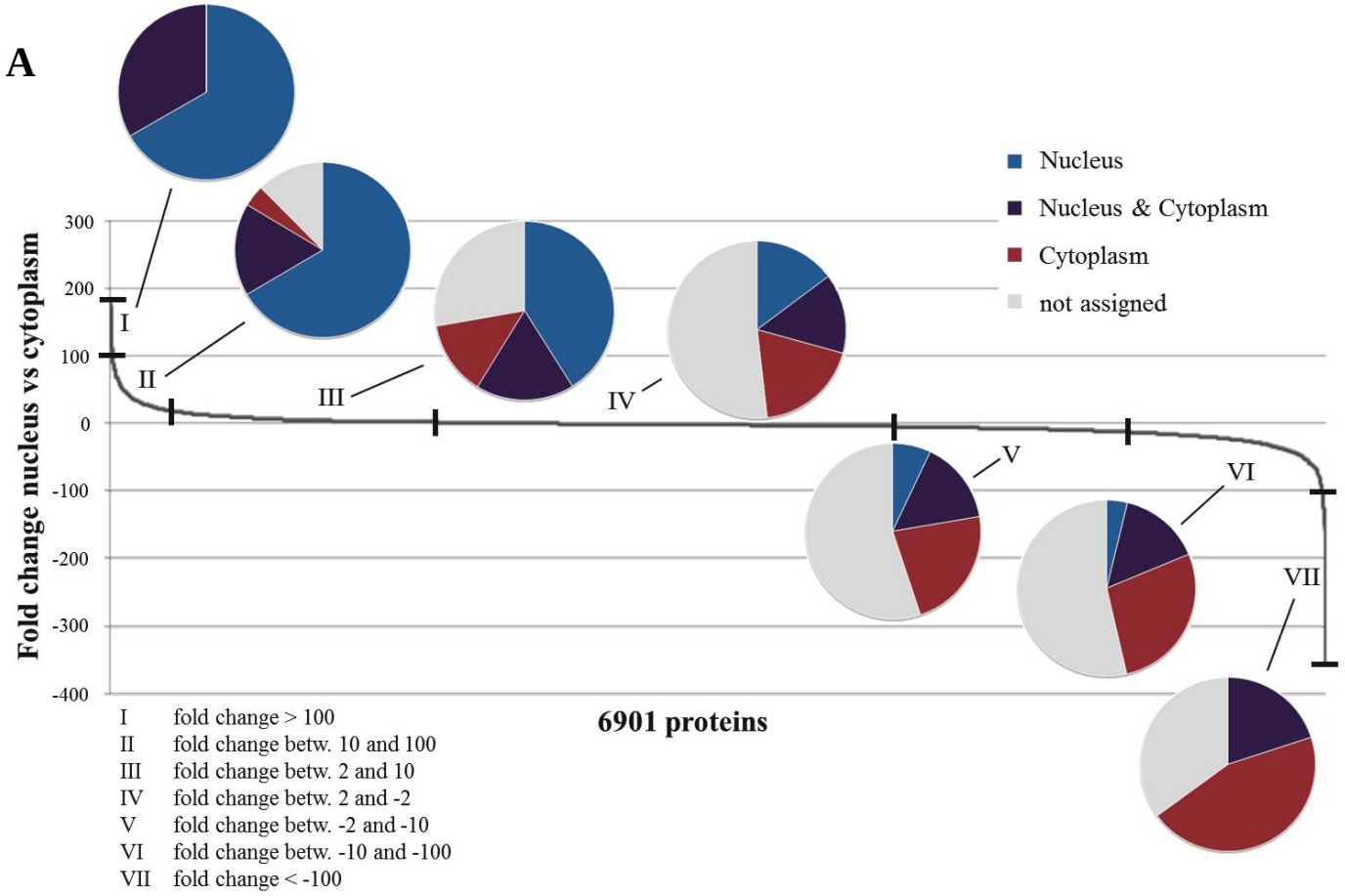
A
Nucleus
Nucleus & Cytoplasm
Cytoplasm
not assigned
Fold change nucleus vs cytoplasm
300
200
100
0
-100
-200
-300
-400
I
II
III
IV
V
VI
VII
6901 proteins
I fold change > 100
II fold change betw. 10 and 100
III fold change betw. 2 and 10
IV fold change betw. 2 and -2
V fold change betw. -2 and -10
VI fold change betw. -10 and -100
VII fold change < -100

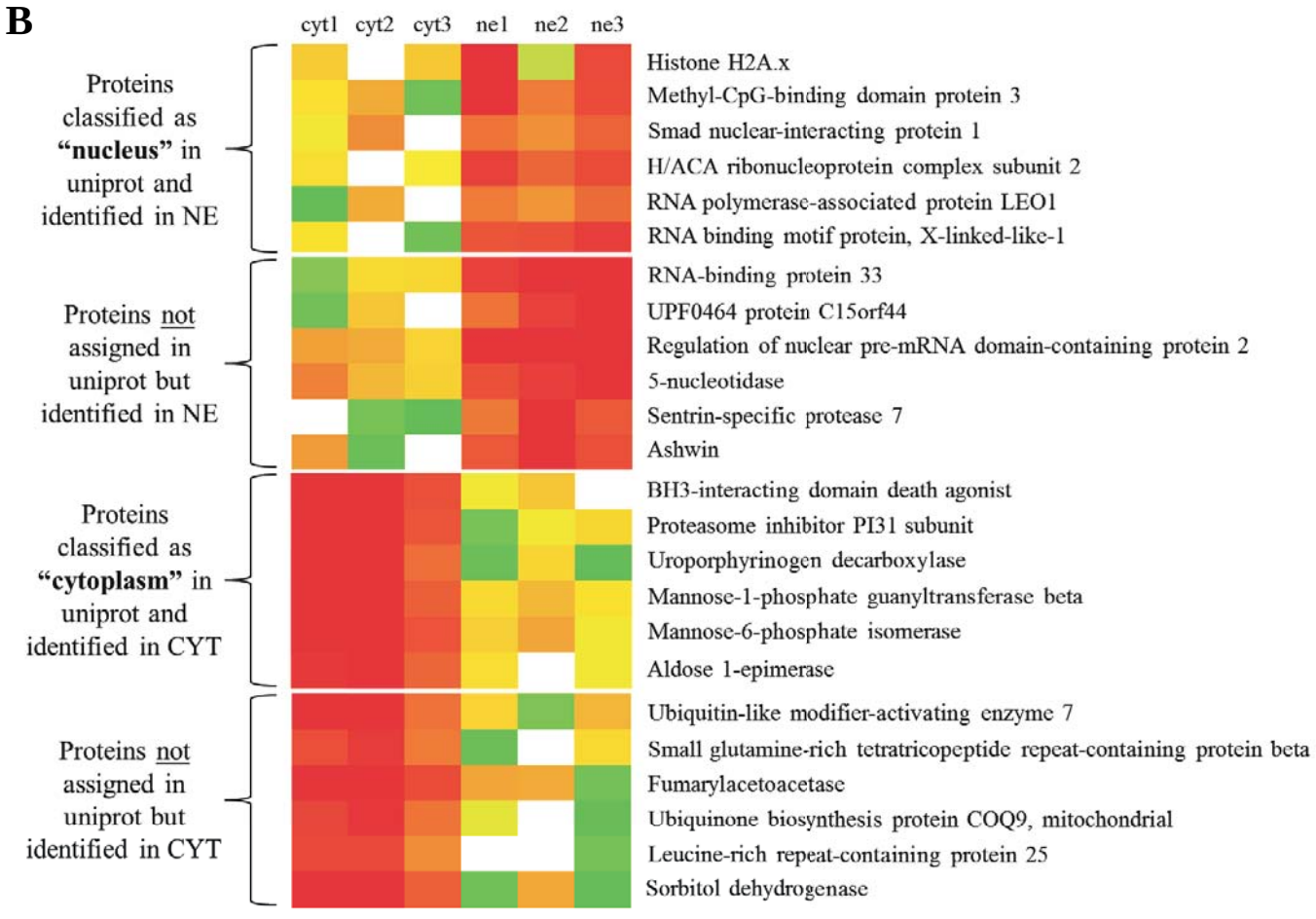
B
cyt1 cyt2 cyt3 ne1 ne2 ne3
Proteins classified as "nucleus" in uniprot and identified in NE
Histone H2A.x
Methyl-CpG-binding domain protein 3
Smad nuclear-interacting protein 1
H/ACA ribonucleoprotein complex subunit 2
RNA polymerase-associated protein LEO1
RNA binding motif protein, X-linked-like-1
Proteins not assigned in uniprot but identified in NE
RNA-binding protein 33
UPF0464 protein C15orf44
Regulation of nuclear pre-mRNA domain-containing protein 2
5-nucleotidase
Sentrin-specific protease 7
Ashwin
Proteins classified as "cytoplasm" in uniprot and identified in CYT
BH3-interacting domain death agonist
Proteasome inhibitor PI31 subunit
Uroporphyrinogen decarboxylase
Mannose-1-phosphate guanyltransferase beta
Mannose-6-phosphate isomerase
Aldose 1-epimerase
Proteins not assigned in uniprot but identified in CYT
Ubiquitin-like modifier-activating enzyme 7
Small glutamine-rich tetratricopeptide repeat-containing protein beta
Fumarylacetoacetase
Ubiquinone biosynthesis protein COQ9, mitochondrial
Leucine-rich repeat-containing protein 25
Sorbitol dehydrogenase

Figure 1

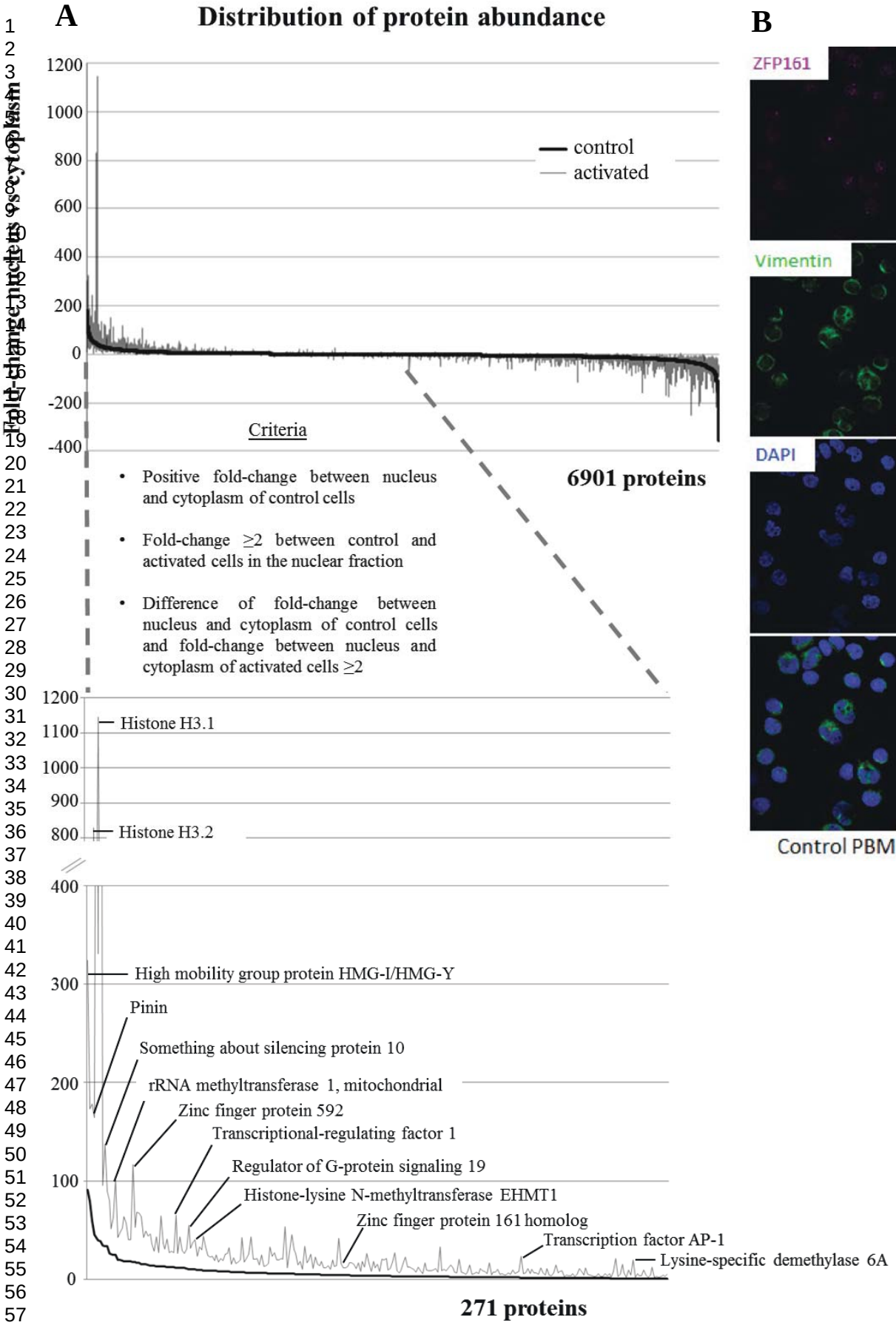
A
Distribution of protein abundance
Fold-change nucleus vs cytoplasm
control
activated
Criteria
• Positive fold-change between nucleus and cytoplasm of control cells
• Fold-change ≥2 between control and activated cells in the nuclear fraction
• Difference of fold-change between nucleus and cytoplasm of control cells and fold-change between nucleus and cytoplasm of activated cells ≥2
6901 proteins
Histone H3.1
Histone H3.2
High mobility group protein HMG-I/HMG-Y
Pinin
Something about silencing protein 10
rRNA methyltransferase 1, mitochondrial
Zinc finger protein 592
Transcriptional-regulating factor 1
Regulator of G-protein signaling 19
Histone-lysine N-methyltransferase EHMT1
Zinc finger protein 161 homolog
Transcription factor AP-1
Lysine-specific demethylase 6A
271 proteins
B
ZFP161
Vimentin
DAPI
Control PBMCs
Activated PBMCs

Figure 2

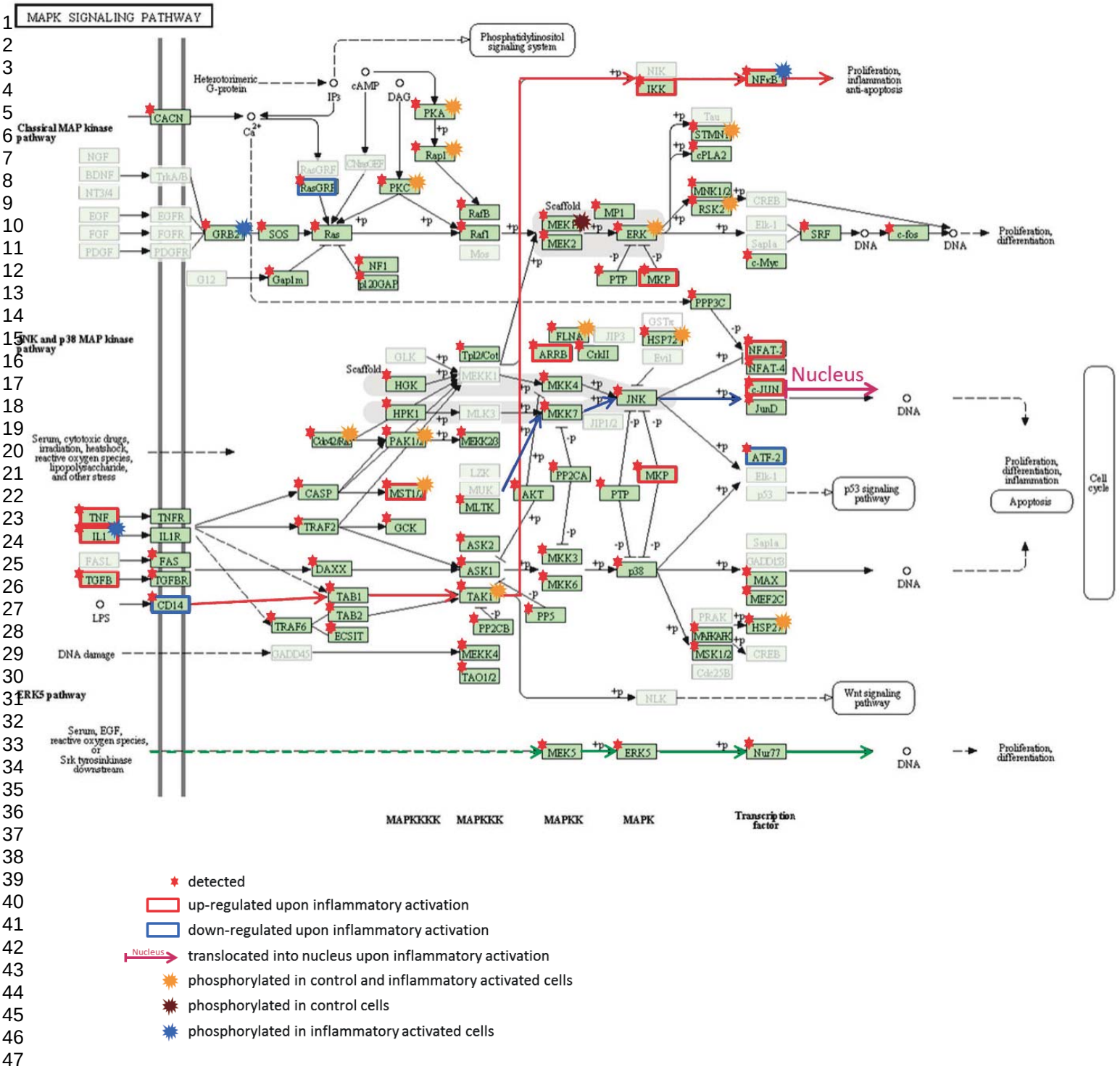
MAPK SIGNALING PATHWAY
Classical MAP kinase pathway
JNK and p38 MAP kinase pathway
ERK5 pathway
Phosphatidylinositol signaling system
Heterotorimeric G-protein
Proliferation, inflammation anti-apoptosis
Proliferation, differentiation
Nucleus
DNA
Serum, cytotoxic drugs, irradiation, heatshock, reactive oxygen species, lipopolysaccharide, and other stress
LPS
DNA damage
Serum, EGF, reactive oxygen species, or Src tyrosinkinase downstream
p53 signaling pathway
Apoptosis
Cell cycle
Wnt signaling pathway
Scaffold
MAPKKKK
MAPKKK
MAPKK
MAPK
Transcription factor
detected
up-regulated upon inflammatory activation
down-regulated upon inflammatory activation
translocated into nucleus upon inflammatory activation
phosphorylated in control and inflammatory activated cells
phosphorylated in control cells
phosphorylated in inflammatory activated cells

Figure 3

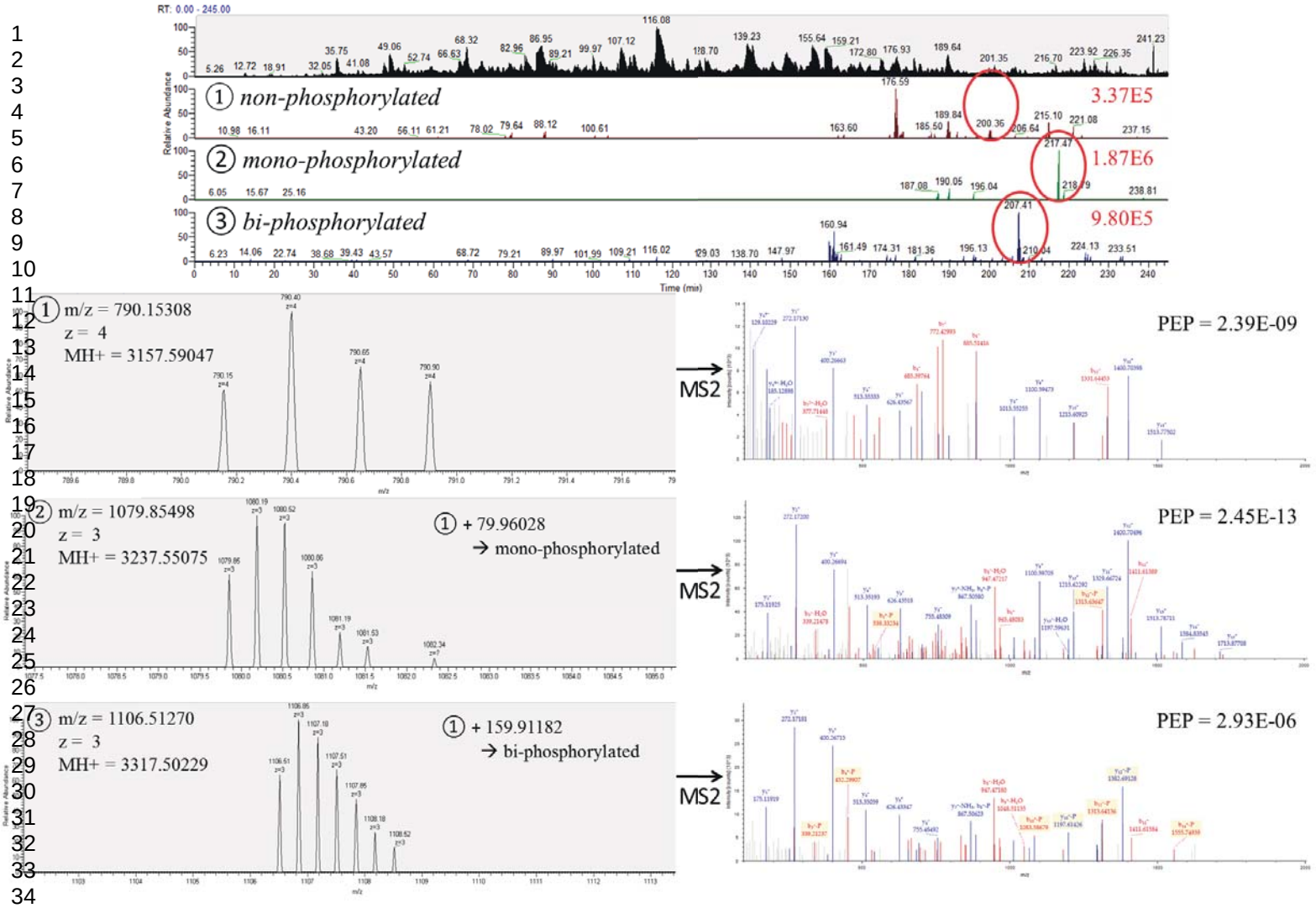
RT: 0.00 - 245.00
Relative Abundance
① non-phosphorylated
3.37E5
② mono-phosphorylated
1.87E6
③ bi-phosphorylated
9.80E5
Time (min)
① m/z = 790.15308
z = 4
MH+ = 3157.59047
MS2
PEP = 2.39E-09
② m/z = 1079.85498
z = 3
MH+ = 3237.55075
① + 79.96028
→ mono-phosphorylated
MS2
PEP = 2.45E-13
③ m/z = 1106.51270
z = 3
MH+ = 3317.50229
① + 159.91182
→ bi-phosphorylated
MS2
PEP = 2.93E-06

Figure 4

3.4. Contribution of human fibroblasts and endothelial cells to the hallmarks of inflammation as determined by proteome profiling

Astrid Slany[a], Andrea Bileck[a], Dominique Kreutz[a], Rupert L. Mayer[a], Besnik Muqaku[a], Christopher Gerner[a]

Molecular & Cellular Proteomics, **2016,** manuscript in press

[a] Department of Analytical Chemistry, Faculty of Chemistry, University of Vienna, Währinger Str. 38, A-1090 Vienna, Austria

Contributions to this publication:

- Conduction of experiments
- Organization of required materials
- Creation of figures
- Involved in data interpretation

MCP Papers in Press. Published on March 29, 2016 as Manuscript M116.058099

ASBMB MOLECULAR & CELLULAR PROTEOMICS MCP

Contribution of human fibroblasts and endothelial cells to the hallmarks of inflammation as determined by proteome profiling

Dedicated to Prof. Bernhard Keppler on the occasion of his 60th birthday

Astrid Slany[1], Andrea Bileck[1], Dominique Kreutz[1], Rupert L. Mayer[1], Besnik Muqaku[1], Christopher Gerner[1]

[1]Department of Analytical Chemistry, Faculty of Chemistry, University of Vienna, Austria

Corresponding author

Christopher Gerner

Department of Analytical Chemistry

University of Vienna

Waehringerstr. 38

1090 Vienna

Austria

christopher.gerner@univie.ac.at

+43-1-4277-52302

Copyright 2016 by The American Society for Biochemistry and Molecular Biology, Inc.

MCP MOLECULAR & CELLULAR PROTEOMICS ASBMB

Running Title

Hallmarks of inflammation: cell type-specific manifestation

ASBMB MOLECULAR & CELLULAR PROTEOMICS MCP

Abbreviations

COX-2, prostaglandin G/H synthase 2; **EC**, endothelial cells; **ECM**, extracellular matrix; **EndMT**, endothelial to mesenchymal transition; **FA,** formic acid; **FDR**, false discovery rate; **GBPs**, guanylate-binding proteins; **HUVEC**, human umbilical vein endothelial cells; **IAA**, iodoacetamide; **IFITs**, interferon-induced proteins with tetratricopeptide repeats; **IFN**, interferon; **IL-1RA**, interleukin-1 receptor antagonist protein; **LAMC2**, laminin subunit gamma-2; **LFQ**, label-free quantification; **LIF**, leukemia inhibition factor; **MEK**, mitogen-activated protein kinase kinase; **MMPs**, matrix metalloproteinases; **Mx1**, interferon-induced GTP-binding protein Mx1; **NHDF**, normal human dermal fibroblasts; **NRCAM**, neuronal cell adhesion molecule; **PBMCs**, peripheral blood mononuclear cells; **PRRX1**, paired mesoderm homeobox protein 1; **PRRX2**, paired mesoderm homeobox protein 2; **TAL1**, T-cell acute lymphocytic leukemia protein 1; **TGFβ2**, transforming growth factor beta-2; **TNC**, tenascin; **TSG6**, tumor necrosis factor-inducible gene 6 protein; **TSP1**, thrombospondin-1; **TSP2**, thrombospondin-2; **VEGF**, vascular endothelial growth factor

ASBMB
MOLECULAR & CELLULAR PROTEOMICS
MCP

Summary

In order to systematically analyze proteins fulfilling effector functionalities during inflammation, here we present a comprehensive proteome study of inflammatory activated primary human endothelial cells and fibroblasts. Cells were stimulated with interleukin 1-beta and fractionated in order to obtain secreted, cytoplasmic and nuclear protein fractions. Proteins were submitted to a data-dependent bottom up analytical platform using a QExactive orbitrap and the MaxQuant software for protein identification and label-free quantification. Results were further combined with similarly generated data previously obtained from the analysis of inflammatory activated peripheral blood mononuclear cells. Applying an FDR of less than 0.01 at both, peptide and protein level, a total of 8370 protein groups assembled from 117599 peptides was identified; mass spectrometry data have been made fully accessible via ProteomeXchange with identifier PXD003406 to PXD003417. Comparative proteome analysis allowed us to determine common and cell type-specific inflammation signatures comprising novel candidate marker molecules and related expression patterns of transcription factors. Cardinal features of inflammation such as interleukin 1-beta processing and the interferon response differed substantially between the investigated cells. Furthermore, cells also exerted similar inflammation-related tasks; however, by making use of different sets of proteins. Hallmarks of inflammation thus emerged, including angiogenesis, extracellular matrix reorganization, adaptive and innate immune responses, oxidative stress response, cell proliferation and differentiation, cell adhesion and migration in addition to monosaccharide metabolic processes, representing both, common and cell type-specific responsibilities of cells during inflammation.

ASBMB MOLECULAR & CELLULAR PROTEOMICS MCP

Introduction

Inflammation is a complex process, which plays, especially in its chronic form, an important role in many diseases of modern civilization such as cardiovascular and neurological disorders and diverse cancers (1-3). While it is possible to cure acute inflammation, chronic inflammation still represents a great challenge and often responds in an unsatisfying fashion to sustained treatment. In acute inflammation, the relations between cause and effects may be rather straight, so that it may be sufficient to block a single activity, for example that of COX-2, in order to achieve relieve of symptoms and subsequent healing. In chronic inflammation, these relations seem to be more complex and a simple treatment may not be successful. Actually, several different cell types are involved in inflammation, contributing to the complex signaling network necessary for the appropriate exertion and completion of this process. Chronic inflammation may occur when specific regulation mechanisms which are necessary to resolve the inflammatory process fail, resulting in an uncontrolled escalation of the ongoing processes (4). Accumulation of pro-inflammatory signaling molecules and effector cells at the site of inflammation (5), the production of new blood vessels enabling the incessant recruitment of inflammatory cells (6), or the excess deposition of extracellular matrix components resulting from an uncontrolled inflammation-related wound healing process (7) can be some of the consequences.

Different cell types may fulfill different functionalities during inflammation. Obviously, each cell type has its repertoire of specific regulatory factors and may contribute to the regulation of inflammation in a specific manner. In this way, all cell types may be cooperating to achieve the fine tuning of the complex process of inflammation. Main players of inflammation, and main targets for anti-inflammatory treatments, are leukocytes, including neutrophils and monocytes as part of the innate immune response, as well as B- and T-lymphocytes, activated in the course of an inflammation-related adaptive immune response. Under normal conditions, when they have fulfilled their tasks, these cells are rapidly neutralized by induction of apoptosis (8). Stromal cells such as fibroblasts and endothelial cells are involved in the process of inflammation as well, and these cells are capable of

ASBMB MOLECULAR & CELLULAR PROTEOMICS MCP

surviving for a longer time and may stay in their functionally activated state when the inflammatory process should be completed, thus possibly contributing to the development of chronic inflammation (9). While the most important players of inflammation have been well described, a systematic analysis of the proteins fulfilling the effector functionalities during inflammation has not yet been undertaken. This would, however, contribute to a better understanding of the ongoing complex processes and may thus support the development of new therapeutic strategies to combat chronic inflammation and related diseases (10).

Here we present a systematic proteome study of inflammatory activated primary human dermal fibroblasts (NHDF) and human umbilical vein endothelial cells (HUVEC). These cells have been analyzed by us previously (11, 12) demonstrating that they display all relevant cell type characteristics of stromal fibroblasts and endothelial cells, and thus represent suitable model systems. A standardized approach has been applied to semi-quantitatively determine and compare the relevant regulatory factors that were up- and downregulated by fibroblasts and endothelial cells upon inflammatory activation. To this end, NHDF and HUVEC were stimulated *in vitro* with the canonical inflammation mediator interleukin-1beta (IL-1β) (13). Secreted, cytoplasmic and nuclear proteins were extracted from the cells and analyzed separately by shotgun proteomics using a QExactive orbitrap mass spectrometer. Results were further combined with data obtained from previous investigations on inflammatory activated peripheral blood mononuclear cells (PBMCs) (14). In this way, cell type-specific inflammation-related functionalities were determined, as well as inflammatory signatures and marker molecules which may be indicative for the inflammatory processes occurring *in vivo*. This motivated us to define hallmarks of inflammation - in the style of the hallmarks of cancer (15) - representing the biological processes essential for the successful resolution of inflammation and to specify responsibilities of fibroblasts, endothelial cells and leukocytes therein.

ASBMB MOLECULAR & CELLULAR PROTEOMICS MCP

Experimental Procedures

Cell culture

Primary human umbilical vein endothelial cells (HUVEC) were purchased from Lonza (Walkersville Inc., USA). HUVEC were cultured in endothelial basal medium supplemented with the EGM-2 SingleQuot Kit (both EBM, Lonza Walkersville Inc., USA), 10% FCS and 100 U/ml penicillin/streptomycin (both ATCC, USA), according to the instructions of the manufacturer. Normal human dermal fibroblasts (NHDF) were kindly provided by Verena Paulitschke from the General Hospital of Vienna. NHDF were cultured in RPMI 1640 (Life Technologies, UK) supplemented with 10% FCS and 100U/ml penicillin/streptomycin (both ATCC, USA) at 37°C and 5% CO_2. Cells were used up to passage 7 and 22 for HUVEC and NHDF, respectively. Experiments were performed in 75cm^2-culture flasks, using approximately 5x10^6 cells per flask. Cell numbers, as well as cell viability which was consistently better than 98%, were determined using a MOXI cell counter (ORFLO, USA). Inflammatory stimulation with 10ng/mL of IL-1β (Sigma-Aldrich, USA) was carried out for 24 hours, as applied in previous studies (11, 16, 17). Control cells were incubated in parallel without IL-1β. After that, cells were washed with PBS and further cultured for 6 hours in 6 ml of serum-free medium. Biological replicates were prepared for each cell type to allow statistical analyses of the resulting data.

Cell fractionation

Supernatants of control and inflammatory activated cells were filtered through 0.2 µm filters (Whatman, Germany) and proteins therein were precipitated overnight with ethanol at -20°C. To obtain the cytoplasmic protein fractions as well as the nuclear protein extracts, we proceeded as previously described (14). In short, cells were lysed in isotonic lysis buffer supplemented with protease inhibitors by applying mechanical shear stress. Cytoplasmic proteins were separated from nuclei by centrifugation and precipitated overnight with ethanol at -20°C. Nuclear proteins were extracted by incubating the nuclei in 500mM NaCl and solubilizing the proteins in NP-40 buffer

ASBMB MOLECULAR & CELLULAR PROTEOMICS MCP

supplemented with protease inhibitors. The extracted proteins were separated from resting cell materials by centrifugation and precipitation of the resulting supernatant with ethanol at -20°C overnight. After precipitation, all samples were dissolved in sample buffer (7.5 M urea, 1.5 M thiourea, 4% CHAPS, 0.05% SDS, 100 mM dithiothreitol (DTT)) and the protein concentrations were determined by means of a Bradford assay (Bio-Rad-Laboratories, Germany).

Sample preparation

For proteomics analyses, we prepared in-solution digests from all three subcellular protein fractions of NHDF and HUVEC, as previously described (14). In short, 20µg of each protein sample was concentrated onto a 3kD MWCO filter (Pall Austria Filter GmbH) pre-washed with LC-MS grade water (Millipore GesmbH); proteins were reduced with DTT and alkylated with iodoacetamide (IAA). After centrifugation at 14000g for 10min, proteins on top of the filter were washed with 50mM ammonium bicarbonate buffer. Trypsin (Roche Diagnostics, Germany) was then added and incubation was performed at 37°C for 18h. After trypsin digestion, peptide samples were cleaned up with C-18 spin columns (Pierce, Thermo Scientific) and eluted two times with 50% acetonitrile (ACN), 0.1% trifluoroacetic acid (TFA) and once with 80% ACN, 0.1% TFA. Samples were finally dried in a speedvac and stored at -20°C until further MS analyses. For cytoplasmic proteins and nuclear extracts, in addition to in-solution digests, in-gel digests were prepared, for one biological replicate in case of NHDF and two in case of HUVEC. This was done as previously described (18). In short, 20µg of each sample was loaded on an SDS-PAGE and allowed to separate for 1.5cm, after what proteins in the gel were stained by an MS-compatible silver staining procedure. Afterwards, each protein band was cut into 4 slices which were again decolored. Upon reduction with DTT and alkylation with IAA, the proteins were digested for 18h at 37°C using trypsin (Roche Diagnostics, Germany). The digested peptides were eluted, once with 50mM ammonium bicarbonate, and twice with 5% FA/50% ACN. The eluted peptide samples were dried and then stored at -20°C until further MS analyses.

LC-MS/MS analysis

ASBMB MOLECULAR & CELLULAR PROTEOMICS MCP

Dried samples were solubilized in 5µl 30% formic acid (FA) containing 10fmol each of 4 synthetic standard peptides (allowing us to verify the quality of the chromatographic separation) and diluted with 40µl mobile phase A (98% H_2O, 2% ACN, 0.1% FA). Of this solution, 10µl were injected into the nano HPLC-system (Dionex Ultimate 3000). Peptides were first concentrated on a 2cm x75µm C18 Pepmap100 pre-column (Thermo Fisher Scientific, Austria) at a flow rate of 10µl/min using mobile phase A. Separation of the peptides was achieved by eluting them from the pre-column to a 50cmx75µm Pepmap100 analytical column (Thermo Fisher Scientific, Austria) applying a flow rate of 300nl/min and using a gradient of 8% to 40% mobile phase B (80% ACN, 20% H_2O, 0.1% FA), over 235min for the analysis of cytoplasmic samples and nuclear fractions, and over 95min in case of secretome analysis. The mass spectrometric analysis was performed on a QExactive orbitrap mass spectrometer, equipped with a nanospray ion source (Thermo Fisher Scientific, Austria), coupled to the nano HPLC system. For detection, MS scans were performed in the range from m/z 400-1400 at a resolution of 70000 (at m/z =200). MS/MS scans were performed choosing a top 12 method for cytoplasmic samples and nuclear fractions and a top 8 method for secretome analysis; HCD fragmentation was applied at 30% normalized collision energy and analysis in the orbitrap at a resolution of 17500 (at m/z =200).

Experimental design and statistical rational

For the investigation of functional signatures, pairs of treated and untreated cells were compared. Technical replicates provided a measure for the coefficient of variation introduced by the applied methodology. In addition, independent cell experiments, here designated as biological replicates, were performed. Furthermore, to assess potential effects of different donors, in case of HUVEC, three individual donors were investigated. Two independent cell experiments each of donor 1 and 2, and three independent cell experiments of donor 3 were performed, thus resulting in seven biological replicates. While quantitative differences concerning the extent of regulation of individual proteins between the donors were evident, the actually regulated proteins were the same in all donors. Consequently, in case of NHDF, the investigation of three biological replicates derived from

ASBMB MOLECULAR & CELLULAR PROTEOMICS MCP

one donor was considered as adequate to assess regulatory effects in these cells. Combining biological and technical replicates finally resulted in a total of fourteen individual LC-MS/MS measurements in case of HUVEC and six in case of NHDF. All replicates were used for statistical analyses. The positive identification of a large number of known inflammation players strongly supports the present strategy. Before statistical evaluation, identified proteins were filtered for reversed sequences, common contaminants and a minimum of three independent experimental identifications in at least one cell type in a given functional state.

Peptide and protein identification

Identification of proteins as well as label-free quantification (LFQ) and statistical analyses were performed using the MaxQuant 1.5.2.8 software including the Andromeda search engine and the Perseus statistical analysis package (19, 20), a commonly used workflow for processing and statistical assessment of shotgun proteomics data. For statistical analysis, data obtained from both biological and technical replicates were used. Furthermore, the obtained data from the current study were combined with data obtained from previous investigations on inflammatory activated PBMCs. Proteins were identified using the UniProt database for human proteins (version 102014 with 20 195 entries, restricted to reviewed entries only), a peptide mass tolerance of 25ppm, an MS/MS match tolerance of 20ppm and a maximum of 2 missed cleavages with trypsin as protease. Search criteria further included carbamidomethylation of cysteines as fixed modification, methionine oxidation as well as N-terminal protein acetylation as variable modifications, and a minimum of two peptide identifications per protein, at least one of them unique. Furthermore, match between runs was performed using a 5min match time window and a 15min alignment time window. For both, peptides and proteins, a false discovery rate (FDR) of less than 0.01 was applied; the FDR was determined by the target-decoy approach. No additional filtering concerning the Andromeda score for accepting MS/MS identifications was recommended by the MaxQuant software when applying a strict FDR. The mass spectrometry-based proteomics data (including raw files, result files and peak list files, peptide

ASBMB MOLECULAR & CELLULAR PROTEOMICS MCP

sequences, precursor charges, mass to charge ratios, amino acid modifications, peptide identification scores, protein accession numbers, number of distinct peptides assigned for each identified protein, percent coverage of each identified protein in each individual experiment and annotated MS2 spectra for each peptide spectrum match) have been deposited to the ProteomeXchange Consortium (21) via the PRIDE partner repository with the dataset identifier PXD003406 to PXD003417 (Supplementary Table S9), accessible via www.proteomeexchange.org. As MaxQuant-derived data are not yet supported for complete submissions, here we used Proteome Discoverer 1.4 running Mascot 2.5 and Uniprot for human proteins (version 112015 with 20193 entries, restricted to reviewed entries only) as search engine. Actually all proteins found to be regulated via MaxQuant were positively identified by Proteome Discoverer as well. Finally, for selected proteins, heat maps representing corresponding LFQ values determined in the respective cell type and cell state, were generated. In case of NHDF, average LFQ-values of the technical replicates were used. In case of HUVEC, the average LFQ-values per donor were used, in this case averaging both technical and biological replicates. Heat maps were generated using an R script (22) based on the raw data obtained from MaxQuant without any further data manipulation.

Quantification

Label-free quantification as described in the former paragraph resulted in LFQ values for each individual protein and was used for quantitative assessment of protein regulation. LFQ values were obtained for all proteins from all experiments (Supplementary Tables S6, S7 and S8) and subjected to a comparative analysis; the same initial protein amount of 20µg used in all experiments served for normalization. Isoforms of individual proteins were summarized into protein groups by the Andromeda software and were not further considered here. Mutual comparisons between untreated and inflammatory activated cells were performed to determine protein groups which were significantly up- or downregulated upon inflammatory activation in each cell type. To this end, using the Perseus statistical analysis package, differences of LFQ values were calculated. Changes in protein abundance values between untreated and stimulated cells were determined by a two-sided t test

ASBMB MOLECULAR & CELLULAR PROTEOMICS MCP

with p<0.05 and a minimum of a twofold abundance difference. All proteins meeting these criteria were considered in the present study as potentially contributing to the regulatory effects taking place during inflammation. In addition, to emphasize the most robust regulatory effects observed within one kind of cell, we determined significantly regulated proteins with a global FDR<0.05 (indicated in Tables 1-4 and Supplementary Tables S1 –S5) as determined by a permutation-based method, referring to Cox *et al.* and Tusher *et al.* (23, 24).

ASBMB MOLECULAR & CELLULAR PROTEOMICS MCP

Results

Proteome profiling of inflammatory activated NHDF and HUVEC

In this study, a systematic investigation of proteins fulfilling important effector functionalities during inflammation has been undertaken. To this end, in-depth proteome profiling data of inflammatory activated primary human fibroblasts (NHDF) and endothelial cells (HUVEC) were generated. Secreted, cytoplasmic and nuclear proteins were extracted from cells and analyzed by shotgun proteomics using a QExactive orbitrap mass spectrometer. Comprehensive proteome profiles were generated by combining all data related to one cell type and cell state. Identification of proteins as well as determination of LFQ-values as abundance measure and statistical analyses of proteins were performed using the MaxQuant and Perseus software (19, 25). Results obtained from previous investigations about inflammatory activated PBMCs (14) were included. As a result, a total of 8370 protein groups assembled from 117599 distinct peptides was identified and semi-quantitatively assessed. Comparative proteome profiling was performed to determine proteins which were regulated in the different cell types upon inflammatory activation. Accordingly, 667 proteins were up- or downregulated ($p<0.05$) with a minimum of twofold change of LFQ values between control and inflammatory activated HUVEC (Supplementary Table S1). Figure 1A shows volcano plots representing the regulation of proteins in the cytoplasm, the nucleus and the secretome of these cells. In activated NHDF, 894 proteins were found to be at least twofold up- or downregulated ($p<0.05$) when compared to controls (Supplementary Table S2). Corresponding volcano plots are represented in Figure 1B. In activated PBMCs, 646 proteins had been found to be regulated (Supplementary Table S3).

Common and cell type-specific protein regulation during inflammation

We first investigated these results with regard to common regulatory processes. Actually, we determined 26 proteins which were found to be regulated in all three kinds of cells upon inflammatory stimulation (Figure 2). Among these, 19 proteins, listed in Table 1A, were consistently

upregulated. Those included well-known pro-inflammatory mediators such as prostaglandin G/H synthase 2 (COX-2), interleukins such as IL-6 and IL-8, and C-X-C motif chemokines such as CXCL1, CXCL2 and CXCL5. Furthermore, proteins involved in the innate immune response, such as complement C3, interferon-induced protein with tetratricopeptide repeats 1 (IFIT1) and receptor-interacting serine/threonine-protein kinase 2 (26), as well as carboxypeptidase D which is involved in antigen presentation (27) were found to be upregulated in all kinds of cells. CCAAT/enhancer-binding protein delta, an important pro-inflammatory transcriptional activator, as well as jun-B, a transcription factor which contributes to the expression of pro-inflammatory molecules such as IL-1β (28), were upregulated likewise. Besides these molecules involved in pro-inflammatory signaling, an anti-inflammatory signaling molecule was also found to be upregulated, namely normal mucosa of esophagus-specific gene 1 protein. This protein is an important regulator of inflammation, initiating a negative-feedback loop in which toll-like receptor stimulation induces microRNA-147 to prevent uncontrolled escalation of inflammation (29).

In a second step, we focused on cell type-specific regulatory processes occurring during inflammation. In general, stimulation of the canonical IL-1β pathway induces the expression of multiple pro- or anti-inflammatory genes capable of regulating the inflammatory response. This includes activation of positive or negative feedback mechanisms able to intensify or reduce the IL-1β response. One of the positive feedback mechanisms implicates the upregulation of IL-1β, whereas upregulation of e.g. interleukin-1 receptor antagonist protein (IL-1RA) is part of a negative feedback mechanism (30). Upregulation of IL-1β and IL-1RA was, however, only observed by us in inflammatory activated NHDF and PBMCs, but not in activated HUVEC. Furthermore, the regulation of IL-1β and IL-1RA was different in NHDF as compared to PBMCs. Both, IL-1β and especially IL-1RA were upregulated mainly in the cytoplasm of NHDF, whereas they were most abundantly upregulated in the supernatant of PBMCs (Figure 3A); these proteins seem to have different functionalities in fibroblasts and leukocytes, as discussed below. Actually, many other proteins were found to be regulated in a cell type-specific way as well. Indeed, 471 and 699 proteins were found to

ASBMB MOLECULAR & CELLULAR PROTEOMICS MCP

ASBMB MOLECULAR & CELLULAR PROTEOMICS MCP

be selectively regulated in activated HUVEC and NHDF, respectively, whereas only 93 proteins were found to be regulated in a similar way in both, HUVEC and NHDF (Figure 2; Supplementary Tables S4 and S5). Proteins of each of these groups are listed in Table 1B-1D.

Importantly, the determination of proteins regulated in only one kind of cell allowed us to designate marker molecules which may be helpful to assess inflammatory processes occurring *in vivo* in a detailed fashion. In Table 1, proteins are listed which may generally indicate inflammation, whereas the marker proteins listed in Table 2 may indicate more specifically the involvement of distinct cell types such as fibroblasts or endothelial in biological samples. We also classified these marker molecules into secreted proteins, membrane-bound proteins from the cell surface, as well as intracellular proteins to support the most appropriate detection strategy.

Because cell type-specific protein regulation may be the result of cell type-specific transcription factor activities, we subjected the proteins specifically regulated in HUVEC, NHDF or PBMCs to the oPOSSUM software (version 3.0); this supports detecting over-represented conserved transcription factor binding sites in the corresponding sets of genes (31). In this way, NFκB and AP1 were identified as most important transcription factors acting in all kinds of investigated cells. Nonetheless, they were obviously inducing different proteins in different cells. Figure 4 illustrates the cell type-specific expression of some proteins targets of NFκB and AP1. Furthermore, some transcription factors were apparently only present or upregulated in one kind of cell. So, T-cell acute lymphocytic leukemia protein 1 (TAL1) was specifically expressed in HUVEC (Figure 4). Several proteins found to be regulated exclusively in activated HUVEC were effectively targets of TAL1, including for example laminin subunit gamma-2 (LAMC2) and neuronal cell adhesion molecule (NRCAM) (Figure 4). Several of the proteins found to be regulated selectively in activated NHDF turned out to be targets of paired mesoderm homeobox protein 2 (PRRX2), such as for example leukemia inhibition factor (LIF) and thrombospondin-2 (TSP2) (Figure 4). We were able to detect PRRX2 in NHDF, but also in HUVEC. Interestingly, PRRX1 was upregulated in inflammatory activated NHDF, but not in activated HUVEC or PBMCs (Figure 4); it is possible that this transcription factor may

ASBMB MOLECULAR & CELLULAR PROTEOMICS MCP

target similar proteins as PRRX2. One of the known targets of PRRX1 and PRRX2, tenascin (TNC), was determined at high levels in NHDF, even though this protein was upregulated in inflammatory activated HUVEC likewise (Figure 4). In conclusion, we observed both cell type-specific expression patterns of transcription factors as well as cell type-specific target gene expression.

Biological processes activated during inflammation

The fact that each kind of inflammatory activated cell type was regulating a very specific set of proteins further raised the question whether the cells were involved in different biological processes during inflammation. To this end, we submitted all proteins found to be regulated in activated NHDF, HUVEC or PBMCs, to the DAVID Functional Annotation Tool for biological processes (32, 33). This determined the most significantly represented biological processes regulated in the cells upon inflammatory activation. Apparently, several common processes were induced in all three kinds of cells during inflammation, namely (i) innate immune response, (ii) cell adhesion and migration, (iii) cell proliferation and differentiation, and (iv) response to oxidative stress. However, execution of these processes was apparently achieved in a cell type-specific way. Indeed, each cell type was up- or downregulating different proteins related to these processes (Supplementary Tables S4 and S5), as exemplified for several proteins in Figure 5. Interestingly, in activated NHDF, even though several proteins related to the innate immune response were upregulated, hardly any interferon (IFN) response was observed upon inflammatory activation. Only IFIT1 was slightly upregulated in these cells, whereas in inflammatory activated PBMCs and HUVEC, several IFN-responsive gene products, such as interferon-induced GTP-binding protein Mx1 (Mx1), interferon-induced proteins with tetratricopeptide repeats (IFITs) and guanylate-binding proteins (GBPs) were strongly upregulated (Figure 3B; Table 3).

Actually, two specific inflammation-related processes were evident only in fibroblasts and endothelial cells, designated here as stromal cells, namely angiogenesis and reorganization of the extracellular matrix (ECM). Table 4A and 4B list regulatory and effector molecules involved in

ASBMB MOLECULAR & CELLULAR PROTEOMICS MCP

angiogenesis. Most of those were classified by applying the DAVID Functional Annotation Tool. This accounts for example for vascular endothelial growth factor C (VEGF-C), and transforming growth factor beta-2 (TGFβ2). Other proteins were described in literature to be involved in angiogenesis, such as for example cathepsin S. Ward *et al.* have shown that antibody-based blocking of cathepsin S leads to inhibition of angiogenesis (34). Plasminogen activator inhibitor 1 is an important regulatory factor of angiogenesis, which is able to both promote and inhibit angiogenesis (35, 36). Neuronal cell adhesion molecule and transforming growth factor-beta-induced protein ig-h3 are involved in angiogenesis as well, as demonstrated by Aitkenhead *et al.* (37). Concerning proteins involved in ECM reorganization, the situation was similar. Several regulator and effector molecules related to this biological process were found significantly up- or downregulated in HUVEC and/or NHDF upon inflammatory activation (Table 4B and 4C). Proteins were again selected using both, the DAVID Functional Annotation Tool (32, 33) as well as relevant information from literature. Finally, we also determined processes which were only accomplished by inflammatory activated fibroblasts, processes related to monosaccharide metabolism and energy generation. Proteins involved in these processes are indicated in Supplementary Table S5.

Hallmarks of inflammation

Through the comparative analysis of inflammatory activated endothelial cells, fibroblasts and leukocytes we were thus able to determine in a comprehensive way proteins fulfilling effector functionalities during inflammation as well as corresponding inflammation-related processes. This motivated us to define hallmarks of inflammation representing the most apparent biological processes occurring during inflammation, and to specify responsibilities of fibroblasts, endothelial cells and leukocytes therein (Figure 6). We included (i) common processes realized by stromal cells and leukocytes, namely the innate immune response, cell adhesion and migration, cell proliferation and differentiation, as well as response to oxidative stress; (ii) processes specifically executed by stromal cells, namely angiogenesis and reorganization of the ECM; (iii) processes fulfilled only by

MCP MOLECULAR & CELLULAR PROTEOMICS ASBMB

fibroblasts related to monosaccharide metabolism; and (iv) a process well-known to be only accomplished by leukocytes, the acquired immune response.

ASBMB MOLECULAR & CELLULAR PROTEOMICS MCP

Discussion

This study focused on inflammation-related proteins in primary human stromal cells, taking NHDF and HUVEC to represent fibroblasts and endothelial cells, respectively. Previously published data on inflammatory stimulated primary human peripheral blood mononuclear cells (PBMCs) were also considered for data interpretation. Comparative proteome profiling revealed 19 proteins which were upregulated in a similar fashion upon inflammatory activation in all three kinds of cells (Table 1A). Obviously, pro-inflammatory agonists such as IL-1β in case of fibroblasts and endothelial cells or LPS/PHA in case of PBMCs can thus trigger similar responses in different cell types. Generally, a pro-inflammatory signal sensed on the cell surface initiates an intracellular signaling cascade, the consequent activation of transcription factors such as AP1 and NFκB and finally the expression of specific genes. Many of the common upregulated proteins were actually NFκB and AP1 target gene products, such as for example IL-6 and COX-2. Besides these common effects, cells were also regulating proteins in a cell type-specific way (Figure 5). The present data demonstrate that each cell type is actually contributing to inflammation in a cell type-specific way by activating its specific repertoire of proteins.

Our observations concerning the expression of the canonical inflammation inducer IL-1β itself in the different kinds of cells indeed point to complex cell type-specific regulatory mechanisms. Firstly, upregulation of IL-1β was only observed in activated NHDF and PBMCs, but not in HUVEC (Figure 3A). Secondly, mechanisms controlling the functionality of IL-1β were apparently different in NHDF and PBMCs. Activated PBMCs abundantly secreted IL-1β, obviously with the aim to activate surrounding cells and reinforce the inflammatory process. However, an upregulation and secretion of interleukin 1 receptor antagonist (IL-1RA) was observed in parallel. While IL-1β binds to interleukin receptor 1 to induce pro-inflammatory signaling in the cell, IL-1RA competes with IL-1β, acting as an anti-inflammatory effector which counter-regulates the pro-inflammatory cascade. The ratio of IL-1β to IL-1RA determines whether the final signal becomes pro- or anti-inflammatory (38). In activated

ASBMB MOLECULAR & CELLULAR PROTEOMICS MCP

NHDF, most of the upregulated IL-1β was found retained inside the cells and, interestingly, IL-1RA was upregulated only in the cytoplasm but not secreted (Figure 3A), producing only the intracellular form of IL-1RA (39). It thus might be that IL-1β, together with IL-1RA, serves as an emergency reserve inside inflammatory activated fibroblasts. In case cells undergo cell death, dying fibroblasts would thus be able to release large amounts of IL-1β, sending rapidly an alert signal and leading to the inflammatory activation of surrounding cells. The simultaneous release of IL-1RA may serve to fine-tune the potent pro-inflammatory signaling. In activated HUVEC, themselves inducing no IL-1β at all, the IL-1β antagonist transforming growth factor beta-2 (TGFβ2) (40), already abundant in untreated cells, was found upregulated (Figure 3A). Physiologically, TGFβ2 together with a continuous and prolonged provision of endothelial cells with IL-1β - rather derived from other cells - is capable of inducing endothelial to mesenchymal transition (EndMT) at later stages of inflammation, during resolution of inflammation and transition to the remodeling phase (40). Downregulation of endothelial markers, such as endothelial nitric oxide synthase and von Willebrand factor, accompanies ongoing EndMT and was actually observed in our experiments (Supplementary Table S1). Most importantly, EndMT is capable of promoting atherosclerosis and strongly correlates with the extent of atherosclerosis (41).

Furthermore, significant differences were also observed concerning the IFN response of cells (Table 3; Figure 3B; Figure 1). Actually, in our experiments, activated HUVEC and PBMCs but not NHDF were readily upregulating several IFN response-related proteins. This observation is supported by data published from Indraccolo *et al.* with regard to several genes selectively induced by IFNs in endothelial cells but not in fibroblasts (42). Some of the corresponding gene products, such as CXCL10, apolipoprotein L3 and IFN-induced protein 44 were found by us to be induced in activated HUVEC, but not in NHDF. One possible explanation for this apparent cell type-specific difference could rely on specific Ras/MEK signaling states. Battcock *et al*. have actually demonstrated that type I IFN cannot establish antiviral states in cells with activated Ras/MEK (43). In HUVEC, the Ras antagonist Ras suppressor protein 1 was found to be 3.5-fold upregulated upon inflammatory

ASBMB MOLECULAR & CELLULAR PROTEOMICS MCP

activation, while in NHDF this protein was found more than 7-fold downregulated (Supplementary Tables S1 and S2). Furthermore, we found dual specificity mitogen-activated protein kinase kinase 1 and 2 (MEK1 and MEK2) to be upregulated in activated fibroblasts, whereas MEK3 was downregulated in activated HUVEC (Supplementary Tables S1 and S2).

These data clearly demonstrated cell type-specific regulatory mechanisms of inflammatory processes. Intriguingly several of the specifically induced proteins are targets of the common transcription factors NFκB or AP1 as exemplified in Figure 4. This points to cell type-specific accessibility of chromatin for these transcription factors as known to account for other cell type-specific gene expression patterns (44). Besides, a cell type-specific inflammatory response might also be regulated in dependence of other, rather cell-type specific transcription factors. Actually, we were able to detect specific transcription factors such as TAL1 in HUVEC and PRRX1 in NHDF (Figure 4). TAL1 may be responsible for the specific induction of LAMC2 and NRCAM in activated HUVEC. PRRX1 may cause the induction of its target TNC as well as the PRRX2 target genes LIF and TSP2 in activated NHDF, as PRRX1 and PRRX2 have been assigned similar functionalities in mesenchymal cells during vasculogenesis (45).

The determination of cell type- and cell state-specific proteins also allowed us to define marker molecules. The identification of pan-markers listed in Table 1 in complex samples such as blood or tissues could serve for the general indication of inflammation without providing information regarding the cell type of origin. In contrast, the identification of cell type-specific inflammation markers as listed in Table 2 would indicate inflammatory activation of fibroblasts or endothelial cells, respectively. This information may elucidate more details regarding the patho-mechanism relevant for the investigated samples. Importantly, such information may become accessible with different kinds of analysis methods including antibody-based technologies or targeted proteomics. In addition, different categories of markers were defined here that can be used for different applications (Table 2): (i) blood-borne markers, i.e. proteins which are secreted by cells in the extracellular space but which do not bind to the extracellular matrix; those may be indicative for a specific inflammatory

ASBMB MOLECULAR & CELLULAR PROTEOMICS MCP

activated cell type in blood samples, using for example ELISA; (ii) membrane-bound proteins from the cell surface, which can be used for FACS analyses; (iii) intracellular proteins which can be used for immunohistochemistry or immunofluorescence. Quantitative monitoring of such markers in clinical samples or appropriate model systems (46) may also help to reveal changes in the functional state of cells in response to specific treatment and, consequently, support the evaluation of specific drug effects.

Another important aim was to determine functionalities related to inflammation, which may be specific for stromal cells. Our data demonstrated that fibroblasts and endothelial cells are both involved in the regulation of angiogenesis and in ECM reorganization. The relatively large number of involved proteins suggests complex regulation and fine-tuning of these important processes (Table 4; Figure 1). Activation of specific factors such as IL-8 and IL-1β may lead to a proangiogenic signaling and the initiation of angiogenesis (47, 48). After this initial phase, other molecules such as matrix metalloproteinases (MMPs) may support the ongoing process by degrading ECM and releasing ECM-bound proangiogenic growth factors (49). Degradation of basement membranes is required to release endothelial cells into the surrounding matrix, growth factors such as VEGF and TGFβ2 supports the formation of new vessels via proliferation (50). Finally, regulatory mechanisms control undesired escalation of angiogenesis. Activation of antiangiogenic factors such as thrombospondin-1 (TSP1) and TSP2, or downregulation of proangiogenic factors such as angiotensin-converting enzyme or c-type lectin domain family 14 member A are involved here (51-54). ECM reorganization is strongly interlinked with angiogenesis and related proteins were found regulated in both cell types as well. Biglycan is a structural component of the ECM but also contributes to blood vessel remodeling, apparently being able to upregulate the expression of VEGF and thus promoting angiogenesis (55). Indeed, this protein, when proteolytically released from the ECM, acts as a danger signal stimulating pro-inflammatory signaling and activating the inflammasome (56). Other components of the ECM, for example laminins, are also important regulators of inflammation and angiogenesis. These proteins are necessary for the recruitment of immune cells to inflammatory loci (57, 58). Interestingly, laminin

ASBMB MOLECULAR & CELLULAR PROTEOMICS MCP

8 (laminin alpha-4beta-1gamma-1), actually observed to be regulated in HUVEC, is involved in the development of inflammatory lesions of the blood brain barrier (59).

Hyaluronan, a glycosaminoglycan of the ECM plays also an important role for the recruitment of immune cells. This molecule is regulated by other components of the ECM such as TSP1 and tumor necrosis factor-inducible gene 6 protein (TSG6) (60). These two proteins were presently observed to be upregulated in stimulated NHDF, indicating that fibroblasts may be involved in regulating the recruitment of leukocytes by endothelial cells during inflammation, which was also observed by McGettrick *et al.* (61). Such interrelations between angiogenesis and ECM reorganization as well as between fibroblasts and endothelial cells are further demonstrated by the interrelation of two important proteins mentioned before, PRRX1 and TNC. The transcription factor PRRX1 regulates vascular development and angiogenesis (62, 63). The PRRX1 target gene product TNC, an ECM glycoprotein, was induced both in fibroblasts and endothelial cells upon inflammatory activation (Figure 4). Tenascin apparently is required for PRRX1-dependent vascularization (64) and regulates angiogenesis during tumor development (65). On the other hand, TNC is also involved in promoting migration of fibroblasts to induce tissue rebuilding in response to injury (66).

Fibroblasts and endothelial cells are thus involved in similar processes during inflammation, each of them fulfilling specific functionalities therein. However, processes related to monosaccharide metabolism and energy generation were found to be specifically regulated during inflammation in fibroblasts. Several proteins related to glycolysis, such as hexokinase 2, triosephosphate isomerase and pyruvate kinase, were found to be upregulated only in these cells, and, similarly, proteins related to the pentose phosphate pathway, such as 6-phosphogluconolactonase and transaldolase (Supplementary Table S5). L-lactate dehydrogenase was found to be upregulated as well, delivering lactate as end product of glycolysis in these cells. Up-regulation of glycolysis and production of lactate, here in the context of inflammation, has also been described to occur in cancer-supporting fibroblasts. These cells have been described to supply cancer cells via autophagy and glycolysis,

ASBMB MOLECULAR & CELLULAR PROTEOMICS MCP

producing high amounts of lactate as energy-rich fuel delivered in a paracrine fashion to cancer cells (67). Also regulators of autophagy, such as lysosome-associated membrane glycoprotein 2 (68) and ras-related protein Rab-7a (69), were found by us to be up-regulated in inflammatory activated fibroblasts (Supplementary Table S5). Considering these aspects, it is not difficult to imagine how inflammation-related processes - when out of control - may contribute to cancer development or other diseases related to chronic inflammation. Especially stromal cells may be critically involved in cancer development as these cells are responsible for processes such as angiogenesis, ECM reorganization and energy supply.

We have chosen suitable model systems representative for fibroblasts and endothelial cells displaying relevant cell functions such as ECM remodeling in fibroblasts, and angiogenesis in endothelial cells. While fibroblasts and endothelial cells derived from other tissues may display slightly different expression patterns (11), the main cell type specific characteristics will be independent from the tissue type of origin. Furthermore, despite a large number of proteins regulated upon inflammatory activation was identified they were clearly related to a rather small number of biological functions. As these biological functions represent the most important activities known to occur during inflammation, hallmarks of inflammation emerged (Figure 6). The consideration of these hallmarks may support our understanding of complex processes occurring during inflammation and related diseases.

Conclusion and Outlook

In this study, the most important players executing complex biological processes involved in the exertion of inflammation were identified. We determined proteins regulated in inflammatory activated endothelial cells, fibroblasts and leukocytes, and elucidated mechanisms which may contribute to the observed cell type-specific regulatory effects. The present results shall contribute to a better understanding of the processes occurring during acute and chronic inflammation and may

ASBMB
MOLECULAR & CELLULAR PROTEOMICS
MCP

thus support the development of new therapeutic strategies to combat chronic inflammation and related diseases. The presented marker molecules may serve to accomplish such tasks by the specific detection of inflammatory activated cells in clinical samples. Furthermore, monitoring the levels of such marker proteins may also support the evaluation of drug effects.

ASBMB MOLECULAR & CELLULAR PROTEOMICS MCP

References

1. Fischer, R., and Maier, O. (2015) Interrelation of oxidative stress and inflammation in neurodegenerative disease: role of TNF. *Oxidative medicine and cellular longevity* 2015, 610813
2. Crusz, S. M., and Balkwill, F. R. (2015) Inflammation and cancer: advances and new agents. *Nature reviews. Clinical oncology*
3. Siti, H. N., Kamisah, Y., and Kamsiah, J. (2015) The role of oxidative stress, antioxidants and vascular inflammation in cardiovascular disease (a review). *Vascular pharmacology* 71, 40-56
4. Perez, D. A., Vago, J. P., Athayde, R. M., Reis, A. C., Teixeira, M. M., Sousa, L. P., and Pinho, V. (2014) Switching off key signaling survival molecules to switch on the resolution of inflammation. *Mediators of inflammation* 2014, 829851
5. Buckley, C. D., Pilling, D., Lord, J. M., Akbar, A. N., Scheel-Toellner, D., and Salmon, M. (2001) Fibroblasts regulate the switch from acute resolving to chronic persistent inflammation. *Trends in immunology* 22, 199-204
6. Kim, Y. W., West, X. Z., and Byzova, T. V. (2013) Inflammation and oxidative stress in angiogenesis and vascular disease. *Journal of molecular medicine* 91, 323-328
7. Wallach-Dayan, S. B., Golan-Gerstl, R., and Breuer, R. (2007) Evasion of myofibroblasts from immune surveillance: a mechanism for tissue fibrosis. *Proceedings of the National Academy of Sciences of the United States of America* 104, 20460-20465
8. Ortega-Gomez, A., Perretti, M., and Soehnlein, O. (2013) Resolution of inflammation: an integrated view. *EMBO molecular medicine* 5, 661-674
9. Naylor, A. J., Filer, A., and Buckley, C. D. (2013) The role of stromal cells in the persistence of chronic inflammation. *Clinical and experimental immunology* 171, 30-35
10. Van Dyke, T. E., and Kornman, K. S. (2008) Inflammation and factors that may regulate inflammatory response. *Journal of periodontology* 79, 1503-1507
11. Slany, A., Meshcheryakova, A., Beer, A., Ankersmit, H. J., Paulitschke, V., and Gerner, C. (2014) Plasticity of fibroblasts demonstrated by tissue-specific and function-related proteome profiling. *Clinical proteomics* 11, 41
12. Slany, A., Paulitschke, V., Haudek-Prinz, V., Meshcheryakova, A., and Gerner, C. (2014) Determination of cell type-specific proteome signatures of primary human leukocytes, endothelial cells, keratinocytes, hepatocytes, fibroblasts and melanocytes by comparative proteome profiling. *Electrophoresis* 35, 1428-1438
13. Dowling, J. K., and O'Neill, L. A. (2012) Biochemical regulation of the inflammasome. *Critical reviews in biochemistry and molecular biology* 47, 424-443
14. Bileck, A., Kreutz, D., Muqaku, B., Slany, A., and Gerner, C. (2014) Comprehensive assessment of proteins regulated by dexamethasone reveals novel effects in primary human peripheral blood mononuclear cells. *Journal of proteome research* 13, 5989-6000
15. Hanahan, D., and Weinberg, R. A. (2000) The hallmarks of cancer. *Cell* 100, 57-70
16. Groessl, M., Slany, A., Bileck, A., Gloessmann, K., Kreutz, D., Jaeger, W., Pfeiler, G., and Gerner, C. (2014) Proteome profiling of breast cancer biopsies reveals a wound healing signature of cancer-associated fibroblasts. *Journal of proteome research* 13, 4773-4782
17. Muqaku, B., Slany, A., Bileck, A., Kreutz, D., and Gerner, C. (2015) Quantification of cytokines secreted by primary human cells using multiple reaction monitoring: evaluation of analytical parameters. *Analytical and bioanalytical chemistry* 407, 6525-6536
18. Slany, A., Haudek, V. J., Gundacker, N. C., Griss, J., Mohr, T., Wimmer, H., Eisenbauer, M., Elbling, L., and Gerner, C. (2009) Introducing a new parameter for quality control of proteome profiles: consideration of commonly expressed proteins. *Electrophoresis* 30, 1306-1328
19. Cox, J., and Mann, M. (2008) MaxQuant enables high peptide identification rates, individualized p.p.b.-range mass accuracies and proteome-wide protein quantification. *Nature biotechnology* 26, 1367-1372

ASBMB MOLECULAR & CELLULAR PROTEOMICS MCP

20. Cox, J., and Mann, M. (2012) 1D and 2D annotation enrichment: a statistical method integrating quantitative proteomics with complementary high-throughput data. *BMC bioinformatics* 13 Suppl 16, S12
21. Vizcaino, J. A., Deutsch, E. W., Wang, R., Csordas, A., Reisinger, F., Rios, D., Dianes, J. A., Sun, Z., Farrah, T., Bandeira, N., Binz, P. A., Xenarios, I., Eisenacher, M., Mayer, G., Gatto, L., Campos, A., Chalkley, R. J., Kraus, H. J., Albar, J. P., Martinez-Bartolome, S., Apweiler, R., Omenn, G. S., Martens, L., Jones, A. R., and Hermjakob, H. (2014) ProteomeXchange provides globally coordinated proteomics data submission and dissemination. *Nature biotechnology* 32, 223-226
22. R Development Core Team (2010) R: A language and environment for statistical computing. *R Foundation for Statistical Computing, Vienna, Austria*
23. Cox, J., Hein, M. Y., Luber, C. A., Paron, I., Nagaraj, N., and Mann, M. (2014) Accurate proteome-wide label-free quantification by delayed normalization and maximal peptide ratio extraction, termed MaxLFQ. *Molecular & cellular proteomics : MCP* 13, 2513-2526
24. Tusher, V. G., Tibshirani, R., and Chu, G. (2001) Significance analysis of microarrays applied to the ionizing radiation response. *Proceedings of the National Academy of Sciences of the United States of America* 98, 5116-5121
25. Aasebo, E., Berven, F. S., Selheim, F., Barsnes, H., and Vaudel, M. (2016) Interpretation of Quantitative Shotgun Proteomic Data. *Methods in molecular biology* 1394, 261-273
26. Zhao, Y., Alonso, C., Ballester, I., Song, J. H., Chang, S. Y., Guleng, B., Arihiro, S., Murray, P. J., Xavier, R., Kobayashi, K. S., and Reinecker, H. C. (2012) Control of NOD2 and Rip2-dependent innate immune activation by GEF-H1. *Inflammatory bowel diseases* 18, 603-612
27. Grolleau, A., Misek, D. E., Kuick, R., Hanash, S., and Mule, J. J. (2003) Inducible expression of macrophage receptor Marco by dendritic cells following phagocytic uptake of dead cells uncovered by oligonucleotide arrays. *Journal of immunology* 171, 2879-2888
28. Fontana, M. F., Baccarella, A., Pancholi, N., Pufall, M. A., Herbert, D. R., and Kim, C. C. (2015) JUNB is a key transcriptional modulator of macrophage activation. *Journal of immunology* 194, 177-186
29. Liu, G., Friggeri, A., Yang, Y., Park, Y. J., Tsuruta, Y., and Abraham, E. (2009) miR-147, a microRNA that is induced upon Toll-like receptor stimulation, regulates murine macrophage inflammatory responses. *Proceedings of the National Academy of Sciences of the United States of America* 106, 15819-15824
30. Weber, A., Wasiliew, P., and Kracht, M. (2010) Interleukin-1 (IL-1) pathway. *Science signaling* 3, cm1
31. Ho Sui, S. J., Mortimer, J. R., Arenillas, D. J., Brumm, J., Walsh, C. J., Kennedy, B. P., and Wasserman, W. W. (2005) oPOSSUM: identification of over-represented transcription factor binding sites in co-expressed genes. *Nucleic acids research* 33, 3154-3164
32. Huang da, W., Sherman, B. T., and Lempicki, R. A. (2009) Systematic and integrative analysis of large gene lists using DAVID bioinformatics resources. *Nature protocols* 4, 44-57
33. Huang da, W., Sherman, B. T., and Lempicki, R. A. (2009) Bioinformatics enrichment tools: paths toward the comprehensive functional analysis of large gene lists. *Nucleic acids research* 37, 1-13
34. Ward, C., Kuehn, D., Burden, R. E., Gormley, J. A., Jaquin, T. J., Gazdoiu, M., Small, D., Bicknell, R., Johnston, J. A., Scott, C. J., and Olwill, S. A. (2010) Antibody targeting of cathepsin S inhibits angiogenesis and synergistically enhances anti-VEGF. *PloS one* 5
35. Bajou, K., Maillard, C., Jost, M., Lijnen, R. H., Gils, A., Declerck, P., Carmeliet, P., Foidart, J. M., and Noel, A. (2004) Host-derived plasminogen activator inhibitor-1 (PAI-1) concentration is critical for in vivo tumoral angiogenesis and growth. *Oncogene* 23, 6986-6990
36. Tashiro, Y., Nishida, C., Sato-Kusubata, K., Ohki-Koizumi, M., Ishihara, M., Sato, A., Gritli, I., Komiyama, H., Sato, Y., Dan, T., Miyata, T., Okumura, K., Tomiki, Y., Sakamoto, K., Nakauchi, H., Heissig, B., and Hattori, K. (2012) Inhibition of PAI-1 induces neutrophil-driven neoangiogenesis and promotes tissue regeneration via production of angiocrine factors in mice. *Blood* 119, 6382-6393

ASBMB MOLECULAR & CELLULAR PROTEOMICS MCP

37. Aitkenhead, M., Wang, S. J., Nakatsu, M. N., Mestas, J., Heard, C., and Hughes, C. C. (2002) Identification of endothelial cell genes expressed in an in vitro model of angiogenesis: induction of ESM-1, (beta)ig-h3, and NrCAM. *Microvascular research* 63, 159-171
38. Langereis, J. D., Oudijk, E. J., Schweizer, R. C., Lammers, J. W., Koenderman, L., and Ulfman, L. H. (2011) Steroids induce a disequilibrium of secreted interleukin-1 receptor antagonist and interleukin-1beta synthesis by human neutrophils. *The European respiratory journal* 37, 406-415
39. Li, B., and Smith, T. J. (2013) Divergent expression of IL-1 receptor antagonists in CD34(+) fibrocytes and orbital fibroblasts in thyroid-associated ophthalmopathy: contribution of fibrocytes to orbital inflammation. *The Journal of clinical endocrinology and metabolism* 98, 2783-2790
40. Maleszewska, M., Moonen, J. R., Huijkman, N., van de Sluis, B., Krenning, G., and Harmsen, M. C. (2013) IL-1beta and TGFbeta2 synergistically induce endothelial to mesenchymal transition in an NFkappaB-dependent manner. *Immunobiology* 218, 443-454
41. Chen, P. Y., Qin, L., Baeyens, N., Li, G., Afolabi, T., Budatha, M., Tellides, G., Schwartz, M. A., and Simons, M. (2015) Endothelial-to-mesenchymal transition drives atherosclerosis progression. *The Journal of clinical investigation* 2015
42. Indraccolo, S., Pfeffer, U., Minuzzo, S., Esposito, G., Roni, V., Mandruzzato, S., Ferrari, N., Anfosso, L., Dell'Eva, R., Noonan, D. M., Chieco-Bianchi, L., Albini, A., and Amadori, A. (2007) Identification of genes selectively regulated by IFNs in endothelial cells. *Journal of immunology* 178, 1122-1135
43. Battcock, S. M., Collier, T. W., Zu, D., and Hirasawa, K. (2006) Negative regulation of the alpha interferon-induced antiviral response by the Ras/Raf/MEK pathway. *Journal of virology* 80, 4422-4430
44. Arvey, A., Agius, P., Noble, W. S., and Leslie, C. (2012) Sequence and chromatin determinants of cell-type-specific transcription factor binding. *Genome research* 22, 1723-1734
45. Higuchi, M., Kato, T., Yoshida, S., Ueharu, H., Nishimura, N., and Kato, Y. (2015) PRRX1- and PRRX2-positive mesenchymal stem/progenitor cells are involved in vasculogenesis during rat embryonic pituitary development. *Cell and tissue research* 361, 557-565
46. Slany, A., Bileck, A., Muqaku, B., and Gerner, C. (2015) Targeting breast cancer-associated fibroblasts to improve anti-cancer therapy. *Breast* 24, 532-538
47. Carmi, Y., Voronov, E., Dotan, S., Lahat, N., Rahat, M. A., Fogel, M., Huszar, M., White, M. R., Dinarello, C. A., and Apte, R. N. (2009) The role of macrophage-derived IL-1 in induction and maintenance of angiogenesis. *Journal of immunology* 183, 4705-4714
48. Qazi, B. S., Tang, K., and Qazi, A. (2011) Recent advances in underlying pathologies provide insight into interleukin-8 expression-mediated inflammation and angiogenesis. *International journal of inflammation* 2011, 908468
49. Rundhaug, J. E. (2005) Matrix metalloproteinases and angiogenesis. *Journal of cellular and molecular medicine* 9, 267-285
50. Holderfield, M. T., and Hughes, C. C. (2008) Crosstalk between vascular endothelial growth factor, notch, and transforming growth factor-beta in vascular morphogenesis. *Circulation research* 102, 637-652
51. Chu, L. Y., Ramakrishnan, D. P., and Silverstein, R. L. (2013) Thrombospondin-1 modulates VEGF signaling via CD36 by recruiting SHP-1 to VEGFR2 complex in microvascular endothelial cells. *Blood* 122, 1822-1832
52. Bornstein, P., Kyriakides, T. R., Yang, Z., Armstrong, L. C., and Birk, D. E. (2000) Thrombospondin 2 modulates collagen fibrillogenesis and angiogenesis. *The journal of investigative dermatology. Symposium proceedings / the Society for Investigative Dermatology, Inc. [and] European Society for Dermatological Research* 5, 61-66
53. Silva, E. A., Eseonu, C., and Mooney, D. J. (2014) Endothelial cells expressing low levels of CD143 (ACE) exhibit enhanced sprouting and potency in relieving tissue ischemia. *Angiogenesis* 17, 617-630
54. Mura, M., Swain, R. K., Zhuang, X., Vorschmitt, H., Reynolds, G., Durant, S., Beesley, J. F., Herbert, J. M., Sheldon, H., Andre, M., Sanderson, S., Glen, K., Luu, N. T., McGettrick, H. M., Antczak,

ASBMB MOLECULAR & CELLULAR PROTEOMICS MCP

P., Falciani, F., Nash, G. B., Nagy, Z. S., and Bicknell, R. (2012) Identification and angiogenic role of the novel tumor endothelial marker CLEC14A. *Oncogene* 31, 293-305
55. Xing, X., Gu, X., Ma, T., and Ye, H. (2015) Biglycan up-regulated vascular endothelial growth factor (VEGF) expression and promoted angiogenesis in colon cancer. *Tumour biology : the journal of the International Society for Oncodevelopmental Biology and Medicine* 36, 1773-1780
56. Nastase, M. V., Young, M. F., and Schaefer, L. (2012) Biglycan: a multivalent proteoglycan providing structure and signals. *The journal of histochemistry and cytochemistry : official journal of the Histochemistry Society* 60, 963-975
57. Kenne, E., Soehnlein, O., Genove, G., Rotzius, P., Eriksson, E. E., and Lindbom, L. (2010) Immune cell recruitment to inflammatory loci is impaired in mice deficient in basement membrane protein laminin alpha4. *Journal of leukocyte biology* 88, 523-528
58. Gonzalez, A. M., Gonzales, M., Herron, G. S., Nagavarapu, U., Hopkinson, S. B., Tsuruta, D., and Jones, J. C. (2002) Complex interactions between the laminin alpha 4 subunit and integrins regulate endothelial cell behavior in vitro and angiogenesis in vivo. *Proceedings of the National Academy of Sciences of the United States of America* 99, 16075-16080
59. Sixt, M., Engelhardt, B., Pausch, F., Hallmann, R., Wendler, O., and Sorokin, L. M. (2001) Endothelial cell laminin isoforms, laminins 8 and 10, play decisive roles in T cell recruitment across the blood-brain barrier in experimental autoimmune encephalomyelitis. *The Journal of cell biology* 153, 933-946
60. Day, A. J., and de la Motte, C. A. (2005) Hyaluronan cross-linking: a protective mechanism in inflammation? *Trends in immunology* 26, 637-643
61. McGettrick, H. M., Smith, E., Filer, A., Kissane, S., Salmon, M., Buckley, C. D., Rainger, G. E., and Nash, G. B. (2009) Fibroblasts from different sites may promote or inhibit recruitment of flowing lymphocytes by endothelial cells. *European journal of immunology* 39, 113-125
62. Murthi, P., Hiden, U., Rajaraman, G., Liu, H., Borg, A. J., Coombes, F., Desoye, G., Brennecke, S. P., and Kalionis, B. (2008) Novel homeobox genes are differentially expressed in placental microvascular endothelial cells compared with macrovascular cells. *Placenta* 29, 624-630
63. Gorski, D. H., and Walsh, K. (2000) The role of homeobox genes in vascular remodeling and angiogenesis. *Circulation research* 87, 865-872
64. Ihida-Stansbury, K., Ames, J., Chokshi, M., Aiad, N., Sanyal, S., Kawabata, K. C., Levental, I., Sundararaghavan, H. G., Burdick, J. A., Janmey, P., Miyazono, K., Wells, R. G., and Jones, P. L. (2015) Role played by Prx1-dependent extracellular matrix properties in vascular smooth muscle development in embryonic lungs. *Pulmonary circulation* 5, 382-397
65. Tanaka, K., Hiraiwa, N., Hashimoto, H., Yamazaki, Y., and Kusakabe, M. (2004) Tenascin-C regulates angiogenesis in tumor through the regulation of vascular endothelial growth factor expression. *International journal of cancer. Journal international du cancer* 108, 31-40
66. Trebaul, A., Chan, E. K., and Midwood, K. S. (2007) Regulation of fibroblast migration by tenascin-C. *Biochemical Society transactions* 35, 695-697
67. Martinez-Outschoorn, U., Sotgia, F., and Lisanti, M. P. (2014) Tumor microenvironment and metabolic synergy in breast cancers: critical importance of mitochondrial fuels and function. *Seminars in oncology* 41, 195-216
68. Eskelinen, E. L. (2006) Roles of LAMP-1 and LAMP-2 in lysosome biogenesis and autophagy. *Molecular aspects of medicine* 27, 495-502
69. Yamaguchi, H., Nakagawa, I., Yamamoto, A., Amano, A., Noda, T., and Yoshimori, T. (2009) An initial step of GAS-containing autophagosome-like vacuoles formation requires Rab7. *PLoS pathogens* 5, e1000670

ASBMB MOLECULAR & CELLULAR PROTEOMICS MCP

Legends

Figure 1: Regulation of proteins in HUVEC (A) and NHDF (B) upon inflammatory activation. Differences in LFQ values (logarithmic scale to the base of two) of proteins determined in activated versus control cells, including corresponding p-values (logarithmic scale), are represented as volcano plots for each subcellular fraction. Proteins related to angiogenesis and/or ECM organization, as well as proteins related to the IFN response are highlighted as indicated. Proteins which were found to be regulated in the same subcellular fraction of the other cell type, respectively, are designated as well.

Figure 2: Quantitative Venn diagrams of proteins regulated in inflammatory activated HUVEC, NHDF and PBMCs demonstrating the cell type-specificity of the inflammatory response. For each kind of cell, the number of protein groups found to be at least twofold up- or downregulated ($p \leq 0.05$) upon inflammatory activation of the cells is represented. In total, we identified 667 protein groups which were regulated in HUVEC, 894 in NHDF and 646 in PBMCs.

Figure 3: Cell type-specific regulation of IL-1β, IL-1RA, TGFβ2 and of proteins related to the IFN response. A. Heat maps of LFQ values for IL-1β, IL-1RA and TGFβ2 are represented, as well as differences of LFQ values for these proteins between control and activated cells (Δ act vs con; logarithmic scale to the base of two) with corresponding p-values (logarithmic scale) determined in the cytoplasm (cyt) and the supernatant (sn) of the cells. Acc.Nr., UniProt accession number. **B.** Heat maps of LFQ values for different IFN-responsive gene products are represented.

Figure 4: Cell type-specific regulation of proteins during inflammation. Heat maps of LFQ values for the canonical transcription factors NFκB and AP1, as well as for corresponding target gene products which were upregulated in a cell type-specific way in HUVEC, NHDF and PBMCs, are represented. LFQ values for cell type-specific transcription factors with target gene products are shown similarly.

Figure 5: Inflammation-related processes realized by all cells, however, by upregulating different proteins. Heat maps of LFQ values for proteins involved in the innate immune response, cell

ASBMB MOLECULAR & CELLULAR PROTEOMICS MCP

adhesion and migration, cell proliferation and differentiation as well as response to oxidative stress are represented.

Figure 6: Hallmarks of inflammation. Hallmarks of inflammation representing the most apparent biological processes executed by HUVEC, NHDF and/or PBMCs are represented.

Table 1: Proteins regulated in a common as well as a cell type-specific way in HUVEC, NHDF and PBMCs. Proteins are listed which were at least twofold up- or downregulated ($p<0.05$) in all three kinds of cells upon inflammatory activation (**A**); proteins which were at least twofold up- or downregulated ($p<0.05$) in inflammatory activated stromal cells, but not in activated PBMCs (**B**); proteins which were at least twofold up- or downregulated ($p<0.05$) in inflammatory activated HUVEC only (**C**); and proteins which were at least twofold up- or downregulated ($p<0.05$) in inflammatory activated NHDF only (**D**). Acc.Nr., UniProt accession number.

Table 2: Candidate marker proteins for inflammatory activated fibroblasts and endothelial cells. Blood-borne markers i.e. secreted proteins, as well as membrane-bound proteins from the cell surface and intracellular proteins were determined for endothelial cells (ECs) and fibroblasts. Differences of LFQ values between control and activated cells (Δ_act vs con; logarithmic scale to the base of two) with corresponding p-values are indicated for each subcellular fraction, cytoplasm (cyt), nuclear extract (ne) and supernatant (sn). Acc.Nr., UniProt accession number.

Table 3: IFN response-related proteins regulated in PBMCs (A), HUVEC (B) and NHDF (C). Many proteins related to the IFN response were found to be regulated in activated HUVEC and PBMCs, whereas in activated NHDF, only IFIT1 was slightly upregulated. Differences of LFQ values between control and activated cells (Δ_act vs con; logarithmic scale to the base of two) with corresponding p-values are indicated for each subcellular fraction, cytoplasm (cyt), nuclear extract (ne) and supernatant (sn). Acc.Nr., UniProt accession number.

Table 4: Proteins related to angiogenesis and ECM reorganization, regulated in HUVEC and NHDF. Proteins related to angiogenesis and ECM reorganization which were found to be at least twofold up

MCP MOLECULAR & CELLULAR PROTEOMICS ASBMB

or downregulated ($p<0.05$) in inflammatory activated HUVEC and/or NHDF are listed. Acc.Nr., UniProt accession number.

ASBMB
MOLECULAR & CELLULAR PROTEOMICS
MCP

Acknowledments

We would like to thank Gerhard Mayer from the PRIDE team for help and support with data submission to ProteomeXchange. Furthermore, we would like to thank Johanna Mader and Peter Frühauf for technical support and Samuel Gerner for programming an R script for generation of the heat maps.

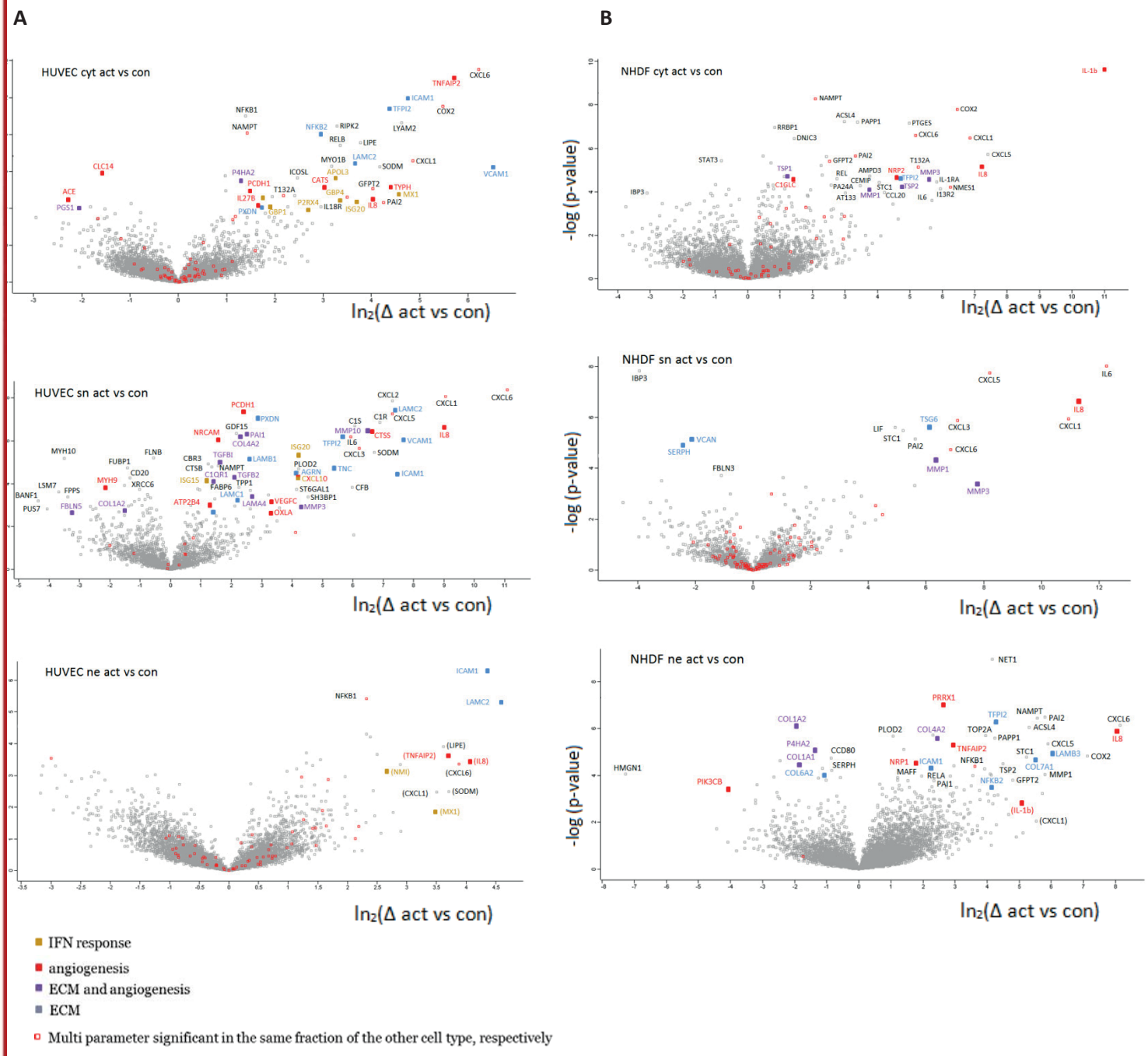
A
B
HUVEC cyt act vs con
NHDF cyt act vs con
HUVEC sn act vs con
NHDF sn act vs con
HUVEC ne act vs con
NHDF ne act vs con
-log (p-value)
ln2(Δ act vs con)
IFN response
angiogenesis
ECM and angiogenesis
ECM
Multi parameter significant in the same fraction of the other cell type, respectively

Figure 1

ASBMB
MOLECULAR & CELLULAR PROTEOMICS
MCP

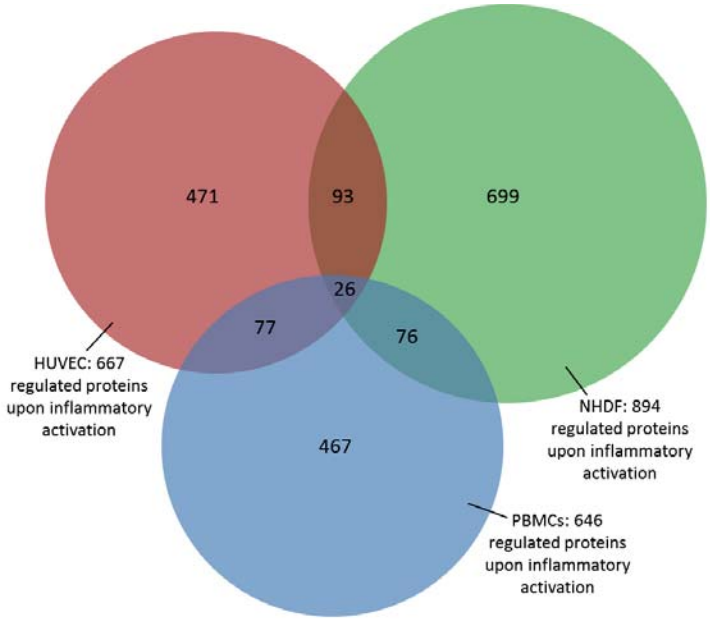

Figure 2

A

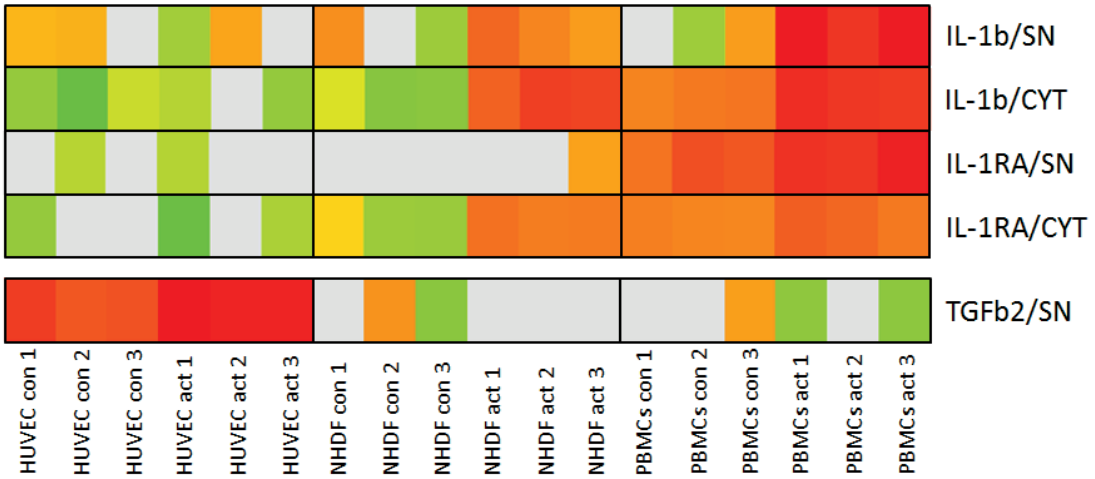

	HUVEC_cyt		HUVEC_sn		NHDF_cyt		NHDF_sn		PBMCs_cyt		PBMCs_sn	
Protein	Δ act vs con	p-value	Δ act vs con	p-value	Δ act vs con	p-value	Δ act vs con	p-value	Δ act vs con	p-value	Δ act vs con	p-value
IL-1b	0.41	3.67E-01	0.24	5.80E-01	**11.01**	**2.28E-10**	**2.10**	**3.60E-02**	**4.20**	**3.31E-05**	**8.05**	**3.71E-08**
IL-1RA	0.92	2.13E-01	0.58	5.76E-01	**5.83**	**3.58E-05**	0.76	3.45E-02	**1.65**	**4.99E-03**	**2.60**	**3.00E-04**
TGFb2	0.55	5.53E-01	**2.14**	**5.60E-05**	0.64	4.63E-01	-0.68	3.07E-01	0.71	3.52E-01	0.64	4.06E-01

B

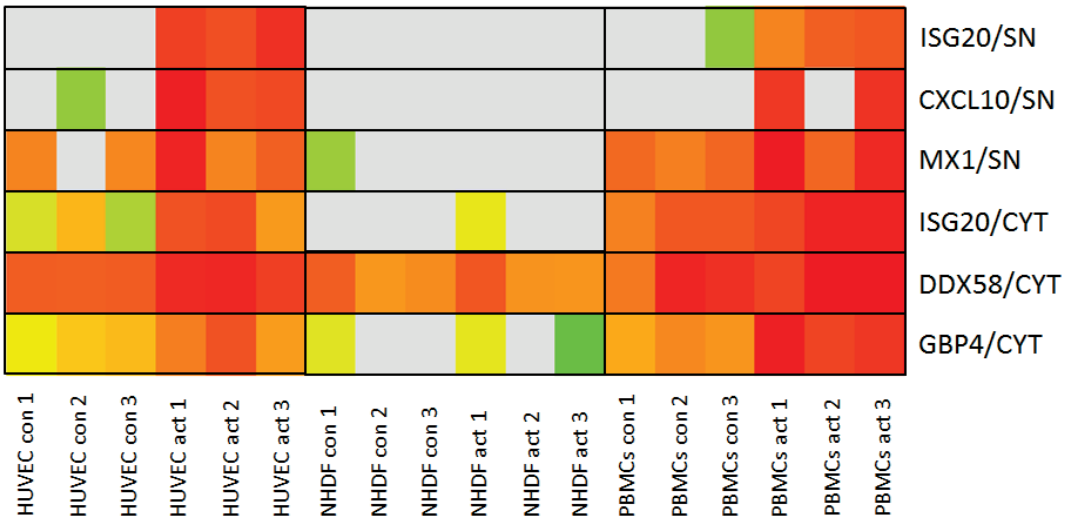

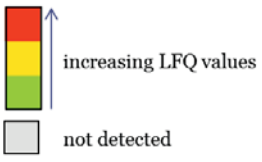

Figure 3

ASBMB
MOLECULAR & CELLULAR PROTEOMICS
MCP

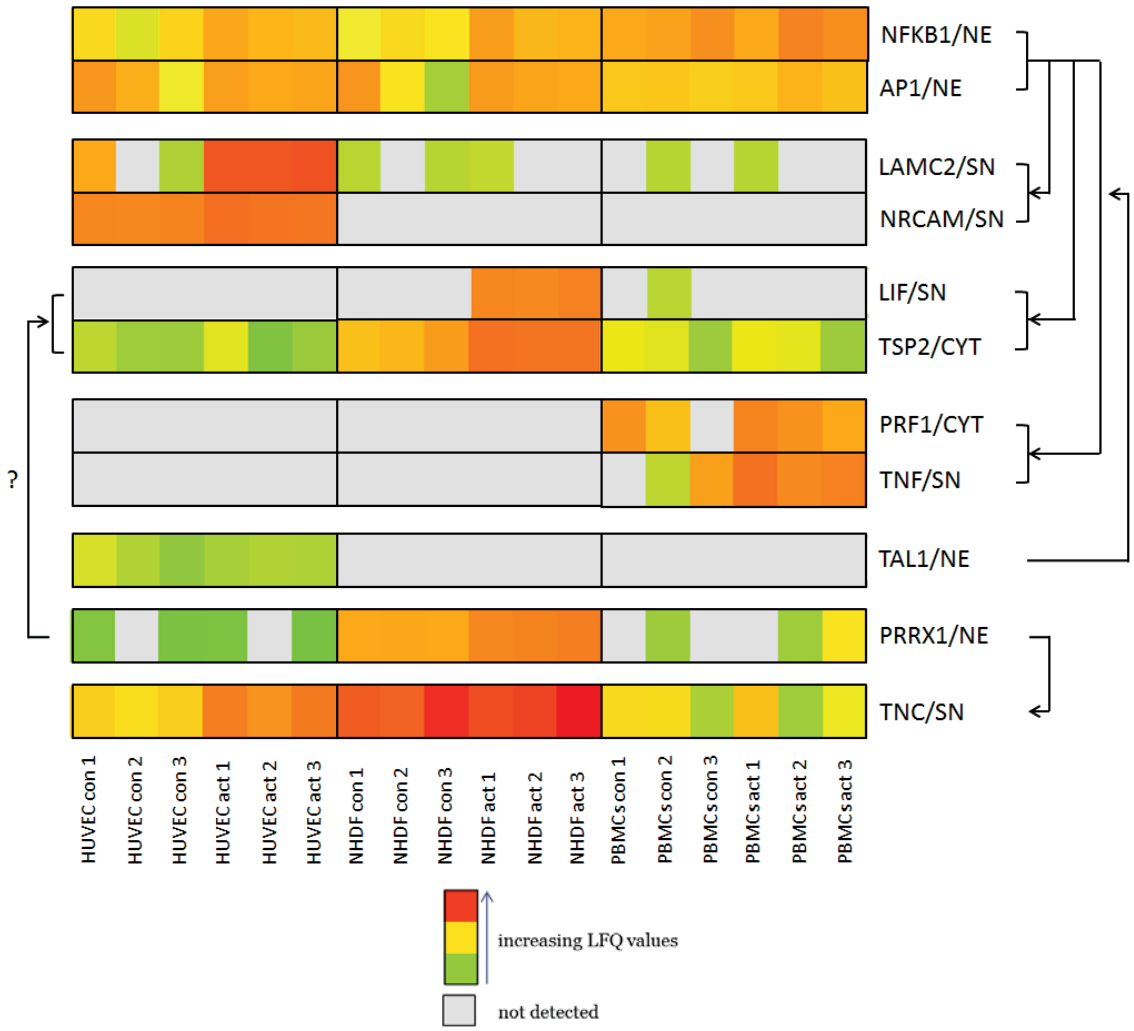

Figure 4

ASBMB
MOLECULAR & CELLULAR PROTEOMICS
MCP

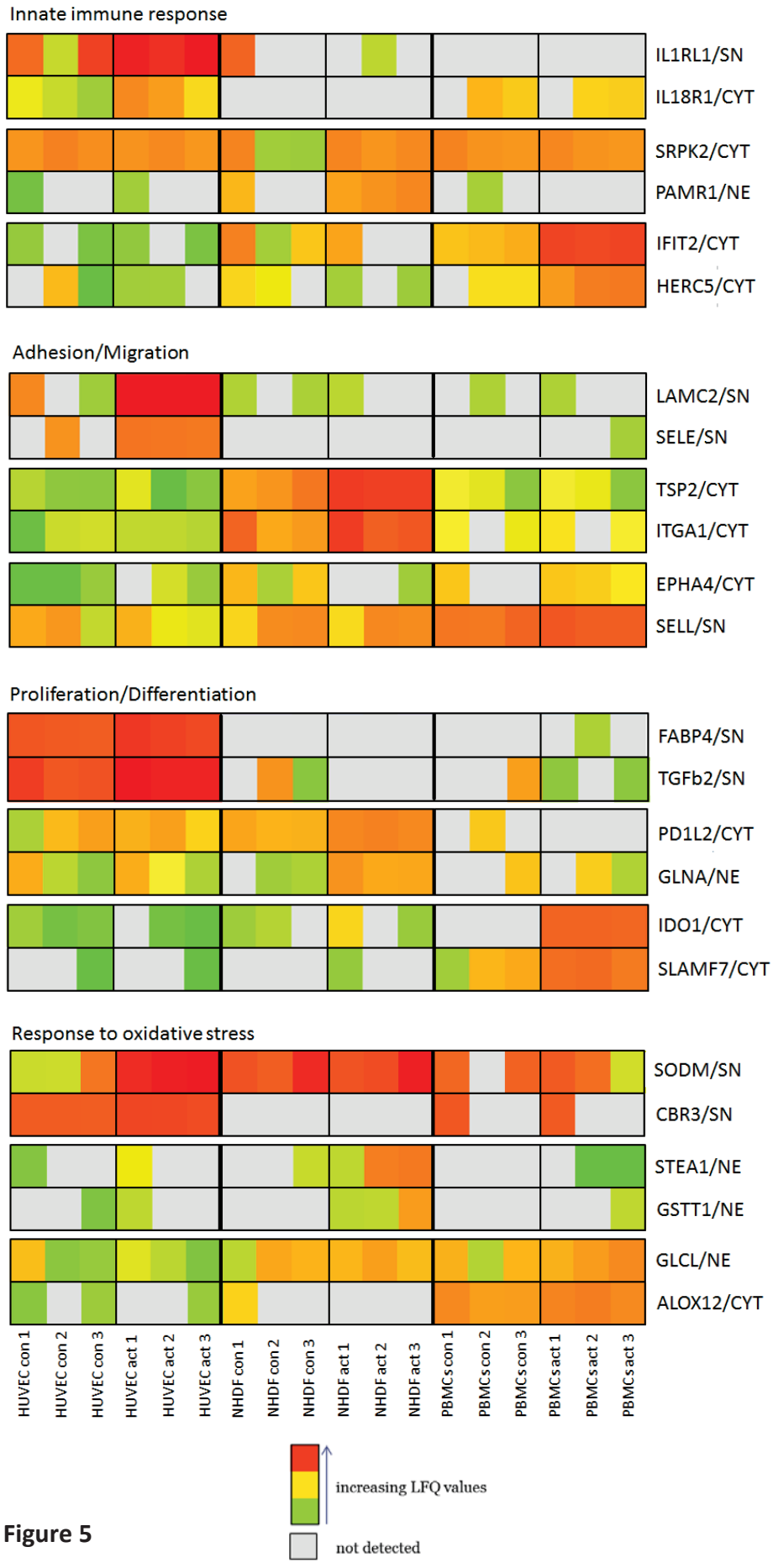

Figure 5

ASBMB
MOLECULAR & CELLULAR PROTEOMICS
MCP

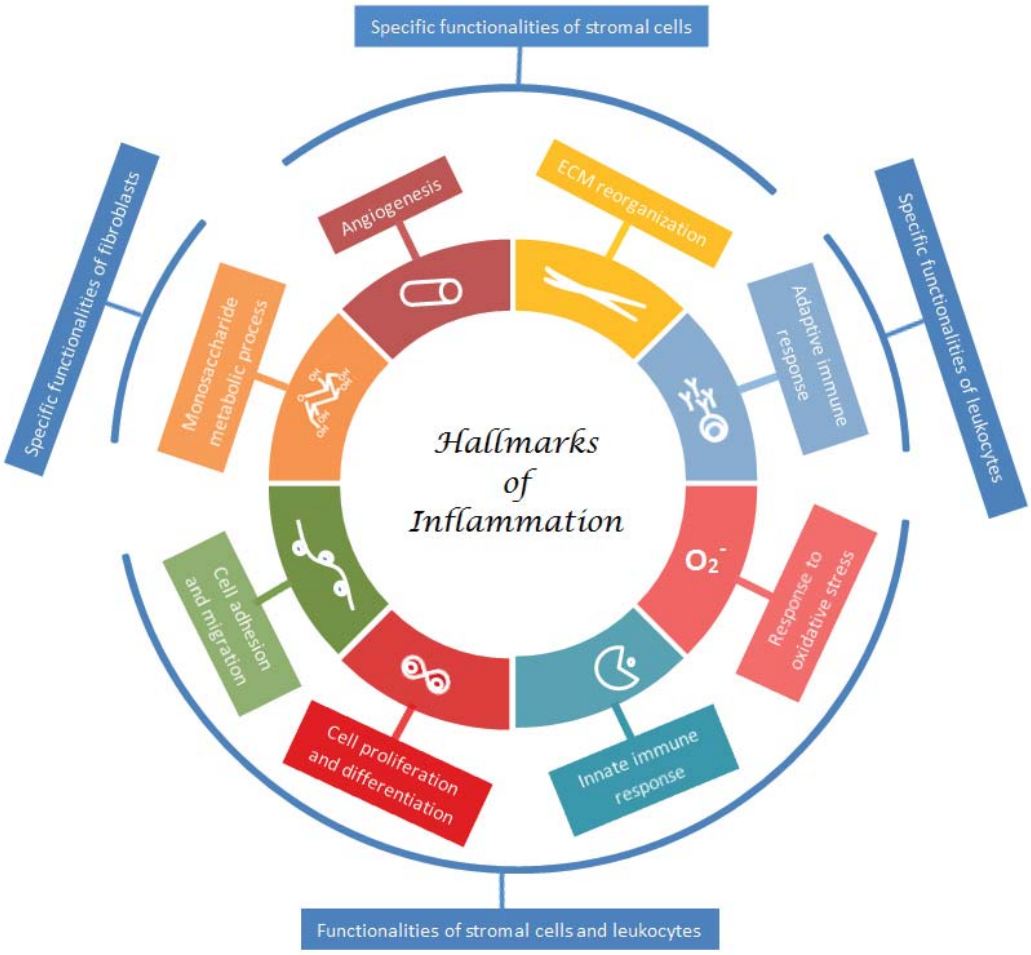

Figure 6

ASBMB
MOLECULAR & CELLULAR PROTEOMICS
MCP

Table 1

Acc.Nr.	Name
A. Proteins regulated in all cell types	
P42830**	C-X-C motif chemokine 5; CXCL5
P09341**	Growth-regulated alpha protein; CXCL1
P05362***	Intercellular adhesion molecule 1; ICAM1
P05231**	Interleukin-6; IL6
P10145**	Interleukin-8; IL8
P43490**	Nicotinamide phosphoribosyltransferase
Q9C002**	Normal mucosa of esophagus-specific gene 1 protein
P05120**	Plasminogen activator inhibitor 2; PAI2
P35354**	Prostaglandin G/H synthase 2; COX-2
P19875*	C-X-C motif chemokine 2; CXCL2
Q9BYK8*	Helicase with zinc finger domain 2
O43353*	Receptor-interacting serine/threonine-protein kinase 2
P01024	Complement C3
O75976	Carboxypeptidase D
P49716	CCAAT/enhancer-binding protein delta
P13500	C-C motif chemokine 2; CCL2
P09914	Interferon-induced protein with tetratricopeptide repeats 1; IFIT1
Q15283	Ras GTPase-activating protein 2
P17275	Transcription factor jun-B
B. Proteins regulated in stromal cells, not in PBMCs	
P08123**	Collagen alpha-2(I) chain
P08572**	Collagen alpha-2(IV) chain
P19876**	C-X-C motif chemokine 3; CXCL3
P80162**	C-X-C motif chemokine 6; CXCL6
O94808**	Glutamine--fructose-6-phosphate aminotransferase [isomerizing] 2
Q00653**	Nuclear factor NF-kappa-B p100 subunit
P19838**	Nuclear factor NF-kappa-B p105 subunit
P05121**	Plasminogen activator inhibitor 1; PAI1
O00469**	Procollagen-lysine,2-oxoglutarate 5-dioxygenase 2
O43353**	Receptor-interacting serine/threonine-protein kinase 2
P08254**	Stromelysin-1; MMP3
P48307**	Tissue factor pathway inhibitor 2
Q01201**	Transcription factor RelB
Q24JP5**	Transmembrane protein 132A
Q03169**	Tumor necrosis factor alpha-induced protein 2
P25774*	Cathepsin S
Q11201*	CMP-N-acetylneuraminate-beta-galactosamide-alpha-2,3-sialyltransferase 1
P02794*	Ferritin heavy chain
Q53EP0*	Fibronectin type III domain-containing protein 3B
Q9UBX5*	Fibulin-5
Q99988*	Growth/differentiation factor 15
Q13751*	Laminin subunit beta-3
Q9UPQ0*	LIM and calponin homology domains-containing protein 1
O60462*	Neuropilin-2
P50479*	PDZ and LIM domain protein 4
C. Proteins regulated in HUVEC only	
P10809*	60 kDa heat shock protein, mitochondrial
O00468*	Agrin
Q06203*	Amidophosphoribosyltransferase
P12821*	Angiotensin-converting enzyme
O95236*	Apolipoprotein L3
Q9NW81*	ATP synthase subunit s-like protein
P50895*	Basal cell adhesion molecule
P15907*	Beta-galactoside alpha-2,6-sialyltransferase 1
P21810*	Biglycan
O75828*	Carbonyl reductase [NADPH] 3
P05997*	Collagen alpha-2(V) chain
P00736*	Complement C1r subcomponent
P09871*	Complement C1s subcomponent
Q9NPY3*	Complement component C1q receptor
P00751*	Complement factor B
Q86T13*	C-type lectin domain family 14 member A
Q16531*	DNA damage-binding protein 1
Q9UBS4*	DnaJ homolog subfamily B member 11
Q9Y5X9*	Endothelial lipase
P16581*	E-selectin
O14980*	Exportin-1
Q96AE4*	Far upstream element-binding protein 1
P14324*	Farnesyl pyrophosphate synthase
P15090*	Fatty acid-binding protein, adipocyte
Q00839*	Heterogeneous nuclear ribonucleoprotein U
O75144*	ICOS ligand
Q01638*	Interleukin-1 receptor-like 1; IL1RL1
Q13478*	Interleukin-18 receptor 1; IL18R1
Q16363*	Laminin subunit alpha-4
P07942*	Laminin subunit beta-1
P11047*	Laminin subunit gamma-1
Q13753*	Laminin subunit gamma-2
Q9H492*	Microtubule-associated proteins 1A/1B light chain 3A
P35580*	Myosin-10
P35579*	Myosin-9
Q92823*	Neuronal cell adhesion molecule
Q99571*	P2X purinoceptor 4
Q92626*	Peroxidasin homolog
P23634*	Plasma membrane calcium-transporting ATPase 4
O15460*	Prolyl 4-hydroxylase subunit alpha-2
Q08174*	Protocadherin-1
Q96PZ0*	Pseudouridylate synthase 7 homolog
Q15262*	Receptor-type tyrosine-protein phosphatase kappa
Q01844*	RNA-binding protein EWS
P09238*	Stromelysin-2; MMP10
P04179*	Superoxide dismutase [Mn], mitochondrial
P24821*	Tenascin
P19971*	Thymidine phosphorylase
Q15025*	TNFAIP3-interacting protein 1
P61812*	Transforming growth factor beta-2; TGFb2
Q15582*	Transforming growth factor-beta-induced protein ig-h3
O95379*	Tumor necrosis factor alpha-induced protein 8
O95407*	Tumor necris factor receptor superfamily member 6B
P30530*	Tyrosine-protein kinase receptor UFO
Q9UK45*	U6 snRNA-associated Sm-like protein LSm7
O43795*	Unconventional myosin-Ib
P19320*	Vascular cell adhesion protein 1; VCAM1
P49767*	Vascular endothelial growth factor C; VEGFC
P12956*	X-ray repair cross-complementing protein 6
D. Proteins regulated in NHDF only	
P30533*	Alpha-2-macroglobulin receptor-associated protein
Q01432*	AMP deaminase 3
P46013*	Antigen KI-67
Q9Y223*	Bifunctional UDP-N-acetylglucosamine 2-epimerase/N-acetylmannosamine kinase
Q96EU7*	C1GALT1-specific chaperone 1
P98194*	Calcium-transporting ATPase type 2C member 1
P10644*	cAMP-dependent protein kinase type I-alpha regulatory subunit
Q9BX69*	Caspase recruitment domain-containing protein 6
P12110*	Collagen alpha-2(VI) chain
Q02388*	Collagen alpha-1(VII) chain
O94921*	Cyclin-dependent kinase 14
Q00535*	Cyclin-dependent-like kinase 5
Q17RY0*	Cytoplasmic polyadenylation element-binding protein 4
P47712*	Cytosolic phospholipase A2
Q13217*	DnaJ homolog subfamily C member 3
P11388*	DNA topoisomerase 2-alpha
Q96F86*	Enhancer of mRNA-decapping protein 3
P00533*	Epidermal growth factor receptor
Q9Y4X5*	E3 ubiquitin-protein ligase ARIH1
Q92598*	Heat shock protein 105 kDa
P52789*	Hexokinase-2
O14929*	Histone acetyltransferase type B catalytic subunit
Q9NPH2*	Inositol-3-phosphate synthase 1
P17936*	Insulin-like growth factor-binding protein 3; IGFBP3
Q8WWN9*	Interactor protein for cytohesin exchange factors 1
Q14627*	Interleukin-13 receptor subunit alpha-2; IL13RA2
P03956*	Interstitial collagenase; MMP1
P15018*	Leukemia inhibitory factor
P00338*	L-lactate dehydrogenase A chain
O60488*	Long-chain-fatty-acid--CoA ligase 4
Q8WYQ5*	Microprocessor complex subunit DGCR8
Q3SY69*	Mitochondrial 10-formyltetrahydrofolate dehydrogenase
Q9NQS3*	Nectin-3
O95631*	Netrin-1
O14786*	Neuropilin-1
P05114*	Non-histone chromosomal protein HMG-14
Q13219*	Pappalysin-1
P54821*	Paired mesoderm homeobox protein 1
Q96HC4*	PDZ and LIM domain protein 5
P42338*	Phosphatidylinositol 4,5-bisphosphate 3-kinase catalytic subunit β isoform
Q9BQ51*	Programmed cell death 1 ligand 2
O14684*	Prostaglandin E synthase
Q8N8S7*	Protein enabled homolog
Q96MK3*	Protein FAM20A
Q92597*	Protein NDRG1
Q8TF72*	Protein Shroom3
Q15293*	Reticulocalbin-1
P50454*	Serpin H1
P09486*	SPARC
P52823*	Stanniocalcin-1
O76061*	Stanniocalcin-2
P10599*	Thioredoxin
P35442*	Thrombospondin-2
Q04206*	Transcription factor p65
P02786*	Transferrin receptor protein 1
Q9NQC7*	Ubiquitin carboxyl-terminal hydrolase CYLD
Q9NR00*	Uncharacterized protein C8orf4
Q15043*	Zinc transporter ZIP14

significant regulation with FDR<0.05 in one (*), two (**) or three kinds of cells (***)

ASBMB
MOLECULAR & CELLULAR PROTEOMICS
MCP

Table 2

Acc.Nr.	Name									
Blood-borne markers for inflammatory activated ECs		**Δ_act vs con_cyt**	**p-value cyt**	**significant with FDR<0.05**	**Δ_act vs con_ne**	**p-value ne**	**significant with FDR<0.05**	**Δ_act vs con_sn**	**p-value sn**	**significant with FDR<0.05**
Q9Y5X9	Endothelial lipase	**3.78**	**2.79E-08**	x	**3.62**	**1.26E-04**		**3.59**	**1.38E-03**	x
Q01638	Interleukin-1 receptor-like 1	-1.31	1.28E-01		-0.84	2.89E-01		**2.17**	**4.41E-07**	x
P09238	Stromelysin-2; MMP10	0.75	1.18E-01		-0.49	2.84E-01		**6.50**	**3.18E-07**	x
P61812	Transforming growth factor beta-2	0.55	5.53E-01		-0.91	2.68E-01		**2.11**	**1.10E-03**	x
O95407	Tumor necris factor receptor superfamily member 6B							**6.71**	**3.49E-06**	x
Membrane-bound markers for inflammatory activated ECs										
P16581	E-selectin; CD62E	**4.63**	**2.40E-09**	x	0.83	2.60E-01		**7.66**	**9.14E-07**	x
O75144	ICOS ligand; CD275	**2.47**	**2.22E-06**	x	-0.44	3.61E-01		**2.63**	**2.06E-04**	x
Q13478	Interleukin-18 receptor 1; CD218a	**2.96**	**8.05E-05**	x	0.30	6.73E-01				
Q99571	P2X purinoceptor 4	**2.67**	**1.34E-04**	x	0.76	3.22E-01				
Q08174	Protocadherin-1	**1.48**	**1.10E-05**	x	0.79	2.71E-01		1.88	1.89E-01	
P19320	Vascular cell adhesion protein 1; CD106	**6.52**	**5.81E-07**	x	1.41	1.35E-01		**2.40**	**3.92E-08**	x
Intracellular markers for inflammatory activated ECs										
O95236	Apolipoprotein L3	**3.25**	**2.34E-06**	x	0.58	3.41E-01		-0.34	4.04E-01	
Q9Y5X9	Endothelial lipase	**3.78**	**2.79E-08**	x	**3.62**	**1.26E-04**		**6.71**	**3.49E-06**	x
P19971	Thymidine phosphorylase	**4.41**	**6.54E-06**	x	-1.04	1.17E-01				
Blood-borne markers for inflammatory activated fibroblasts										
P15018	Leukemia inhibitory factor; LIF							**4.93**	**2.53E-06**	x
P52823	Stanniocalcin-1	**4.06**	**3.63E-05**	x	**5.22**	**1.63E-05**	x	**5.21**	**3.26E-06**	x
O76061	Stanniocalcin-2	0.04	9.65E-01		0.80	4.08E-01		**1.05**	**2.37E-04**	x
Membrane-bound markers for inflammatory activated fibroblasts										
Q14627	Interleukin-13 receptor subunit alpha-2; CD213a2	**5.94**	**7.15E-05**	x	0.88	1.85E-01				
Q9NQS3	Nectin-3; CD113	**2.30**	**1.66E-05**	x	0.51	6.02E-01				
Q9BQ51	Programmed cell death 1 ligand 2; CD273	**2.26**	**6.05E-06**	x	0.25	7.94E-01				
Q15043	Zinc transporter ZIP14	**2.43**	**2.42E-06**	x	2.24	8.41E-02				
Intracellular markers for inflammatory activated fibroblasts										
P47712	Cytosolic phospholipase A2	**2.57**	**4.86E-05**	x	1.48	1.40E-01				
P00533	Epidermal growth factor receptor	**1.40**	**2.05E-02**		**4.13**	**2.95E-04**	x			
O14684	Prostaglandin E synthase	**4.98**	**6.81E-08**	x	**2.96**	**3.82E-05**	x			
P35442	Thrombospondin-2	**4.75**	**6.14E-05**	x	**4.50**	**3.17E-05**	x	**2.43**	**1.75E-03**	

ASBMB
MOLECULAR & CELLULAR PROTEOMICS
MCP

Table 3

Acc.Nr.	Name	Δ_act vs con_cyt	p-value cyt	significant with FDR<0.05	Δ_act vs con_ne	p-value ne	significant with FDR<0.05	Δ_act vs con_sn	p-value sn	significant with FDR<0.05
A. Proteins related to IFN response, upregulated in PBMCs upon inflammatory activation										
O14879	Interferon-induced protein with tetratricopeptide repeats 3	**7.54**	**5.30E-07**		1.51	2.05E-01		**3.99**	**3.21E-03**	
P09913	Interferon-induced protein with tetratricopeptide repeats 2	**6.75**	**3.37E-06**		-0.83	2.76E-01		**3.19**	**4.91E-02**	
Q96PP8	Guanylate-binding protein 5	**2.48**	**1.17E-05**		0.45	4.61E-01		0.17	8.81E-01	
Q15646	2-5-oligoadenylate synthase-like protein	**5.85**	**3.17E-05**		**4.07**	**6.82E-04**				
P14902	Indoleamine 2,3-dioxygenase 1	**7.63**	**4.51E-05**		-1.90	1.12E-01				
P20591	Interferon-induced GTP-binding protein Mx1; MX1	**3.53**	**6.57E-05**		1.46	2.07E-01		**2.46**	**7.11E-03**	
Q96PP9	Guanylate-binding protein 4; GBP4	**4.76**	**1.15E-04**		-0.28	6.06E-01				
P09914	Interferon-induced protein with tetratricopeptide repeats 1	**4.95**	**1.81E-04**		0.82	5.39E-01		1.26	3.31E-01	
Q92985	Interferon regulatory factor 7	**4.01**	**2.04E-04**		**4.63**	**3.40E-03**				
Q9BYX4	Interferon-induced helicase C domain-containing protein 1	**6.77**	**2.49E-04**		0.97	2.28E-01				
P05161	Ubiquitin-like protein ISG15	**5.33**	**4.91E-04**		**4.03**	**2.44E-05**		**4.28**	**1.27E-03**	
Q9UII4	E3 ISG15--protein ligase HERC5	**4.95**	**1.10E-03**		**5.35**	**7.80E-04**				
Q8TCB0	Interferon-induced protein 44	**4.23**	**1.17E-03**		**2.31**	**4.52E-02**				
P32455	Interferon-induced guanylate-binding protein 1	**1.02**	**1.70E-03**		0.72	4.19E-01		2.46	1.29E-01	
Q9NQ25	SLAM family member 7	**5.18**	**2.61E-03**		0.84	3.68E-01				
P20592	Interferon-induced GTP-binding protein Mx2	**6.41**	**4.51E-03**		1.98	1.80E-01				
Q96J88	Epithelial-stromal interaction protein 1	**3.87**	**7.36E-03**		**5.85**	**9.84E-05**				
Q08380	Galectin-3-binding protein	**2.77**	**9.29E-03**		**6.62**	**1.11E-07**	x	0.85	3.17E-01	
Q96AZ6	Interferon-stimulated gene 20 kDa protein; ISG20	**2.40**	**1.28E-02**		2.45	1.87E-01		**2.67**	**9.62E-04**	
P31941	DNA dC->dU-editing enzyme APOBEC-3A	**5.16**	**1.60E-02**		0.97	1.60E-01				
Q9Y244	Proteasome maturation protein	**2.69**	**2.38E-02**		-0.59	6.65E-01				
Q8N8V2	Guanylate-binding protein 7	**3.19**	**4.36E-02**		0.72	1.99E-01				
P02778	C-X-C motif chemokine 10; CXCL10	2.08	1.11E-01		**3.31**	**5.55E-02**		**3.00**	**2.39E-02**	
Q8WXG1	Radical S-adenosyl methionine domain-containing protein 2	1.33	1.28E-01		**4.99**	**2.49E-03**				
P52630	Signal transducer and activator of transcription 2	1.00	1.34E-01		**4.22**	**5.75E-04**				
O95786	Probable ATP-dependent RNA helicase DDX58; DDX58	1.61	1.99E-01		**3.70**	**2.05E-04**		0.72	5.64E-01	
P42224	Signal transducer and activator of transcription 1-alpha/bet	0.45	3.83E-01		**2.77**	**1.90E-03**		0.53	6.11E-01	
Q02556	Interferon regulatory factor 8	0.73	4.47E-01		**2.32**	**1.09E-02**				
Q16666	Gamma-interferon-inducible protein 16	0.35	5.11E-01		**1.93**	**4.09E-02**		1.03	2.63E-01	
P80075	C-C motif chemokine 8							**3.35**	**1.90E-05**	
Q14258	E3 ubiquitin/ISG15 ligase TRIM25	-0.08	4.01E-01		0.50	3.80E-01		**1.61**	**4.71E-02**	
B. Proteins related to IFN response, upregulated in HUVEC upon inflammatory activation										
O95236	Apolipoprotein L3	**3.25**	**2.34E-06**	x	0.58	3.41E-01				
P20591	Interferon-induced GTP-binding protein Mx1; MX1	**4.57**	**1.81E-05**	x	**3.48**	**1.43E-02**		**2.53**	**2.04E-02**	
O95786	Probable ATP-dependent RNA helicase DDX58; DDX58	**1.75**	**2.63E-05**	x	-0.66	1.36E-01		-0.90	2.20E-01	
Q96PP9	Guanylate-binding protein 4; GBP4	**3.34**	**3.91E-05**	x	-0.68	1.31E-01				
Q96AZ6	Interferon-stimulated gene 20 kDa protein; ISG20	**3.69**	**5.00E-05**	x	**2.77**	**1.44E-02**		**4.22**	**4.43E-06**	x
P32455	Interferon-induced guanylate-binding protein 1	**1.91**	**7.91E-05**	x	0.52	3.77E-01		1.19	3.77E-01	
Q99571	P2X purinoceptor 4	**2.67**	**1.34E-04**	x	0.76	3.22E-01				
Q9BYX4	Interferon-induced helicase C domain-containing protein 1	**2.67**	**1.43E-03**		-0.17	7.62E-01				
Q13287	N-myc-interactor	**1.15**	**2.02E-03**		**2.67**	**7.72E-04**				
P32456	Interferon-induced guanylate-binding protein 2	**1.07**	**2.40E-03**		-0.37	6.04E-01		-0.85	2.58E-01	
Q13325	type I interferon signaling pathway; antiviral	**1.91**	**3.77E-03**		0.82	1.78E-01				
Q07000	HLA class I histocompatibility antigen, Cw-15 alpha chain	**2.45**	**4.66E-03**		**1.45**	**1.18E-02**				
O00478	Butyrophilin subfamily 3 member A3	**1.45**	**6.85E-03**		0.62	2.75E-01				
P20592	Interferon-induced GTP-binding protein Mx2	**1.26**	**1.07E-02**		1.11	1.69E-01				
O14879	Interferon-induced protein with tetratricopeptide repeats 3	**2.02**	**1.28E-02**		0.09	8.38E-01		-0.24	7.00E-01	
P09914	Interferon-induced protein with tetratricopeptide repeats 1	**1.99**	**2.21E-02**		1.03	1.84E-01		-0.12	7.73E-01	
Q8TCB0	Interferon-induced protein 44	**1.06**	**4.16E-02**		0.07	8.94E-01				
P05161	Ubiquitin-like protein ISG15	1.06	6.72E-02		1.20	2.44E-01		**1.18**	**6.17E-05**	x
Q00978	Interferon regulatory factor 9	0.38	5.87E-01		**1.28**	**1.57E-02**				
P02778	C-X-C motif chemokine 10; CXCL10	0.11	8.18E-01		0.79	1.30E-01		**4.23**	**4.21E-05**	x
C. Proteins related to IFN response, upregulated in NHDF upon inflammatory activation										
P09914	Interferon-induced protein with tetratricopeptide repeats 1	-0.99	4.77E-02		-0.58	7.07E-01		**1.01**	**2.76E-02**	

ASBMB MOLECULAR & CELLULAR PROTEOMICS MCP

Table 4

Acc.Nr.	Name	HUVEC	NHDF
A. Proteins involved in angiogenesis			
P12821	Angiotensin-converting enzyme; CD143	down*	-
Q96EU7	C1GALT1-specific chaperone 1	-	up*
P25774	Cathepsin S	up*	up
Q86T13	C-type lectin domain family 14 member A	down*	-
Q9NPY3	Complement component C1q receptor; CD93	up*	-
P01584	Interleukin-1 beta	-	up*
Q14213	Interleukin-27 subunit beta	up*	-
P10145	Interleukin-8	up*	up*
Q96RQ9	L-amino-acid oxidase	up*	-
P35579	Myosin-9	down*	-
Q92823	Neuronal cell adhesion molecule	up*	-
O14786	Neuropilin-1	-	up*
O60462	Neuropilin-2	up	up*
P54821	Paired mesoderm homeobox protein 1	-	up*
P42338	Phosphatidylinositol 4,5-bisphosphate 3-kinase catalytic subunit beta isoform	-	down*
P23634	Plasma membrane calcium-transporting ATPase 4	up*	-
Q92597	Protein NDRG1	-	up*
Q08174	Protocadherin-1	up*	-
P19971	Thymidine phosphorylase	up*	-
Q03169	Tumor necrosis factor alpha-induced protein 2	up*	up*
P49767	Vascular endothelial growth factor C	up*	-
B. Proteins involved in angiogenesis and ECM reorganization			
P21810	Biglycan	down*	-
P02452	Collagen alpha-1(I) chain	-	down*
P08123	Collagen alpha-2(I) chain	down*	down*
P08572	Collagen alpha-2(IV) chain	up*	up*
Q9UBX5	Fibulin-5	down*	down
P03956	Interstitial collagenase; MMP1	-	up*
Q16363	Laminin subunit alpha-4	up*	-
P05121	Plasminogen activator inhibitor 1	up*	up
O15460	Prolyl 4-hydroxylase subunit alpha-2	up*	down*
P08254	Stromelysin-1, MMP3	up*	up*
P09238	Stromelysin-2, MMP10	up*	
P07996	Thrombospondin-1	down	up*
P35442	Thrombospondin-2	-	up*
P61812	Transforming growth factor beta-2	up*	-
Q15582	Transforming growth factor-beta-induced protein ig-h3	up*	-
C. Proteins involved in ECM reorganization			
O00468	Agrin	up*	-
Q02388	Collagen alpha-1(VII) chain	-	up*
P05997	Collagen alpha-2(V) chain	up*	-
P12110	Collagen alpha-2(VI) chain	-	down*
P05362	Intercellular adhesion molecule 1	up*	up*
P07942	Laminin subunit beta-1	up*	-
Q13751	Laminin subunit beta-3	up	up*
P11047	Laminin subunit gamma-1	up*	-
Q13753	Laminin subunit gamma-2	up*	-
Q00653	Nuclear factor NF-kappa-B p100 subunit	up*	up*
Q92626	Peroxidasin homolog	up*	
P50454	Serpin H1	-	down*
P24821	Tenascin	up*	-
P48307	Tissue factor pathway inhibitor 2	up*	up*
P98066	Tumor necrosis factor-inducible gene 6 protein; TSG6	up	up*
P19320	Vascular cell adhesion protein 1	up*	-
P13611	Versican core protein	-	down*

*significant regulation with FDR<0.05

4. Conclusions

Although inflammation-related processes are in the focus of numerous research institutions already for decades, many important questions remain unsolved. In clinical practice, biomarkers for inflammation such as C-reactive protein (CRP) are readily available and the determination of these markers represents the most important and widely used bioassays. However, since CRP is rather unspecific, more specific markers for inflammatory activities and states of cells and tissues could dramatically improve diagnosis and monitoring of for example arteriosclerosis or neurodegenerative processes and are still urgently required. Furthermore, a detailed and individualized prediction of drug effects during a therapeutic intervention is not yet possible, resulting in rather empirical approaches to find best working drugs. A comprehensive investigation of complex molecular processes may actually support the determination of appropriate marker molecules as well as improved prediction of therapeutic effects.

The present doctoral thesis demonstrates that comprehensive analysis of regulatory molecular processes involved in acute inflammation is feasible. The detectable molecular events range from ligand-induced receptor activation, the exertion of downstream signaling cascades including kinase activities, the translocation of transcription factors as well as the subsequent transcriptional activation of target genes resulting in specific protein synthesis. Detailed insights into these molecular processes were obtained by a powerful proteomic approach based on nanoflow liquid chromatography and high resolution mass spectrometry. Furthermore, an increased data density achieved by iterative method optimization allowed the elucidation of expected as well as unexpected effects of commonly used drugs such as dexamethasone or more specific compounds such as cannabinoids. In conclusion, here I demonstrate that the application of a mass spectrometry-based screening approach resulted in comprehensive assessments of complex molecular inflammation-related processes. The presented methods are fully compatible for dealing with biological model systems as well as clinical samples. The comprehensive screening for molecular events resulted in the identification of representative marker molecules. Targeted mass spectrometry methods were demonstrated to support high-throughput analysis with very high accuracy. These methods and tools shall be used for the improvement of diagnostic procedures as well as for the evaluation of drug mechanisms of action including side effects.

5. Abstract

Inflammatory responses are indispensable physiological processes involved in the defense mechanism of an organism. These processes are characterized by a complex interplay of different types of immune cells with an underlying network of intersecting signaling pathways. Mass spectrometry-based proteomics analysis was applied in order to investigate cellular processes during inflammatory stimulation as well as in response to therapeutic interventions. As a highly relevant *in vitro* model system, primary human peripheral blood mononuclear cells (PBMCs) were chosen, which were inflammatory stimulated using lipopolysaccharide and phytoheamagglutinin. Furthermore, cells were treated with dexamethasone and the synthetic cannabinoid CP47,497-C8, respectively. The treatment of inflammatory activated PBMCs with dexamethasone was performed to obtain insight into anti-inflammatory mechanisms induced by drug treatment and to investigate its potency to suppress pro-inflammatory cellular activities. In contrast, the assessment of CP47,497-C8-treated quiescent PBMCs demonstrated the power of this analysis strategy to disclose inflammation-related processes independent of a classical inflammatory stimulus. Cellular samples were fractionated into supernatant, cytoplasmic and nuclear protein fractions and subsequently enzymatically digested. Comprehensive proteome profiles were then generated using a high resolution QExactive orbitrap mass spectrometer and label-free quantitative data analysis was performed using MaxQuant.

Comparative proteome profiling of quiescent and inflammatory activated PBMCs revealed the identification of 85501 peptides compiled to 6886 proteins. Thereof, 469 proteins were significantly regulated upon inflammatory activation including the classical inflammatory mediators IL-1β, IL-6, CXCL2 and GROα. Furthermore, it was clearly demonstrated that dexamethasone is unable to counter-regulate all inflammation-induced proteins. Based on the high data density, the entire c-JUN, ERK5 and NF-κB signaling cascade was mapped in a semi-quantitative fashion. Furthermore, 2731 phosphopeptides derived from 991 proteins were identified in a highly confident fashion. Due to the efficient subcellular fractionation it was further possible to assess inflammation-related nuclear translocation of proteins, for example of histone-modifying proteins and transcription factors. In conclusion, this thesis demonstrates the power of mass spectrometry-based proteomics regarding not only the identification of proteins, but also the assessment of protein regulations, post-translational modifications and nuclear translocation events in order to comprehensively characterize the complex molecular processes during inflammation.

6. Zusammenfassung (German Abstract)

Entzündungsprozesse sind die Folge von physiologisch essentiellen Abwehrstrategien höherer Organismen gegen Pathogene. Diese Prozesse sind durch ein komplexes Zusammenspiel unterschiedlichster Zelltypen charakterisiert, dem ein Netzwerk verschränkter Signaltransduktionswege zugrunde liegt. Massenspektrometrie-basierende Proteomanalysen wurden zur Untersuchung der zellulären Prozesse während entzündlicher Stimulation und auch der zellulären Reaktion auf anti-entzündliche Wirkstoffe eingesetzt. Als biologisch relevantes *in vitro* Modell wurden primäre humane mononukleäre Zellen des peripheren Blutes herangezogen, welche mit Lipopolysaccharid und Phytohämagglutinin entzündlich stimuliert wurden. In weiterer Folge wurden die Effekte von Dexamethason und dem synthetischen Cannabinoid CP47,497-C8 auf die Entzündungsprozesse untersucht. Die Behandlung entzündlich stimulierter Zellen mit Dexamethason wurde durchgeführt um einerseits Einblicke in anti-entzündliche Mechanismen zu erhalten und andererseits die Fähigkeit des Medikamentes pro-entzündliche Zellaktivitäten zu unterbinden, zu evaluieren. Die Behandlung von ruhenden Zellen mit dem synthetischen Cannabinoid hingegen zeigte die besondere Eignung des Verfahrens, die Beeinflussung von Entzündungsprozessen auch aufgrund von nicht-klassischen Stimulantien genau untersuchen zu können. Die zellulären Proben wurden in zytoplasmatische Protein, Kernproteine und sezernierte Proteine aus dem Zellüberstand fraktioniert und enzymatisch verdaut. Umfassende Proteomprofile wurden mit Hilfe eines hochauflösenden QExactive Orbitrap Massenspektrometers und der MaxQuant-Software erstellt.

Vergleichende Proteomanalysen von ruhenden und entzündlich stimulierten mononukleären Zellen des peripheren Blutes ergaben die Identifikation von 85501 unterschiedlichen Peptiden, die zur Identifikation von 6886 Proteinen führte. Davon waren 469 Proteine durch die entzündliche Stimulation signifikant reguliert, unter anderem auch die klassischen entzündlichen Mediatoren IL-1β, IL-6, CXCL2 und GROα. Es konnte auch gezeigt werden, dass Dexamethason nicht in der Lage ist, alle durch entzündliche Stimulation hoch regulierten Proteine wieder hinunter zu regulieren. Basierend auf der hohen Datendichte konnte der gesamte c-JUN, ERK5 und NF-κB Signalweg semiquantitativ abgebildet werden. Des Weiteren konnten 2731 Phosphopeptide, welche von 991 Proteinen stammen, mit hoher Sicherheit erfasst werden. Aufgrund der effizienten subzellulären Fraktionierung war es auch möglich Entzündungs-assoziierte Translokations-Ereignisse in den Zellkern von beispielsweise Histon-modifizierenden Enzymen und Transkriptionsfaktoren zu verfolgen. Schließlich zeigt diese Arbeit nicht nur die Leistungsfähigkeit von Massenspektrometrie-basierenden Analysestrategien hinsichtlich der Identifikation von Proteinen, sondern auch bezüglich der Untersuchung von Proteinregulationen, post-translationalen Modifikationen und Kerntranslokation von Proteinen, welche zur detaillierten Charakterisierung von komplexen Mechanismen im Rahmen von Entzündungsprozessen erforderlich sind.

7. Scientific Contributions

7.1. List of Publications

1. Weiss, T.; Taschner-Mandl, S.; Bileck, A.; Slany, A.; Kromp, F.; Rifatbegovic, F.; Frech, C.;Windhager, R.; Kitzinger, H.; Tzou, C.H.; Ambros, P.F.; Gerner, C.; Ambros, I.M. Comprehensive in-depth cell and tissue omics-analysis unravels the human Schwann cell repair phenotype. *Glia* **2016, manuscript submitted**

2. Slany, A.; Bileck, A.; Kreutz, D.; Mayer, R.L.; Muqaku, B.; Gerner, C. Contribution of human fibroblasts and endothelial cells to the hallmarks of inflammation as determined by proteome profiling. *Mol Cell Proteomics* **2016, manuscript in press**

3. Bileck, A.; Mayer, R.L.; Kreutz, D.; Weiss, T.; Slany, A.; Gerner, C. Shotgun proteomics of primary human cells enables the analysis of signaling pathways and nuclear translocations related to inflammation..*J Proteome Res* **2015, manuscript under revision**

4. Smidak, R.; Mayer, R. L.; Bileck, A.; Gerner, C.; Mechtcheriakova, D.; Stork, O.; Lubec, G.; Li, L., Quantitative proteomics reveals protein kinases and phosphatases in the individual phases of contextual fear conditioning in the C57BL/6J mouse. *Behav Brain Res* **2016,** 303, 208-17.

5. Meier, S. M.; Muqaku, B.; Ullmann, R.; Bileck, A.; Kreutz, D.; Mader, J. C.; Knasmuller, S.; Gerner, C., Proteomic and Metabolomic Analyses Reveal Contrasting Anti-Inflammatory Effects of an Extract of Mucor Racemosus Secondary Metabolites Compared to Dexamethasone. *PLoS One* **2015,** 10, (10), e0140367.

6. Slany, A.; Bileck, A.; Muqaku, B.; Gerner, C., Targeting breast cancer-associated fibroblasts to improve anti-cancer therapy. *Breast* **2015,** 24, (5), 532-8.

7. Bileck, A.; Ferk, F.; Al-Serori, H.; Koller, V. J.; Muqaku, B.; Haslberger, A.; Auwarter, V.; Gerner, C.; Knasmuller, S., Impact of a synthetic cannabinoid (CP-47,497-C8) on protein expression in human cells: evidence for induction of inflammation and DNA damage. *Arch Toxicol* **2015**.

8. Muqaku, B.; Slany, A.; Bileck, A.; Kreutz, D.; Gerner, C., Quantification of cytokines secreted by primary human cells using multiple reaction monitoring: evaluation of analytical parameters. *Anal Bioanal Chem* **2015,** 407, (21), 6525-36.

9. Paulitschke, V.; Berger, W.; Paulitschke, P.; Hofstatter, E.; Knapp, B.; Dingelmaier-Hovorka, R.; Fodinger, D.; Jager, W.; Szekeres, T.; Meshcheryakova, A.; Bileck, A.; Pirker, C.; Pehamberger, H.; Gerner, C.; Kunstfeld, R., Vemurafenib resistance signature by proteome analysis offers new strategies and rational therapeutic concepts. *Mol Cancer Ther* **2015,** 14, (3), 757-68.

10. Bileck, A.; Kreutz, D.; Muqaku, B.; Slany, A.; Gerner, C., Comprehensive assessment of proteins regulated by dexamethasone reveals novel effects in primary human peripheral blood mononuclear cells. *J Proteome Res* **2014,** 13, (12), 5989-6000.

11. Groessl, M.; Slany, A.; Bileck, A.; Gloessmann, K.; Kreutz, D.; Jaeger, W.; Pfeiler, G.; Gerner, C., Proteome profiling of breast cancer biopsies reveals a wound healing signature of cancer-associated fibroblasts. *J Proteome Res* **2014,** 13, (11), 4773-82.

12. Slany, A.; Haudek-Prinz, V.; Meshcheryakova, A.; Bileck, A.; Lamm, W.; Zielinski, C.; Gerner, C.; Drach, J., Extracellular matrix remodeling by bone marrow fibroblast-like cells correlates with disease progression in multiple myeloma. *J Proteome Res* **2014,** 13, (2), 844-54.

7.2. List of Oral Contributions

2015 BSPR British Society for Proteome Research Meeting 2015 (Reading, United Kingdom): "Evaluation of signalling pathways in primary human peripheral blood mononuclear cells by in-depth proteome profiling"

2015 ASAC-JunganalytikerInnenforum 2015 (Innsbruck, Austria):"Comprehensive LC-MS/MS analyses enables assessment of signaling pathways in human blood cells"

2015 23. Jahrestagung der Biomedizinischen AnalytikerInnen (Graz, Austria): "Proteom-Analysen zeigen unerwartete Effekte von Dexamethason in primären humanen mononukleären Zellen des peripheren Blutes"

2014 APRS Austrian Proteomics Research Symposium (Salzburg, Austria): "Proteome profiling of breast cancer biopsies reveals a wound healing signature of cancer-associated fibroblast"

2013 1st international Symposium on Profiling (Lisbon, Portugal): "Proteome profiling of primary human multiple myeloma cells in comparison to the established multiple myeloma cell line RPMI-8226"

2012 APRS Austrian Proteomics Research Symposium (Graz, Austria):"Characterization of tumor-stroma interactions by means of marker proteins in multiple myeloma"

7.3. List of Poster Contributions

2014 13th Annual World Congress of the Human Proteome Organization (Madrid, Spain): "Molecular Profiling of Peripheral Blood Mononuclear Cells (PBMCs) for the Identification of Cellular Responses to Dexamethasone"

2010 7. Jahrestagung Deutsche Vereinte Gesellschaft für Klinische Chemie und Laboratoriumsmedizin (Mannheim, Germany): "Establishment of a multiplex assay for the detection of the potential tumor biomarkers CXCL-1, IGFBP-6, STC-1 and periostin by means of Luminex™ technology"

Ich habe mich bemüht, sämtliche Inhaber der Bildrechte ausfindig zu machen und ihre Zustimmung zur Verwendung der Bilder in dieser Arbeit eingeholt. Sollte dennoch eine Urheberrechtsverletzung bekannt werden, ersuche ich um Meldung bei mir.

– A.B.
April, 2016